UNIVERSITY OF SOUTHAMPTON

ELECTROSTATIC BACTERIAL CONTROL

By

JONATHAN OLIVER NOYCE

A thesis submitted for the degree of

DOCTOR OF PHILOSOPHY

FACULTY OF ENGINEERING AND APPLIED SCIENCE
DEPARTMENT OF ELECTRONICS AND COMPUTER SCIENCE

December 2002

UNIVERSITY OF SOUTHAMPTON

ABSTRACT

FACULTY OF ENGINEERING AND APPLIED SCIENCE

ELECTRONICS AND COMPUTER SCIENCE

Doctor of Philosophy

ELECTROSTATIC BACTERIAL CONTROL

By Jonathan Oliver Noyce

Since the onset of the first application of antibiotics, selective pressure on the micro-organism community has established the emergence of resistant strains. Now at the turn of the 21st century, multi-drug resistant bacteria are commonplace. Even disinfectants are now becoming tolerated at previously lethal doses. The search to find new chemical agents and decontamination methods is paramount, if the fight against pathogenic organisms is to continue.

The following work describes the bactericidal effect of either negative or positive ions, generated by an electrical corona discharge in nitrogen. Bacterial samples were selected for the study to represent both Gram-negative and Gram-positive species, and naturally occurring resistant phenotypes that exist in everyday environmental conditions. These were *Escherichia coli*, *Staphylococcus aureus*, starved *Pseudomonas veronii* cells or *Pseudomonas veronii* biofilms. Samples were placed into a custom-built multi-point-to-plane ion generator, situated within a sealed chamber. Under a nitrogen atmosphere, to prevent ozone formation, microbial samples were exposed to either negative or positive ions for various time periods and corona current levels. The results from this study have demonstrated an antibacterial effect of both negative and positive unipolar ions, with significant reductions (up to two log) in bacterial numbers for all the target samples. Of the two polarities, positive ions were significantly more effective than negative at reducing microbial load, with a mean kill rate of 72% compared to 50% for negative. This could possibly be due to the net negative surface charge that exists on the cell walls of both Gram-negative and Gram-positive bacteria.

Gram-negative bacteria have been shown to be more susceptible to ionic challenge than Gram-positive, with *S.aureus* achieving higher viability results after treatment, compared to both *E.coli* and *P.veronii*. This is possibly due to the lower peptidoglycan content in their cell walls. As to a mechanism for microbial death, this is possibly due to the Mendis *et al* cell wall disruption model (2001), which is proposed to function by accumulation of charge at the outer membrane surface. The attractive force that exists between oppositely charged groups on either side of the cell wall cause it to narrow and eventually collapse. The proposed Mendis model noted that the physical mechanism for the structural disruption of bacteria is only effective for Gram-negative ones like *E.coli* and *P.veronii*, which possess thin outer membranes and small quantities of peptidoglycan. However, data provided in this study conclusively shows disruption to the Gram-positive cell wall after ionic challenge, indicating an alternative mechanism, possibly through interference with the selective permeability properties. This technology could provide a novel method of disinfection where the use of toxic biocides is inappropriate.

Contents

Table of Figures

List of Tables

Preface

This research is multidisciplinary and encompasses concepts from both electrical engineering and biological subjects. In order to understand the ideas presented in this thesis, background information on bacteria and the required electrostatic theory has been provided for comprehension by scientists of any discipline in *Chapter one*. The aims and objectives of this project are additionally provided in this chapter. Descriptions of the experiments conducted during this research, including all materials used, apparatus design and procedures are described in *Chapter Two*. Written and graphical presentation of the results of all conducted experiments is shown in *Chapter Three*. Finally, the effect of negative or positive ionic challenge on bacterial samples is discussed in *Chapter four* with conclusions drawn and further work described.

Acknowledgements

I would like to thank my supervisor, Professor John Hughes, for his endless assistance, advice and guidance throughout this project. I would also like to thank my colleagues, Dr. Lindsey Gaunt, Dr. Karen Jerrim, Dr. Neil Goodman and Miss Sabrina Higgins for their advice and assistance in literary and laboratory projects. I am also grateful for the support and guidance from Dr. David O'Connor and his research group, for all matters concerning microbiology and Dr. Pauline Handley for the provision of *P.veronii* – bio.

With regards to financial matters, I would like to thank the Engineering and Physical Sciences Research Council and Reckitt-Benckiser for their support.

Finally, I would like to thank my parents for their encouragement, and Ellie, for her patience and never-ending support throughout this PhD.

Abbreviations

A	amps
ATP	adenosine triphosphate
C	coulomb
CDC	centre for disease control and prevention
CDSC	public health laboratory service communicable disease surveillance centre
$CFUml^{-1}$	colony forming units per ml
CGB	cantoni giolitti broth
CPC	cetylpyridinium chloride
DC	direct current
DLVO	derjaguin landau verwey and overbeck
DNA	deoxyribonucleic acid
E	electric field strength
ECD	enhanced corona discharge
EPS	exopolysaccharide
GI	gastro intestinal
I	current
kV	kilovolts
$lmin^{-1}$	litres per minute
LPS	lipopolysaccharide
MRSA	methicillin-resistant *Staphylococcus aureus*
NAG	N-acetylglucosamine
NAM	N-acetylmuramic acid
$O.D_{630nm}$	optical density at a wavelength of 630nm
Ω	ohms
O_3	ozone
ppGpp	guanosine 3-5-biophosphate
RH	relative humidity
$RLUs^{-1}$	relative light units per second
RNA	ribonucleic acid
Sm^{-1}	siemens per metre
SEM	standard error of the mean
S9: P.I	ratio of syto-9 to propidium iodide
ToneSB	tryptone soy broth
TSB	tryptic soy broth
V	volts

Chapter One

Introduction

1.1) Bacteria

Our bodies consist of some 10^{14} cells; numerically 90% of them are bacteria (Gilbert and McBain, 2001). Bacteria are prokaryotic organisms (*Figure* 1.1), a diverse group of ubiquitous organisms, all of which consist of a single cell that lacks a distinct nuclear membrane and has a cell wall of unique composition. This is in contrast to eukaryotes; organisms whose cells have chromosomes that are separated from the cytoplasm by a double membrane nuclear envelope. Eukaryotic cells additionally possess distinct cytoplasmic organelles, including the golgi apparatus, mitochondria and rough and smooth endoplasmic reticulum.

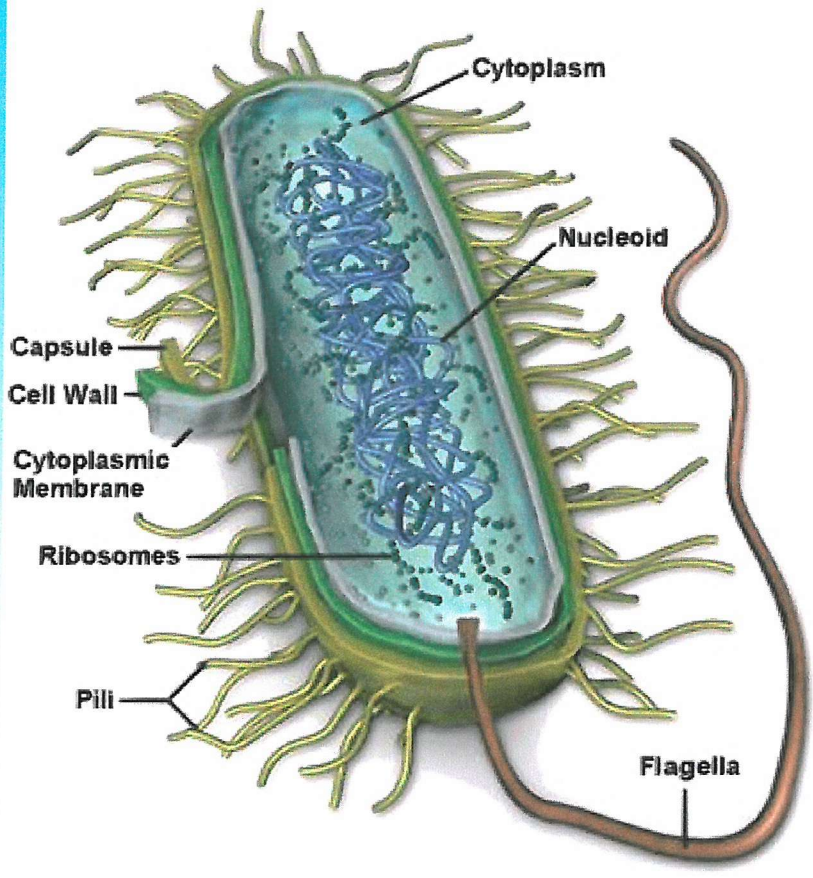

Figure 1.1) Diagram of a typical Gram – negative bacterium

(Wessells and Hopson, 1988)

The majority of bacteria range in size from 0.5 to 5μm. Many are capable of movement, bearing flagella or cilia. A bacterial cell may be spherical (coccus), rodlike (bacillus), spiral (spirillum), comma shaped (vibrio), corkscrew shaped (spirochaete), or filamentous. Recently bacteria have been subdivided into Eubacteria and Archaebacteria, with Eubacteria further divided into two groups, either 'Gram-positive' or 'Gram–negative'. This sub-division is based on their ability to take up the dye crystal violet, and due to the presence (Gram-negative, *Figure* 1.2, *Page* 4) or absence (Gram-positive, *Figure* 1.3, *Page* 5) of an outer membrane in their cell walls. The thickness of the cell wall ranges from 15-80nm for Gram-positive bacteria and 10nm for Gram-negative. Beneath this protective wall lies a plasma membrane, enclosing a single cytoplasmic compartment containing deoxyribonucleic acid (DNA), ribonucleic acid (RNA), protein synthesising complexes and a variety of enzymes (White, 1995).

As previously mentioned, the typical feature of the Gram-negative bacteria cell wall is the highly organised outer membrane, composed of an asymmetrical bilayer of phospholipid and lipopolysaccharide (LPS). This membrane constitutes a significant permeability barrier containing specific diffusion pores, formed of integral porin proteins connecting the periplasm of the cell to the external environment. A wide range of both Gram-positive and Gram-negative bacteria additionally possess an envelope layer consisting of polysaccharide, termed a capsule, which prevents immunological intervention mechanisms, including adhesion by antibodies or complement, and phagocytosis by macrophages.

The cell wall maintains the shape of the cell and protects the cytoplasmic membrane from rupture due to high internal osmotic pressure. The single, intrinsic component that confers structural integrity to the cell wall is peptidoglycan, a macromolecule not found in eukaryotes. Peptidoglycan consists of chains of amino sugars (N-acetylglucosamine, NAG, and N-acetylmuramic acid, NAM) crosslinked to a tripeptide of alanine, glutamic acid and lysine. Within Gram-positive bacteria, peptidoglycan accounts for 50% of their total mass and 10-20% in Gram-negative (Rang *et al*, 1998).

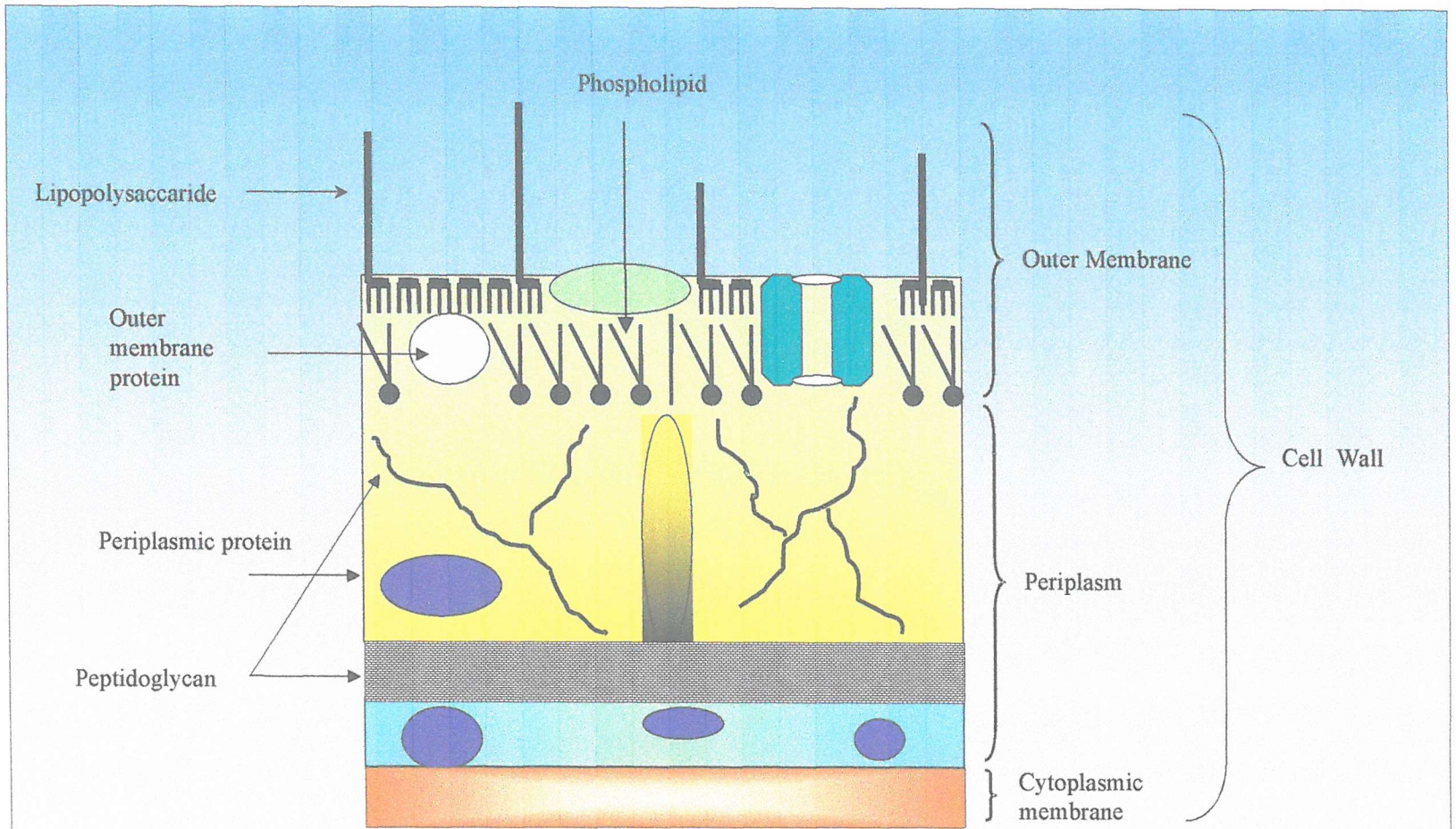

Figure 1.2) Cross sectional diagram through the cell wall of a typical Gram-negative bacterium.
(Adapted from Mozes, 1991)

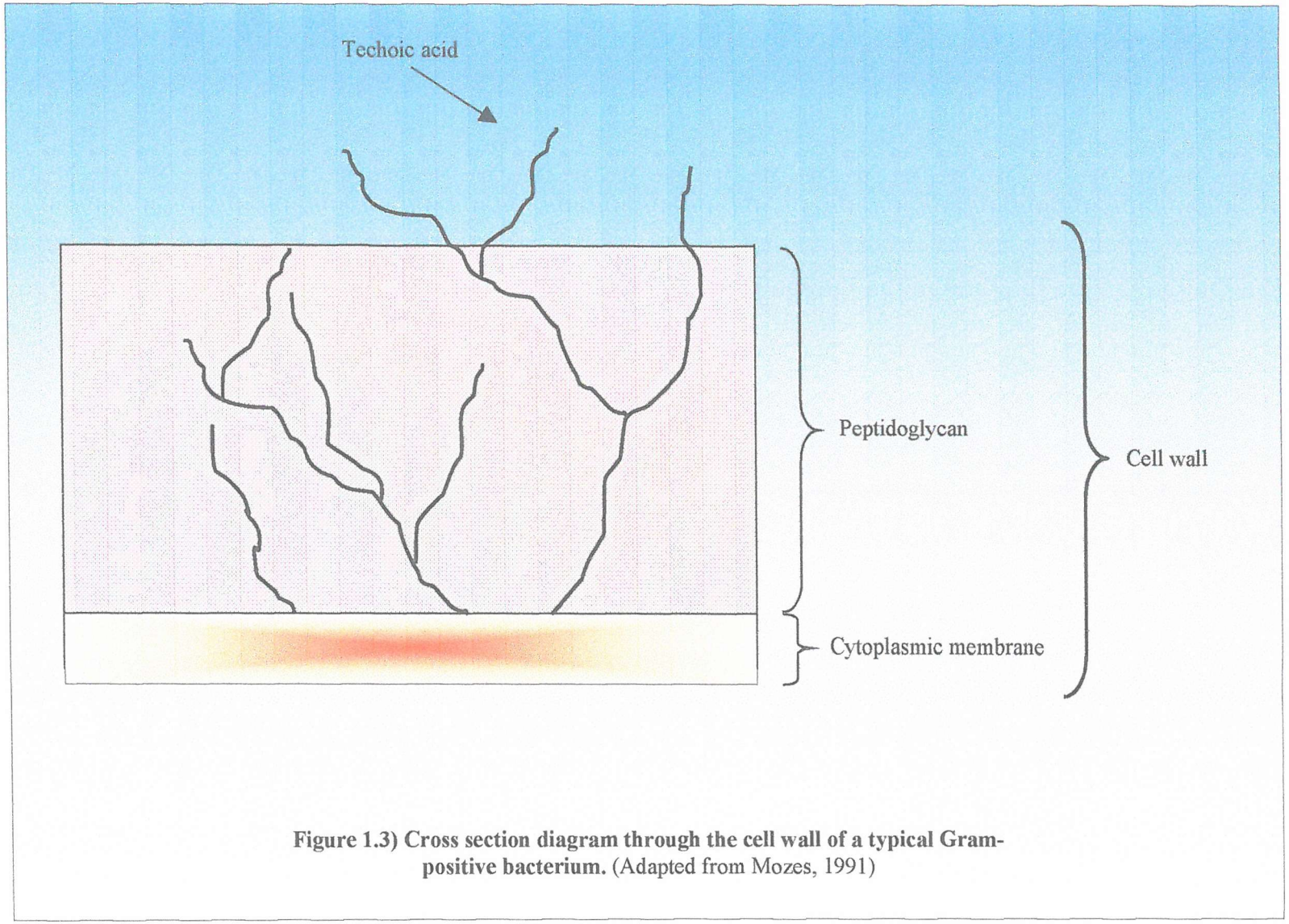

Figure 1.3) Cross section diagram through the cell wall of a typical Gram-positive bacterium. (Adapted from Mozes, 1991)

In most bacteria, growth involves an increase in cell mass and the number of ribosomes, duplication of the bacterial chromosome, synthesis of new cell wall and plasma membrane, partitioning of the two chromosomes, septum formation, and cell division. This asexual process of reproduction is called binary fission. The prokaryotic chromosome is a single DNA molecule that first replicates, and then attaches each copy to a different part of the cell membrane. When the cell begins to pull apart, the replicated and original chromosomes are separated. Following cell splitting (cytokinesis), there are then two cells of identical genetic composition (except for the rare chance of a spontaneous mutation).

In addition to binary fission, some prokaryotes undergo a form of sexual reproduction termed conjugation, seen in bacteria, ciliate protozoa and certain fungi, in which nuclear material is exchanged during the temporary fusion of two cells (conjugants). In bacterial genetics, a donor bacterium (male) contributes some or all of its DNA (in the form of a replicated set) to a recipient (female). The 'female' then incorporates this genetic information into its own chromosome by recombination and then passes the recombined set on to its progeny by replication.

The ability of bacteria to divide and increase in number can be easily demonstrated by plotting a growth curve (*Figure* 1.4, *Page* 7). The bacteria are cultured in sterile nutrient medium and incubated at the optimum temperature for growth. Samples are removed at intervals and the number of viable bacteria are counted. A logarithmic growth curve is plotted, which shows various phases. In the lag (or latent) phase, there is only a small increase in numbers as the bacteria adjust to the new conditions, imbibe water, and synthesize ribosomal RNA and enzymes. The length of this phase depends on the medium used to culture the bacteria before the investigation and which phase the cells were already in.

As the time taken for a cell population to double in numbers or generation time decreases, they enter the log or exponential phase, in which the cells reach a maximum

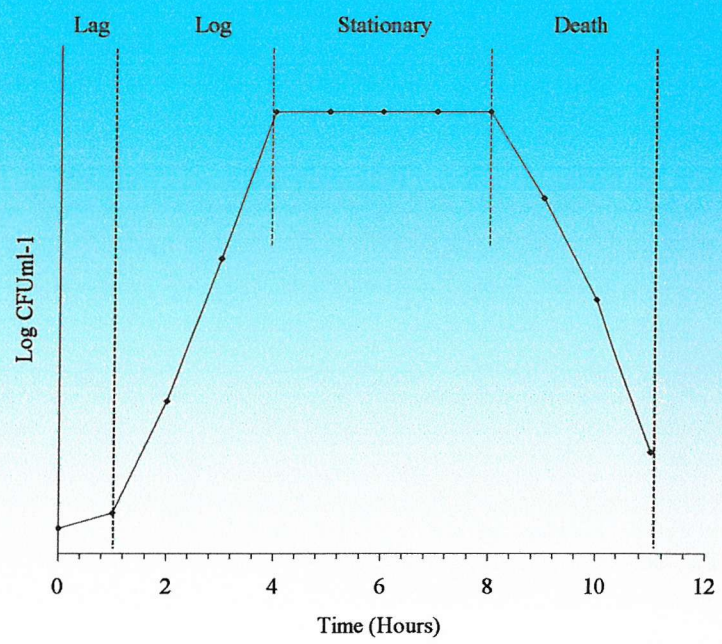

Figure 1.4) Schematic of a Bacterial Growth Curve.

(Adapted from Mann, 1996)

rate of reproduction and the number of bacteria increases directly with time, giving a straight slope on a logarithmic scale. For example, the fastest generation time for *Escherichia coli* (*E.coli*) is 21 minutes. Growth rate can be estimated in this phase. With time, as the population grows, it enters the stationary phase, when the nutrients and electron acceptors are depleted and the pH drops as carbon dioxide and other waste poisons accumulate. As the cell's energy stores are depleted the rate of cell division decreases. The death (or final) phase occurs when the rate at which the bacteria die exceeds the rate at which they are produced. The population declines as the levels of nutrients fall and toxin levels increase.

The archetypal Gram-negative species is *E.coli*. This organism colonizes the gastro intestinal (GI) tract of most warm-blooded animals within hours or a few days after birth. The bacterium is ingested in foods or water, or obtained directly from other individuals handling the infant. The human bowel is usually colonized within 40 hours of birth, with *E.coli* adhering to the mucus overlying the large intestine. Once established,

an *E.coli* strain may persist for months or years. *E.coli* is the head of the large bacterial family, *Enterobacteriaceae* (the enteric bacteria), which are facultatively anaerobic (the bacterium can grow in the presence or absence of O_2) Gram-negative rods. They live in the intestinal tracts of animals in good health and disease, and under aerobic conditions produce characteristic "mixed acids and gas" as end products. For *E.coli,* anaerobic respiration is possible as it is able to utilize NO_3 (nitrate) or NO_2 (nitrite) as the final electron acceptors for respiratory electron transport processes. In part, this adapts *E.coli* to its intestinal (anaerobic) and its extraintestinal (aerobic or anaerobic) habitats (Lederberg, 2000).

E.coli is a consistent inhabitant of the human intestinal tract, and it is the predominant facultative organism found there; however, it makes up a very small proportion of the total bacterial content. The anaerobic bacterial species in the bowel outnumber *E.coli* by at least 20:1. However, the regular presence of *E.coli* in the human intestine and faeces has led to tracking the bacterium in nature, as an indicator of faecal pollution. As such, it is taken to mean that, wherever *E.coli* is found, there may be faecal contamination (White, 1995).

Another common genus of gram-negative bacteria is *Pseudomonas*. They are rod shaped, mostly aerobic and motile, possessing one or more polar flagella. A distinctive trait is the ability of several species to produce characteristic water-soluble fluorescent pigments. They are found in soil and water. One particular species, *Pseudomonas veronii* (*P.veronii*) is predominantly found in water. A genetically modified strain designated *P.veronii* – Bio, has been generated to include the gene for luciferase (see Kerr *et al*, 2000). The addition of this enzyme has allowed the viability of this bacterium to be determined through light output, as luminescence has been shown to correlate with viability via the following reaction:

Reduced flavin mononucleotide + Nonanal (Aldehyde) + Oxygen

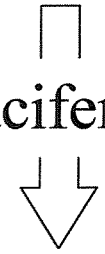

Oxidised flavin mononucleotide + nonanoic acid + water + Light

The bioluminescent capability of this bacterium allows tests to be conducted where conventional methods of determining viability are not appropriate or possible, such as investigations involving biofilms or the effects of starvation on bacteria.

Staphylococci are non-motile, Gram-positive spherical bacteria that occur in microscopic clusters. They are facultative anaerobes that grow by aerobic respiration or by fermentation that yields principally lactic acid. Bacteriological culture of the nose and skin of normal humans invariably yields *staphylococci*. They are perfectly spherical cells, about 1μm in diameter and grow in clusters due to division in two planes. *Staphylococcus aureus* (*S.aureus*) causes a variety of pyogenic (pus-forming) infections and toxinoses in humans. It causes superficial skin lesions such as boils and styes. More serious infections include pneumonia, mastitis, meningitis, and urinary tract infections; and deep-seated infections, such as osteomyelitis and endocarditis. *S.aureus* is a major cause of hospital acquired (nosocomial) infection of surgical wounds and infections associated with indwelling medical devices. *S.aureus* additionally causes food poisoning by releasing enterotoxins into food, and toxic shock syndrome by release of pyrogenic exotoxins into the blood stream (Lederberg, 2000).

1.2) Bacterial Pathogenicity and Antibiotics

One of the major characteristics of some micro-organisms is their ability to cause disease in humans, animals and plants, and infectious disease is one of the primary reasons why the development of microbiological science has taken place. Diseases in

plants and animals are also of great importance from the human perspective as we are extremely dependent upon these organisms to satisfy our food requirements.

Until the relatively recent development of vaccines and antibiotics, human societies have been beset by acute epidemic infectious diseases, caused by planktonic cells of such specialised pathogens as *Vibrio cholerae* and *Yersinia pestis*. However, more than half of the infectious diseases that affect mildly immuno-compromised individuals involve bacterial species that are either commensal with the human body or are common in our environments. For example, the skin bacterium *Staphylococcus epidermidis* and the aquatic bacterium *Pseudomonas aeruginosa* can cause devastating chronic infections in compromised hosts (Levy, 1998).

Bacteria are amongst the most successful living organisms on the planet and their ubiquity ensures that humans are obliged to live in constant and intimate contact with a wide variety of species. Although the number of species capable of causing disease is relatively few, many others have the ability to do so given the right conditions (Setti and Micetich, 1998). Infection can either be prevented through disinfecting processes, such as administration of antiseptics, disinfectants and preservatives to our immediate environment, or treated through antibiotic administration. Of the two, prevention is therapeutically the best option, although not necessarily possible for all situations.

Microbial pathogenicity has been defined as the structural and biochemical mechanisms whereby micro-organisms cause disease. Pathogenicity in bacteria may be associated with unique structural components of the cells (e.g. capsules, LPS or other cell wall components) or active secretion of substances that either damage host tissues or protect the bacteria against host defences. Infection may imply colonization, multiplication, invasion or persistence of a pathogen on or within a host, but infectious disease is used to describe an infection that causes significant overt damage to the host. There are two broad qualities of pathogenic bacteria that underlie the means by which they cause disease: invasiveness and toxigenesis. Invasiveness is the ability to invade tissues. This

encompasses mechanisms for colonization (adherence and initial multiplication), ability to bypass or overcome host defence mechanisms, and the production of extracellular substances that facilitate the actual invasive process. Toxigenesis is the ability to produce toxins. Toxic substances, both soluble and cell-associated, may be transported by blood and lymph and cause cytotoxic effects at tissue sites remote from the original point of invasion or growth (Volk, 1996).

Toxigenesis is an underlying mechanism by which many bacterial pathogens produce disease. At a chemical level, there are two types of bacterial toxins, LPS, associated with Gram-negative bacteria including *E.coli*, *Salmonella*, *Shigella*, *Pseudomonas*, *Neisseria* and *Haemophilus*, and proteins, which are released from bacterial cells and may act at tissue sites far removed from the site of bacterial growth. The cell-associated LPS toxins are referred to as endotoxins and the extracellular diffusible proteins are referred to as exotoxins (Mann, 1996).

The biological activity of endotoxin is associated with the lipid component (Lipid A) and immunogenicity is associated with the polysaccharide components of LPS. Endotoxin elicits a variety of inflammatory responses in an animal due to its activation of complement by the alternative pathway, which is often part of the pathology of Gram-negative bacterial infections. Compared to the classic exotoxins of bacteria, endotoxins are less potent and less specific in their action, as they do not act enzymatically.

Exotoxins are typically soluble proteins secreted by living bacteria during exponential growth. The production of the toxin is generally specific to a particular bacterial species that produces the disease associated with the toxin (e.g. only *Clostridium tetani* produces tetanus toxin; only *Corynebacterium diphtheriae* produces the diphtheria toxin). Usually, virulent strains of the bacterium produce the toxin while non-virulent strains do not, and the toxin is the major determinant of virulence. At one time it was thought that exotoxin production was limited mainly to Gram-positive bacteria, but now

it has been shown that both Gram-negative bacteria additionally produce soluble protein toxins (Volk, 1996).

Certain protein toxins have very specific cytotoxic activity (i.e., they attack specific types of cells). For example, tetanus or botulinum toxins attack only neurons. But some toxins (as produced by *staphylococci*, *streptococci*, *clostridia*, etc.) have fairly broad cytotoxic activity and cause non-specific death of all sorts of cells and tissues, eventually resulting in necrosis. Toxins that are phospholipases act in this way. They cleave phospholipids that are regular components of host cell membranes, resulting in the death of the cell by leakage of cellular contents.

The discovery of the first antibiotic, penicillin, by Alexander Flemming in 1928, represents one of the greatest medical advances in recent history, and the turning point for reversing the inevitable mortality that bacterial infection once brought. Flemming could not have imagined that his chance observation of a contaminant mould inducing bacterial lysis would have dramatic, worldwide implications. By 1943, drug companies were mass-producing penicillin and its application revolutionised our ability to combat pathogenic bacteria (Tan *et al*, 2000).

Antibiotics are low-molecular weight substances that are produced as secondary metabolites by certain groups of micro-organisms, especially *Streptomyces*, *Bacillus*, and a few moulds that are inhabitants of soils (*Penicillium* and *Cephalosporium*). Antibiotics may have a cidal (killing) effect, or a static (inhibitory) effect on a range of microbes. The range of bacteria or other micro-organisms that are affected by a certain antibiotic is expressed as its spectrum of action. Antibiotics effective against prokaryotes, which kill or inhibit a wide range of Gram-positive and Gram-negative bacteria are said to be broad spectrum. If effective mainly against Gram-positive or Gram-negative bacteria, they are narrow spectrum. If effective against a single organism or disease, they are referred to as limited spectrum (Rang *et al*, 1998)

Antibiotics exert selective toxicity towards microbial cells by targeting the cellular differences that exist between prokaryotes and eukaryotes. Differences that include the,

- Cell wall:

  As previously described, peptidoglycan is vital to the integrity of the cell wall. If the biosynthesis of peptidoglycan is inhibited by antibiotic action then the integrity of the bacterial cell fails, leading to eventual lysis and death. A classic compound that interferes with peptidoglycan synthesis is Vancomycin. Hydrophilic components manufactured within the cell, destined for the peptidoglycan cell wall are carried through the hydrophobic cell membrane attached to a large lipid carrier (C_{55}). Vancomycin prevents the release of the peptidoglycan pre-cursor from the C_{55} lipid carrier molecule. This type of antibiotic is bactericidal.

- Protein synthesis:

  Inhibiting protein synthesis has also proved to be very effective as an antibiotic mechanism. Although the basic components to protein synthesis are the same for both eukaryotes and prokaryotes, there are important differences in ribosome structure, namely the size of the sub units. Bacterial ribosomes are smaller with a sedimentation coefficient value of 70 Svedberg units, incorporating two subunits of size 50S and 30S. In contrast, the eukaryotic ribosome is 80S with sub units of 60s and 40S. Selectivity of the antibiotic occurs via binding to the 50S or 30S sub units of the bacterial ribosome. Consequently, some of these compounds can be taken in high quantities without undue toxicity to humans. Streptomycin binds to the 30S subunit, producing a change in codon – anticodon recognition, which results in miscoding of bacterial proteins. This type of antibiotic is bactericidal.

- Anti-metabolites:

  The synthesis of folate is an example of a metabolic pathway found in bacteria but not in humans. Folate is necessary for the production of DNA in both bacteria and man. However, man has a mechanism for taking up folate into the cells from a dietary intake. In contrast, bacteria must manufacture their own folate using the enzyme dihydropteroate synthetase i.e. they have no mechanism to take it up. Sulphonamides such as sulphadiazine competitively inhibit this enzyme, as they are

structural analogues of para - aminobenzoic acid, the precursor for folic acid. This type of antibiotic is bacteriostatic.

- Nucleic acid synthesis:

The DNA helix is twisted itself, resulting in supercoiling. Initiation of DNA synthesis requires the local unwinding of the supercoil and the introduction of a negative supercoil. The enzyme responsible for this is DNA gyrase or topoisomerase II. The unwound coil is used as a template for DNA synthesis. Nalidixic acid inhibits DNA gyrase and is used in urinary tract infections with Gram-negative organisms (Mann, 1996).

1.3) Bacterial Resistance to Antimicrobial Agents

With the widespread application of penicillin, particularly during the Second World War, it was only a matter of time before selective environmental pressure induced survival of the most resistant bacterial strains.

"*If the collective bacterial flora in a community possesses genes that confer resistance to a given antibiotic, and the community continues to use the drug persistently, bacteria able to defy eradication will emerge and multiply*" (Levy, 1998).

In fact, as early as 1947, a bacterial enzyme capable of neutralising penicillin was described and later designated beta-lactamase (Frère, 1995). However, these early lessons were ignored and continued overuse of antibiotics in humans, animals and the plant industry, have been the major factor in the development of multi-drug resistant strains, such as the notorious methicillin-resistant *Staphylococcus aureus* (MRSA).

The prevalence of resistant bacteria has arisen as a consequence of mutational events and/or the acquisition of resistant genes, followed by a selection process. Cellular mechanisms exist to ensure that DNA replication is error-free, however, mistakes do occur. As each mutation confers only a slight alteration in susceptibility, bacteria need to accumulate several mutations to become intrinsically resistant to antibiotics. Once

created, genes that confer resistance can be integrated into the bacterial chromosome to be inherited from one generation to the next, or maintained within an extra-chromosomal plasmid. Once stored on plasmids, resistance-conferring genes can be easily transferred to other bacteria by conjugation or transduction (Tan *et al*, 2000).

From the first reported outbreaks of bacterial resistance, international groups have tracked the progress of multi-drug-resistant strains, including the Centre for Disease Control and Prevention (CDC) in Atlanta, USA, and the Public Health Laboratory Service Communicable Disease Surveillance Centre (CDSC) in the United Kingdom. As early as 1968, 12,500 people in Guatemala died in an epidemic of *Shigella* diarrhoea due to the responsible micro-organism possessing a plasmid that endowed resistance to four different antibiotics (Davies, 1996). More recently, data supplied by the CDSC have shown that in 1994, some 2% of all cases involving infection by *Staphylococcal* bacterium in England and Wales were caused by MRSA. Four years later this figure had increased to 30% (Tan *et al*, 2000).

The development of resistant strains has been met with alternative antibiotics and combination therapy, but continued use has created strains of bacteria resistant to nearly all. Even glycopeptide antibiotics such as vancomycin, the drug of last resort, are no longer effective against some strains. In fact, vancomycin resistant *Enterococcus* species emerged in the late 1980s and then in 1997 the inevitable happened, the first report of the clinician's nemesis, vancomycin-resistant *Staphylococcus aureus* (Levy, 1998). In response to this, there has been an international call for the application of antibiotic rotational schemes to conquer the problem of resistance. By implementing this strategy, there is a high probability that in the absence of an antibiotic, bacteria will disregard genes that confer resistance, therefore rendering them vulnerable to the antibiotic on its reintroduction (Roccanova and Rappa, 2000).

However, until such programmes are introduced, diseases once conquered in western society are continuing to re-emerge with devastating consequences. The bacterium

Mycobacterium tuberculosis, responsible for Tuberculosis and killing millions during the nineteenth and early twentieth century has returned as a multi-drug resistant strain (Handal and Olsen, 2000). As antibiotic administration continues, an increasing number of micro-organisms that were previously arrested in the past are returning in mutated forms, and the death rates for communicable diseases such as Tuberculosis rise every year in Western countries (Slavkin, 1997).

Apart from the discovery and exploitation of the natural peptide anti-microbial agents that form part of the innate immune systems of plants and animals, there have been few antibiotics developed in recent years (Tan *et al*, 2000). In addition, there is the alarming onset of resistance to biocides such as antiseptics, disinfectants and preservatives (Russell, 1998). The most resistant types of micro-organisms to disinfectants are believed to be the prions followed by coccidian with bacterial spores and mycobacterium being the most resistant types of bacteria (McDonald and Russell, 1999). Gram-negative bacteria are generally more resistant than Gram-positive cocci such as *staphylococci* and *enterococci* (Russell, 1998). With this in mind there will be a continued requirement for new and potent anti-microbial agents, together with techniques suitable for the control and destruction of bacteria.

1.4) Bacteria and biocide tolerance

Strategies to control infection additionally include the use of biocides in the form of antiseptics and disinfectants. Biocide is a general term to describe a chemical agent that inactivates micro-organisms. Since the first use of chlorinated lime hand wash by Dr. Ignaz Semmelweiss 150 years ago, these agents have become indispensable in infection control programmes. Today, a wide variety of biocides are found in a large number of hospital and personal care products. Some biocides may be applied topically and are then generally referred to as antiseptics. Disinfectants are biocides that are used on inanimate objects. An increasing apprehension of microbial contamination of everyday living environments has lead to an increased use of antiseptics and disinfectants both inside and outside of health care settings. Biocides have been incorporated into such

diverse items as surgical scrubs, surface disinfectants, laundry soaps, hand washes, cosmetics, toothpastes, cutting boards and even toys (White and McDermott, 2001).

By their very nature, biocides are too toxic to be used internally. Biocides tend to have a broader spectrum of activity than antibiotics. This does not however, necessarily reflect a lack of target specificity. Mechanistic understanding of biocide action is at present poor, the common view being that cellular effects occur by gross membrane damage, protein coagulation, or by cytoplasmic 'poisoning'. In fact, some believe that there is a common series of events starting with interactions of the biocide with the cell surface, followed by penetration into the cell and interaction with multiple targets within the cell (Russell, 1997).

The concept of drug resistance, as applied to antibiotics in clinical settings cannot be applied to biocides. The multi-target nature of many biocides means that mutation within a single target is unlikely to result in treatment failure. Furthermore, toxicity problems associated with high-level antibiotic therapy do not generally apply to biocides. As with antibiotics, alterations in biocide sensitivity may be acquired, but these are more frequently related to intrinsic properties of the organism, because of spontaneous mutation or adaptation. Non-susceptibility may occur in bacteria due to the nature of the outer cell layers, resulting in exclusion of the agent (Russell and Russell, 1995). Biocides initially interact with bacteria at the cell surface, where intrinsic resistance is largely a function of the chemical composition and structure of the cell surface. For example, Gram-positive bacteria are generally more susceptible to biocide action than are Gram-negative bacteria, due to the absence of an outer membrane, which restricts entry of many types of chemical agents including antibacterials (Nikaido, 1994). Resistance due to physiological specifications can occur in bacterial spores and in biofilms (Brown and Gilbert, 1993).

A major mechanism of acquired biocide resistance relates to alterations in drug access. Reduction in cell surface permeability, via the loss of porin proteins through gene

deletion may facilitate reduced biocide susceptibility. Heir *et al* (1995) showed that a single amino acid modification in a membrane permease protein of *staphylococci* caused insensitivity to quaternary ammonium compounds. Biocides can be actively secreted by efflux pumps, such as the mechanism that occurs in metal resistant micro-organisms isolated from polluted environments (Neis and Silver, 1995). Insensitivity can also result from enzymic or chemical inactivation of the agent. For example, hydrogen peroxide may be inactivated by microbially synthesised catalase or peroxidase (Fiorenza and Ward, 1997).

As with chemotherapeutic antimicrobials, resistance to biocides can occur via target mutation or acquisition of foreign genes residing on plasmids. Plasmid mediated biocide resistance was initially described in *P.aeruginosa* (Sondossi *et al*, 1985). Since then, numerous reports have described plasmid-mediated resistance or increased tolerance to numerous biocides. Plasmid encoded resistance to antiseptics and disinfectants have also been reported in members of the *Enterobacteriaceae* family and *S.aureus* (Leelaporn *et al*, 1994).

Recent evidence has suggested a link between the use of biocides and the emergence of antibiotic resistance although a relationship has not been conclusively demonstrated one way or the other. There are similarities between antibiotic and biocide resistance, and Gram-negative bacteria that have developed resistance to biocides may also be insusceptible to some antibiotics, possibly as a result of outer membrane modifications (Russell, 2000).

1.5) Bacteria and Starvation-Induced Resistance

During periods of nutrient availability bacterial growth is rapid. However, in their natural environment nutrient deficiency is more widespread. Starvation survival has been defined as the physiological state resulting from an insufficient amount of nutrients, for the growth (increase in size) and multiplication of micro-organisms

(Morita, 1982). In the majority of cases, the restriction of growth is due to the absence of a carbon source.

As expected, the generation time for bacterial populations in natural conditions are considerably longer than those created under laboratory conditions. The mean generation time of bacteria in nature are 210 days in deep sea water, 20 days in deciduous woodland soil and 5-20 hours for *Salmonella* species and pathogenic strains of *E.coli* in host tissues (Matin *et al*, 1989). Bacterial populations use nutrients efficiently to generate rapid increases in biomass, however, this in turn means that they are nutritionally starved most of the time. Nevertheless, these organisms can survive for extremely long periods in the absence of nutrients (Kolter *et al*, 1993).

Bacterial evolution has seen the development of systems to counteract the effects of environmental stress, whether that be heat, oxidative or starvation. These systems can be divided into two classes. The first class comprises specific systems, which are induced by sub lethal doses of a chemical or physical stress, and permit survival against a challenge dose of the same agent. However, some cross protection to non-homologous stresses may occur. The second class comprises more general systems, which prepare cells to survive towards very different environmental stresses, without the need for prior exposure to them. These general systems are induced in stationary phase, under starvation conditions or sometimes also in hyperosmotic environments (Pichereau, *et al*, 2000). With regards to the two systems, the resistance produced by starvation is even more protective than preadaptation of growing cells (Siegele and Kolter, 1992).

During normal exponential growth, bacterial cells undergo cycles of cell growth and division in which daughter cells are identical to the mother cell. In order to ensure their survival, bacteria should be able to make an orderly transition when starved, such that the cell cycle is not arrested randomly. The sudden arrest of growth in response to starvation could halt key metabolic processes, in particular DNA replication, at stages

at which severe and irreparable damage could occur. In addition, bacteria must be able to remain viable during long periods of starvation and return to the exponential growth when starvation is relieved (Kolter *et al*, 1993). Many bacteria have evolved highly sophisticated mechanisms that allow them to maintain cell viability during starvation and resume growth rapidly when nutrients again become available.

Some bacteria, such as *Bacillus* species or *Clostridium* species, undergo major differentiation programmes, leading to the formation of highly resistant spores. In contrast members of bacterial genera such as *Escherichia*, *Salmonella* and *Vibrio* do not generate differentiated cells as a result of starvation. However, while it is evident that certain species do not form classical spores, starvation does induce a programme that results in a metabolically less active and more resistant state, which confer on the cells some properties of classical spores (Pichereau *et al*, 2000).

In response to starvation, the non-differentiating bacteria undergo a concerted, rapid change in the pattern of gene expression. The metabolic reprogramming leads to a cellular state of enhanced resistance to a great number of stress conditions. Carbon starved *E.coli* are more resistant to heat shock, oxidative stress and osmotic challenge than exponential phase cells (Jenkins *et al*, 1990; Jenkins *et al*, 1988). *Escherichia faecalis* cells starved of glucose develop strong cross protection against such diverse treatments as heat, ethanol, acid, osmotic, oxidative or bile salt stresses. Under complete starvation established by incubation in tap water, *E.faecalis* cells become more resistant to the heat, acid and sodium hypochlorite stresses in addition to UV irradiation (Hartke *et al*, 1998).

As bacterial cells become starved their overall metabolic rate decreases, but some level of endogenous metabolism is maintained. This allows the starved cells to maintain some level of adenosine triphosphate (ATP) and the proton motive force across the membrane. One function of endogenous metabolism is to maintain the ability to transport substrates into the cell. If this ability is compromised, the starved cell will be

unable to resume growth when nutrients become available in the surrounding environment. Several adjustments are made in order to maintain some level of endogenous metabolism. For example, although the rate of total protein synthesis decreases under nutrient limitation conditions, the synthesis of specific starvation induced proteins is important to protect the cells against deprivation (Giard *et al*, 1996). The starved cell synthesises 30 to 50 proteins involved in maintaining viability during prolonged starvation. They also synthesize proteins needed for the cells to recover from starvation and resume growth when nutrients become available. The existence of such proteins is demonstrated by observations that blocking protein synthesis at the same time that cells are starved leads to decreased viability (Siegele and Kolter, 1992). In rapidly growing *E.coli* cells, the bulk of the nucleic acid is stable. However, RNA stability decreases when cells enter a starved state and 20% to 40% of total RNA is lost during the first several hours of starvation. Unlike protein and RNA, DNA remains stable in most bacteria, even during prolonged starvation (Siegele and Kolter, 1992).

Examination of starved cells using light microscopy reveals distinct differences in cell morphology compared to actively growing cells. *E.coli* cells become much smaller and almost spherical when they enter a starvation state. These changes in cell size and shape are accompanied by changes in the sub cellular compartments, the cytoplasm is condensed and the volume of the periplasm increases (Lange and Henggearonis, 1991). In addition, lipid, DNA and RNA contents are diminished during the transition from growth to non-growth. The reduction in cell volume is even more apparent in marine bacteria, which greatly decrease in size during starvation and form what are termed ultramicrocells, as small as $0.03\mu m^3$ (Kjelleberg *et al*, 1987). Ultramicrocells result from cells that undergo several cell divisions without an increase in biomass and then further decrease in their size as a result of endogenous metabolism. However, not all bacteria alter their morphology. The Gram-positive bacterium *Staphylococcus faecalis* does not significantly shrink during glucose starvation or incubation in an oligotrophic environment (Hartke *et al*, 1998).

The surface properties of starved cells are also different from those of growing cells. The surface of many marine bacteria becomes increasingly hydrophobic and the cells become more adhesive during starvation. Changes in the fatty acid composition of the cell membranes have been seen during starvation of several species, including *E.coli* and certain *Vibrio* species. (Kjelleberg *et al*, 1987). The cell wall synthesised during amino acid starvation has a different structure from the cell wall synthesised during growth. Structural changes that appear to protect bacterial cells from the lytic effects of penicillin (Nystrom and Kjelleberg, 1989).

Part of the initial response to starvation for a particular nutrient, such as carbon, nitrogen, or phosphate, is to induce the expression of a group of genes whose functions are designed to help the cell cope with that particular starvation stress. Each of these systems appears to function via a sensor component that monitors the availability of a specific nutrient, either directly or indirectly. A decrease in the level of the nutrient results in the activation of a transcriptional regulator that turns on expression of the genes in that regulon. When even the induction of these regulons is not sufficient to secure enough of the limiting nutrient, growth ceases and the cells enter the starvation state (Siegele and Kolter, 1992).

A variety of unusual nucleotides have been suggested as possible factors in cellular responses to nutrient deprivation. One of the best understood is the nucleotide guanosine 3-5-biophosphate (ppGpp). When rapidly growing *E.coli* cells are subjected to starvation, a panalopy of metabolic and physiological changes occur that constitute an adaptational response to the altered extracellular conditions. An important conservational aspect of this response is the rapid curtailment of rRNA and tRNA synthesis, leading to the lower rates of ribosome formation and eventually, protein synthesis. This adaptational response is termed the stringent response and is mediated through the production of ppGpp (*Figure* 1.5, *Page* 23). Although the knowledge on stringent response and ppGpp production centres around *E.coli*, recent evidence has shown the presence of similar pathways in other organisms, including *Staphylococci* species, *Streptococci* species and *Bacillus subtilis* (Mukherjee, *et al* 1998).

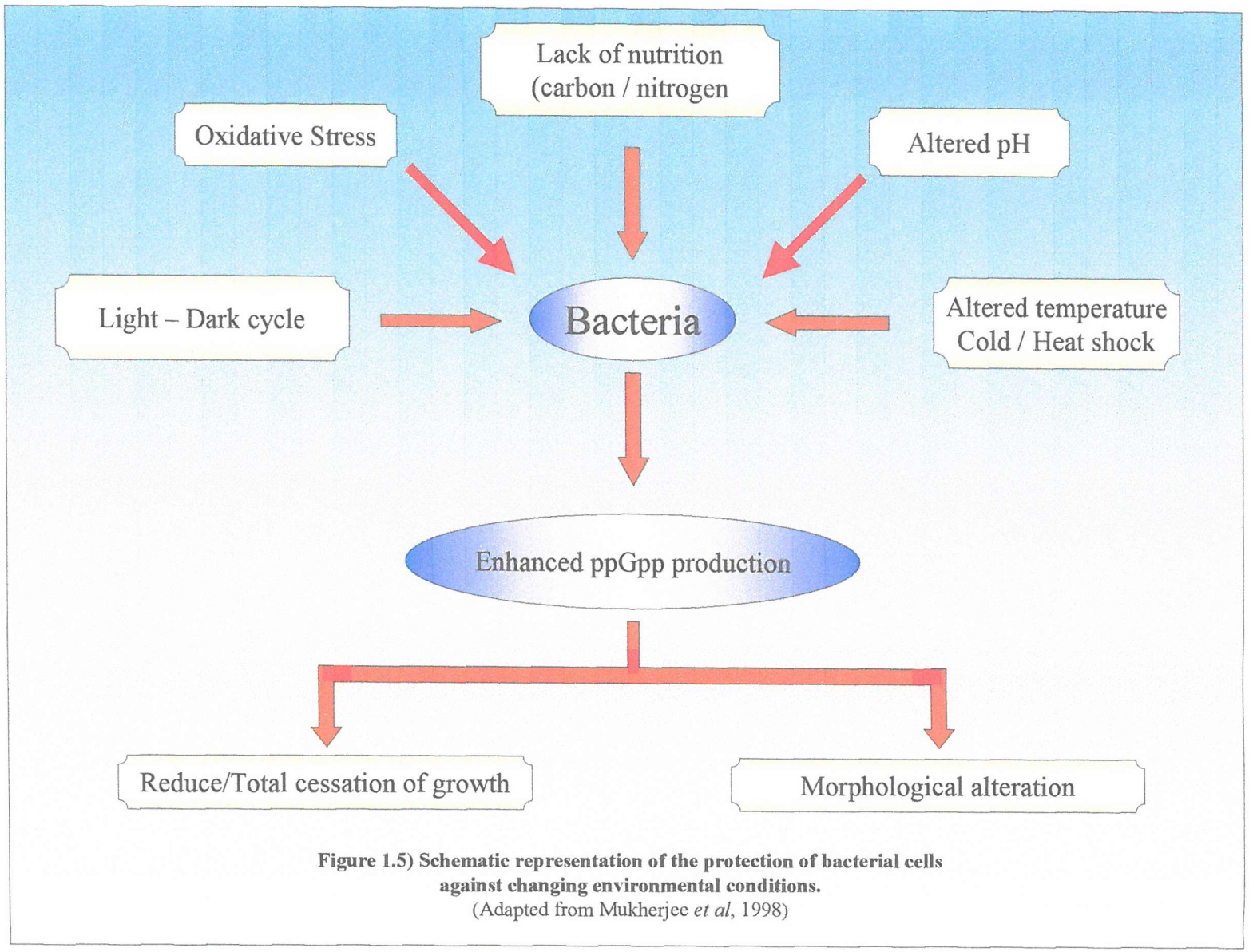

Figure 1.5) Schematic representation of the protection of bacterial cells against changing environmental conditions.
(Adapted from Mukherjee *et al*, 1998)

Thus, ppGpp seems to serve as an emergency break to stop production of protein synthesising machinery, when substrates for protein synthesis are in short supply. However, basal level synthesis of ppGpp is always necessary for the fine control of growth rate. Conservation of energy by fine-tuning of growth rate and protection of cells from changing environmental conditions are the two main features for stringent response. The production and maintenance of ppGpp under stress conditions are controlled by the genes *relA* and *spoT*, which code for two ppGpp synthetases, PSI and PSII respectively. There is a strong homology between the two enzymes produced by these two genes from different species. Some recent observations indicate that ppGpp may have a wide variety of functions in bacterial growth apart from ribosome synthesis or growth rate control. It is involved in a variety of biological functions including peptidoglycan synthesis, control of cell cycle, antibiotic production and DNA replication (Mukherjee, *et al* 1998).

1.6) Bacterial Biofilms

Issues concerning the targeting of bacteria in the natural world have been redefined and revolutionised by the fact that the majority of bacteria preferentially exist as biofilms. Micro-organisms exist in every part of our environment, and wherever they are found, they are growing attached to surfaces, enveloped within an extracellular matrix.

Biofilms have been defined in a number of ways by various researchers, constructed to be inclusive of the many environments in which biofilms are found and disciplines that the subject covers. The initial definition of a biofilm consisted of micro-organisms and extracellular substances in association with a substratum (Reid *et al*, 1995). Costerton *et al* (1995) supplied a definition of biofilms as matrix-enclosed bacterial populations, adherent to each other and/or surfaces or interfaces. Palmer and White (1997) tried to be more comprehensive and defined a biofilm as a collection of micro-organisms (including cells in culture) and their associated extracellular products at an interface, and generally attached to a biological (other cells or tissues) or abiological (mineral or synthetic) substratum.

Biofilms can be considered as microbial ecosystems representing different microbial strains and species in aggregation, which efficiently co-ordinate and co-operate to protect themselves against environmental stresses, and facilitate the nutrient uptake for survival (Sihorkar and Vyas, 2001). Biofilms constitute a protected mode of growth that allows survival in a hostile environment. The structures that form in biofilms contain channels in which nutrients can circulate, and cells in different regions of a biofilm exhibit different patterns of gene expression. The complexity of biofilm structure and metabolism has lead to the analogy of biofilms to tissues of higher organisms (Costerton *et al*, 1999).

Although many bacteria can grow in a free-living 'planktonic' state, it is quite common for them to adhere to surfaces by producing extracellular polysaccharide or in some cases, by means of specialised structures termed holdfasts. The adherent bacteria produce micro-colonies, leading to the development of biofilms, which initially may be composed of only one bacterial type, but frequently develop to contain several bacteria living in a complex community. In fact, almost every surface exposed to liquids and nutrients will be colonised. Biofilms develop preferentially on inert surfaces, or on dead tissue, and occur commonly on medical devices. They can also form on living tissue as in the case of endocarditis (Lambe *et al*, 1991).

Microbial biofilms can have positive outcomes such as a healthy intestine and the female genito-urinary tract. However, biofilms are predominantly associated with negative outcomes, such as pathogenic organisms infecting a patient with a medical implant or the biofilm on our teeth, leading to the development of cavities (dental caries) when bacteria such as *Streptococcus mutans* degrade sugars to organic acids (Habash and Reid, 1999). On most of the occasions where biofilms are a nuisance, the term microbial fouling or biofouling is generally implied. Biofouling refers to the undesirable formation of a layer of living micro-organisms and their decomposition products as deposits on the surfaces in contact with liquid media. In the dairy and food industry, biofouling causes serious problems, such as impeding the flow of heat across surfaces and

increases in the fluid frictional resistance at surfaces, leading to energy and production losses. In addition, biofilms that form on surfaces such as poultry offer considerable problems of cross and post-processing contamination (Kumar and Anand, 1998).

Before a biofilm can even form, adhesion of planktonic bacteria to a surface is required and for the majority of bacteria a conditioning film is essential. The role of the conditioning film cannot be underestimated in biofilm formation, as many bacteria do not have the mechanisms allowing them to adhere directly or strongly onto bare implant surfaces, with the exception of *Staphylococcus epidermidis* (Veenstra *et al*, 1996). Medical implants are a good example (*Figure* 1.6, *Page* 27). Prior to implantation a medical device is a clean, sterile surface, composed of various polymers termed biomaterials. Following implantation, bodily fluids, such as blood and saliva surround the implant forming a conditioning film. This film itself may not completely cover the entire implant surface but may form a mesh-like covering (Busscher *et al*, 1991). The creation of a conditioning film alters the surface characteristics of implants, such that bacteria can adhere more rapidly to the biomaterial surface (Reid *et al*, 1995).

With a conditioning film in place, the next stage in biofilm development is the approach and attachment of micro-organisms. The actual mechanisms of attachment to materials are still under investigation, although several theories have been proposed to explain the detailed interactions that occur as a microbe approaches and then attaches to a surface. One of the leading theories is the Derjaguin Landau Verwey and Overbeck (DLVO) theory of colloidal stability, involving the effects of hydrophobicity and surface charge (Habash and Reid, 1999).

The DLVO theory describes two boundaries, determined by the form of the potential energy function experienced by an organism as it approaches a surface. This will involve two terms; van der Waals' interactions that dominate at short distances, and electrostatic forces which act over longer length scales. The net result is two potential energy minima.

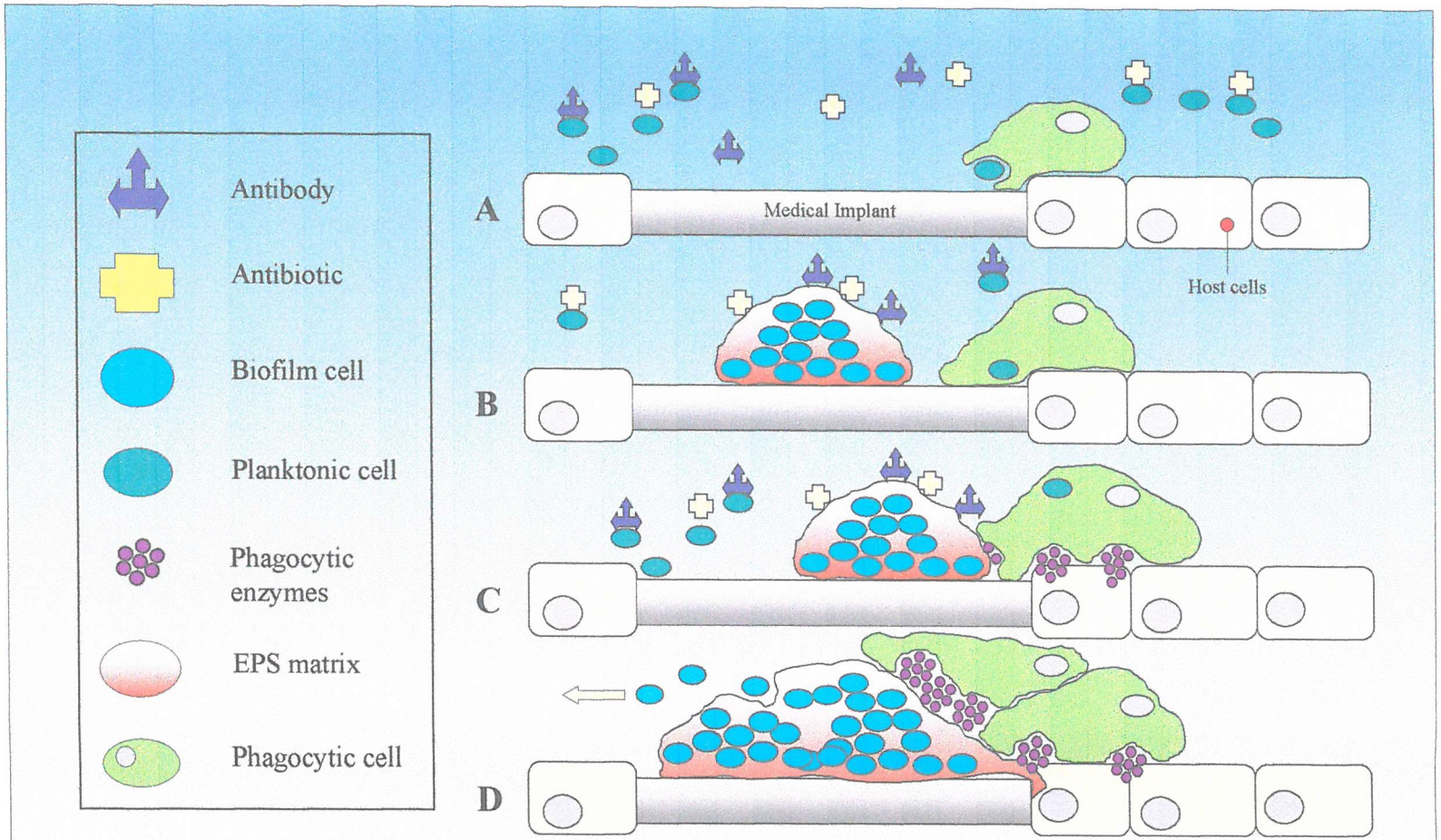

Figure 1.6) Diagram of a medical Biofilm. A) Planktonic bacteria can be cleared by antibodies and phagocytes. **B)** Adherent bacterial cells form biofilms preferentially on inert surfaces, and these sessile communities are resistant to antibiotics, antibodies and phagocytosis. **C)** Phagocytes are attracted to the biofilms. Phagocytosis is frustrated but phagocytic enzymes are released. **D)** Phagocytic enzymes damage tissue around the biofilm and planktonic bacteria are released from the biofilm. (Adapted from Costerton *et al*, 1999)

Numerous groups have shown the majority of bacterial membranes to possess a net negative charge provided by phosphate, carboxylate and less commonly sulphate groups in the cell wall and capsular molecules (James, 1991). To date, from a total of 156 strains studied, only two have demonstrated a positive charge at neutral pH, *Staphylococcus epidermidis* and *Streptococcus thermophilus* (Jucker *et al*, 1996). If and when a bacterium overcomes the barrier of electrostatic repulsion, at the boundary between the secondary and primary minima, it can approach closely to the surface where irreversible attachment can then take place (Vanloosdrecht *et al*, 1989).

At this stage, hydrophobic interactions are required to remove layers of water from between the bacteria and the solid surface for the microbe to be able to reach the surface. With the water molecules removed, the bacterium moves closer to the solid surface (<1.5nm), where a wide variety of short-range interactions can take place, directly attaching the bacterium to the solid surface. For a bacterium to attach strongly to a substratum, many types of interactions are required, as the sum of all types of adhesion interactions is far greater than any single one. The end result is an irreversibly bound bacterium (Busscher and Weerkamp, 1987).

Following initial attachment, bacteria can commence growth and colonisation to establish themselves firmly on a surface. A first step is the production of polysaccharides, which anchor the organisms to the surface. Both the growth rate of organisms on a surface and the strategies used by micro-organisms to spread over a surface are important for colonisation. These strategies are species specific, affecting the distribution of a biofilm on a surface, which can form patchy networks or contiguous films. Potential colonisation strategies include mother cells attaching to a surface and the release of daughter cells, which migrate to other locations and themselves become mother cells. Slow migration and spreading are other mechanisms by which cells grow on a surface and divide, and the daughter cells migrate prior to their division (Habash and Reid, 1999).

The final stage of microbial colonisation of a surface is the formation of a biofilm structure. At this point, the micro-organisms have created for themselves a microenvironment, protective against many antimicrobial agents and host immune defence mechanisms. The biofilm provides a buffer to changing environment conditions, easier access to nutrients via mass transfer, and elimination of metabolic wastes. It allows the formation of microbial consortia, creating a synergistic environment where the by-products from one type of organism can act as a substrate for another (Habash and Reid, 1999). A summary of biofilm development can be seen in *Figure* 1.7 (*Page* 30).

Bacterial infection can be a serious problem, particularly with regards to antibiotic resistance. However, of primary concern is the intrinsic resistance of biofilms to antimicrobial agents. They are reported to be anything between 50 and 1000 times less susceptible to antibiotics than their planktonic counterparts (McBain and Gilbert, 2001). When trying to kill micro-organisms, a biofilm is often the target, yet the way they grow makes them resistant. Electron micrographs of the surfaces of medical devices that have been the foci of device-related infections, show the presence of large numbers of slime encased bacteria. Tissues taken from non-device related chronic infections also show the presence of biofilm bacteria surrounded by an exopolysaccharide matrix. These biofilm infections may be caused by a single species or by a mixture of bacterial species or fungi (Costerton *et al*, 1999).

Sessile bacterial cells release antigens and stimulate the production of antibodies, but the antibodies are not effective in killing bacteria within biofilms and may cause immune complex damage to surrounding tissues. Even in individuals with excellent cellular and humeral immune reactions, biofilm infections are rarely resolved by the host defence mechanisms. Antibiotic therapy typically reverses the symptoms caused by planktonic cells released from the biofilm, but fails to kill the biofilm itself (Marrie *et al*, 1982).

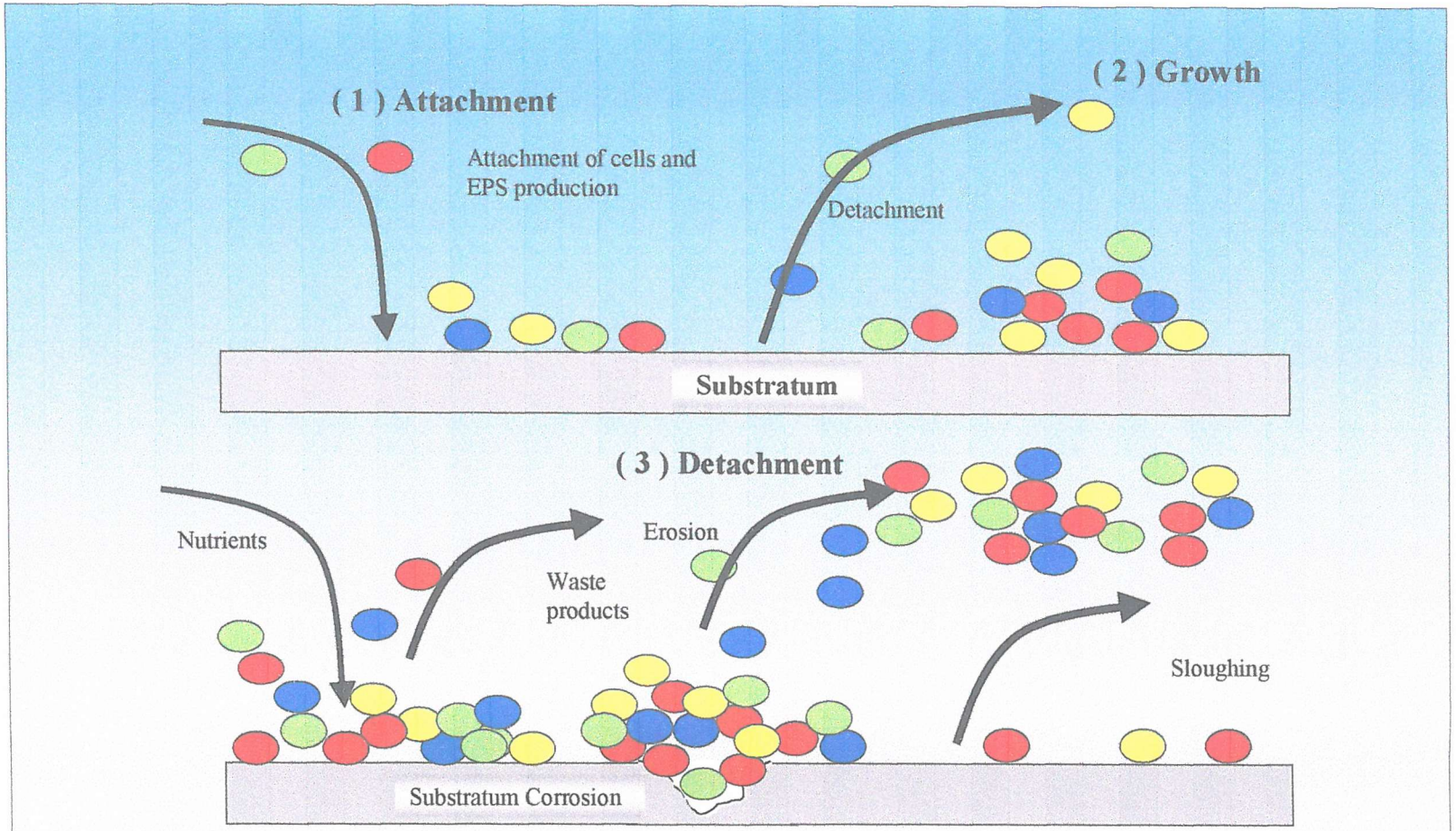

Figure 1.7) Biofilm Development condensed into three main stages.

The attachment of cells to a surface (1), cellular growth and production of exopolysaccharide matrix (2) and finally, detachment of individual cells and large pieces of biofilm (sloughing). (Adapted from Stoodley *et al*, 1999)

For this reason, biofilm infections typically show recurring symptoms, after cycles of antibiotic therapy, until the sessile population is surgically removed from the body. Planktonic bacterial cells are released from biofilms, and evidence supports the notion that there is a natural pattern of programmed detachment. Therefore, biofilms can act as niduses of acute infection if the mobilised host defences cannot eliminate the planktonic cells that are released at any one time during the infection (Dasgupta *et al*, 1989).

The reasons for biofilm resistance to host defences and antibiotic therapy are yet to be conclusively determined. However, it is likely that biofilms evade antimicrobial challenges by multiple mechanisms. One theory proposes the failure of an agent to penetrate the full depth of the biofilm. Polymeric substances contained within the matrix of a biofilm are known to retard the diffusion of antibiotics and solutes in general diffuse at slower rates within biofilms than they do in water (Ishida *et al*, 1998). Antibiotics have been shown to penetrate biofilms readily in some cases and poorly in others, depending on the particular agent and biofilm. Mathematical models predict that a formidable penetration barrier should be established, if the antimicrobial agent is deactivated in the outer layers of the biofilm faster than it diffuses. This is true for reactive oxidants such as hypochlorite and hydrogen peroxide. These antimicrobial oxidants are products of the oxidative burst of phagocytic cells, and poor penetration of reactive oxygen species may partially account for the inability of phagocytic cells to destroy biofilm micro-organisms (Costerton *et al*, 1999).

A second hypothesis to explain reduced biofilm susceptibility to antibiotics proposes that at least some of the cells in a biofilm experience nutrient limitation, and therefore exist in a slow growing or starved state. As previously described, starved cells are less susceptible to antimicrobial agents. Spatial heterogeneity in the physiological state of bacteria within model biofilms has been demonstrated by a variety of microscopic techniques. Such heterogeneity of biofilms constitutes an important survival strategy because at least some of the cells, which represent a wide variety of different metabolic states, are almost certain to survive any metabolically directed attack. A third

mechanism, which is more speculative than the preceding hypotheses, is that at least some of the cells in a biofilm adopt a distinct and protected phenotype. This phenotype is not a response to nutrient limitation, but a biologically programmed response to growth on a surface (Stewart, 1998).

1.7) Electrical Phenomena

There are two types of electric charge referred to as positive (+) and negative (-), and the unit of charge is the coulomb (C) named after the 18th century French physicist Charles de Coulomb. The unit of negative charge is the charge on a single electron (1.602×10^{-19} C), which is equal but opposite to the positive charge on a proton. Large-scale matter that consists of equal numbers of electrons and protons is electrically neutral. If however, there is an excess of electrons then the body is negatively charged and conversely, if an excess of protons exists then a positive charge results (Blin-Stoyle, 1997). An atom or a group of atoms, which have lost one or more electrons i.e., have more protons than electrons, are termed positive ions or cations. If however, one or more electrons are gained then the atom or group of atoms are termed negative ions or anions. Two particles that have similar charges i.e. both negative or both positive, interact by repelling each other. Particles that have dissimilar charges interact by attracting each other. A flow of charged particles constitutes an electric current (I). The nature of the charge carrier is dependent on the conductor, for example, in metals the charge carriers are electrons, and in gases, charge is carried by ions (positive or negative).

The ratio between the applied voltage and the current is termed the resistance, a measure of the component's opposition to the flow of electric charge. The resistance, measured in ohms (Ω) of a component of unit length with unit cross sectional area is a property of the material known as resistivity, measure in ohm metres. The reciprocal of resistivity is the conductivity measured in siemens metre^{-1} (S m^{-1}). Typical conductivity readings for a conductor are 10^{8} S m^{-1}, and an insulator 10^{-12} S m^{-1}.

Electrons in a single isolated atom move in orbits around the nucleus representing discrete levels of energy. When atoms are brought together to form solids (separation distances ~ 0.1nm), electrons are influenced by adjacent atomic nuclei, and the once sharply defined energy levels become bands of allowed energy. The outer, or valence electrons are smeared into a wider band termed the valence band and energy levels that correspond to excited states of the outer electrons form a conduction band. At any temperature above absolute zero, some electrons will have sufficient thermal energy to transfer from the valence band to the empty conduction band. Metals such as copper and aluminium are good conductors of electrical current, as the number of mobile or free electrons is high, allowing electrons to be accelerated by an electric field and move throughout the crystal lattice of the solid. In essence, electrons do not belong to any atom in particular, but are delocalised (Blin-Stoyle, 1997).

Unipolar charge gives rise to an electric field, which is defined as a region in which an electric charge experiences a force due to the distribution of other charges (Taylor and Secker, 1994). The electric field strength (E) at any point in an electric field is defined as the force per unit charge experienced by a unit positive charge placed at that point. An electric field may be represented by lines, which indicate the path that would be followed by a positive charge placed in that field (*Figure* 1.8, *Page* 34)). Electric field lines must always commence on a positive charge and terminate on a negative charge. As electric field lines begin and end on a charge, a high density of field lines implies a high charge density and a high electric field (Cross, 1987).

If a negative charge is in the vicinity of a fixed positive charge then an attractive force is experienced between them (*Figure* 1.9, *Page* 34)). In moving the negative charge from point X to point Y, work has to be done against the attractive force, thereby increasing the potential energy of the negative charge. The difference in the potential energy between points X and Y is defined as the potential difference between the two points, and is measured in volts (V).

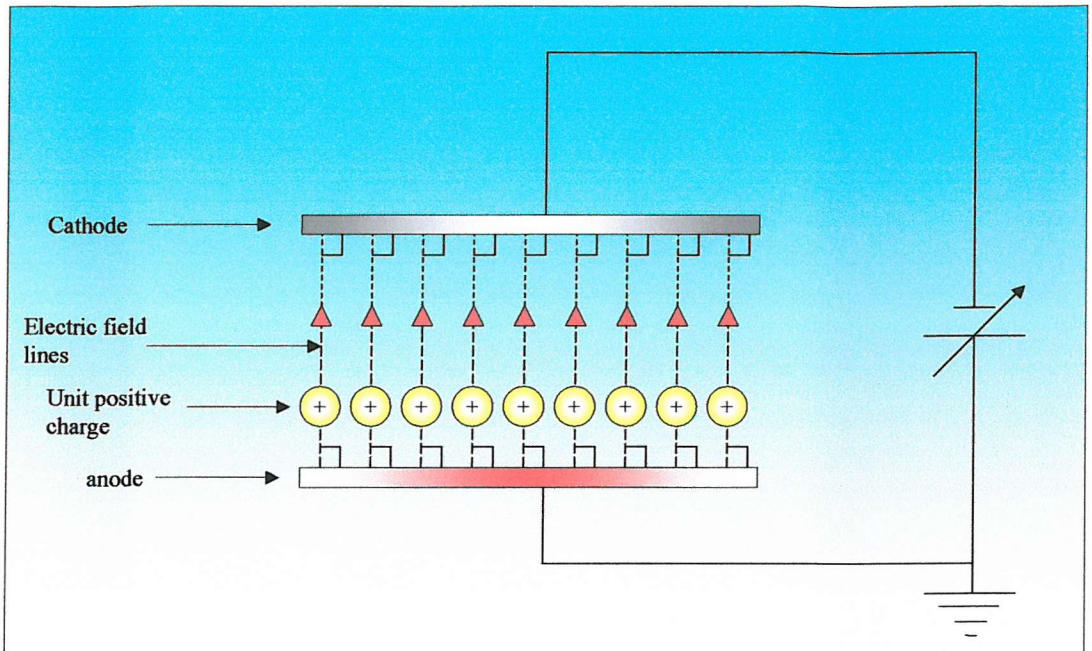

Figure 1.8) An example of a uniform electric field between two oppositely charged electrodes. (Adapted from Taylor and Secker, 1994)

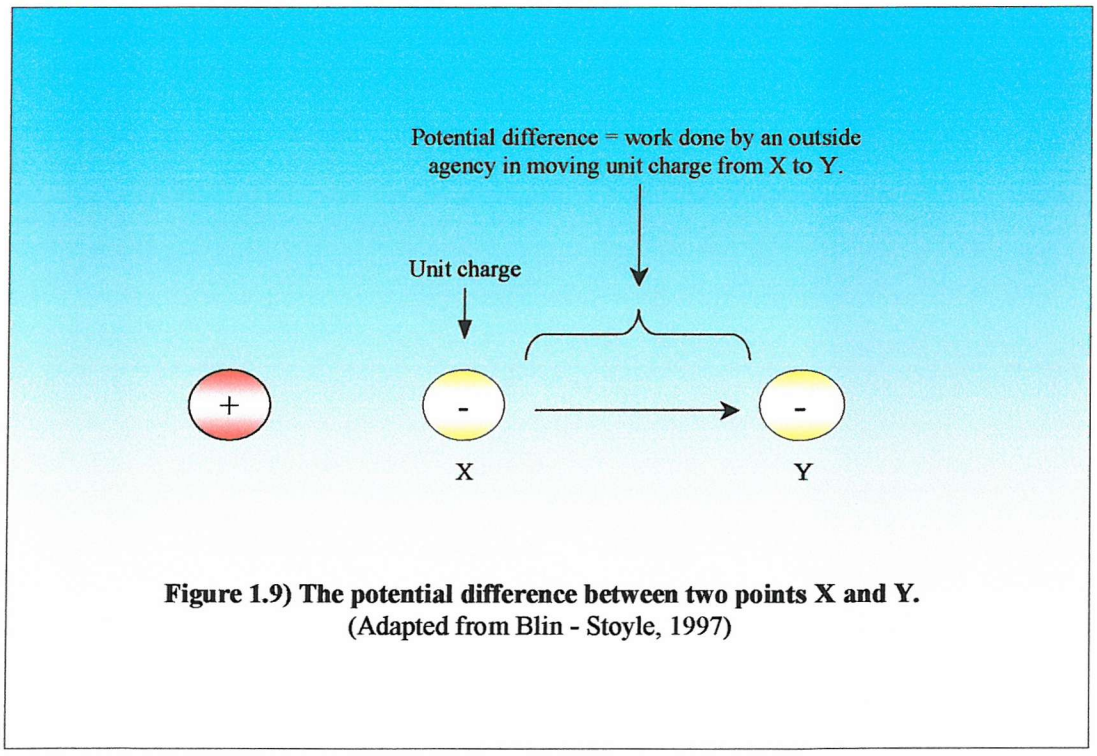

Figure 1.9) The potential difference between two points X and Y.
(Adapted from Blin - Stoyle, 1997)

1.8) Electrical Coronas

In many applications of electrostatics, negative or positive charge may be applied to a surface by means of a direct current (DC) corona discharge. This is produced when a high voltage is applied between two non-uniform electrodes such as a cylinder with a wire at its axis, or a point and a plane (*Figure* 1.10, *Page* 36). In such an arrangement, the electric field at the terminus of the point electrode is considerably higher, as shown by the convergence of the electric field lines. With electrical coronas, ions of a particular polarity can be created by simply changing the polarity of the applied voltage i.e. a positive point electrode voltage will produce positive ions and conversely a negative applied voltage will produce negative ions. The predominant negative ions produced by a corona discharge in air are CO_4^-, CO_3^- and O_3^-. With a positive point electrode O_2^+ and N_2^+ are dominant.

In pure nitrogen, or other gases to which electrons do not readily attach, the current associated with a negative corona may be predominantly electronic (Taylor and Secker, 1994). However, the existence of free electrons (or electrons with a long mean free time) in a gas at atmospheric pressure is unlikely, and so the precise nature of negative charge carriers in high electronegative gases is somewhat uncertain. It is possible that a complex dynamic state is created where ions and partially free electrons co-exist. Therefore, throughout this thesis, in order to simplify the terminology and to avoid confusion, the current generated by a negative corona discharge in pure nitrogen will be designated as, and assumed to be, ionic.

When a negative high voltage is applied in air, electrons within the high field region are liberated from both the point electrode and naturally occurring negative ions. These electrons accelerate away from the point electrode, driven by the high electric field and gain sufficient energy to ionise any atom with which they collide. Ionisation occurs when energy in excess of the electron potential is absorbed by an atom, yielding a free electron and a positive ion. The liberated electrons are in turn accelerated by the high electric field causing further ionisation reactions. Light is emitted during the ionisation

process and in air a blue glow can be seen around the sharp electrode that gives the discharge the name corona (*Figure* 1.11).

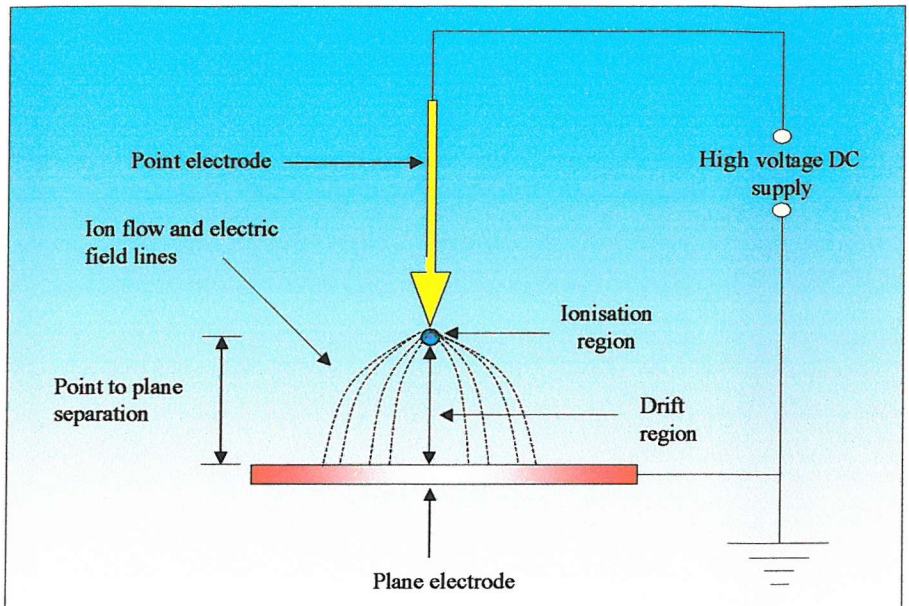

Figure 1.10) A typical point to plane corona geometry.
(Adapted from Taylor and Secker, 1994)

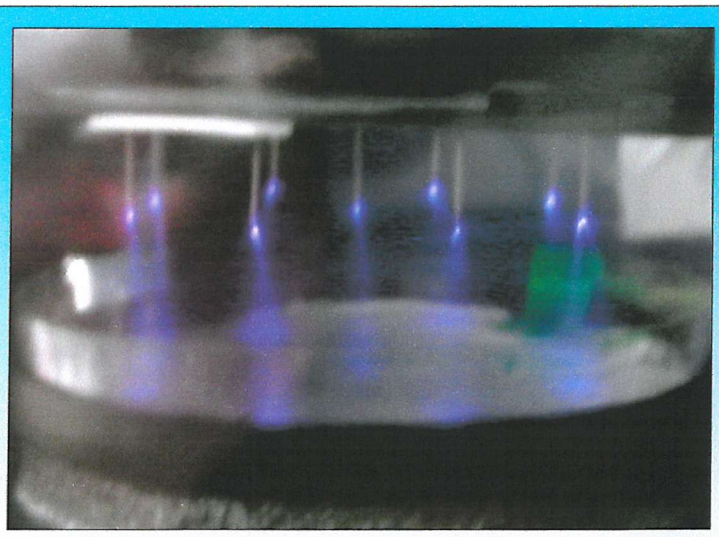

Figure 1.11) A nine point to plane corona set up with negative applied voltage (14kV, 350μA) showing the characteristic blue glow of photon emission during ionisation. (Taken from own experimental work)

As the ionisation collisions escalate an electron avalanche is established, termed the Townsend α-process, in which the electron population grows exponentially (Taylor and Secker, 1994). The electron multiplication process continues until new electrons are released at a point within the inter-electrode space where they are unable to gain sufficient energy from the electric field to cause additional ionisation. Electrons that have insufficient energy to form new electron – positive ion pairs, attach to high electronegative atoms, such as oxygen or fluorine, to form negative ions. The positive ions that are formed are attracted to the negative point electrode and gain energy from the electric field. On collision with the point electrode, secondary electrons are released which add to the discharge ionisation process. When the point electrode is positive, electrons created by ionisation within the high field region are attracted to the point, and positive ions drift towards the planar electrode. The positive ions that reach the plane have insufficient energy to generate secondary electrons (Cross, 1987).

For both positive and negative coronas, the really distinguishing feature is the existence of a drift region connecting the ionisation region with the eventual low field, passive electrode. In this drift region, ions and electrons move and react with neutral gas species, but with too low an energy to ionise. In fact the ions drifting through the inter-electrode space possess ~ 0.06 electron volts ($1eV = 1.602 \times 10^{-19}J$) of kinetic and potential energy (Goldman *et al*, 1985). This collision-dominated process ensures that virtually all momentum and energy (~99%) extracted by the ions from the electric field is transferred to the neutral gas species (Sigmond, 1989). As a result, a fairly strong, axial gas jet is formed which is termed the ion wind. The wind is a bulk movement of the gas and not of the ions alone and typical velocities in air are in the order of $1m\ s^{-1}$ (Cross, 1987).

The ions that are created by the discharge modify the electric field that exists between the two electrodes by decreasing the field near the point and increasing the field near the plane. The result is that although the field is not uniform in the absence of ions, the field across the drift region of the corona discharge when ions are present can be assumed to

be constant. Lying approximately between V/X and V/2X, where X is the inter-electrode space in metres and V is the applied voltage in kV. The field of a corona discharge at the plane electrode is normally in the order of 300 kV m^{-1} (Taylor and Secker, 1994).

With regards to the unipolar current density in positive and negative point-to-plane coronas, the distribution over the plane electrode is set according to Warberg's law, represented in *Figure* 1.12. The observed distribution usually falls sharply to zero at around 65°, due to the fact that ions drift along the field lines and that field lines terminating outside 65° usually originate on the point surface outside the ionisation region (Goldman *et al*, 1985). The corona current density on a plane arising from a single point electrode is typically 10^{-4} to 10^{-3} A m^{-1} (Taylor and Secker, 1994).

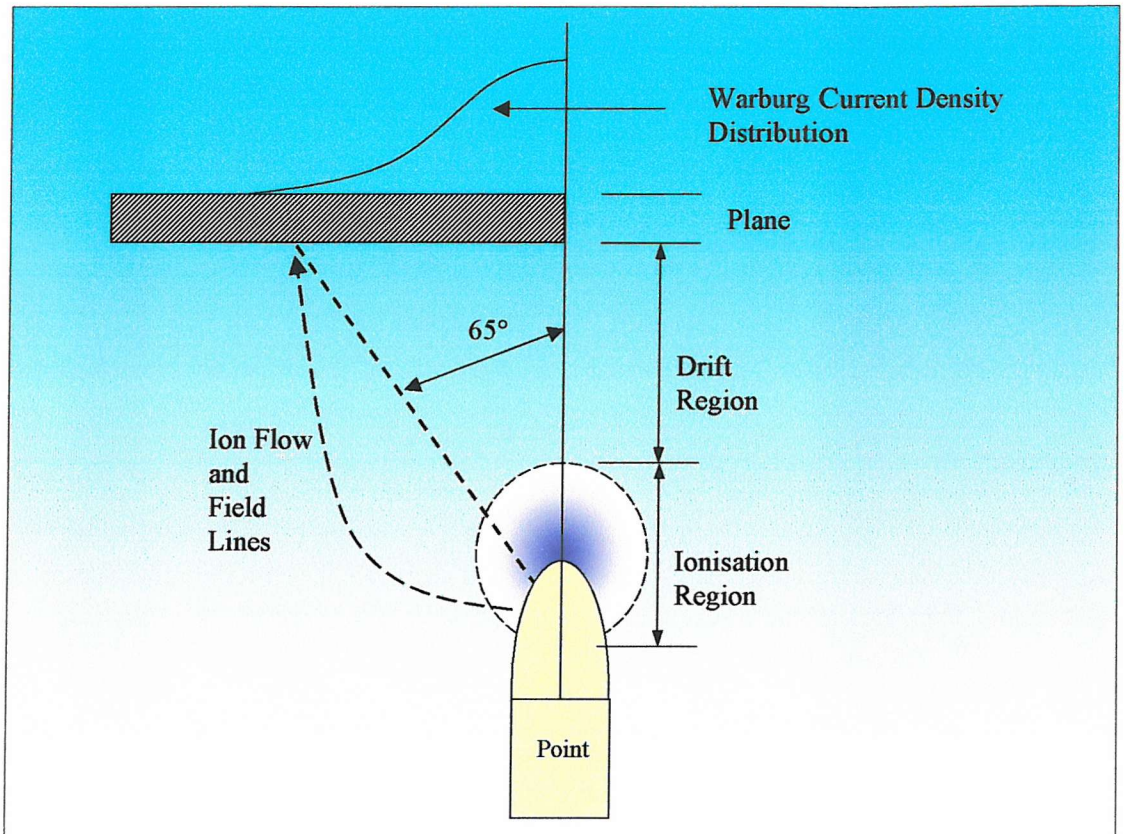

Figure 1.12) Distribution in the current density of a point to plane corona. (Adapted from Goldman *et al*, 1985)

For electrostatic applications, the fact that unipolar corona drift regions contain ions of one polarity is the primary reason for their extended use as charging methods in electrostatic apparatus such as precipitators, paint guns and photocopiers. Applying a positive or negative charge to a surface is reasonably straight forward as objects placed in the drift zone will intercept the ion wind and become charged according to the polarity of the sharp electrode (Taylor and Secker, 1994).

1.9) Electrical Coronas and Ozone Production in air

One of the most potent products of corona discharges in air is ozone (O_3). Large scale industrial ozone reactors utilise a positive corona discharge, generally using air or oxygen filled short gaps, where one of the electrodes is covered with an insulating layer in order to prevent breakdown of the gas (Goldman *et al*, 1985). Within these discharges high-energy electrons provide a high yield of atomic oxygen, which in turn combines with molecular oxygen to produce ozone, bluish in colour, with a pungent and characteristic odour.

Ozone is a potent disinfectant and has been utilised as a sanitizer in European water treatment plants since the beginning of the century (Kim *et al*, 1999). The use of ozone allows the natural taste of the water to be preserved, thus avoiding the smell of other commonly used disinfectants, such as chlorine. In addition, the high oxidising power and spontaneous decomposition makes the use of ozone an efficient mechanism for decreasing microbial load. Given the right conditions, relatively low concentrations of ozone (<1ppm) and short contact time (<10 seconds) is sufficient to inactivate a large number of bacterial species including *P.fluorescens*, *E.coli* O157:H7 and *L.mesenteroides* (Kim, 1998).

Kowalski *et al* (1998) conducted a series of tests examining the effect of high airborne ozone concentrations on *E.coli* and *S.aureus* to determine if airborne ozone could be used to inactivate pathogenic agents. Petri dishes inoculated with the micro-organisms were placed into a chamber (volume 72 litres) and exposed for time periods ranging

from 10 to 480 seconds, to ozone concentrations ranging from 300 to 1500 ppm. The results obtained demonstrated that high i.e. >300<1500ppm, airborne ozone could effectively kill bacterial cells and sterilise surfaces.

In a similar series of tests, Moore *et al* (2000) evaluated the efficacy of ozone to act as a terminal disinfectant against different micro-organisms of importance to the food industry. Stainless steel squares ($5cm^2$) were inoculated with one of five bacteria, either *E.coli*, *S.aureus*, *Serratia liquefaciens*, *Listeria innocua* or *Rhodotorula rubra*, and placed into a temperature and relative humidity controlled chamber (volume 154 litres). The ozone concentration within the chamber ranged from 2ppm to 5ppm and the exposure time was four hours. Their results demonstrated that relatively low levels of gaseous ozone, when applied to contaminated steel surfaces exhibit potent bactericidal properties. In fact, a four-hour exposure to 2ppm ozone resulted in at least a 5-log reduction in the viability of four of the five bacteria tested.

With regards to the direct effects against bacteria, ozone initially targets the bacterial membrane glycoproteins, glycolipids, or certain amino acids such as tryptophan, in addition to acting on the sulfhydryl groups of certain enzymes, resulting in the disruption of normal cellular activity. Bacterial death is rapid and is often attributed to changes in cell permeability followed by cell lysis (Greene *et al*, 1993).

1.10) Electrical Coronas and Bacterial Decontamination

Studies to date have demonstrated that exposure to electrical coronas in air will stop the growth of bacterial cells. In a series of tests conducted by Sigmond *et al* (1999), the bactericidal efficiencies of various well-defined corona types were investigated against the bacterium *E.coli*. The research group exclusively worked with the point-to-plane corona geometry in air and altered the point polarity and material to produce the desired corona. Their results demonstrated that the manipulation of corona parameters could affect the production of bactericidal agents. The primary one monitored was ozone, with a concentration of 35-40ppm at the agar surface. Other possible antibacterial

agents produced, although not identified, were nitrogen oxide species and hydrogen peroxide. Sigmond concluded that any reduction in viability was due to ozone and that charged particles and photons could only play a minor role.

Yan *et al* (1991), utilised a corona discharge to sterilise a traditional Chinese powder of moulds and bacteria. Experiments were conducted in air and thus ozone was produced. However, Yan concluded that the quantity of sterilisation recorded was not completely due to ozone alone. Instead, the authors concluded that the corona current itself was responsible, particularly with AC coronas.

Garate *et al* (1998), conducted tests utilising an enhanced corona discharge (ECD), against *E.coli* and *Bacillus subtilis*. The ECD tests consisted of a line of pins attached to a brass tube pierced with a series of tiny holes. Less electronegative gases such as argon or nitrogen were then fed into the brass tube, which subsequently escaped through the holes to provide a local atmosphere around the point electrodes. Using this experimental set up significant kill rates were achieved. However, experiments were still conducted in air and thus were subject to possible ozone and oxide contamination, although the authors fail to mention if ozone was recorded.

Thus the use of the corona discharge for biological decontamination is not entirely novel, although to date the continued possibility of ozone contamination prevents the elucidation of determining the effect of ions alone. Therefore, although corona ionisation offers a relatively simple technique for ion generation, the ions will always be accompanied by ozone. Where the effects of ions alone are to be evaluated, it is necessary to eliminate ozone production.

1.11) Project Aims

Since the onset of the first application of antibiotics, selective pressure on the micro-organism community has established the emergence of resistant strains. Now, some fifty-nine years later, multi drug resistant bacteria are common place, immune to even

our most potent weapons. Even disinfectants are now becoming tolerated at previously lethal doses. The search to find new chemical agents and decontamination methods is paramount if the war against pathogenic organisms is to continue. Electrical coronas have been utilised before for the purposes of sterilisation, although the majority of effects have been attributed to the oxidising agent ozone. Electrostatic technology utilising either positive or negative ionic exposure alone is yet to be fully evaluated and could provide a potentially novel approach to the control of bacterial populations.

In summary, the aims of this investigation are:
To establish the effect of exposure to unipolar ions, either positive or negative on Gram-positive and Gram-negative bacterial species. In addition, unipolar ionic effects on more resistant phenotypes, including starved bacterial cells and mono-species biofilms will be investigated. Ionic treatments will be applied using a purpose built nine-point electrode corona discharge and the following bacterial species will be used: *Escherichia coli*, *Staphylococcus aureus* and *Pseudomonas veronii*.

The following investigations will be conducted:

- Ionic treatments in air and the specific contribution of ozone towards any reduction in bacterial viability.
- Ionic treatments under a nitrogen atmosphere. Effect of current and exposure time on log phase bacterial cells.
- Ionic treatments under a nitrogen atmosphere. Effect of current and exposure time on starved bacterial cells.
- Ionic treatments under a nitrogen atmosphere. Effect of current and exposure time on mono-species biofilms.
- Effects of varying temperature, relative humidity, electrical current and electric field.
- Physiological effects of exposure to unipolar ions in nitrogen. Effect of ionic challenge on Gram-negative and Gram-positive cell walls.

Chapter Two

Materials and Methods

2.1) Materials and apparatus

Escherichia coli DH5-α (*E.coli*) was provided by Dr. David O'Connor, University of Southampton, England. *Pseudomonas veronii* BL146-Bio (*P.veronii*) was provided by Dr. Pauline Hadley, University of Manchester, England. *Staphylococcus aureus* type 8532 (*S.aureus*) was provided by the National Collection of Type Cultures, Public Health Laboratory Service, London, England. All organisms were stored at –20°C in 50% glycerol.

Tryptic soy broth (TSB), TSB with agar, tryptone soy broth (ToneSB), agar, glycerol, ethyl alcohol (98.86%), nonanal aldehyde, cetylpyridinium chloride, congo red powder, tween-80 and giolitti cantoni broth (CGB) were all supplied by Sigma chemicals, Poole, Dorset, England. The BacLight L-7012 cell wall integrity staining kit was supplied by Cambridge Bioscience, Cambridge, England. Ozone readings were taken using a Dräger multi-gas detector, Model 31, Dräger Sicherheitstechnik GmbH, Germany. DC current was measured using a series eight universal Avometer, model Mk-7, Avometer, Megger Instruments, Dover, England. Voltage was measured and applied using a Brandenberg high voltage unit, Brandenberg ltd, 939 London Road, Thornton Heath, England. Light output from *P.veronii* was quantified using a Sirius model luminometer, Berthold Detection Systems, Pforzheim, Germany.

2.2) Preparation of *E.coli* cells

Working stock plates were prepared by aseptically transferring cells stored at -20°C to a TSB agar plate. This plate was then incubated for eighteen hours at 37°C to generate visible colonies. After incubation, the plate was stored at 4°C and replaced every three weeks. Cells stored for longer than this became non-viable. Cells maintained on TSB agar stock plates, were aseptically transferred to 10mls of sterile TSB. The inoculated TSB was then incubated at 37°C on a fixed speed rocker (Grant/Boekel model BFR25, Shepreth, Cambridgeshire, England) for a period of eighteen hours. Cells were harvested by pipetting 1ml of culture into eppendorfs, which was washed twice in sterile, distilled water by centrifugation (Micro Centaur, Model: MSB010.CX2, Sanyo Gallenkamp PLC, Middlesex, England) at room temperature (21° ± 3°C, ten minutes,

3200 × g), and then resuspended in 1ml of sterile, distilled water. Resuspending in sterile, distilled water at room temperature dramatically reduced further cell division and improved assessment of cell number. Once resuspended, the optical density (for a given wavelength, an expression of the transmittance of an optical element) at a wavelength of 630nm ($O.D_{630nm}$) was taken (plate reader model ELX-800, Biotek Instruments, England) and used to calculate the number of colony forming units per ml ($CFUml^{-1}$) using *Figure* 2.1. With the number of $CFUml^{-1}$ known for the suspension, the volume required to produce plates with ~ 300 CFU at a dilution of 10^{-5} could be determined.

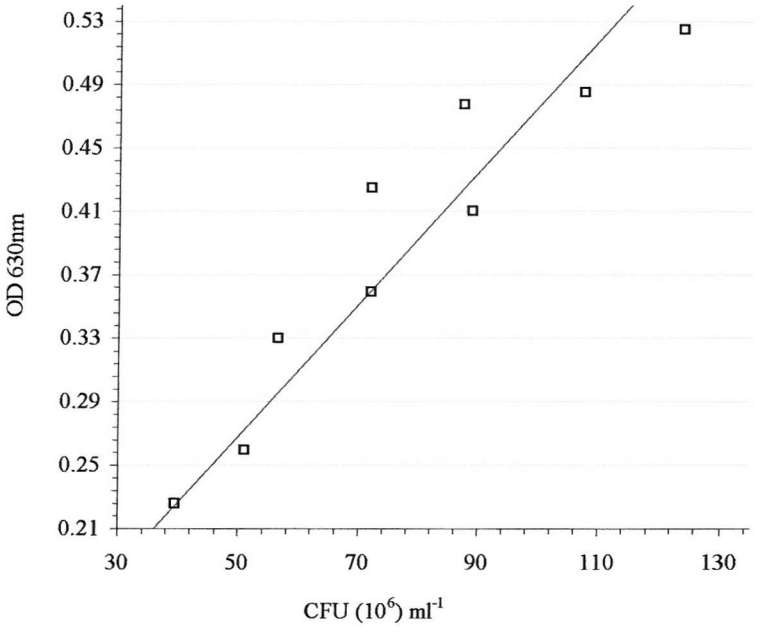

Figure 2.1) Relationship between optical density and $CFUml^{-1}$ for *E.coli*. 10mls of TSB was inoculated with *E.coli* cells and incubated on a rocker for eighteen hours at 37°C. From the culture 1ml aliquots were removed, washed twice by centrifugation and resuspended in varying volumes of sterile, distilled water ranging from 200µl to 1.5ml. The optical density reading (630nm) was taken for each new suspension, prior to plating out at a dilution of 10^{-6}. Plates were subsequently incubated for eighteen hours at 37°C and the number of colonies counted.

2.3) Preparation of *P.veronii* cells

Working stock plates were prepared by aseptically transferring cells stored at -20°C to a ToneSB agar plate. This plate was then incubated for nineteen hours at 30°C to generate visible colonies. After incubation, the plate was stored at 4°C and replaced

every two weeks as cells stored for longer than this became non-viable. Cells maintained on ToneSB agar plates, were aseptically transferred to 10mls of sterile ToneSB. The inoculated ToneSB was then incubated at 30°C on a rocker for a period of nineteen hours. Cells were harvested by pipetting 1ml of the *P.veronii* culture into eppendorfs and washed twice in sterile, distilled water by centrifugation (21° ± 3°C, ten minutes, 3200 × g), and then resuspended in 1ml of sterile, distilled water. Once resuspended, cells were left at room temperature (21 ± 3°C) and the $O.D_{630nm}$ was taken and used to calculate the number of $CFUml^{-1}$ using *Figure* 2.2.

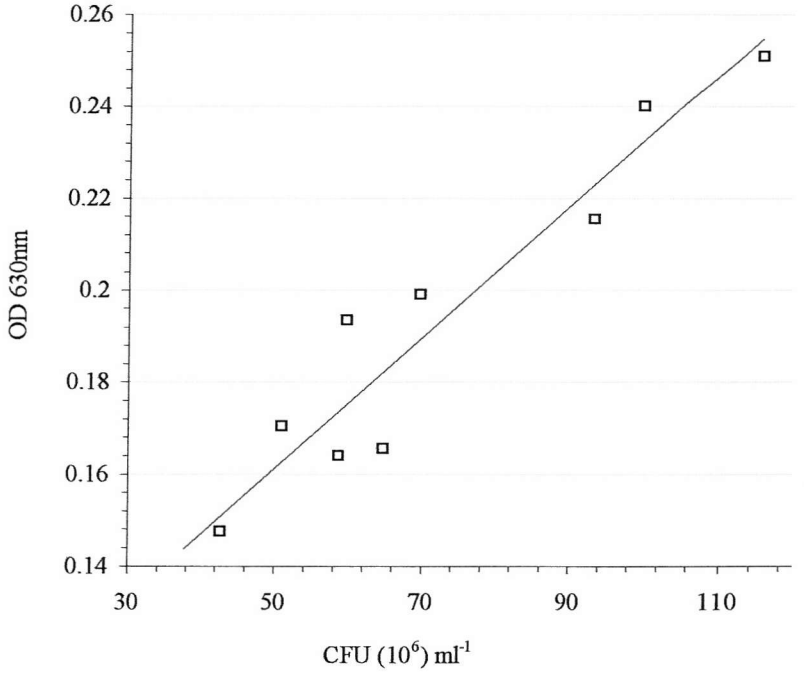

Figure 2.2) Relationship between optical density and $CFUml^{-1}$ for *P.veronii*. 10mls of ToneSB was inoculated with *P.veronii* cells and incubated on a rocker for nineteen hours at 30°C. From the culture 1ml aliquots were removed, washed twice by centrifugation and resuspended in varying volumes of sterile, distilled water ranging from 200µl to 1.5ml. The optical density reading (630nm) was taken for each new suspension, prior to plating out at a dilution of 10^{-6}. Plates were subsequently incubated for nineteen hours at 30°C and the number of colonies counted.

2.4) Preparation of *S.aureus* cells

Working stock plates were prepared by aseptically transferring cells stored at -20°C to a CGB agar plate. This plate was then incubated for nineteen hours at 30°C to generate visible colonies. After incubation, the plate was stored at 4°C and replaced every three

weeks as cells stored for longer than this became non-viable. Cells maintained on CGB agar plates, were aseptically transferred to 10mls of sterile CGB, which was then incubated at 30°C on a rocker for a period of nineteen hours. Cells were harvested by pipetting 1ml of culture into eppendorf tubes and washed twice in sterile, distilled water by centrifugation (21° ± 3°C, ten minutes, 3200 × g), and then resuspended in 1ml of sterile, distilled water. Once resuspended, the $O.D_{630nm}$ reading was taken and used to calculate the number of $CFUml^{-1}$ using *Figure* 2.3. With the number of $CFUml^{-1}$ known, the volume required to produce plates with ~ 300 CFU at a dilution of 10^{-5} could be determined.

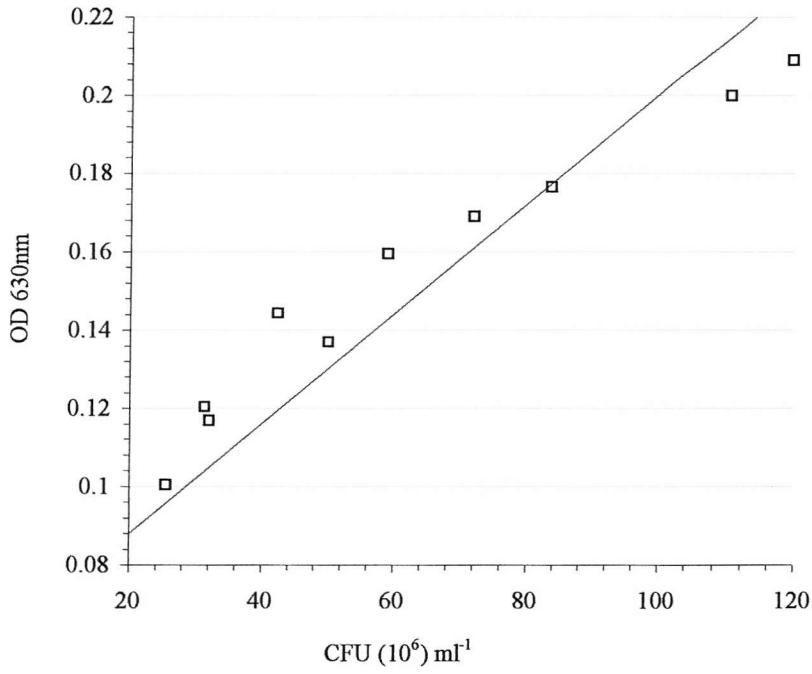

Figure 2.3) Relationship between optical density and $CFUml^{-1}$ for *S.aureus*. 10mls of CGB was inoculated with *S.aureus* cells and incubated on a rocker for nineteen hours at 30°C. From the culture 1ml aliquots were removed, washed twice by centrifugation and resuspended in varying volumes of sterile, distilled water ranging from 200µl to 1.5ml. The optical density reading (630nm) was taken for each new suspension, prior to plating out at a dilution of 10^{-6}. Plates were incubated for nineteen hours at 30°C and the number of colonies counted.

2.5) Preparation of experimental *E.coli* plates

Sterile TSB agar was poured into standard 88mm diameter petri dishes and allowed to set. Once set, plates were stored at 4°C and dried at 37°C for two hours prior to inoculation to remove excess condensation. From the resuspended *E.coli* solution

(*Section* 2.2), an appropriate volume was removed and resuspended in sterile, distilled water to give a concentration of 300 × 10^6 $CFUml^{-1}$. The resuspended *E.coli* culture was serially diluted in sterile, distilled water through five 1:10 dilutions and each plate was inoculated with 100µl of the final dilution, which was spread evenly over the surface of the TSB agar with a glass spreader. These conditions were found to generate plates with 300 ± 50 CFU. Plates were refrigerated at 4°C until required and used within 72hours of inoculation. Control plates incubated after 72hours refrigeration showed a significant reduction in CFU number, compared to control plates incubated at time zero. Prior to testing, experimental plates were removed from the fridge and left at room temperature for fifteen minutes to acclimatise.

2.6) Preparation of experimental *S.aureus* plates

Sterile CGB agar was poured into standard 88mm diameter petri dishes and allowed to set. Once set, plates were stored at 4°C and dried at 37°C for two hours prior to inoculation to remove excess condensation. From the resuspended *S.aureus* solution (*Section* 2.4), an appropriate volume was removed and resuspended in sterile, distilled water to give a concentration of 300 × 10^6 $CFUml^{-1}$. This new suspension was serially diluted in sterile, distilled water through five 1:10 dilutions and each plate was inoculated with 100µl of the final dilution, which was spread evenly over the surface of the CGB agar with a glass spreader. These conditions were found to generate plates with 300 ± 60 CFU. Plates were refrigerated at 4°C until required and used within 96 hours of inoculation. Control plates incubated after 96 hours refrigeration showed a significant reduction in CFU number compared to control plates incubated at time zero. Prior to testing, experimental plates were removed from the fridge and left at room temperature for fifteen minutes to acclimatise.

2.7) Preparation of starved *P. veronii* aluminium foil coupons

Nutrient availability to bacteria in the natural world is extremely inconsistent. Consequently, micro-organisms are in a starvation state most of the time. Under starvation conditions bacteria enter a physiological state that provides increased resistance to a host of exterior challenges. To ascertain the effect of unipolar ions on

starved bacteria, *P.veronii* cells prepared as in *Section* 2.3 were used. Once resuspended in sterile, distilled water, the cells were left at room temperature for a period of twenty four hours. Plating out the resuspended culture after 24 hours demonstrated a decrease in viability of 12 ± 2%. With the number of $CFUml^{-1}$ determined from *Figure* 2.2, the suspension was centrifuged (21° ± 3°C, ten minutes, 3200 × g) and resuspended to give a final concentration of 500×10^6 viable $CFUml^{-1}$, accounting for a 14% decrease in viability.

For the *P.veronii* experiments, aluminium foil coupons (20 × 20mm) were utilised as the inoculating receptacle instead of ToneSB agar plates. This was done for two reasons,

1) The use of a non-nutrient medium surface reflected a more realistic, environmental existence, which also ensured that the cells remained in a starvation state.
2) To ascertain cell viability it would not be necessary to plate out cells, incubate and count colonies, as this would be determined using the bioluminescent capability of the cells. To ascertain the number of viable cells, the inoculated coupons would simply be read in the Sirius luminometer.

Individual aluminium foil coupons were cut and placed into 88mm petri dishes (five coupons per dish). To ensure that the foil coupons remained flat and in position, a spot of glycerol was pipetted onto the petri dish base prior to foil placement. To each foil square 100µl of 24hour starved cell suspension was added (~50×10^6 viable CFU). The cell suspension drops were then allowed to dry at 30°C for 120 minutes to remove all water, forming residue spots on the foil coupons (*Figure* 2.4, *Page* 50). Any loss in microbial viability due to the drying process was accounted for by control coupons, which were not exposed to experimental procedures. Once dry, coupons remained stable for four hours i.e. there was no significant difference in readings of coupons read at time zero and those read at time zero plus four hours. Control coupons analysed after four hours showed a significant reduction in cell viability.

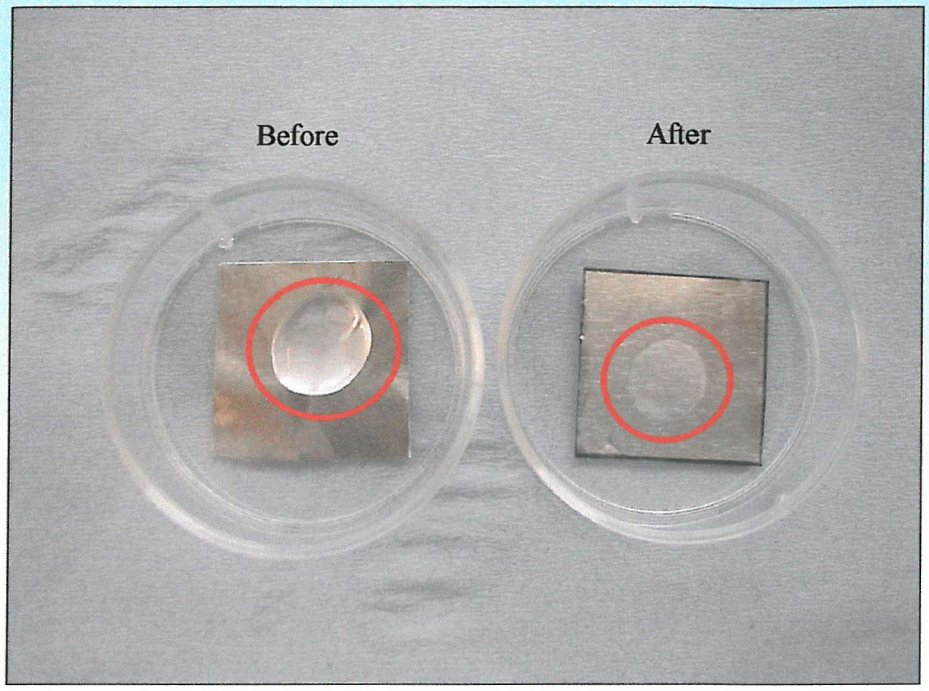

Figure 2.4) Picture of *P.veronii* coupons inoculated with 100µl of *P.veronii* suspension, before and after two hours incubation at 30°C

2.8) Relationship between *P.veronii* viability and bioluminescence readings in relative light units per second ($RLUs^{-1}$)

To determine if *P.veronii* viability related directly to bioluminescence, a *P.veronii* suspension as described in *Section* 2.3 was resuspended at a concentration of 50×10^6 CFU ml^{-1}. Half of the suspension was removed and placed in ethyl alcohol for three hours to kill all cells and then washed twice in sterile, distilled water by centrifugation (21° ± 3°C, ten minutes, 3200 × g), and then resuspended in sterile, distilled water at 50×10^6 CFU ml^{-1}. The viable and non-viable suspensions were then mixed to give the following proportions of percent alive cells: zero, 20%, 50%, 80% and 100%. From each new suspension 1ml was taken and 50µl of nonanal added to obtain a reading in $RLUsec^{-1}$.

2.9) Relationship between *P.veronii* bioluminescence readings in $RLUs^{-1}$ and number of $CFUml^{-1}$

To ascertain the relationship between readings obtained in $RLUs^{-1}$ and the number of CFU ml^{-1}, a *P.veronii* suspension as described in *Section* 2.3 was resuspended at a concentration of 50×10^6 CFU ml^{-1}. This suspension was then diluted to give suspensions of 40, 30, 25, 20, 15, 10, 5, 4, 3 and 2×10^6 $CFUml^{-1}$. From each dilution 1ml was taken and 50µl of nonanal added to obtain a reading in $RLUsec^{-1}$. The number of $CFUml^{-1}$ was subsequently plotted against the $RLUsec^{-1}$ reading for that dilution.

2.10) Preparation of *P.veronii* biofilms

In their natural environment bacterial cells rarely exist in a planktonic state, choosing to congregate and form complex micro-colonies and subsequent biofilms. Once formed, the biofilm provides a protective mode of growth that is highly resistant to numerous antibacterial agents. To ascertain the effect of unipolar ionic exposure on a monospecies bacterial biofilm, *P.veronii* foil coupons (as described in *Section* 2.7) were placed into individual 35mm diameter petri dishes. The coupons were held in place by the addition of a small quantity of petroleum jelly to the base of the dish. With the inoculated coupons in position, 3mls of ToneSB was added to each dish, which was then placed into an incubator at 30°C for a period of 24hours. At the end of this period, biofilm formation could be clearly seen across the surface of the foil coupons (*Figure* 2.5, *Page* 52) and was confirmed through the application of Congo red staining (*Section* 2.11).

Following the 24hour incubation period, the TSB medium was removed by transfer pipette and the coupons gently washed once with sterile, distilled water to remove non-adhered cells. With the coupons washed, 3mls of sterile, distilled water was added to each petri dish, which were then placed back in the incubator at 30°C for a further 24hours. The removal of the nutrient broth ensured that all cells within the biofilm were forced into a starvation state. Previous investigations had shown that actively growing biofilms were highly susceptible to desiccation, which was a necessary process for the latter part of this protocol. *P.veronii* biofilms not starved for 24hours,

demonstrated significant reductions in cell viability compared to biofilms that had been incubated in sterile, distilled water. Following the 24hour incubation period, the water was removed by transfer pipette and the coupons allowed to dry at 30°C for ninety minutes. Once dry, biofilm coupons remained stable for a period of five hours. Control biofilm coupons analysed after five hours showed a significant reduction in cell viability.

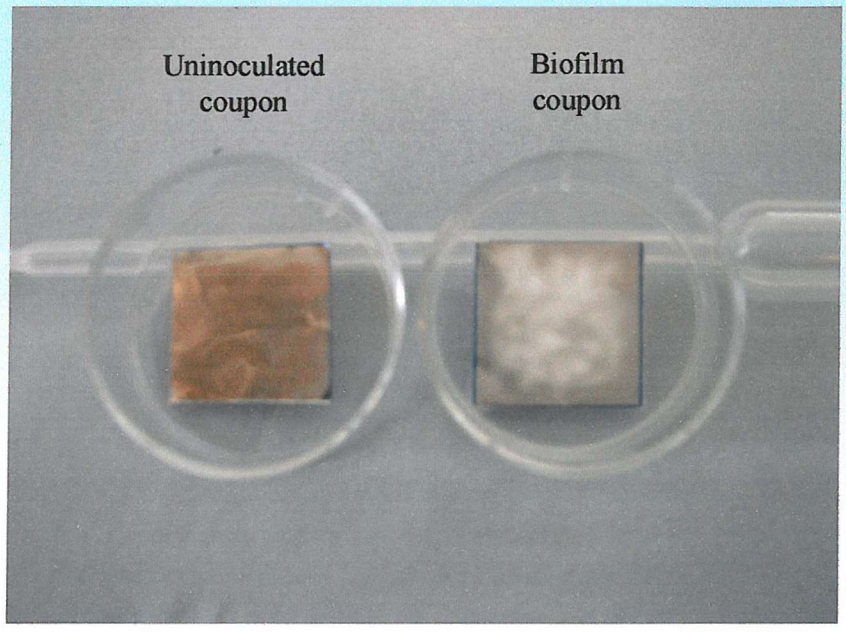

Figure 2.5) Picture of a *P.veronii* biofilm. Inoculated foil coupon after 24hours incubation in Tone SB

2.11) Congo red staining for bacterial biofilms

The primary identifying characteristic of a biofilm, compared to a planktonic cell or bacterial colony is the production of exopolysaccharide (EPS). Bacterial biofilms can be identified through the application of a Congo red staining technique described by Serralta *et al* (2001), which specifically stains for EPS. *P.veronii* biofilms described in *Section* 2.10 were grown, except that no 24hour incubation in sterile, distilled water occurred. After the incubation in ToneSB, all nutrient medium was removed by gently washing twice with sterile, distilled water. To precipitate the EPS from the coupons,

1ml of 10mM cetylpyridinium chloride (CPC) was added. After a five-minute incubation with the CPC, 500µl of the solution was transferred to a clean 35mm petri dish and allowed to dry at 37°C for two hours, forming a residue spot in the base. Once dry, 2mls of Congo red solution (10mls saturated aqueous Congo Red solution with 5mls, 10% Tween 80) was added to each petri dish and incubated at room temperature for fifteen minutes. After incubation with Congo red, the residue spots were gently washed twice with distilled water and analysed.

As a comparison, planktonic *P.veronii* cells were also stained. *P.veronii* cells were prepared as described in *Section* 2.3 and resuspended at a concentration of 500×10^6 $CFUml^{-1}$. From this suspension 500µl was transferred to a 35mm petri dish containing 500µL CPC. After five minutes, 500µl was removed and treated in an identical fashion as described above.

2.12) Voltage – current relationship for a point plane corona in air

For the initial ionic exposure experiments with *E.coli* and *S.aureus*, a nutrient medium agar plate would be acting as the plane electrode. To establish the ability of this medium to act as a plane electrode, a set of nine pins (point radius of 45µm) spaced to allow uniform plate coverage, were placed at a distance of 25mm above either a TSB or CGB agar plate (*Figure* 2.6, *Page* 54). The agar plate was earthed by inserting a copper wire through a small hole in the side of the petri dish directly into the medium. Voltage, negative or positive, was applied to the pin electrodes in 1kV increments and the current flowing was measured in the earthed lead of the circuit. Two other plane electrodes were tested for comparison; an aluminium foil plane and an agar plate with an aluminium base (prepared by placing an aluminium foil disc in the base of a petri dish and then subsequently pouring TSB agar over it) (*Figure* 2.7, *Page* 55). In both cases the planes were earthed via a direct connection to the aluminium foil.

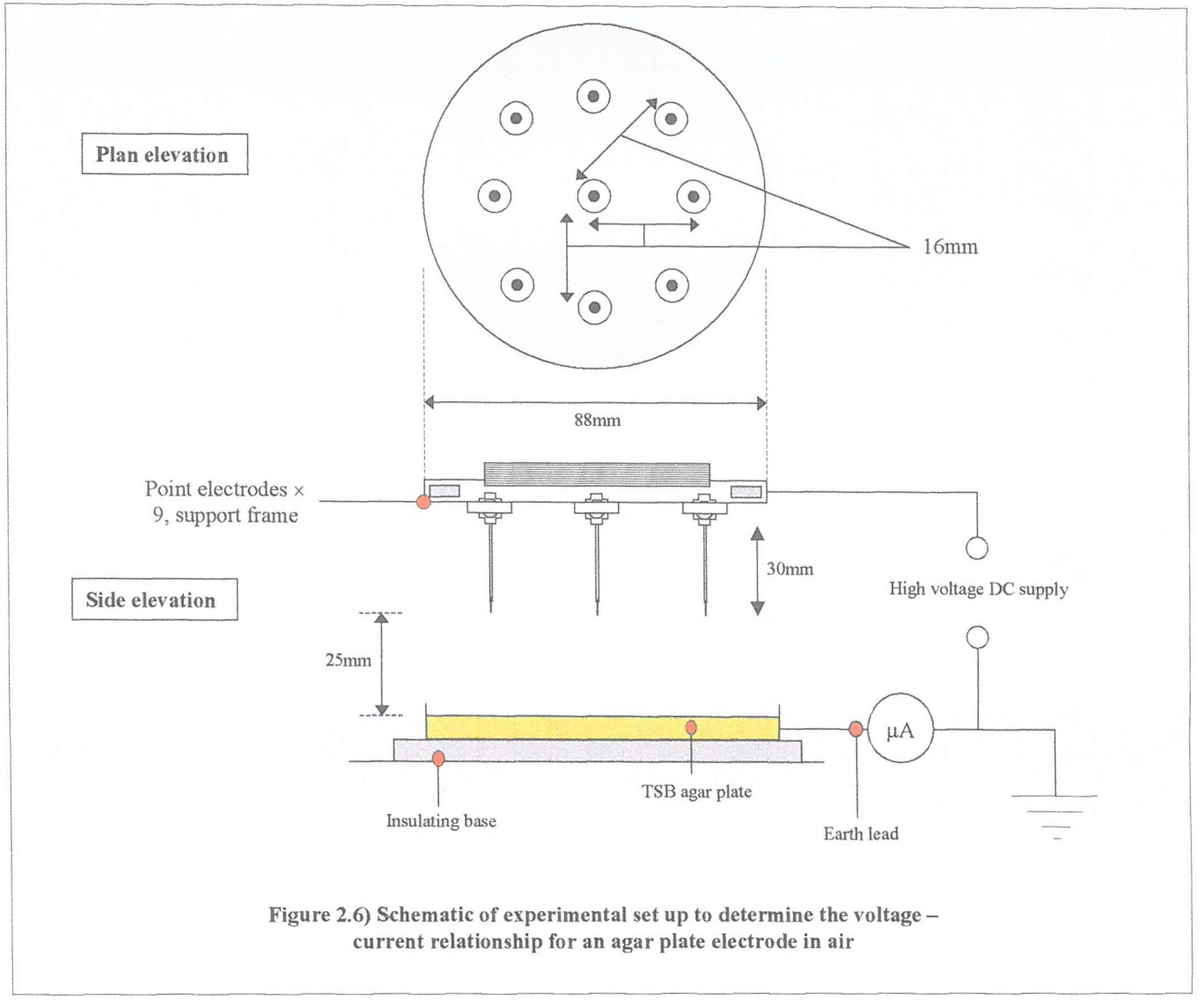

Figure 2.6) Schematic of experimental set up to determine the voltage – current relationship for an agar plate electrode in air

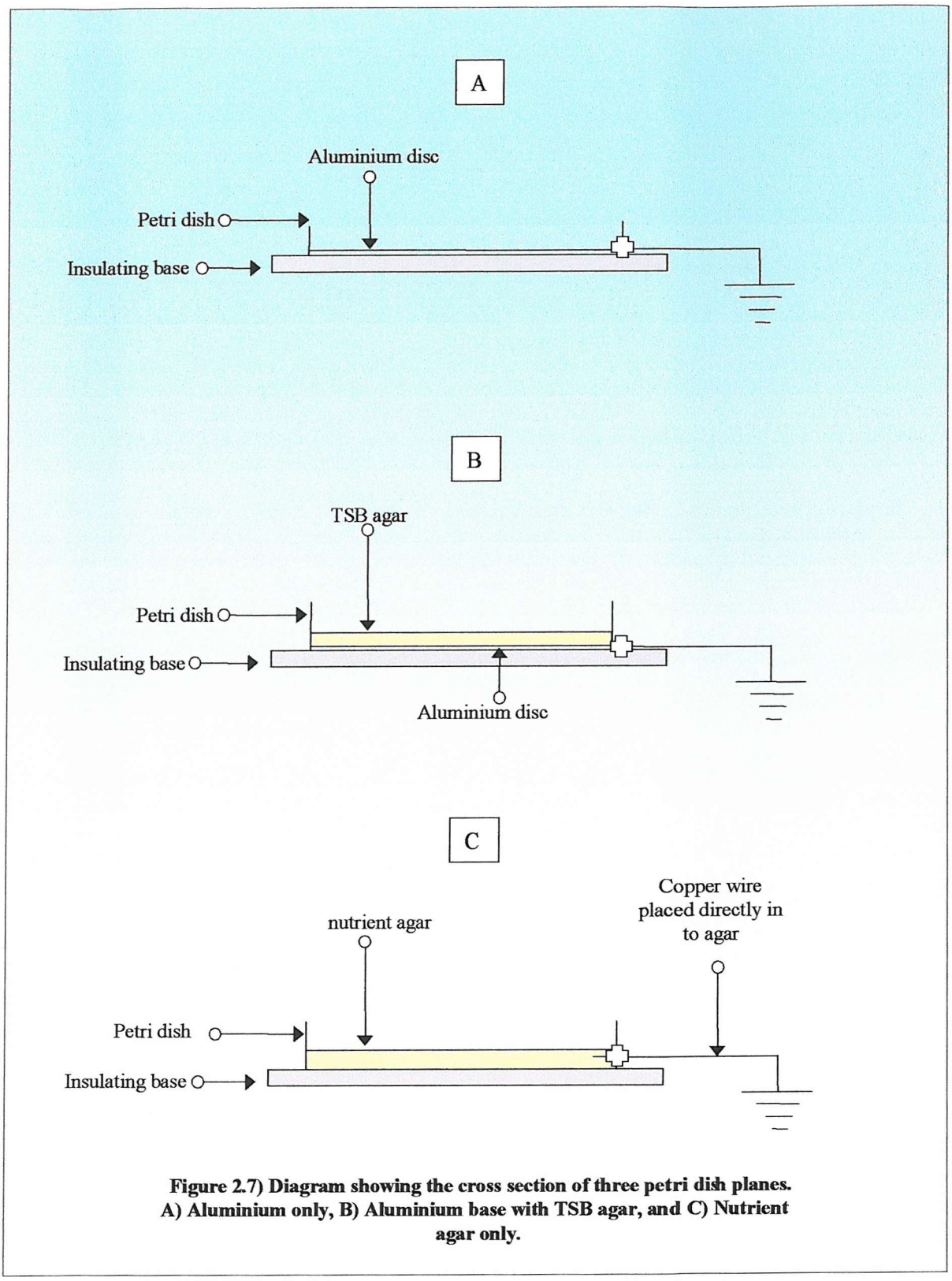

Figure 2.7) Diagram showing the cross section of three petri dish planes. A) Aluminium only, B) Aluminium base with TSB agar, and C) Nutrient agar only.

Temperature and relative humidity (RH) readings within close proximity of the experimental set up were recorded using an electronic probe (model 625, Testo Ltd, Alton, Hampshire, England). This was achieved by placing the tip of the probe level with the pin electrodes, at a distance approximately 15mm from the outer edge of the support frame. Tests were conducted at ambient room temperature (21 ± 3°C). For tests using an aluminium plane electrode, RH remained at the room level of 47 ± 6%. However, for tests using nutrient agar as the plane electrode, there was water evaporation from the agar plate surface, and as a consequence mean RH levels were 75 ± 4%.

To ascertain the effect of RH on the voltage – current relationship for a point to plane corona in air, tests using an aluminium foil plane electrode were conducted within a RH controlled room. RH within the room was controlled using the combination of a humidifier (model 2000-V, Munters, Huntingdon, England) and a dehumidifier (model MD08, Munters, Huntingdon, England). The apparatus shown in *Figure* 2.6 (*Page* 54) was used. Three different relative humidity levels were selected, 20%, 40% or 70%. The required RH level was selected, then the voltage, negative or positive, was applied to the pin electrodes in 1kV increments and the current flowing was measured in the earthed lead of the circuit.

2.13) *E.coli,* starved *P.veronii, S.aureus* or *P.veronii* biofilm exposure to negative or positive ionic exposure in air

For all experiments a point to plane geometry was utilised to generate an electrical corona and the set up shown in *Figure* 2.6 (*Page* 54) was used. The plane in each case was either an inoculated 88mm diameter agar plate (*E.coli* or *S.aureus*) or for *P.veronii* coupons (starved cells or biofilms), an 87mm diameter aluminium metal disc placed into a petri dish. For each *P.veronii* replicate, four inoculated foil coupons (starved cells or biofilms) were placed one at a time onto the aluminium plane electrode directly beneath one of the point electrodes. For each *E.coli* or *S.aureus* replicate, an inoculated plate was positioned beneath the point electrodes and earthed. The point to plane distance was adjusted to 25mm and the current was measured in the earth lead of the

circuit. Tests were conducted at ambient room temperature (21 ± 3°C) and for tests using coupons, RH was the ambient room level i.e. 47 ± 6%. For tests using agar plates, the mean RH level was 75 ± 4%. Either agar plates or coupons were exposed for a period of either ten or thirty minutes to either a negative or positive corona discharge. The current for both polarities was maintained at either 25μA or 50μA for each time period. Six replicates were completed for each time and current regime, for each bacterial sample.

The ozone concentration near the plate surface was recorded using the Dräger multi gas detector at the beginning, and then at two minutes before the termination of each experiment. This involved the use of glass, calibrated, blue Dräger tubes, which when attached to the hand held pump, allowed a gas sample to be sucked through the tube. In the presence of ozone, white discolouration occurred giving a reading in parts per million, which was subsequently corrected for atmospheric pressure. In each case the tip of the Dräger tube was placed at the same point on the edge of the petri dish. When the current was maintained at either 25μA or 50μA, for a negative applied voltage the ozone concentration remained constant at 1.0ppm. In contrast, when a positive voltage was applied to the point electrodes, the ozone concentration increased to 1.4ppm for both current regimes. The plate mass was recorded before and after exposure to determine any change in mass. Post treatment, sample plates were incubated at either 37°C for eighteen hours or 30°C for nineteen hours for *E.coli* and *S.aureus* respectively.

After the incubation period the numbers of CFU on each plate were counted using a stereomicroscope (model SDZ-PL, Kyowa Optical, Japan). Control plates were treated identically except that no corona discharge was initiated. Post exposure, *P.veronii* cell and biofilm coupons were transferred to individual, 35mm petri dishes and incubated in 3mls of Tone SB for 30 minutes. This allowed surviving cells to be resuscitated and a preliminary study had shown that a thirty-minute incubation with ToneSB was required to produce consistent and detectable readings. To initiate bioluminescence from viable cells, 50μl of nonanal was added to each petri dish in turn, prior to

placement in the luminometer for reading. In contrast to *P.veronii* cell coupons, the biofilm coupons required a six-minute incubation with the nonanal to obtain an optimal reading. This additional time was possibly required to allow aldehyde penetration of the biofilm matrix. Control coupons (cellular and biofilm) were treated identically but were not exposed to a corona discharge. Readings obtained from the luminometer were expressed in $RLUsec^{-1}$ and converted to $CFUml^{-1}$.

2.14) *E.coli*, starved *P.veronii*, *S.aureus* or *P.veronii* biofilm exposure to ozone

During experiments 2.13, ozone concentration was recorded at 1.0ppm and 1.4ppm for negative and positive ionic exposure respectively. To establish the effect of exposure to ozone without unipolar ions, either agar plates (*E.coli* / *S.aureus*) or coupons (*P.veronii* cells / *P.veronii* biofilms) were exposed to an ozone concentration of either 1.0ppm or 1.4ppm. This was achieved using an ozone production unit (model STRG-Pc-uTube, Starna Industries ltd, England) (*Figure* 2.8, *Page* 59). Inoculated samples, either plates or coupons were placed at a distance of 30mm directly beneath the outlet pipe of the ozone unit and exposed for a period of thirty minutes. Ozone concentration at the plate surface was measured using the Dräger multi gas detector. Plate mass was recorded before and after exposure to determine any change. Six replicates were completed for each ozone concentration, for each bacterial sample.

Post treatment sample plates were incubated at either 37°C for eighteen hours or 30°C for nineteen hours for *E.coli* and *S.aureus* respectively. Following the incubation period the numbers of CFU on each plate were counted using a stereomicroscope. *P.veronii* and biofilm coupons were transferred to individual, 35mm petri dishes and incubated in 3mls of Tone SB for 30 minutes, prior to reading in the luminometer as described in *Section* 2.13. Control plates and coupons were treated identically except that no exposure to ozone occurred.

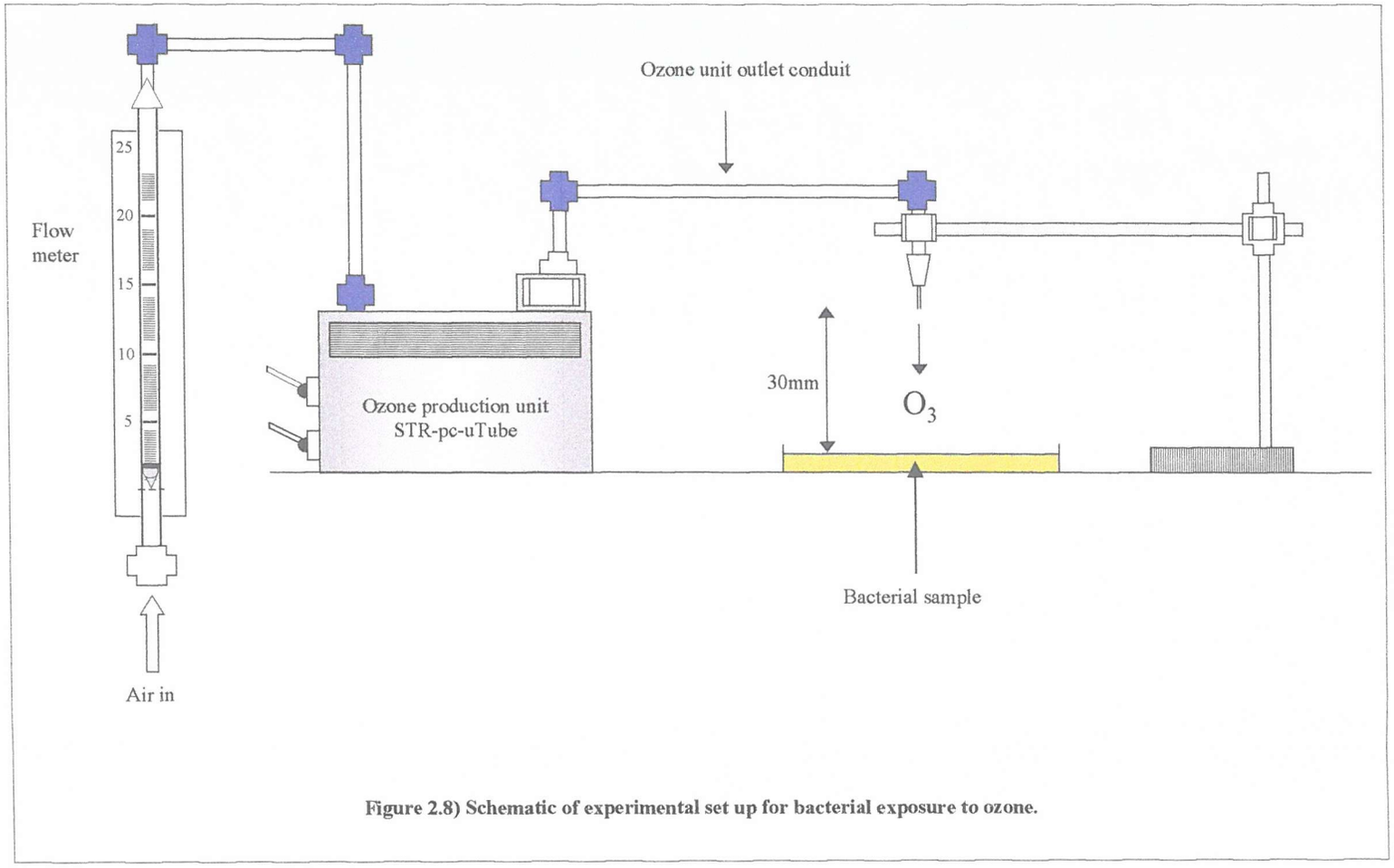

Figure 2.8) Schematic of experimental set up for bacterial exposure to ozone.

2.15) Voltage – current relationship for a point to plane corona in nitrogen

In order to eliminate ozone production it was necessary to conduct experiments in an oxygen free environment. To achieve this, a sealed chamber of volume 10 litres (dimensions: height 150mm, width 260mm, length 257mm), was used and flushed with nitrogen gas (N_2 – oxygen free, BOC Gases, Manchester, England) to remove atmospheric oxygen. To establish the effect of a nitrogen only atmosphere on the voltage – current relationship of either a positive or negative corona discharge, the experimental set-up shown in *Figure* 2.9 (*Page* 61) was used. A ninepin electrode set-up (arranged as in *Figure* 2.6) was used to ensure uniform coverage of the plane electrode, which was either a nutrient agar plate or an aluminium disc. The point to plane distance was 25mm.

Nitrogen flow in litres per minute ($lmin^{-1}$) through the chamber was measured using a rotameter attached to the outlet pipe. To allow thorough mixing of the bottled nitrogen with the atmospheric gases within the chamber, multi-directional gas jets were generated by forcing the incoming nitrogen through a 400mm, perforated, flexible tube (2mm diameter) that was attached to the inside edge of the chamber. After an initial flushing period of fifteen minutes at a flow rate of 15 l min^{-1}, the flow rate was reduced to 1 l min^{-1}. This flushing period was calculated to reduce the oxygen concentration in the chamber to 0.000001%. However, as a precaution, ozone readings were taken during experiments by attaching a Dräger tube to a sampling pipe (total length 60mm) that terminated at a distance of 6mm from the point electrodes. During all experiments using this set up no ozone was detected.

Voltage, negative or positive, was applied to the pin electrodes in 1kV increments and the current flowing was measured in the earthed lead of the circuit. Temperature and RH readings within the chamber were taken by inserting the Testo electronic probe through an access port in the side of the chamber. When positioned in the port the probe formed an airtight seal and remained in situ during experiments. All tests were conducted at ambient room temperature (21 ± 3°C).

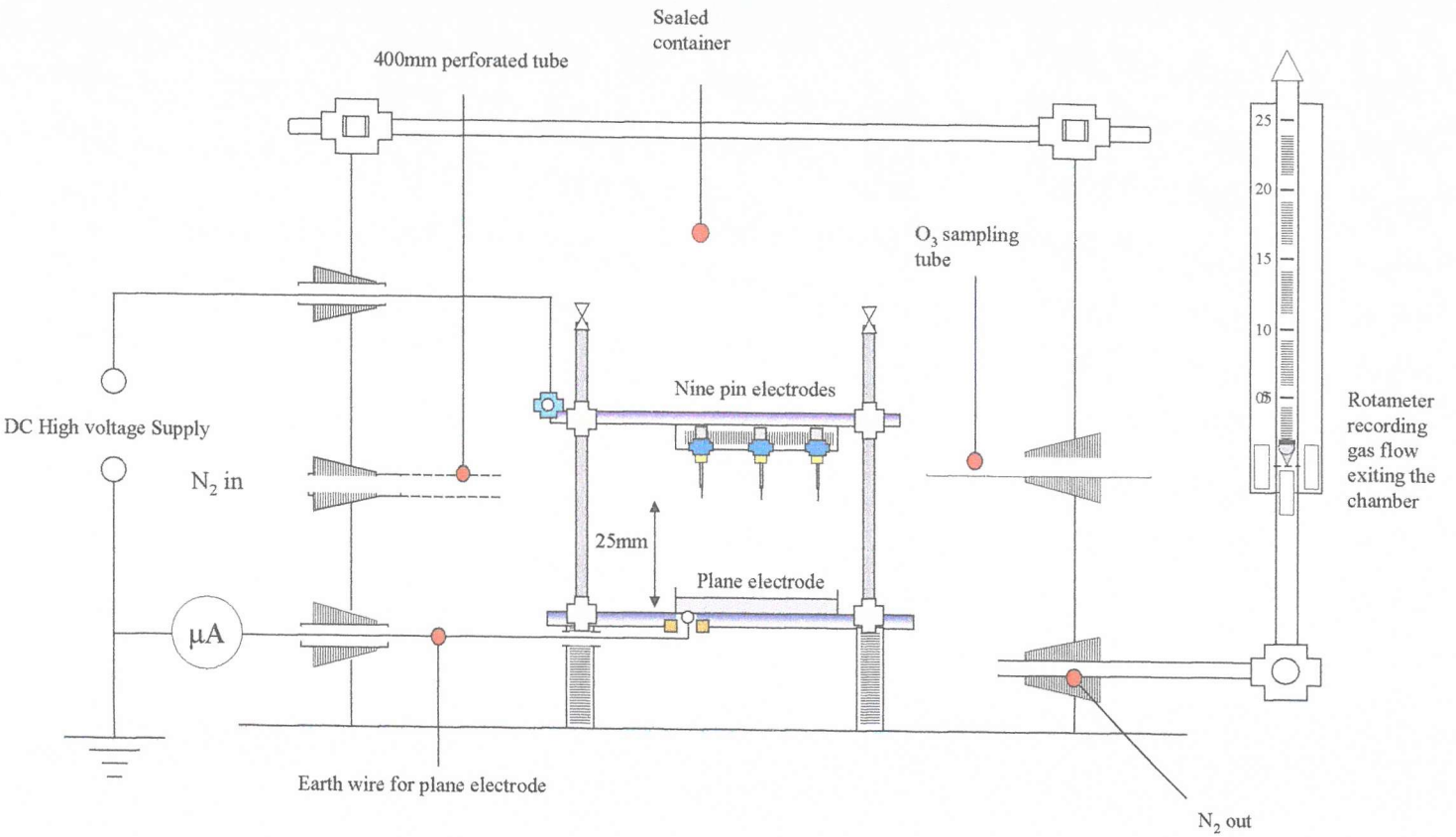

Figure 2.9) Schematic of experimental set up to determine the voltage – current relationship for a corona discharge in nitrogen.

For tests involving the use of an aluminium plane electrode the RH inside the chamber remained at the level of the bottled nitrogen i.e. 8%. For tests involving the use of nutrient agar plates the mean RH level inside the chamber was 77 ± 5%, due to water evaporation.

To establish the effect of RH level on the I-V relationship, the experimental set up shown in *Figure* 2.10 (*Page* 63) was used. The RH inside the chamber was altered by passing the nitrogen through a sealed, glass beaker (200ml) containing 10mls of water and then through a sealed, glass tube (300ml) containing varying quantities of silica gel. Depending on the quantity of silica gel present, the RH level could be selected within a ± 6% range (*Table* 2.1), which remained stable for a thirty-minute period. The interelectrode distance was 25mm and the plane electrode was an aluminium disc (diameter 87mm). After an initial flushing period of sixteen minutes at a flow rate of 15 l min^{-1}, the flow rate was reduced to 1lmin^{-1}. Voltage, positive or negative was then applied to the pin electrodes in 1kV increments and the current flowing was measured in the earthed lead of the circuit.

Silica gel (g)	Final R.H. % ± 6%
10	20
8	40
4	70

Table 2.1) Quantity of silica gel required for final relative humidity reading for experimental set-up shown in *Figure* 2.10

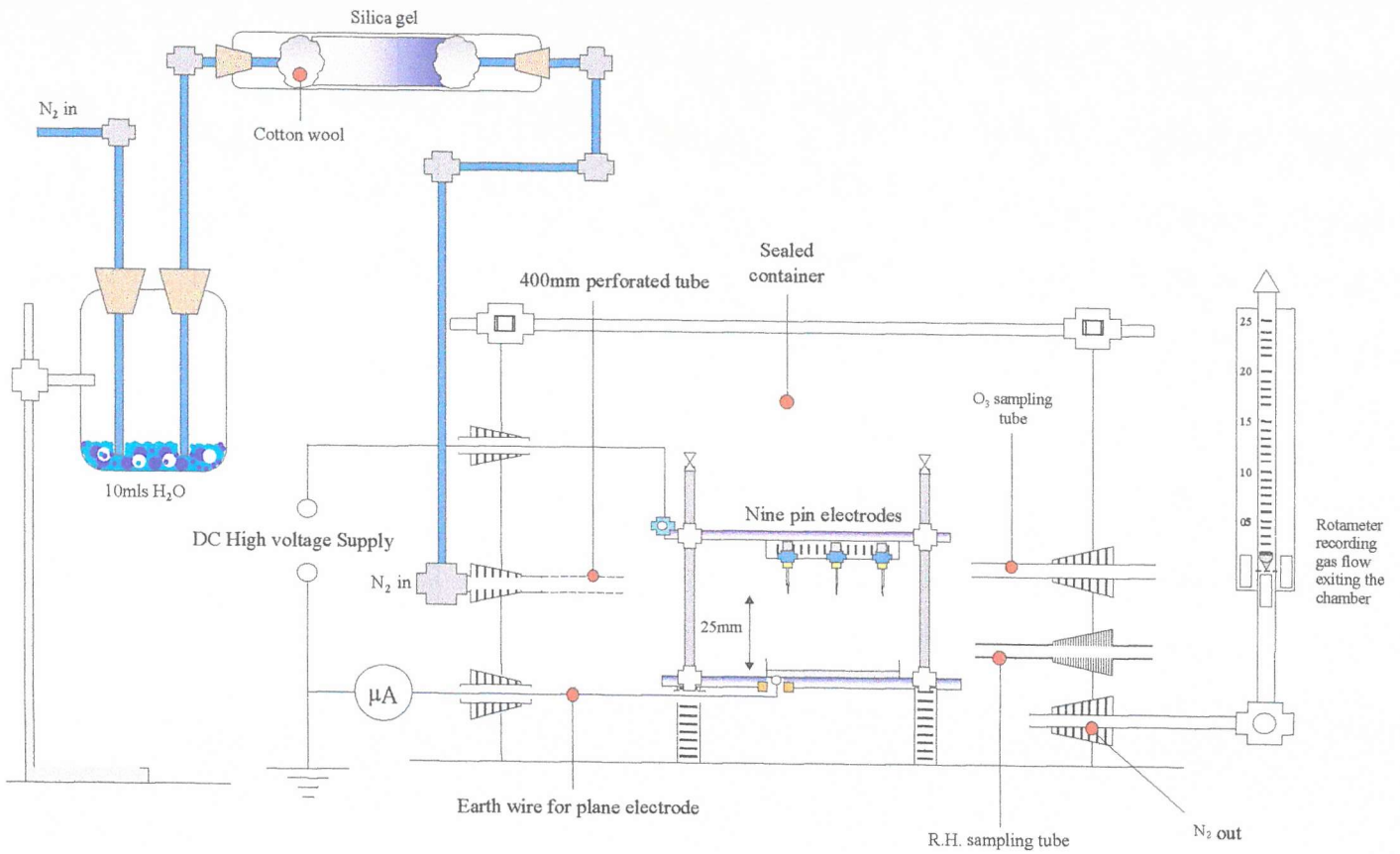

Figure 2.10) Schematic of experimental set up for establishing the current – voltage relationship in nitrogen with varying levels of relative humidity

2.16) *E.coli*, starved *P.veronii*, *S.aureus* or *P.veronii* biofilm exposure to negative or positive ionic exposure in nitrogen

The experimental set-up described in *Section* 2.15 was used. Due to the non-electronegative properties of nitrogen, for negative polarity experiments the current would increase over time for a constant applied voltage (*Figure* 3.19, *Page* 96), an effect that was independent of plane electrode material. To compensate for this and to allow comparisons between experiments, a constant current was achieved by manually adjusting the voltage applied to the pin electrodes. In contrast to negative applied voltage, positive polarity demonstrated no increase in current over time for a constant applied voltage. With RH levels of 77 ± 5%, the maximum current for negative or positive applied voltage, before electrical breakdown of the gas was 350 ± 15μA and 220 ± 15μA respectively. Therefore, tests in a nitrogen sealed chamber were limited to 350μA for negative and 200μA for positive.

Temperature and RH readings within the chamber were taken with the Testo electronic probe as described in *Section* 2.15. All tests were conducted at ambient room temperature (21 ± 3°C). For tests involving the use of an aluminium plane electrode, the RH inside the chamber remained at the level of the bottled nitrogen (8%). For tests involving the use of nutrient agar plates the mean RH level inside the chamber was 77 ± 5%. For negative ionic exposure, inoculated samples (plates or coupons) were exposed to a variable point electrode voltage to provide a constant current of 100μA, 200μA or 350μA. With a positive applied voltage, plates or coupons were exposed to a constant current of 100μA or 200μA. Exposure times for each current regime were either ten, thirty or sixty minutes. Six replicates were completed for each time and current regime, for each bacterial sample.

2.16.1) *E.coli* or *S.aureus* exposure to ions in nitrogen

After exposure to negative or positive ions, plates were incubated at 37°C for a period of eighteen hours or 30°C for a period of nineteen hours for *E.coli* and *S.aureus* respectively. After the incubation period the numbers of CFU on each plate were

counted and compared to controls. Control plates were placed into an identical chamber and exposed to the same nitrogen atmosphere, temperature and RH as the sample plates. However, no ions were generated.

2.16.2) *P.veronii* exposure to ions in nitrogen

For starved *P.veronii* cell or *P.veronii* biofilm experiments, an 87mm diameter aluminium metal disc placed into a petri dish was used as the plane electrode. For each replicate, four foil coupons were placed one at a time onto the aluminium plane electrode directly beneath one of the nine point electrodes. Control coupons were placed into an identical chamber and exposed to the same nitrogen atmosphere, temperature and RH as the sample coupons. However, no ions were generated. Post exposure, sample and control coupons were treated as described in *Section* 2.13.

2.17) *E.coli,* starved *P.veronii, S.aureus, or P.veronii* biofilm exposure to either negative or positive ions within an electric field – free region in nitrogen

Ions generated within the ionisation region of the point electrode drift towards the planar electrode under the influence of the electric field that exists between the two electrodes. Collisions with neutral species generates a bulk movement of gas in the direction of the planar electrode, with >99% of the kinetic energy of the ions transferred. This mechanism of momentum sharing gives rise to an ion wind.

However, ions approaching the planar electrode are still under the influence of the electric field. Depending on the current regime and polarity of previous tests, the applied point electrode voltage ranged from 4kV to 10kV. Based on these values, the electric field of the drift region was calculated to be between $80kVm^{-1}$ and $400kVm^{-1}$. To establish the effect of ionic interactions without the influence of an electric field, either inoculated agar plates or inoculated foil coupons were exposed to ions within a field free region for a period of either 60, 120 or 180 minutes (*Figure* 2.11, *Page* 66).

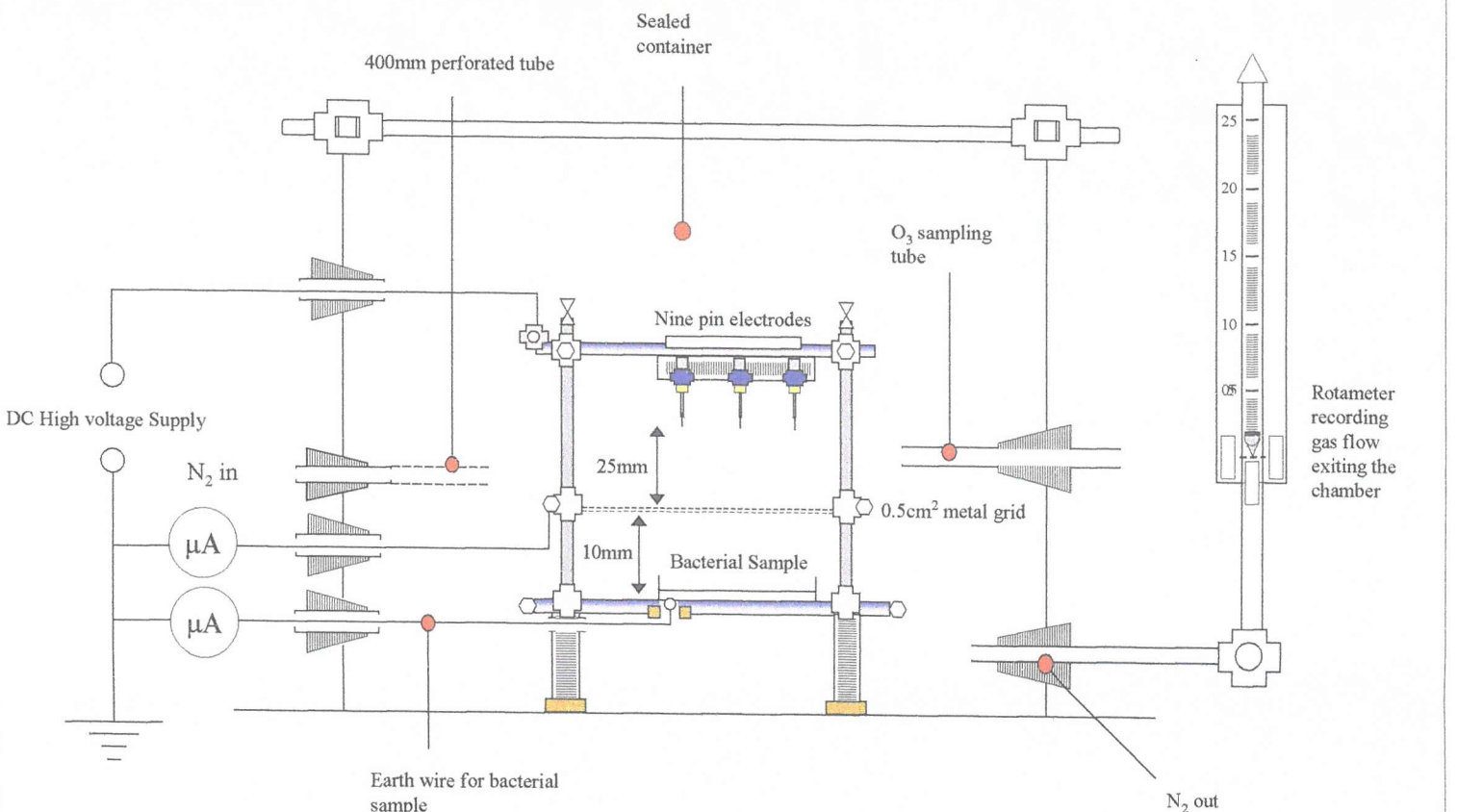

Figure 2.11) Schematic of experimental set up for bacterial exposure to negative or positive ions within an electric field-free region in nitrogen

With bacterial samples positioned between two earthed planes, any effect of an electric field was minimised or eliminated. For these experiments the first plane electrode was an earthed, 87mm diameter, 0.5cm^2 metal grid. Bacterial samples, either inoculated plates or an 87mm diameter metal disc with adhered *P.veronii* cellular or *P.veronii* biofilm coupons, were earthed and placed beneath the grid plane at a distance of 10mm. As described in *Section* 2.15, a nitrogen atmosphere was provided via an initial flushing period of fifteen minutes at a flow rate of 15 l min^{-1}, then 1 l min^{-1} for the duration of each experiment.

Voltage was applied, either positive or negative, to the series of nine point electrodes positioned at a distance of 25mm from the 0.5cm^2 metal grid electrode, and the current was measured in the earth lead of the grid plane. With a metal grid acting as the plane electrode, the ion wind was free to pass through and impinge onto the bacterial sample beneath. Although the majority of gas molecules reaching the bacterial sample would be neutral species, a proportion of charged species were able to penetrate the grid as a direct result of their momentum. The amount of current reaching the bacterial sample was measured using an Electrometer (Model 602, Keithley Instruments, Ohio, USA), placed in series with the bacterial sample earth lead. Temperature and RH readings were taken as described in *Section* 2.15. All experiments were performed at room temperature (21° ± 3°C) and for tests involving the use of an aluminium planar electrode the RH inside the chamber remained at the level of the bottled nitrogen i.e. 8%. For tests involving the use of nutrient agar plates, the mean RH level inside the chamber was 77 ± 5%.

Bacterial samples were exposed to a current of 0.75 ± 0.2μA. For a negative applied voltage this equated to a current of 300μA from the grid plane electrode. For positive corona, this equated to a current of 200μA. After exposure, *E.coli* or *S.aureus* plates were incubated at 37°C for a period of eighteen hours or 30°C for nineteen hours respectively and compared to controls. *P.veronii* coupons (starved cells or biofilms) were incubated in separate 35mm dishes with 3mls ToneSB for thirty minutes, prior to luminometer reading with 50μl nonanal as described in *Section* 2.13.

2.18) Scanning electron micrographs of *P.veronii* and *S.aureus*

In order to ascertain the physiological effect of ionic treatment in nitrogen on either Gram-negative or Gram-positive bacterial cells, scanning electron micrographs were taken of *P.veronii* or *S.aureus* cells after a sixty-minute exposure to either 200μA negative or positive ions in nitrogen. Bacterial cells were prepared as described in *Sections* 2.3 and 2.4. Once the cells were resuspended in sterile, distilled water the $O.D_{630nm}$ readings were taken and used to calculate the number of CFU ml^{-1} from *Figures* 2.2 and 2.3 respectively. With the number of CFUml^{-1} determined, both suspensions were resuspended at 500×10^6 CFU ml^{-1}.

Individual aluminium foil coupons (20 × 20 mm) were cut and placed into 88mm petri dishes and held in position with a spot of glycerol. To each foil coupon 100μl of either *S.aureus* or *P.veronii* cell suspension was added (~50×10^6 CFU). The cell suspension drops were then allowed to dry at 30°C for 120 minutes to remove all water, forming residue spots on the foil coupons. Once dry, sample coupons were exposed to ionic treatment as described above. Post treatment, control and sample coupons were prepared and photographed (Dr Alan Page, Biomedical Imaging unit, University of Southampton).

2.19) BacLight™ staining for bacterial cell wall integrity

To further elucidate the effects of ionic exposure on bacterial cells, a cell wall integrity staining technique was employed. The BacLight™ staining kit is composed of two separate nucleic acid stains; Syto-9 and Propidium iodide, which when used in conjunction with each other can differentiate between bacterial cells that have either intact or damaged cell walls. Syto-9 has an emission wavelength of 530nm (green) and stains all cells regardless of cell wall condition. In contrast, Propidium iodide has an emission wavelength of 630nm (red) and only stains cells with disrupted cell walls. In addition, Propidium iodide when bound to nucleic acid masks the emission of bound Syto-9. Using this technique, bacterial cells are stained and subsequently incubated at room temperature for fifteen minutes. Post incubation the cells are analysed using a spectrometer to obtain emission readings for both Syto-9 and Propidium iodide and the

results given as a ratio of Syto-9 to Propidium iodide (S9: P.I). Due to the nature of the stain, samples containing healthy cells will have higher ratios due to the greater Syto-9 emission. In contrast, samples containing cells with damaged cell walls will show a reduction in the ratio, due to the higher Propidium iodide emission and its masking effect on Syto-9.

E.coli, *S.aureus* and *P.veronii* cells were prepared as described in *Sections* 2.2, 2.3 and 2.4 respectively. Once resuspended in sterile, distilled water the $O.D_{630nm}$ was taken for each cell suspension and used to calculate the number of $CFUml^{-1}$. With the number determined, each cell suspension was resuspended at 500×10^6 $CFUml^{-1}$. The *P.veronii* suspension was left for 24hours at room temperature to starve the cells. The *E.coli* and *S.aureus* suspensions were used immediately. Aluminium foil coupons (20 × 20 mm) were cut and placed into 88mm diameter petri dishes (six per dish) and held in place with a drop of glycerol. To inoculate the coupons, 100µl of cell suspension (either *E.coli*, *S.aureus* or starved *P.veronii*) was added and then allowed to dry at 30°C for 120 minutes to remove all water and form residue spots. Once dry, sample coupons (four per replicate) were exposed to either 100µA or 200µA positive or negative ionic treatment in nitrogen for either thirty or sixty minutes. Post treatment, coupon residue spots were rehydrated by adding 100µl of sterile, distilled water and left at room temperature for sixty minutes. Six replicates were completed for each time and current regime, for each bacterial sample.

Post hydration, 80µl of bacterial suspension was removed from each coupon and transferred into separate wells of a white, 96 well plate. To each well, 80µl of BacLight dye (6µl Syto-9, 6µl Propidium iodide and 2mls sterile, distilled water) was added and thoroughly mixed using the pipette. The plate was then placed in darkness to incubate at room temperature for a period of fifteen minutes. Following incubation with the dye, the plate was read using a luminescence spectrometer (model LS 50B, Perkin Elmer Ltd, England) using the specified excitation and emission wavelengths for Syto-9 (Ex: 485nm, Em: 530nm) and Propidium iodide (Ex: 485nm, Em: 630nm).

2.20) Negative or positive ionic exposure and effect on nutrient agar

To establish if a corona discharge could affect the ability of either TSB agar or CGB agar medium to support either *E.coli* or *S.aureus* colony formation respectively, un-inoculated plates were exposed to either 200μA negative or positive corona in air or nitrogen for a period of 120 minutes. Experimental set-ups described in *Sections* 2.13 (Air) and 2.16 (N_2) were used. Post treatment, plates were inoculated immediately with either *E.coli* cells (as described in *Section* 2.5) or *S.aureus* cells (*Section* 2.6) and incubated at 37°C for eighteen hours or 30°C for nineteen hours respectively. After incubation, the numbers of CFU on each plate were counted using a stereomicroscope and compared to control plates, which received no ionic treatment.

2.21) Negative or positive ionic exposure and aluminium foil

For the *P.veronii* experiments (starved cells or biofilms), aluminium foil was acting as the inoculating surface instead of nutrient agar. Thus, the possibility existed that the corona discharge was interacting with the foil to produce compounds that could affect bacterial viability. To remove this possibility, uninoculated aluminium foil coupons ($2cm^2$) were placed onto an 87mm diameter metal disc, and held in place with a small drop of glycerol. The foil coupons were then exposed to 200μA positive or negative corona current in air or nitrogen for a period of 120 minutes. Following treatment, the coupons were inoculated immediately with *P.veronii* as described in *Section* 2.7 and once dry, incubated with TSB for thirty minutes, followed by luminometer reading with 50μl nonanal. Control coupons were prepared according to the standard protocol, but were not exposed to a corona discharge.

2.22) Effect of current on bacterial viability

Throughout these tests, bacterial cells have been exposed to both ionic interactions and electrical currents ranging from 1 to 350μA. To establish the effect of electrical current alone, the experimental set up shown in *Figure* 2.12 (*Page* 71) was used. Bacterial cells were cultured, harvested, washed and resuspended in sterile, distilled water to a cell density of 300×10^6 $CFUml^{-1}$. For tests using *E.coli* or *S.aureus*, standard petri dishes were replaced with rectangular dishes (120mm × 80mm).

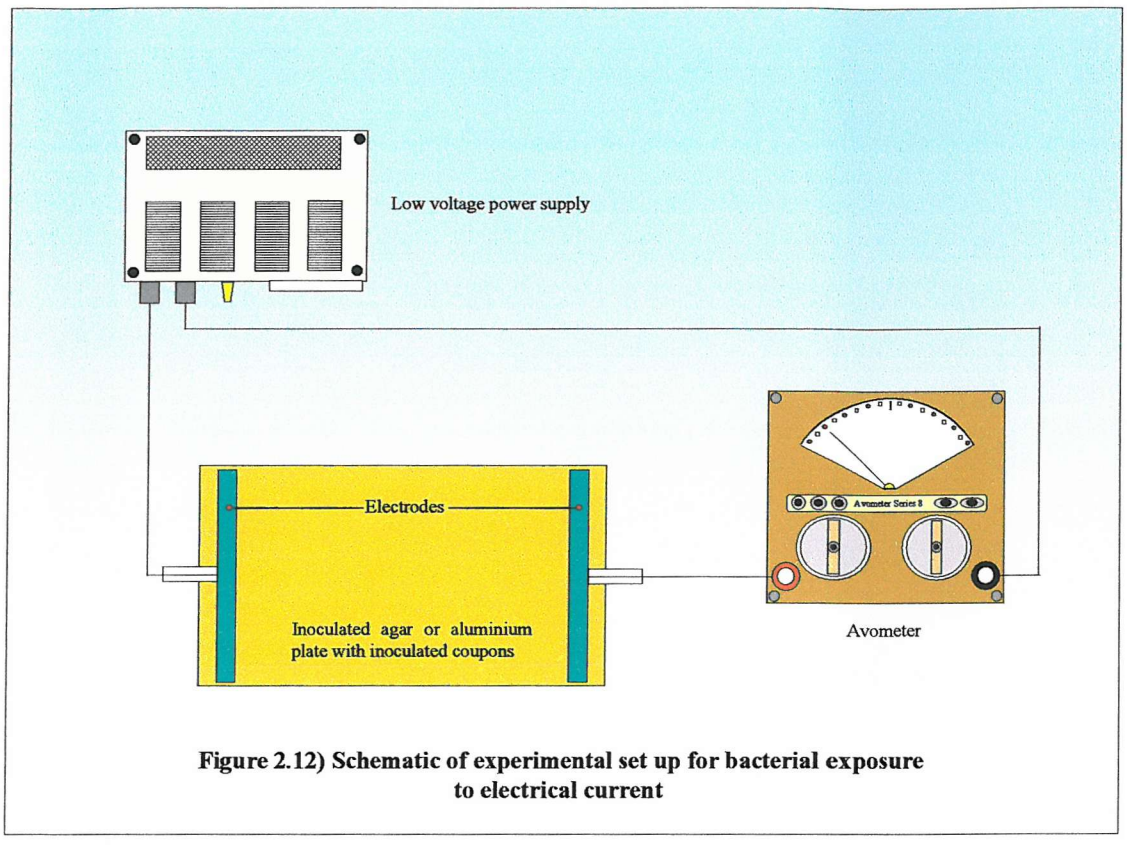

Figure 2.12) Schematic of experimental set up for bacterial exposure to electrical current

Dishes were filled with nutrient agar to a depth of 4mm and allowed to set. Once set, dishes were stored at 4°C and dried at 37°C for two hours prior to inoculation to remove excess condensation. The resuspended *E.coli* or S.aureus cultures were serially diluted in sterile, distilled water through five 1:10 dilutions and each dish was inoculated with 100µl of the final dilution, which was spread evenly over the surface of the nutrient agar with a glass spreader. To allow placement of the aluminium plate electrodes (4mm × 79mm) on the surface of the agar at each end of the dish, only the central third of the nutrient agar was inoculated.

For tests using inoculated *P.veronii* coupons (starved cells or biofilms) an aluminium plate (120 × 80mm) acted as the conduction platform. Coupons were placed in the central third to allow placement of electrodes at each end, which were connected to a low voltage power supply. Voltage was applied to the electrodes and the current measured using a series-8 Avometer. Bacterial cells were treated with 500µA of

current for 180 minutes. Post treatment, agar dishes were incubated at 37°C for a period of eighteen hours or 30°C for a period of nineteen hours for *E.coli* and *S.aureus* respectively. After incubation, the number of CFU on each plate were counted using a stereomicroscope and compared to control plates. *P.veronii* coupons (starved cells or biofilms) were incubated in separate 35mm dishes with 3mls ToneSB for thirty minutes, prior to luminometer reading with 50µl nonanal as described in *Section* 2.13.

2.23) Effect of RH on ionic treatment of *E.coli* and *S.aureus* cells

During ionic treatment of *E.coli* and *S.aureus* cells, the mean RH level was 77 ± 5% due to evaporation of water from the agar plate. This is in contrast to the tests conducted with *P.veronii*, where the RH was that of the bottled nitrogen i.e. 8%. In order to ascertain the effect of RH on ionic exposure, *E.coli* and *S.aureus* cells were cultured and resuspended in water as described in *Sections* 2.2 and 2.4 respectively. By taking $O.D_{630nm}$ readings and using *Figures* 2.1 and 2.3, the number of $CFUml^{-1}$ was obtained for the *E.coli* and *S.aureus* suspensions respectively. With the number of $CFUml^{-1}$ known, an appropriate volume was removed and resuspended in water to give a concentration of 700×10^6 $CFUml^{-1}$. For the RH tests, aluminium foil coupons ($2cm^2$) would be acting as the inoculating receptacle.

From each bacterial suspension, 100µl was taken and pipetted onto aluminium foil squares (~70×10^6 CFU). The cell suspension drops were then allowed to dry at 30°C for 120 minutes to remove all water, forming residue spots on the foil coupons. Once dry, bacterial coupons were exposed to 200µA positive or negative corona current in nitrogen for a period of sixty minutes, with RH levels of 8, 20, 40 or 70% ± 6%. The apparatus described in *Section* 2.15 was used (*Figure* 2.10, *Page* 63). For each replicate four bacterial coupons, either *E.coli* or *S.aureus* were placed one at a time onto the plane electrode directly beneath one of the point electrodes. After an initial flushing period of sixteen minutes at a flow rate of 15 l min^{-1}, the flow rate was reduced to 1 l min^{-1} and the voltage applied to the pin electrodes. Six replicates were completed for each RH regime and for each bacterial sample.

Post exposure, bacterial residue spots were rehydrated by adding 100µl of appropriate nutrient medium and incubated at room temperature for one hour. Following the incubation, 100µl was removed and serially diluted in sterile water through four 1:10 dilutions. From the final dilution, nutrient agar plates were inoculated with 100µl, which was spread evenly over the surface with a glass spreader. Agar plates were then incubated at 37°C for a period of eighteen hours or 30°C for a period of nineteen hours for *E.coli* and *S.aureus* respectively. After incubation the numbers of CFU on each plate were counted using a stereomicroscope and compared to control plates. Control bacterial coupons were treated identically except no exposure to corona ions occurred.

2.24) *E.coli*, starved *P.veronii*, *S.aureus* or *P.veronii* biofilm exposure to evaporation

The movement of ions under the influence of the electric field that exists between the point and plane electrodes generates an ion wind. To determine if this evaporative wind was contributing to the reduction in bacterial viability, either inoculated plates (*E.coli* or *S.aureus*) or coupons (starved *P.veronii* / *P.veronii* biofilms) were exposed to a gas flow similar to that generated by a positive ion wind in nitrogen i.e. ~ 1.7 m s^{-1}. Ion wind velocity readings were obtained by placing a gas velocity meter (model AV2, Airflow Developments Ltd, High Wycombe, Buckinghamshire, England) beneath the grid electrode of the experimental set-up shown in *Figure* 2.11 (*Page* 66). With the gas velocity meter in place, the chamber was flushed with nitrogen (15 l min^{-1}, 15mins) and then voltage was applied to the point electrodes to produce a current of 200µA from the grid electrode and the ion wind velocity recorded. Readings were also obtained for a negative applied voltage with a current of 350µA.

Bacterial samples were exposed to an evaporative wind through the use of a variable speed electric fan placed at a distance of 80mm above the sample (*Figure* 2.13, *Page* 74). The flow of gas generated by the fan was calibrated by the use of the air velocity meter.

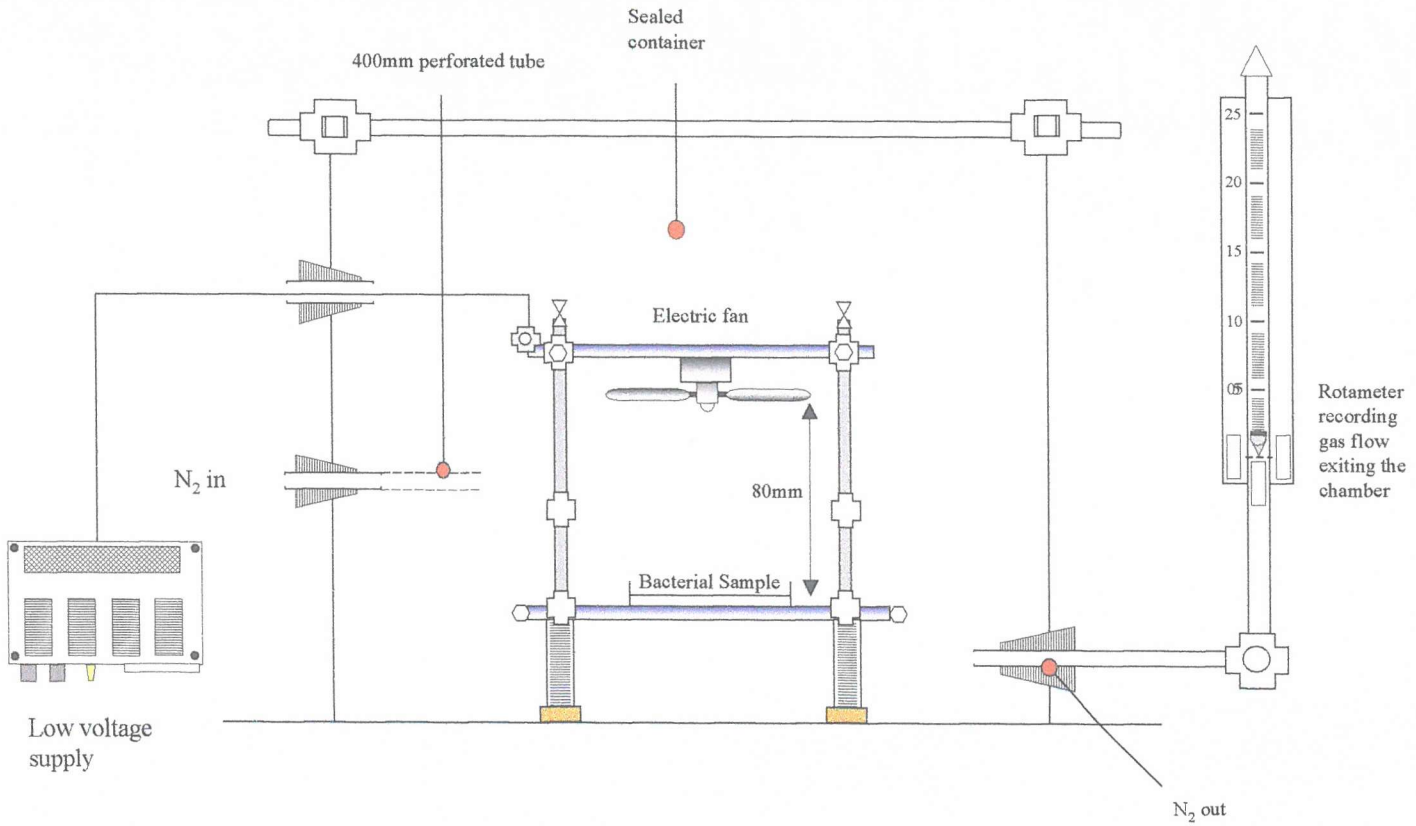

Figure 2.13) Schematic of experimental set up for bacterial exposure to non-ionic gas flow in nitrogen

After an initial flushing period of fifteen minutes at a flow rate of 15 l min^{-1}, the nitrogen flow rate was reduced to 1 l min^{-1} and the electric fan was switched on. Either plates or coupons (adhered using glycerol to an 87mm diameter aluminium disc) were placed beneath the fan and exposed for a period of 180 minutes. Plate mass before and after treatment was recorded and loss in mass was within the same limits produced by exposure to either positive or negative corona ion wind. After the exposure, plates were incubated at 37°C for a period of eighteen hours or 30°C for a period of nineteen hours for *E.coli* and *S.aureus* respectively. After incubation the number of CFU on each plate were counted using a stereomicroscope and compared to control plates. *P.veronii* coupons (starved cells or biofilms) were incubated in separate 35mm dishes with 3mls ToneSB for thirty minutes, prior to luminometer reading with 50µl nonanal as described in *Section* 2.13.

2.25) *E.coli*, starved *P.*veronii, S.*aureus, or P.veronii* biofilm exposure to a nitrogen only atmosphere

E.coli, *P.veronii* and *S.aureus* are facultative aerobes, i.e. they are not reliant on oxygen for respiration. To evaluate exposure to an oxygen free environment i.e. N_2 only, for an extended period of time, either inoculated plates (*E.coli* / *S.aureus*) or coupons (starved *P.veronii* cells / *P.veronii* biofilms) were placed into a sealed container (volume 10 litres) and exposed to a nitrogen only atmosphere for a period of 180 minutes. After the exposure, plates were incubated at 37°C for a period of eighteen hours or 30°C for a period of nineteen hours for *E.coli* and *S.aureus* respectively. After incubation the number of CFU on each plate were counted using a stereomicroscope and compared to control plates. *P.veronii* coupons were incubated in separate 35mm dishes with 3mls ToneSB for thirty minutes, prior to luminometer reading with 50µl nonanal as described in *Section* 2.13.

2.26) Effect of temperature on negative or positive ionic treatment in nitrogen

Throughout the previous experiments temperature readings were recorded, resulting with a mean value of 21 ± 3°C. The fluctuation in temperature was due to seasonal changes and the ambient laboratory temperature reflected this. The nitrogen gas was

always within 0.5°C of the ambient laboratory temperature. To establish if temperature could affect the antibacterial efficiency of ionic exposure, a series of tests were conducted at two set temperature levels. This was achieved through the addition of a heating element in the base of the experimental chamber. By simply switching the element on and off various temperature levels could be achieved. Temperature was monitored using the electronic probe as described in *Section* 2.15.

Two different temperature levels were selected to reflect winter (18°C) and summer (24°C) laboratory conditions. Nitrogen gas was flushed through the chamber to remove all atmospheric oxygen and the heating element activated until the desired temperature was achieved. Either inoculated agar plates (*E.coli/ S.aureus*) or aluminium coupons (*P.veronii/ P.veronii* biofilms) were exposed to 100μA of either negative or positive ions at an inter-electrode distance of 25mm, for a period of sixty minutes. After exposure, plates were incubated at 37°C for a period of eighteen hours or 30°C for nineteen hours for *E.coli* and *S.aureus* respectively. Post incubation, the number of CFU on each plate were counted and compared to controls. Sample and control *P.veronii* coupons (starved cells or biofilms) were incubated in separate 35mm dishes with 3mls ToneSB for thirty minutes, prior to luminometer reading with 50μl nonanal.

2.27) Statistical analysis

Data was expressed as the mean ± the standard error of the mean (SEM). For group comparison a Mann-Whitney *U*-test was used. For relationships between variables a Spearman rank correlation was used. Statistical significance was defined as $P<0.05$. Statistical procedures were performed using SPSS version 10.0.5, and graphical analyses were performed with Microsoft's Excel, version 6.0.

Chapter Three

Results

3.1) Relationship between *P.veronii* viability and bioluminescence readings in $RLUs^{-1}$

Initial experiments investigated the relationship between viability of *P.veronii* cells and bioluminescence. As shown in *Figure* 3.1 a significant positive correlation (rho = 0.96, $p<0.01$) was found between $RLUsec^{-1}$ and % viable cells, allowing subsequent results to be directly linked to the viability of *P.veronii*.

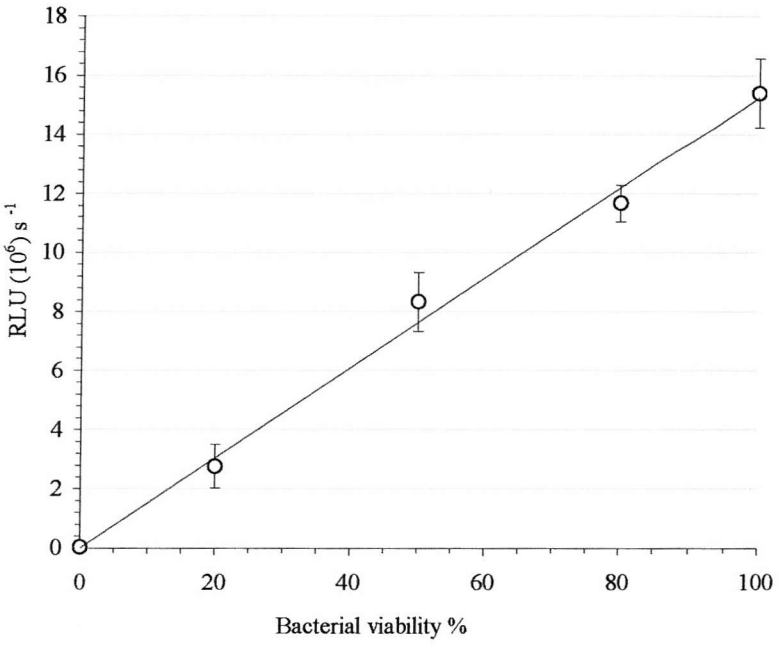

Figure 3.1) Relationship between relative light units per second and viability. A 19hour *Pseudomonas veronii* resuspended at a concentration of 50×10^6 $CFUml^{-1}$. Half of the suspension was removed and placed in ethyl alcohol for three hours to kill all cells and then washed twice in sterile, distilled water by centrifugation (21° ± 3°C, ten minutes, 3200 × g), and then resuspended in sterile, distilled water at 50×10^6 $CFUml^{-1}$. The viable and non-viable suspensions were then mixed to give the following proportions of percent alive cells: zero, 20%, 50%, 80% and 100%. From each new suspension 1ml was taken and 50µl of nonanal added to obtain a reading in $RLUsec^{-1}$. Points represent the mean (n = 3).

3.2) Relationship between *P.veronii* bioluminescence readings in $RLUs^{-1}$ and number of $CFUml^{-1}$

A significant positive correlation (rho = 0.92, $p<0.01$) was found between $RLUsec^{-1}$ and $CFUml^{-1}$. From this data 1 $RLUsec^{-1}$ unit equates to 3.5 $CFUml^{-1}$ (*Figure* 3.2, *Page* 79). From these results and to enable comparisons between bacterial types, subsequent data concerning units in $RLUsec^{-1}$ were converted to $CFUml^{-1}$.

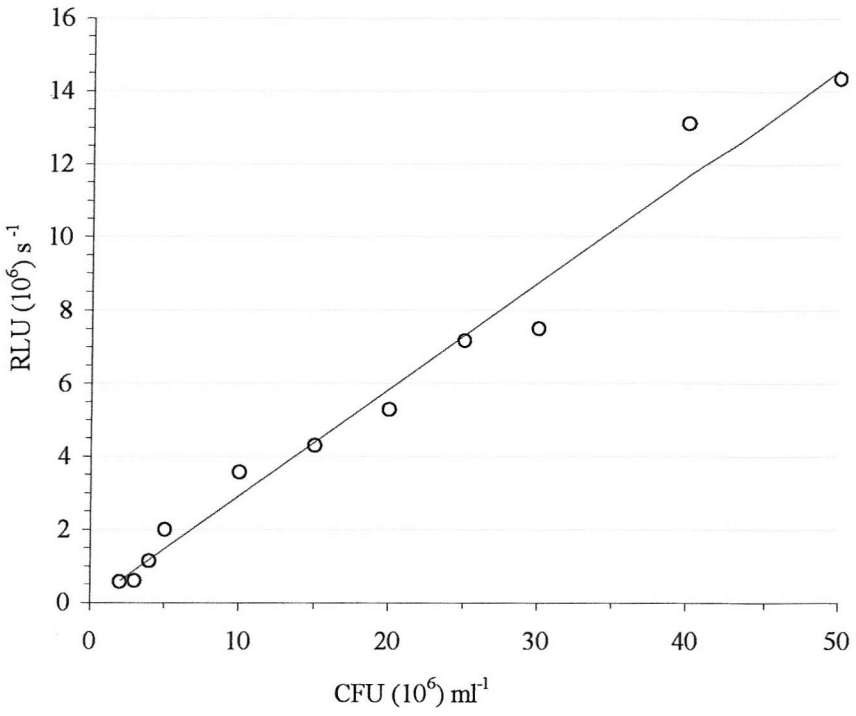

Figure 3.2) Relationship between relative light units per second and colony forming units per ml. A 19hour *Pseudomonas veronii* culture was resuspended at a concentration of 50 x 10^6 $CFUml^{-1}$. This suspension was then diluted to give suspensions of 40, 30, 25, 20, 15, 10, 5, 4, 3 and 2 x 10^6 $CFUml^{-1}$. From each dilution 1ml was taken and 50µl of nonanal added to obtain a reading in $RLUsec^{-1}$. The number of $CFUml^{-1}$ was subsequently plotted against the $RLUsec^{-1}$ reading for that dilution.

3.3) Congo red staining for biofilm formation

To confirm the formation of *P.veronii* biofilms, Congo red staining was employed (*Page* 52). *Figure* 3.3 (*Page* 80) shows the result of staining either the precipitated biomaterial from the *P.veronii* coupons or planktonic cells. Biofilm formation on the coupons was confirmed, as the precipitated sample clearly stained red due to the presence of EPS. For the planktonic cellular sample no staining has occurred, confirming no EPS formation and consequently no biofilm status.

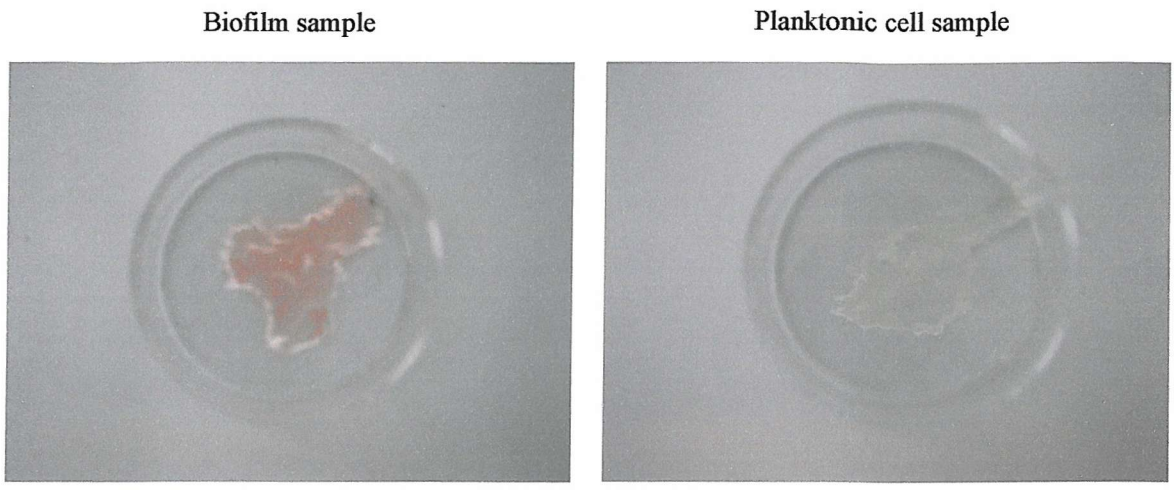

Figure 3.3) Congo red staining of biofilm coupons and planktonic *P.veronii* cells. Either biofilm coupons, or planktonic cells suspended in distilled water, were treated with 10mM cetylpyridinium chloride. After a five-minute incubation, 500µl of each solution was transferred to a clean 35mm petri dish and allowed to dry at 37°C for two hours, forming a residue spot. Once dry, 2mls of Congo red solution was added to each petri dish and incubated at room temperature for fifteen minutes. After incubation with Congo red, the residue spots were gently washed twice with distilled water and analysed.

3.4) Voltage – Current relationship for a point to plane corona in air

In the proposed experiments in which *E.coli* or *S.aureus* would be subjected to ionic exposure, a TSB or CGB agar plate would be acting as the plane electrode. Failure of the nutrient agar plates to conduct charge would prevent the onset of corona. Thus, initial experiments investigated the ability of these nutrient agar plates to perform electrically as ground planes. This was compared to an aluminium plane and a TSB agar plate with an aluminium base. *Figure* 3.4 (*Page* 81) shows the voltage – current relationship for the four different plane electrodes with negative applied voltage. The end point of each curve represents electrical breakdown of the interelectrode gas.

Both the TSB and CGB agar plates produced virtually identical I-V curves, although for any given applied voltage the magnitude of the current recorded from the TSB plate was greater than from the CGB plate, but not significantly so ($p>0.05$). With an applied voltage of 13kV, the current measured from the TSB and CGB plates was

246μA and 209μA respectively. The modification of the TSB agar plate with the addition of aluminium foil in the base, significantly increased the electrical characteristics of the media and shifted the I-V curve for the TSB plate to the left i.e. increased the recorded current for a given applied voltage. With an applied voltage of 12kV the mean current recorded from the TSB and TSB hybrid plane electrodes was 225μA and 280μA respectively. With the aluminium plane electrode there was no significant difference in the current recorded for applied voltages up to 12kV when compared to the TSB hybrid plane. However, the I-V curve for the aluminium plane did extend up to 405μA (15kV) before breakdown.

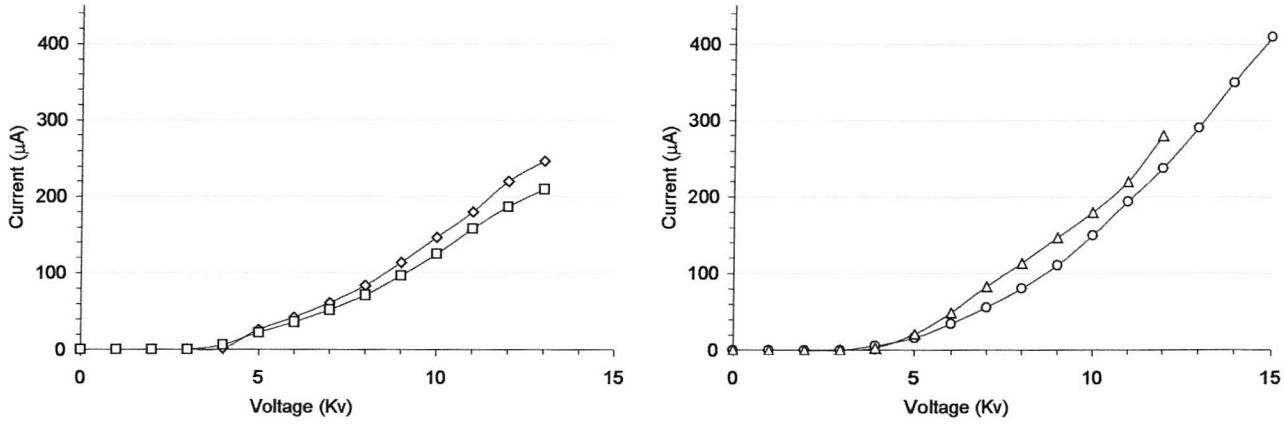

Figure 3.4) Voltage-current relationship for four different plane electrodes with a negative point electrode in air. A nine pin to plane corona geometry was used at an interelectrode distance of 25mm. Four different plane electrodes were tested. TSB agar plate (◇), a CGB agar plate (□), an aluminium disc (○) and a TSB agar plate with an aluminium base (△). Voltage was applied to the pin electrodes in 1kV increments and the current in μA recorded. Points represent the mean (n = 4).

Aluminium, like all metals, is a good conductor of electrical charge (due to the delocalisation of their electrons), and was expected to be more conductive than the TSB or CGB agar media. The conductivity of the TSB and CGB agar media was $3.3 \times 10^{4}Sm^{-1}$ and $1.9 \times 10^{4}Sm^{-1}$ respectively. In comparison, the hybrid TSB plate and aluminium plane had conductivity readings of $2.4 \times 10^{5}Sm^{-1}$ and $1.4 \times 10^{7}Sm^{-1}$ respectively. Both the TSB and CGB agar were sufficiently conductive to allow corona onset, thus allowing standard agar plates to be used without the need for modification i.e. the insertion of aluminium foil into the base of the petri dish.

The effect of changing the polarity of the point electrodes to positive can be seen in *Figure* 3.5. For all plane electrodes significantly less current was recorded in comparison to negative corona. However, negative coronas typically generate greater current levels due to the higher number of electrons that escape attachment as the electric field intensifies around the point electrode. With an applied positive voltage of 15kV the magnitude of current flowing through the TSB and CGB plates was 76μA and 69μA respectively. The TSB hybrid and aluminium plane electrodes significantly ($p<0.05$) enhanced these values to 95μA and 127μA respectively, current levels that reflect their respective conductivity readings.

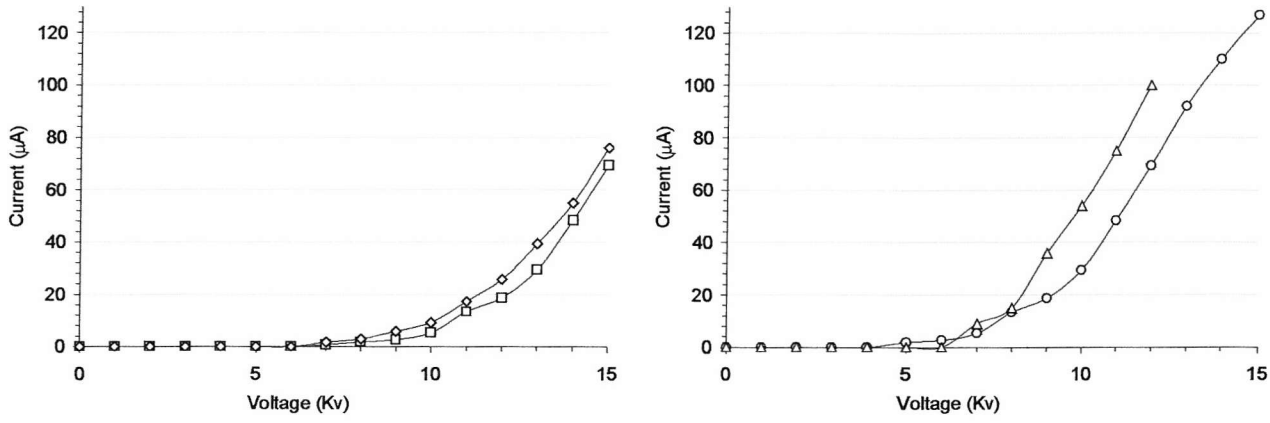

Figure 3.5) Voltage-current relationship for four different plane electrodes with a positive point electrode in air. A nine pin to plane corona geometry was used at an interelectrode distance of 25mm. Four different plane electrodes were tested. TSB agar plate (◇), a CGB agar plate (□), an aluminium disc (○) and a TSB agar plate with an aluminium base (△). Voltage was applied to the pin electrodes in 1kV increments and the current in μA recorded. Points represent the mean (n = 4).

With the use of nutrient agar plates as plane electrodes, there was water evaporation from the plate surface due to the action of the ion wind, and consequently relative humidity (RH) levels increased during the course of each test. The effect of RH on the negative and positive I-V relationship for a point to aluminium plane electrode can be seen in *Figure* 3.6 (*Page* 83). Regardless of polarity, increasing the RH level reduced the applied voltage required for a given current value. As the RH level increased the water vapour pressure in the inter-electrode space approached saturation. This in turn increased the conductivity of the air, resulting in higher current levels for a given applied voltage. This effect also explains why the TSB hybrid plane with a lower

conductivity value produced a similar I-V curve to the aluminium plane, as the mean RH level recorded during measurements was significantly greater at 75%, compared to 47% for the aluminium plane.

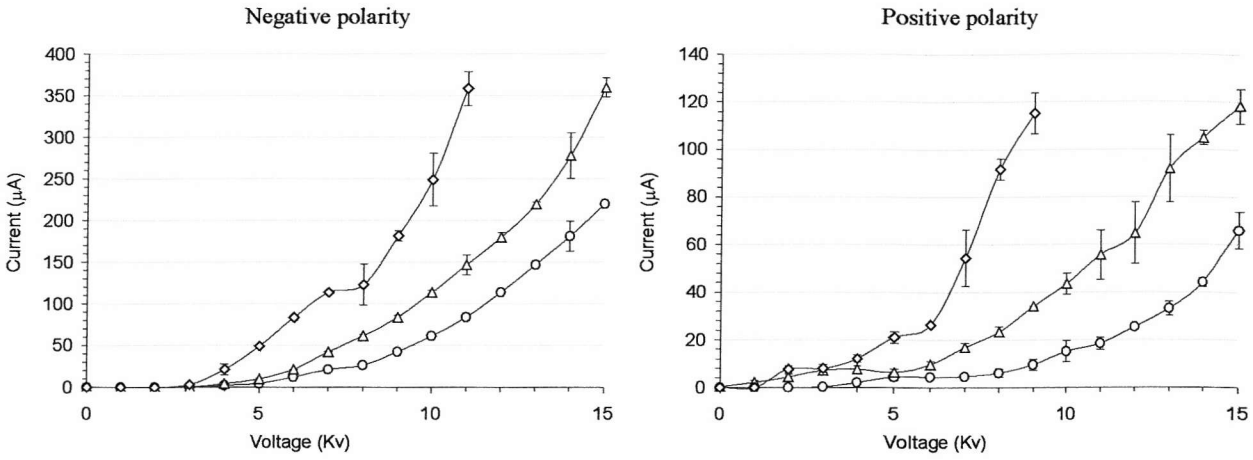

Figure 3.6) Effect of RH on the voltage-current relationship for a negative or positive corona discharge in air. A nine pin to aluminium foil plane corona geometry was used at an interelectrode distance of 25mm. Three different RH levels were tested, 20% (◯), 40% (△) and 70% (◇). Voltage was applied to the pin electrodes in 1kV increments and the current in μA recorded. Points represent the mean (n = 4) ± S.E.M.

3.5) Effect of negative or positive ionic exposure in air on *E.coli*, starved *P.veronii*, *S.aureus* or *P.veronii* biofilms

A series of experiments investigated the effect of either negative or positive ionic exposure in air on bacterial samples. Inoculated plates or coupons were exposed to either 25μA or 50μA current flow for a period of either ten or thirty minutes. Exposure to 25μA of negative or positive ions for *E.coli*, *S.aureus*, starved *P.veronii* cells and *P.veronii* biofilms can be seen in *Figures* 3.7 to 3.10 (*Pages* 84 to 85).

From *Figure* 3.7 it can be seen that both corona polarities produced a significant reduction ($p<0.05$) in the number of *E.coli* $CFUml^{-1}$, but only after an exposure time of thirty minutes. The shorter exposure time of ten minutes was insufficient to produce any significant effect. It is also apparent that negative corona exposure at 25μA was significantly ($p<0.05$) more efficient at disinfecting the plates with a mean $CFUml^{-1}$ reduction of 39%, compared to positive corona exposure with a mean reduction of 24% after thirty minutes.

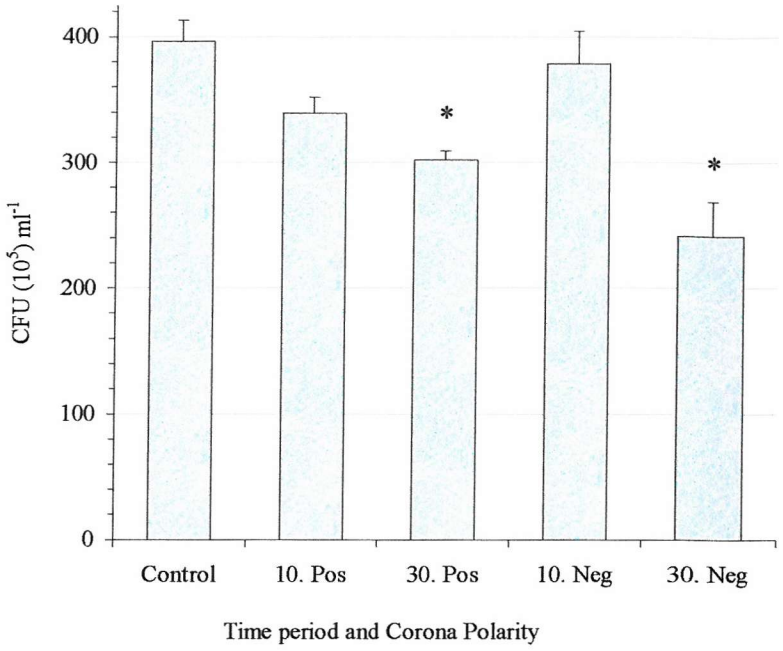

Figure 3.7) Effect of 25μA negative or positive ionic exposure in air on *E.coli*. A set of nine pins equally spaced above an agar plate at a point to plane distance of 25mm was used. Voltage was applied to the pin electrodes to give a current of 25μA, for 10 or 30 minutes. Plates were subsequently incubated at 37°C for eighteen hours and the number of CFU counted and compared to controls (time zero). Bars represent the mean (n = 6) ± S.E.M. and * indicates $p<0.05$.

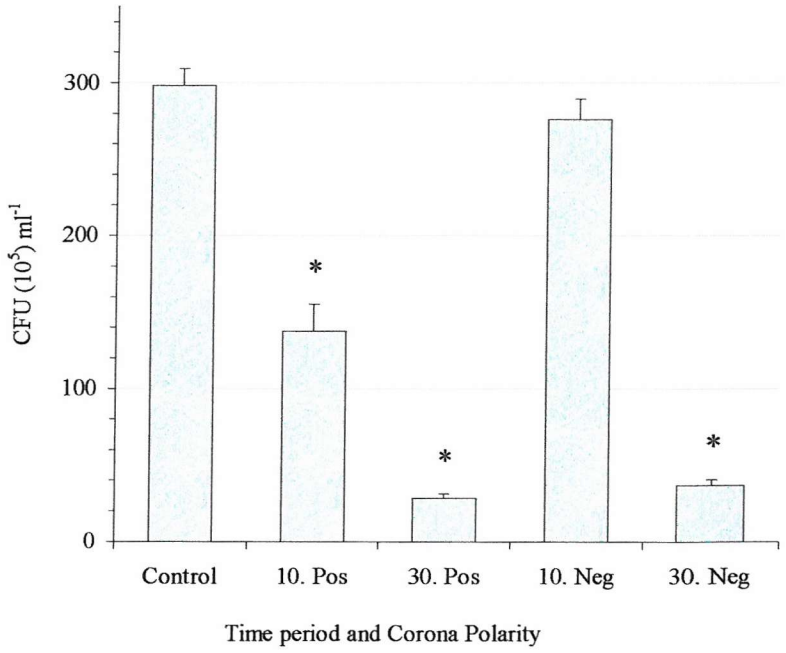

Figure 3.8) Effect of 25μA negative or positive ionic exposure in air on *S.aureus*. A set of nine pins equally spaced above an agar plate at a point to plane distance of 25mm was used. Voltage was applied to the pin electrodes to give a current of 25μA, for 10 or 30 minutes. Plates were subsequently incubated at 30°C for nineteen hours and the number of CFU counted and compared to controls (time zero). Bars represent the mean (n = 6) ± S.E.M. and * indicates $p<0.05$.

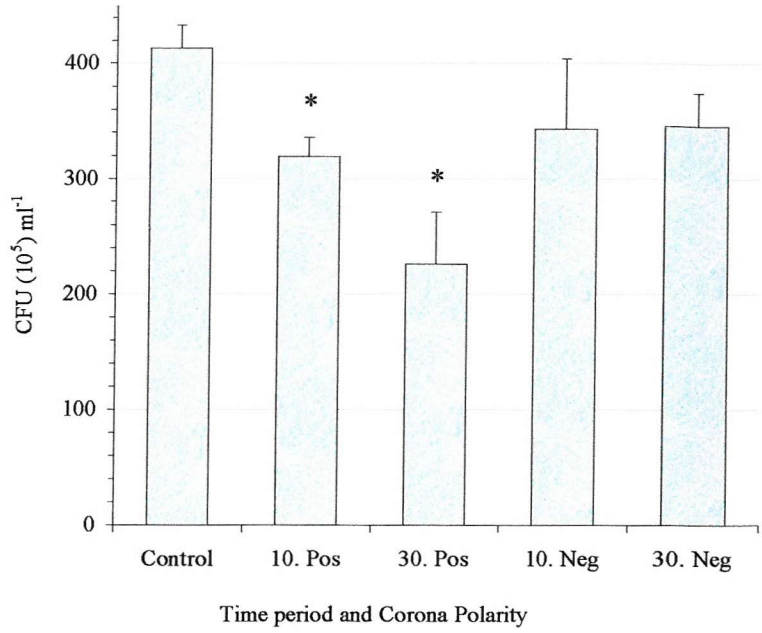

Figure 3.9) Effect of 25μA negative or positive ionic exposure in air on starved *P.veronii*. A set of nine pins spaced equally above an 87mm diameter metal disc, at a distance of 25mm was used. Inoculated foil coupons ($2cm^2$) were positioned on the disc directly beneath a pin electrode. Voltage was applied to the pin electrodes to produce 25μA current for a period of either 10 or 30 minutes. Coupons were subsequently incubated in TSB for thirty minutes prior to reading in a luminometer with 50μl nonanal and compared to controls. Bars represent the mean (n = 6) ± S.E.M. and * indicates $p<0.05$.

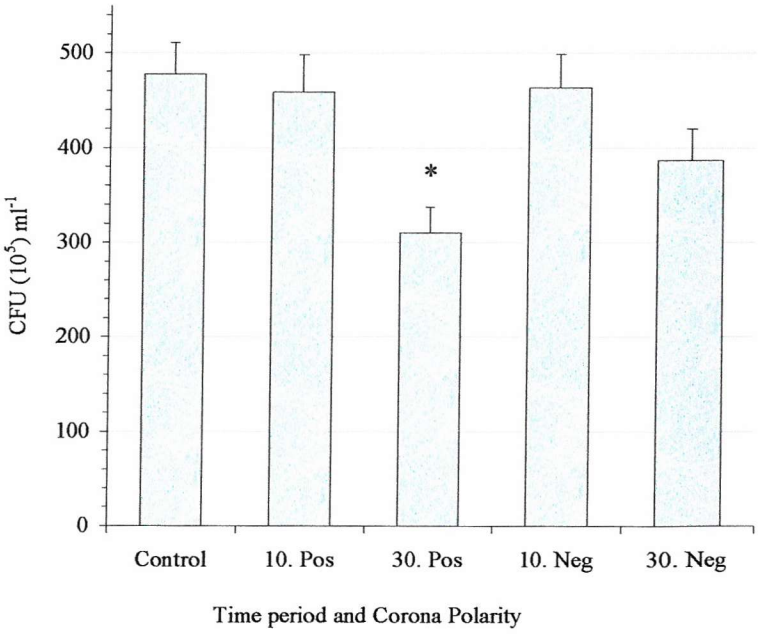

Figure 3.10) Effect of 25μA negative or positive ionic exposure in air on *P.veronii* biofilms. A set of nine pins spaced equally above an 87mm diameter metal disc, at a distance of 25mm was used. Biofilm foil coupons ($2cm^2$) were positioned on the disc directly beneath a pin electrode. Voltage was applied to the pin electrodes to produce 25μA current for a period of either 10 or 30 minutes. Biofilms were subsequently incubated in TSB for thirty minutes prior to reading in a luminometer with 50μl nonanal and compared to controls. Bars represent the mean (n = 6) ± S.E.M. and * indicates $p<0.05$.

For *S.aureus*, ten minutes negative corona exposure was insufficient to have any effect on the number of $CFUml^{-1}$ (*Figure* 3.8). However, the longer exposure period of thirty minutes did produce a significant reduction of 88%. Changing the corona polarity to positive produced significant reductions in cell viability with both time regimes. After ten and thirty minute exposures the mean $CFUml^{-1}$ number was 138×10^5 and 28×10^5 $CFUml^{-1}$ respectively, representing mean reductions of 54% and 90%. Comparisons between sample groups for thirty minutes negative or positive exposure showed no significant difference.

In contrast to treatments of *E.coli* and *S.aureus*, after ten or thirty minutes exposure on starved *P.veronii* cells (*Figure* 3.9) with a negative applied voltage, there was no significant reduction ($p<0.05$). However, with a positive applied voltage there were significant reductions ($p<0.05$) in the number of $CFUml^{-1}$ for the ten and thirty minute time regimes, with mean reductions of 23% and 45% respectively. With *P.veronii* biofilms as the bacterial target (*Figure* 3.10) there was no significant reduction in $CFUml^{-1}$ number for both time periods with a negative corona. With a positive applied voltage there was a significant reduction ($p<0.05$) in the number of $CFUml^{-1}$, but only after thirty minutes exposure with a mean reduction of 35%. The effect of increasing the corona current to 50μA can be seen in *Figures* 3.11 to 3.14 (*Page*s 87 - 88).

For *E.coli* (*Figure* 3.11) exposure to negative corona at this current level had no significant effect after ten minutes. However, thirty minutes exposure produced a mean reduction of 70%. In contrast to 25μA exposure where negative treatment was more detrimental, the positive corona discharge at 50μA was more effective at reducing the number of $CFUml^{-1}$. Significant differences ($p<0.05$) between control and sample plates were found for both time regimes when the point electrodes were positive. After 10 minutes exposure, the mean reduction in $CFUml^{-1}$ number was 68%, increasing to 99% after thirty minutes.

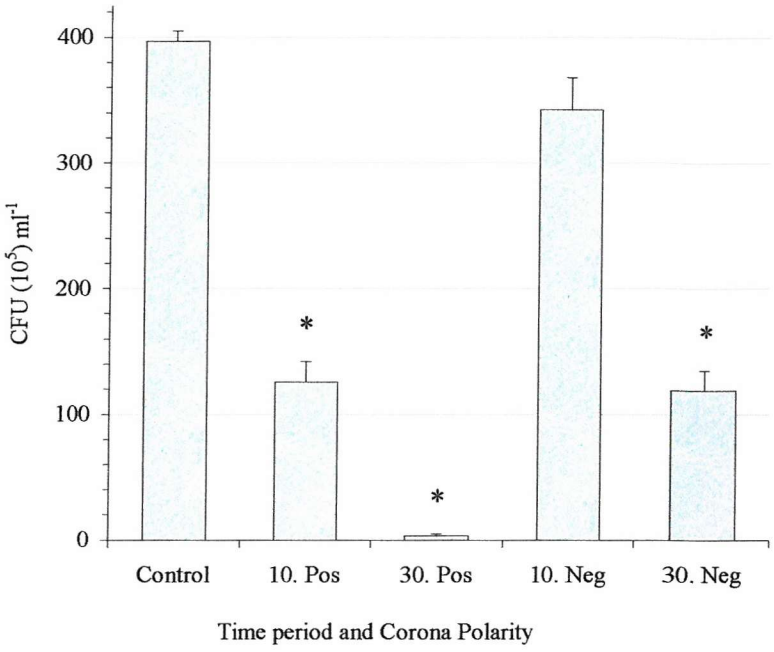

Figure 3.11) Effect of 50μA negative or positive ionic exposure in air on *E.coli*. A set of nine pins equally spaced above an agar plate at a point to plane distance of 25mm was used. Voltage was applied to the pin electrodes to give a current of 50μA, for 10 or 30 minutes. Plates were subsequently incubated at 37°C for eighteen hours and the number of CFU counted and compared to controls (time zero). Bars represent the mean (n = 6) ± S.E.M. and * indicates $p<0.05$.

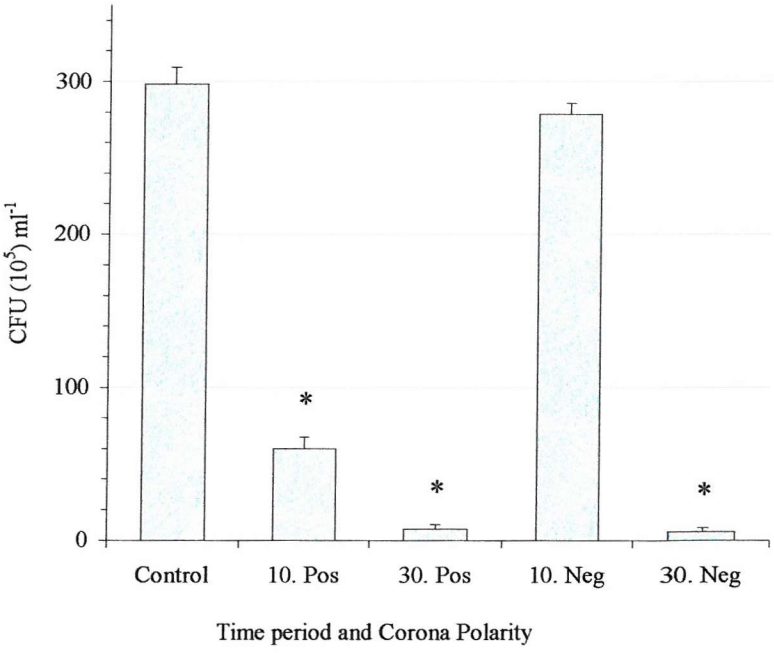

Figure 3.12) Effect of 50μA negative or positive ionic exposure in air on *S.aureus*. A set of nine pins equally spaced above an agar plate at a point to plane distance of 25mm was used. Voltage was applied to the pin electrodes to give a current of 50μA, for 10 or 30 minutes. Plates were subsequently incubated at 30°C for nineteen hours and the number of CFU counted and compared to controls (time zero). Bars represent the mean (n = 6) ± S.E.M. and * indicates $p<0.05$.

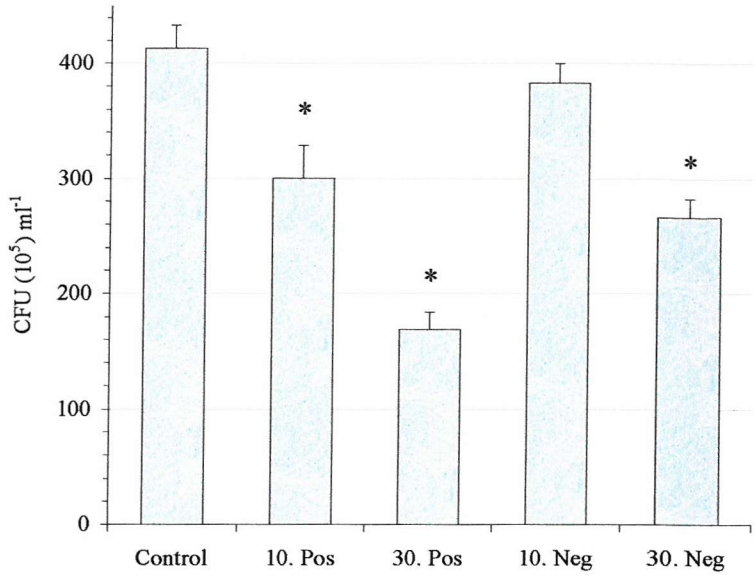

Figure 3.13) Effect of 50μA negative or positive ionic exposure in air on starved *P.veronii*. A set of nine pins spaced equally above an 87mm diameter metal disc, at a distance of 25mm was used. Inoculated foil coupons ($2cm^2$) were positioned on the disc directly beneath a pin electrode. Voltage was applied to the pin electrodes to produce 50μA current for a period of either 10 or 30 minutes. Coupons were subsequently incubated in TSB for thirty minutes prior to reading in a luminometer with 50μl nonanal and compared to controls. Bars represent the mean (n = 6) ± S.E.M. and * indicates $p<0.05$.

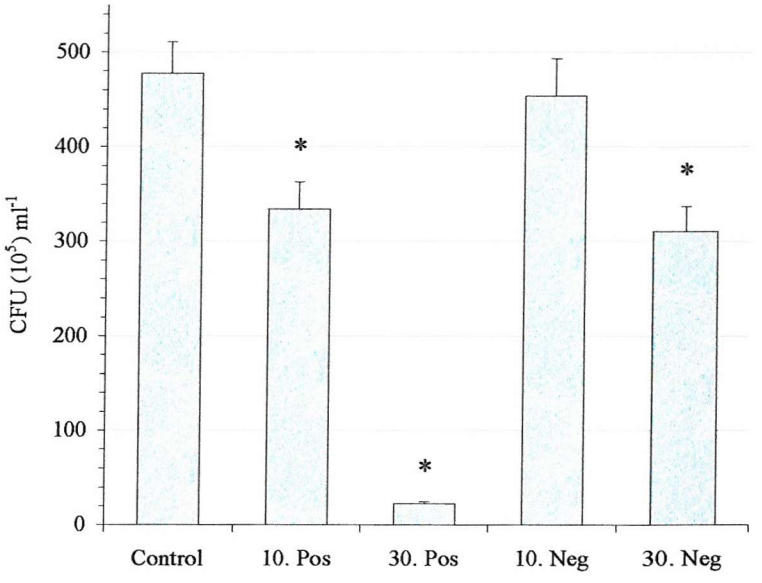

Figure 3.14) Effect of 50μA negative or positive ionic exposure in air on *P.veronii* biofilms. A set of nine pins spaced equally above an 87mm diameter metal disc, at a distance of 25mm was used. Biofilm foil coupons ($2cm^2$) were positioned on the disc directly beneath a pin electrode. Voltage was applied to the pin electrodes to produce 50μA current for a period of either 10 or 30 minutes. Biofilms were subsequently incubated in TSB for thirty minutes prior to reading in a luminometer with 50μl nonanal and compared to controls. Bars represent the mean (n = 6) ± S.E.M. and * indicates $p<0.05$.

As with the previous current regime for *S.aureus*, there was no significant difference after ten minutes exposure with 50μA negative current (*Figure* 3.12). Comparisons between the thirty minute sample groups for 25μA and 50μA negative exposure revealed a significant difference ($p<0.05$), with a greater mean reduction of 98% with 50μA. With a positive 50μA current there were significantly greater reductions ($p<0.05$) after ten and thirty minutes exposure, compared to 25μA, with mean reductions in cell viability of 80% and 97% respectively.

With 50μA negative polarity there was no significant reduction after ten minutes exposure on starved *P.veronii* cells (*Figure* 3.13). Increasing the exposure time to thirty minutes produced a significant difference ($p<0.05$) between sample and control coupons with a mean reduction of 36%. With a positive applied voltage there was a significant reduction in the number of $CFUml^{-1}$ after ten minutes with a mean reduction of 27%. At thirty minutes this figure had significantly increased ($p<0.05$) to 59%, representing a mean number of $CFUml^{-1}$ of 168×10^5, compared to the control value of 413×10^5 $CFUml^{-1}$. However, comparisons with sample groups for 25μA positive exposure found no significant difference.

Ten minutes 50μA negative exposure proved ineffective at decreasing biofilm viability (*Figure* 3.14). However, increasing the exposure time to thirty minutes did significantly ($p<0.05$) reduce the number of $CFUml^{-1}$ with a mean reduction of 35%. Positive corona treatment at this current level proved effective for both time regimes. At ten and thirty minutes the mean number of $CFUml^{-1}$ was 334×10^5 and 22×10^5 respectively compared to the control value of 477×10^5. Representing mean reductions of 30% and 95% respectively and significant increases ($p<0.05$) in cell death compared to 25μA positive treatment.

A summary of the results of exposure to either 25μA or 50μA negative or positive corona in air is shown in *Table* 3.1.

Bacterial target	Negative polarity				Positive polarity			
	25μA		50μA		25μA		50μA	
	10mins	30mins	10mins	30mins	10mins	30mins	10mins	30mins
E.coli	5	39*	14	70*	15	24*	68*	99*
S.aureus	7	88*	7	98*	54*	90*	80*	97*
Starved *P.veronii*	17	16	7	36*	23*	45*	27*	59*
P.veronii Biofilm	3	19	5	35*	4	35*	30*	95*

Table 3.1) Summary of the mean % reduction in CFUml^{-1}number for either 25μA or 50μA negative or positive corona exposure in air, against four different bacterial targets. * Indicates $p<0.05$ compared to control group. Highlighted boxes represent significantly greater reductions in cell viability ($p<0.05$) compared to 25μA exposure for the same polarity and time regime.

From these results it can be seen that an increase in either the exposure time or the current level resulted in greater reductions in the number of viable CFUml^{-1}. For each polarity and current regime, increasing the exposure time from ten to thirty minutes reduced the viable cell count, although not significantly for all cases. Of the four bacterial targets, *S.aureus* was the most susceptible to the effects of either a negative or positive corona discharge in air, with mean reductions in the number of CFUml^{-1} after ten or thirty minutes of 37% and 93% respectively (mean values for both 25μA and 50μA sample data). *E.coli* proved to be more resistant than *S.aureus* with mean reductions of 26% and 58% after ten or thirty minute treatments. The starved *P.veronii* cells and the *P.veronii* biofilms preserved their reputation as highly resistant phenotypes, with mean reductions after thirty minutes exposure of 39% and 46% respectively. Of the two polarities, positive ionic exposure was more efficient at disinfecting inoculated samples with a mean reduction of 53% compared to 40% for

negative. However, this could have been due to the higher ozone concentration of 1.4ppm compared to 1.0ppm with a negative applied voltage.

3.6) Effect of ozone on *E.coli*, starved *P.veronii*, *S.aureus* or *P.veronii* biofilms

During exposure to either 25μA or 50μA negative or positive corona current in air, the ozone concentration was recorded (*Section* 2.13, *Page* 57). For a negative applied voltage the ozone concentration was 1.0ppm for both current regimes compared to 1.4ppm with positive applied voltage. Using an ozone production unit (*Section* 2.14, *Page* 58), inoculated samples were exposed to the same concentrations, thus allowing the contribution of ozone, without unipolar ions to be evaluated. The effect of exposure to either 1.0ppm or 1.4ppm ozone for thirty minutes for the four bacterial samples can be seen in *Figures* 3.15 to 3.18 (*Pages* 93 - 94).

For *E.coli*, both ozone concentrations produced significant differences ($p<0.05$) in the number of $CFUml^{-1}$ between control and sample plates (*Figure* 3.15). Exposure to 1.0ppm decreased cell number from the control value of 353×10^5 to 234×10^5 $CFUml^{-1}$, representing a mean reduction of 34%. Comparisons with the thirty minute sample group for 50μA negative exposure in air revealed a significant difference ($p<0.05$) with corona exposure producing a 70% reduction. With an ozone concentration of 1.4ppm the mean reduction in cell number was not significantly different to thirty minutes 50μA positive corona treatment, with a mean reduction of 93%, compared to 99%.

As shown in *Figure* 3.16, both 1.0ppm and 1.4ppm ozone produced significant reductions ($p<0.05$) in the number of *S.aureus* $CFUml^{-1}$ with mean reductions of 78% and 97% respectively. Exposure to 50μA negative treatment for thirty minutes reduced the mean number of $CFUml^{-1}$ to 5.8×10^5, compared to 65×10^5 $CFUml^{-1}$ for ozone alone, a significant difference ($p<0.05$) of 20%. Analysis between the sample groups for thirty minutes 50μA positive ionic exposure in air and ozone exposure at 1.4ppm demonstrated no significant difference.

Exposure to the lower ozone concentration of 1.0ppm failed to reduce the number of starved *P.veronii* cells (*Figure* 3.17), which is in contrast to thirty minutes 50μA negative exposure where the mean $CFUml^{-1}$ number was significantly reduced to 266×10^5. Increasing the ozone concentration to 1.4ppm produced a significant difference ($p<0.05$) between sample and control coupons with a mean reduction of 49% (413×10^5 to 211×10^5 $CFUml^{-1}$). Thirty minutes positive corona exposure at 50μA produced a mean reduction of 59%, although the difference was not significant.

For biofilm sample groups Exposure to 1.0ppm ozone failed to affect biofilm viability (*Figure* 3.18). In contrast, negative corona exposure of 50μA produced a significant reduction of 35%. Exposure to 1.4ppm ozone produced a significant difference ($p<0.05$) between sample and control coupons with a mean reduction of 40% (477×10^5 to 286×10^5 $CFUml^{-1}$). However, 50μA positive treatment induced a greater reduction of 95%, significantly different ($p<0.05$) to the ozone sample group. A summary of results for bacterial exposure to ozone is shown in *Table* 3.2.

Bacterial target	Ozone concentration	
	1.0ppm	1.4ppm
E.coli	34*	93*
S.aureus	78*	97*
Starved *P.veronii*	3	49*
P.veronii Biofilm	20	40*

Table 3.2) Summary of the mean % reduction in $CFUml^{-1}$number after exposure to either 1.0ppm or 1.4ppm ozone for thirty minutes, against four different bacterial targets. * Indicates $p<0.05$ compared to control group. Highlighted boxes represents significantly less reduction in cell viability ($p<0.05$) compared to 50μA negative corona exposure in air for 1.0ppm, and 50μA positive challenge for 1.4ppm.

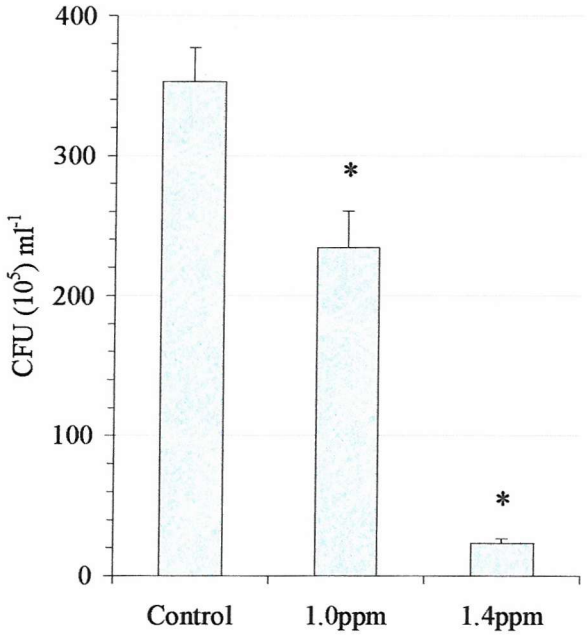

Figure 3.15) Effect of ozone on *E.coli*. Inoculated TSB agar plates were placed at a distance of 30mm from the outlet pipe of an ozone generator. Plates were exposed to an ozone concentration of either 1.0ppm or 1.4ppm for thirty minutes. After exposure, plates were incubated at 37°C for eighteen hours and the number of CFU counted and compared to controls. Bars represent the mean (n = 6) ± S.E.M. and * indicates $p<0.05$.

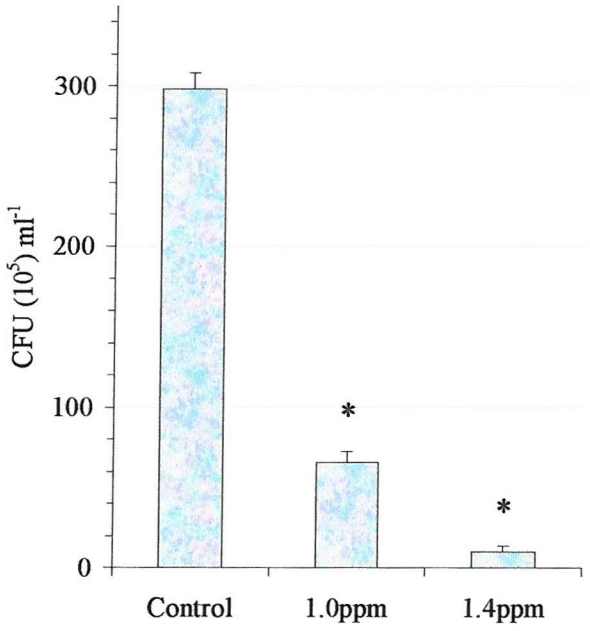

Figure 3.16) Effect of ozone on *S.aureus*. Inoculated TSB agar plates were placed at a distance of 30mm from the outlet pipe of an ozone generator. Plates were exposed to an ozone concentration of either 1.0ppm or 1.4ppm for thirty minutes. After exposure, plates were incubated at 30°C for nineteen hours and the number of CFU counted and compared to controls. Bars represent the mean (n = 6) ± S.E.M. and * indicates $p<0.05$.

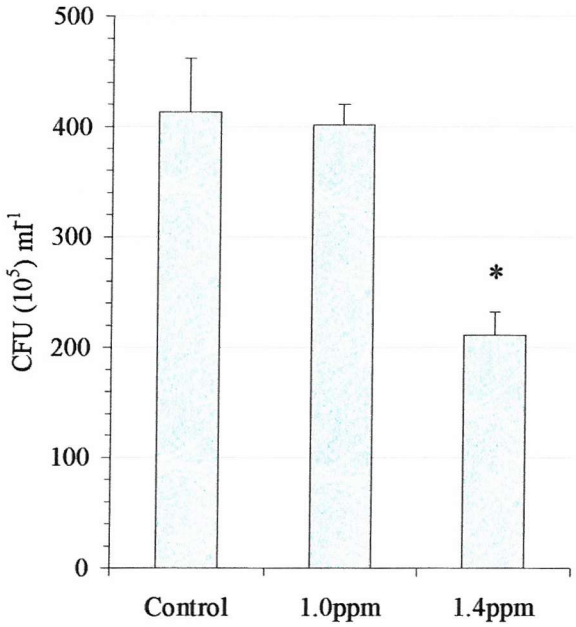

Figure 3.17) Effect of ozone on starved *P.veronii*. Inoculated foil coupons ($2cm^2$) were placed at a distance of 30mm from the outlet pipe of an ozone generator. Coupons were exposed to an ozone concentration of either 1.0ppm or 1.4ppm for thirty minutes. Post exposure coupons were incubated in TSB for thirty minutes prior to reading in a luminometer with 50µl nonanal and compared to controls. Bars represent the mean (n = 6) ± S.E.M. and * indicates $p<0.05$.

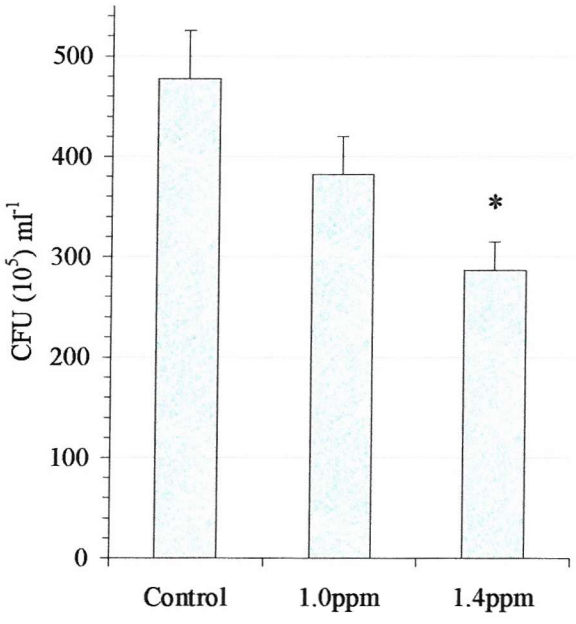

Figure 3.18) Effect of ozone on *P.veronii* biofilms. Biofilm coupons ($2cm^2$) were placed at a distance of 30mm from the outlet pipe of an ozone generator. Coupons were exposed to an ozone concentration of either 1.0ppm or 1.4ppm for thirty minutes. Post exposure biofilms were incubated in TSB for thirty minutes prior to reading in a luminometer with 50µl nonanal and compared to controls. Bars represent the mean (n = 6) ± S.E.M. and * indicates $p<0.05$.

Treatment of bacterial samples with ozone, a well-documented disinfectant was expected to significantly reduce the number of $CFUml^{-1}$ for all the bacterial targets. However, negative corona exposure in air at 50μA with an ozone concentration of 1.0ppm produced significantly greater reductions in cell number for all bacterial types. Based on these data it is apparent that some component of a negative corona discharge in air other than ozone, is contributing towards the disinfection of bacterial samples. Although from these results it is not possible to say what contribution negative ions themselves are making.

Comparisons between positive corona treatment at 50μA and exposure to 1.4ppm ozone, only showed a significant difference for the biofilm group, which once again suggests other contributory factors towards cellular death other than ozone, but only where biofilms are concerned. For the remaining bacterial targets, these results suggest that ozone is the dominant agent of death for bacteria when exposed to a positive corona discharge in air. However, it may be the case that positive ions are antibacterial but any effect is masked by the ozone.

3.7) Voltage – current relationship for a point to plane corona in nitrogen

To remove the influence of ozone, experiments were conducted within a nitrogen only atmosphere. The effect on the voltage – current relationship of a nitrogen atmosphere can be seen in *Figures* 3.19 and 3.20 (*Page* 96). One initial point to note is the significantly greater current that is generated by both polarities in nitrogen before electrical breakdown, when compared to same applied voltages in air, a phenomenon that is probably due to the complete removal of electronegative atoms such as oxygen or fluorine, to which electrons usually attach in a corona discharge. Initial experiments utilising a negative corona in nitrogen demonstrated a novel response. As shown in *Figure* 3.19, for a constant applied negative voltage of 3kV there was an increase in current with time that was independent of plane electrode material. This behaviour is yet to be fully explained, although as previously described, the non-electronegative properties of nitrogen are probably responsible. Particularly as electrons carry a higher proportion of the current in nitrogen, compared to a negative discharge in air.

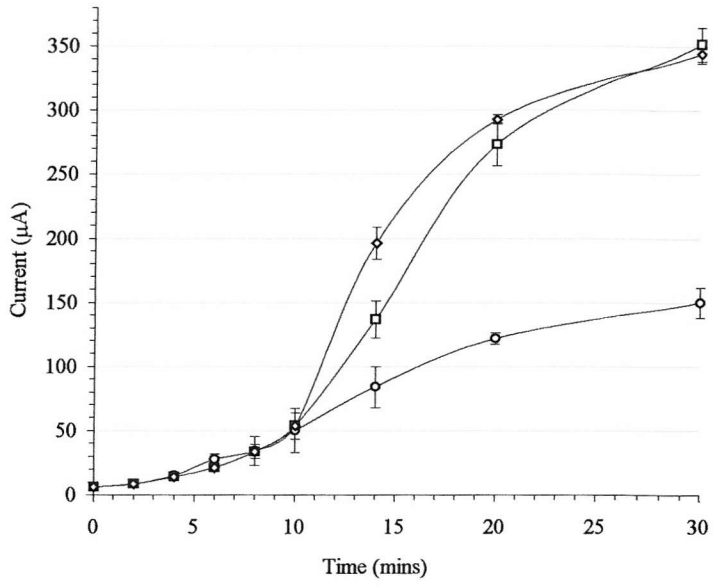

Figure 3.19) Current-time relationship for three different plane electrodes with negative point electrodes in nitrogen. A nine pin to plane corona geometry was used at an interelectrode distance of 25mm. Nitrogen was flushed through the sealed chamber at a flow rate of 15L/minute for fifteen minutes prior to voltage application and then reduced to 1l/min during tests. Three different plane electrodes were tested. TSB agar plate (◇), a CGB agar plate (□), and an aluminium disc (○). Voltage of 3kV was applied to the pin electrodes and the current in μA recorded over a thirty minute period. Points represent the mean (n = 4) ± S.E.M.

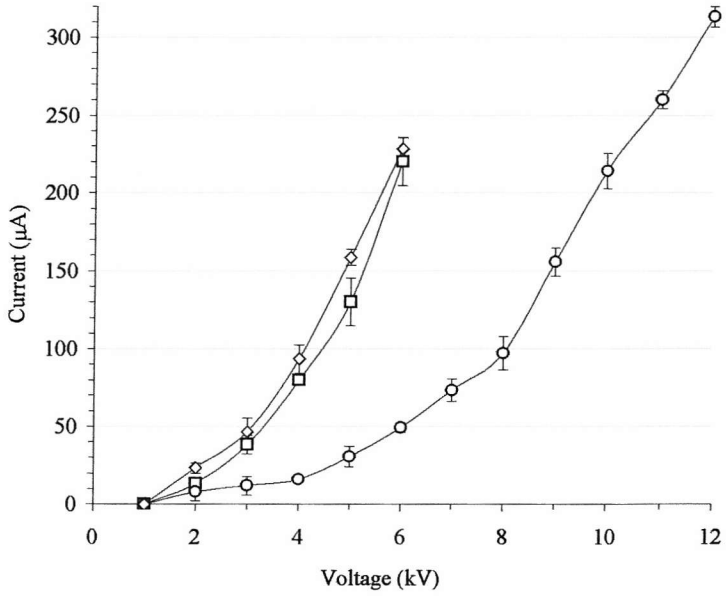

Figure 3.20) Voltage-current relationship for three different plane electrodes with a positive point electrode in nitrogen. A nine pin to plane corona geometry was used at an interelectrode distance of 25mm. Nitrogen was flushed through the sealed chamber at a flow rate of 15L/minute for fifteen minutes prior to voltage application and then reduced to 1l/min during tests. Three different plane electrodes were tested. TSB agar plate (◇), a CGB agar plate (□), and an aluminium disc (○). Voltage was applied to the pin electrodes in 1kV increments and the current in μA recorded. Points represent the mean (n = 4) ± S.E.M.

With both TSB and CGB acting as the plane electrodes, the current rose rapidly after ten minutes from 14μA for both types of media, increasing to mean values of 293μA and 273μA respectively after twenty minutes. After thirty minutes the current recorded from the TSB and CGB electrodes had reached 344μA and 355μA respectively. No significant difference was found between the I-V curves for TSB and CGB, and further increases in applied voltage resulted in electrical breakdown of the nitrogen. With aluminium foil acting as the plane electrode the increase in current over the thirty minute period was the same as the agar electrodes up to ten minutes. After this time point, the I-V curve for the aluminium plane took a distinctly different path with a mean current at thirty minutes of 150μA, a significant difference of ~ 200μA compared to the TSB and CGB curves. This will be discussed later with respect to relative humidity.

The current-voltage relationship for a positive corona in nitrogen is shown in *Figure* 3.20. In contrast to a negative applied voltage there was no increase in current for a fixed positive voltage. A similar I-V relationship to a positive corona in air occurred, but with significantly greater current levels recorded as previously described. For an applied positive voltage of 10kV with an aluminium plane electrode, the mean current level in air was 7μA, compared to 210μA in nitrogen. With TSB and CGB agar plane electrodes, an applied voltage of 6kV generated currents of 220μA and 228μA respectively. This is in contrast to the positive I-V curve in air, where no current was generated for an applied voltage of 6kV when nutrient plates were used as plane electrodes. With TSB and CGB agar plates, applied positive voltages >6kV and currents >210μA caused electrical breakdown of the inter-electrode space. The aluminium foil base electrode conducted a mean current of 313μA for an applied positive voltage of 12kV. Although greater current levels were achieved before electrical breakdown, higher applied voltages were necessary. For example, a voltage of 10kV was required to produce 200μA current compared to 6kV using nutrient agar plates.

As previously stated in the materials and methods chapter (*Section* 2.15, *Page* 62), the RH in the chamber was ~8% when aluminium was used as a plane electrode compared to the mean RH value of 77% with agar plates. The effect of relative humidity on the negative or positive voltage – current relationship in a nitrogen atmosphere, can be seen in *Figures* 3.21 and 3.22 respectively. Both polarities demonstrated a shift in the respective curves to the left as the RH level increased. A pattern that was also seen for I-V curves in air and possibly explains why current levels recorded from the nutrient agar plates were greater than those for the aluminium plane electrode, in spite of the greater conductivity level of aluminium. With regards to positive polarity corona, the increasing RH also significantly ($p<0.05$) reduced the maximum current level before breakdown, possibly by reducing the insulating properties of the nitrogen gas. For example, at an RH level of 20% the mean maximum current was 385μA, compared to 311μA and 325μA at 40% and 70% RH respectively.

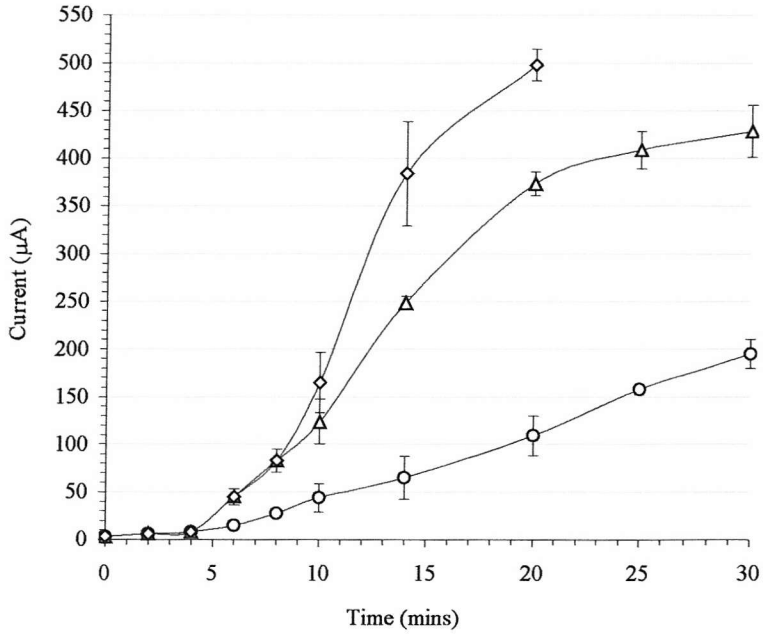

Figure 3.21) Effect of RH on the Voltage-current relationship for a negative corona discharge in nitrogen. A nine pin to plane corona geometry was used at an interelectrode distance of 25mm. Nitrogen was flushed through the sealed chamber at a flow rate of 15L/minute for sixteen minutes prior to voltage application and then reduced to 1l/min during tests. Three different RH levels were tested, 20% (○), 40% (△) and 70% (◇). Voltage of 3kV was applied to the pin electrodes and the current in μA recorded over a thirty minute period. Points represent the mean (n = 4) ± S.E.M.

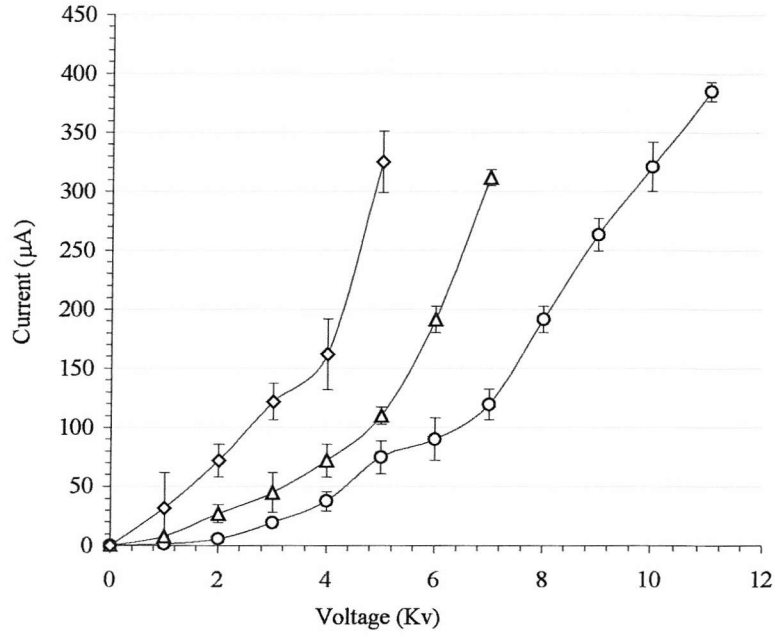

Figure 3.22) Effect of RH on the Voltage-current relationship for a positive corona discharge in nitrogen. A nine pin to aluminium foil plane corona geometry was used at an interelectrode distance of 25mm. Nitrogen was flushed through the sealed chamber at a flow rate of 15L/minute for sixteen minutes prior to voltage application and then reduced to 1l/min during tests. Three different RH levels were tested, 20% (◯), 40% (△) and 70% (◇). Voltage was applied to the pin electrodes in 1kV increments and the current in µA recorded. Points represent the mean (n = 4).

3.8) Effect of negative or positive ionic exposure in nitrogen on *E.coli, P.veronii, S.aureus* or *P.veronii* biofilms

Ozone is produced by an electrical corona in the presence of oxygen. Thus, removing all atmospheric oxygen was a viable solution to eliminating ozone disinfection of the inoculated bacterial samples. With the I-V characteristics of either a negative or positive corona discharge in nitrogen established, a series of experiments were conducted within a sealed chamber flushed through with nitrogen gas to remove atmospheric oxygen. The effect of 100µA negative exposure in nitrogen on the four different bacterial samples can be seen in *Figures* 3.23 to 3.26 (*Pages* 100 to 101).

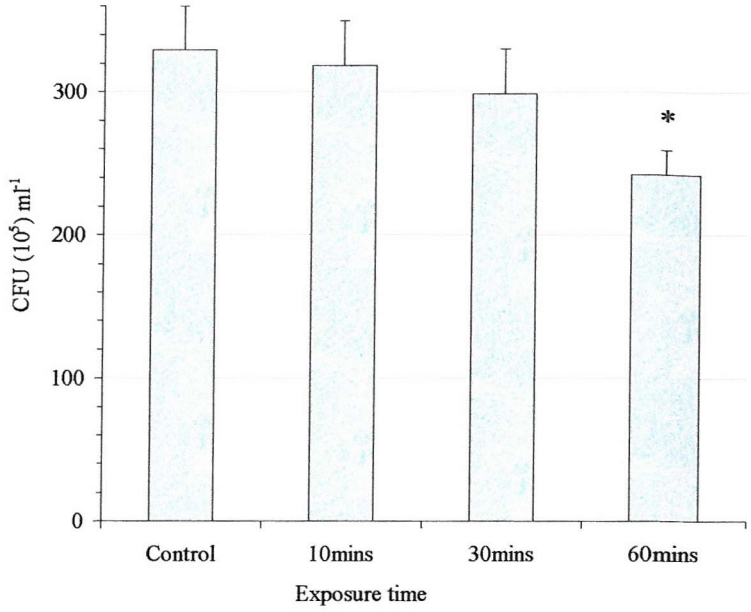

Figure 3.23) Effect of 100μA negative ionic exposure in nitrogen on *E.coli*. A set of nine pins spaced equally above an inoculated agar plate at a distance of 25mm was used. Nitrogen was flushed through the sealed chamber at a flow rate of 15L/minute for fifteen minutes prior to exposure and then reduced to 1l/min during exposure . Variable voltage was applied to the pin electrodes to produce 100μA current for a period of either 10, 30 or 60 minutes. Plates were subsequently incubated at 37°C for eighteen hours and the number of CFU counted and compared to controls. Bars represent the mean (n = 6) ± S.E.M. and * indicates $p<0.05$.

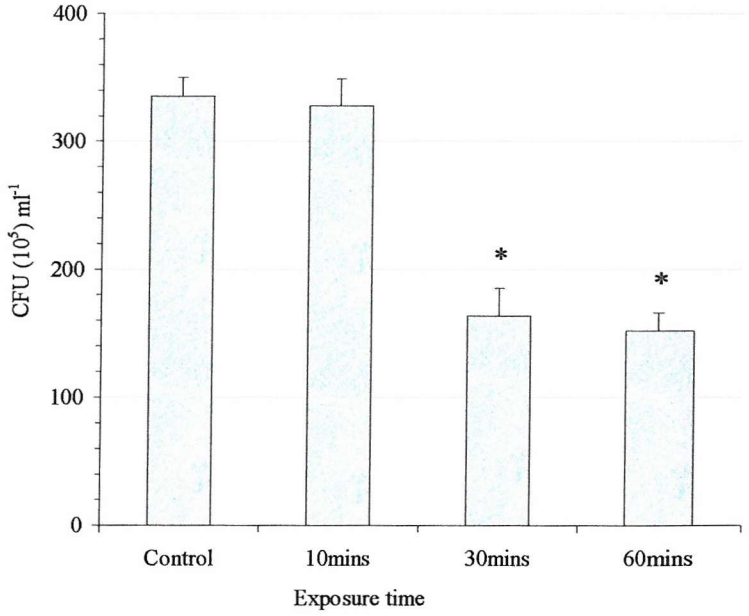

Figure 3.24) Effect of 100μA negative ionic exposure in nitrogen on *S.aureus*. A set of nine pins spaced equally above an inoculated agar plate at a distance of 25mm was used. Nitrogen was flushed through the sealed chamber at a flow rate of 15L/minute for fifteen minutes prior to exposure and then reduced to 1l/min during exposure. Variable voltage was applied to the pin electrodes to produce 100μA current for a period of either 10, 30 or 60 minutes. Plates were subsequently incubated at 30°C for nineteen hours and the number of CFU counted and compared to controls. Bars represent the mean (n = 6) ± S.E.M. and * indicates $p<0.05$.

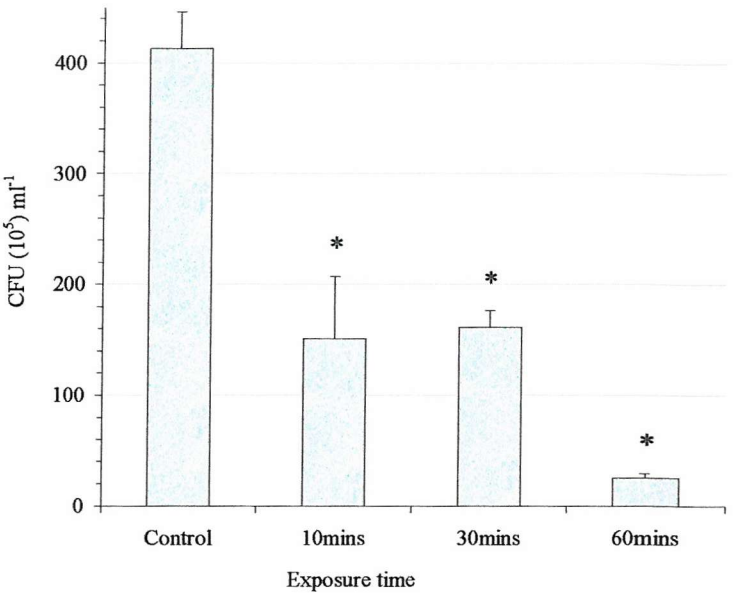

Figure 3.25) Effect of 100μA negative ionic exposure in nitrogen on starved *P.veronii*. A set of nine pins spaced equally above an 87mm diameter metal disc, at a distance of 25mm was used. Inoculated foil coupons ($2cm^2$) were positioned on the disc directly beneath a pin electrode. Nitrogen was flushed through the sealed chamber at a flow rate of 15L/minute for fifteen minutes prior to exposure and then reduced to 1l/min during exposure. Variable voltage was applied to the pin electrodes to produce 100μA current for a period of either 10, 30 or 60 minutes. Coupons were subsequently incubated in TSB for thirty minutes prior to reading in a luminometer with 50μl nonanal and compared to controls. Bars represent the mean (n = 6) ± S.E.M. and * indicates $p<0.05$.

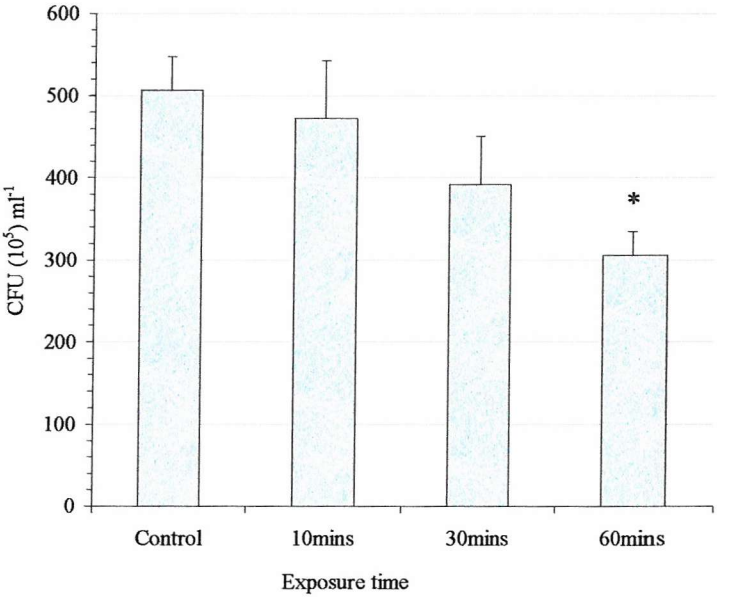

Figure 3.26) Effect of 100μA negative ionic exposure in nitrogen on *P.veronii* biofilms. A set of nine pins spaced equally above an 87mm diameter metal disc, at a distance of 25mm was used. Biofilm foil coupons ($2cm^2$) were positioned on the disc directly beneath a pin electrode. Nitrogen was flushed through the sealed chamber at a flow rate of 15L/minute for fifteen minutes prior to exposure and then reduced to 1l/min during exposure. Variable voltage was applied to the pin electrodes to produce 100μA current for a period of either 10, 30 or 60 minutes. Biofilms were subsequently incubated in TSB for thirty minutes prior to reading in a luminometer with 50μl nonanal and compared to controls. Bars represent the mean (n = 6) ± S.E.M. and * indicates $p<0.05$.

For *E.coli* (*Figure* 3.23), exposure to 100μA negative current for either ten or thirty minutes demonstrated no significant difference ($p<0.05$) between control and sample plates. However, increasing the exposure time to sixty minutes did significantly reduce the number of $CFUml^{-1}$ by 26%, from a mean control value of 329×10^5 to 242×10^5 $CFUml^{-1}$. With *S.aureus* as the bacterial target (*Figure* 3.24) ten minutes exposure failed to elicit a response. Significant reductions were produced for thirty and sixty-minute exposure periods with mean reductions of 51% and 55% respectively. Although the reduction at sixty minutes was marginally greater, there was no significant difference when compared to the sample group at thirty minutes.

For starved *P.veronii* (*Figure* 3.25) there were significant reductions in the number of $CFUml^{-1}$ for all time periods. After ten minutes the mean number of $CFUml^{-1}$ had decreased from a control value of 413×10^5 to 151×10^5 $CFUml^{-1}$, a mean reduction of 64%. The thirty minute sample group showed no significant difference ($p>0.05$) to the sample group for ten minutes exposure with a mean reduction of 61%. However, increasing the treatment time to sixty minutes did produce a significant difference ($p<0.05$) when compared to the sample group at thirty minutes, with a mean value of 26×10^5 $CFUml^{-1}$, corresponding to a mean reduction of 94%.

P.veronii Biofilms proved more resistant when compared to the other bacterial targets, as there was no significant reduction in the number of $CFUml^{-1}$ for either ten or thirty minute exposures (*Figure* 3.26). Only a treatment time of sixty minutes produced a significant difference with a mean reduction of 40% (506×10^5 $CFUml^{-1}$ to 306×10^5 $CFUml^{-1}$). The effect of changing the exposure polarity to positive with the same current level of 100μA can be seen in *Figures* 3.27 to 3.30 (*Pages* 103 to 104).

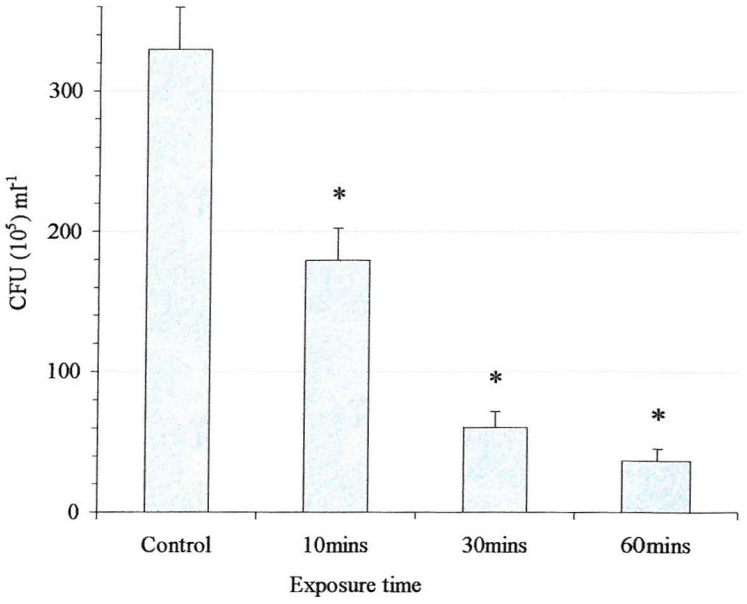

Figure 3.27) Effect of 100μA positive ionic exposure in nitrogen on *E.coli*. A set of nine pins spaced equally above an inoculated agar plate at a distance of 25mm was used. Nitrogen was flushed through the sealed chamber at a flow rate of 15L/minute for fifteen minutes prior to exposure and then reduced to 1l/min during exposure. Voltage was applied to the pin electrodes to produce 100μA current for a period of either 10, 30 or 60 minutes. Plates were subsequently incubated at 37°C for eighteen hours and the number of CFU counted and compared to controls. Bars represent the mean (n = 6) ± S.E.M. and * indicates $p<0.05$.

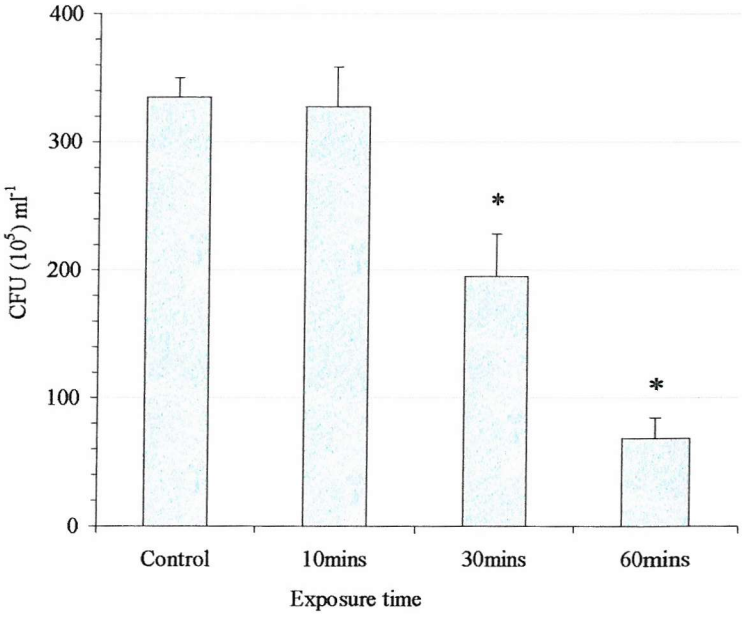

Figure 3.28) Effect of 100μA positive ionic exposure in nitrogen on *S.aureus*. A set of nine pins spaced equally above an inoculated agar plate at a distance of 25mm was used. Nitrogen was flushed through the sealed chamber at a flow rate of 15L/minute for fifteen minutes prior to exposure and then reduced to 1l/min during exposure. Voltage was applied to the pin electrodes to produce 100μA current for a period of either 10, 30 or 60 minutes. Plates were subsequently incubated at 30°C for nineteen hours and the number of CFU counted and compared to controls. Bars represent the mean (n = 6) ± S.E.M. and * indicates $p<0.05$.

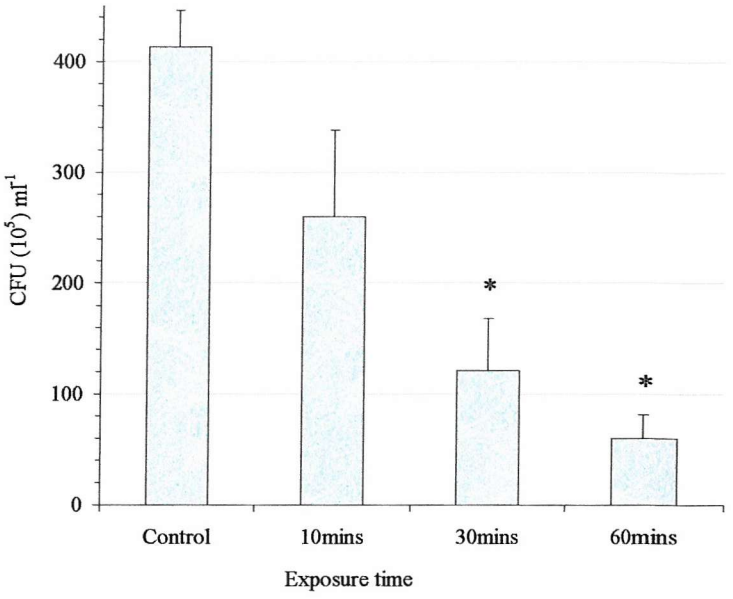

Figure 3.29) Effect of 100μA positive ionic exposure in nitrogen on starved *P.veronii*. A set of nine pins spaced equally above an 87mm diameter metal disc, at a distance of 25mm was used. Inoculated foil coupons ($2cm^2$) were positioned on the disc directly beneath a pin electrode. Nitrogen was flushed through the sealed chamber at a flow rate of 15L/minute for fifteen minutes prior to exposure and then reduced to 1l/min during exposure. Voltage was applied to the pin electrodes to produce 100μA current for a period of either 10, 30 or 60 minutes. Coupons were subsequently incubated in TSB for thirty minutes prior to reading in a luminometer with 50μl nonanal and compared to controls. Bars represent the mean (n = 6) ± S.E.M. and * indicates $p<0.05$.

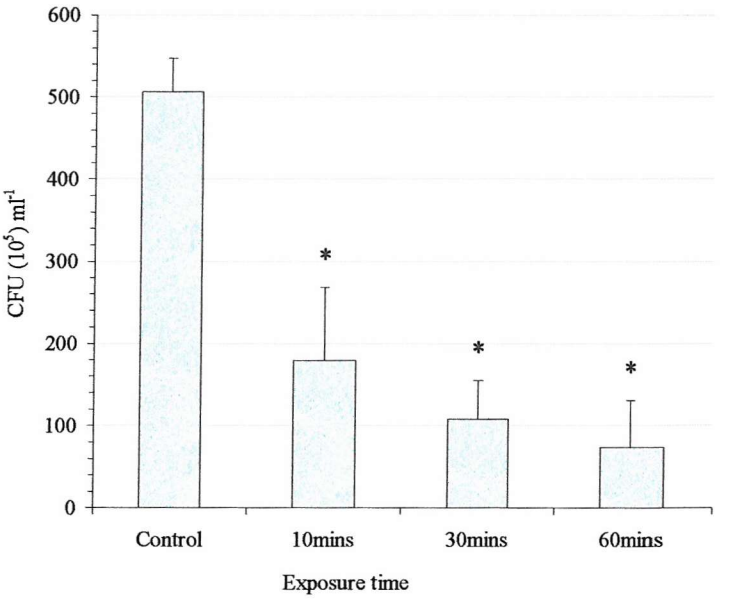

Figure 3.30) Effect of 100μA positive ionic exposure in nitrogen on *P.veronii* biofilms. A set of nine pins spaced equally above an 87mm diameter metal disc, at a distance of 25mm was used. Biofilm foil coupons ($2cm^2$) were positioned on the disc directly beneath a pin electrode. Nitrogen was flushed through the sealed chamber at a flow rate of 15L/minute for fifteen minutes prior to exposure and then reduced to 1l/min during exposure. Voltage was applied to the pin electrodes to produce 100μA current for a period of either 10, 30 or 60 minutes. Biofilms were subsequently incubated in TSB for thirty minutes prior to reading in a luminometer with 50μl nonanal and compared to controls. Bars represent the mean (n = 6) ± S.E.M. and * indicates $p<0.05$.

With *E.coli* (*Figure* 3.27) as the sample organism, positive ions proved more effective than negative, with significant reductions of 46%, 82% and 89% for ten, thirty and sixty minutes respectively. Analysis between sample groups for ten and thirty minute treatments demonstrated a significant difference ($p<0.05$) with a decrease in the mean $CFUml^{-1}$ number from 179×10^5 to 60×10^5 respectively. However, there was no significant difference between sample groups for thirty and sixty minute exposures to 100μA positive ions. Compared with 100μA negative exposure, 100μA positive treatment produced significantly greater reductions ($p<0.05$) in the number of $CFUml^{-1}$ for all time periods.

There was no significant effect on the mean number of *S.aureus* cells after ten minutes exposure (*Figure* 3.28). However, after thirty or sixty minutes treatment, the mean number of $CFUml^{-1}$ was significantly reduced from a control value of 335×10^5 to 195×10^5 and 69×10^5 respectively, representing mean reductions of 42% and 79%. Analysis between the sixty-minute sample groups for 100μA negative or positive treatment of *S.aureus*, showed positive exposure to be significantly more effective at reducing $CFUml^{-1}$ number.

For starved *P.veronii* (*Figure* 3.29) there were only significant effects after thirty minutes positive exposure with a mean reduction of 71%. Further increasing the exposure time to sixty minutes resulted in a mean reduction in $CFUml^{-1}$ number of 85%, although there was no significant difference ($p<0.05$) when compared to the sample group for thirty minutes. In contrast to results for *E.coli* and *S.aureus*, where positive exposure at this current level was significantly more detrimental, 100μA negative exposure (*Figure* 3.25) demonstrated significantly greater reductions ($p<0.05$) for the sixty minute sample group.

With *P.veronii* biofilms (*Figure* 3.30) there were significant reductions in $CFUml^{-1}$ number for all exposure times with mean reductions of 65%, 79% and 85% for ten, thirty and sixty minutes respectively. However, there was no significant difference ($p<0.05$) between sample groups for each time period. Compared to negative exposure

at the same current level, positive treatment proved significantly more effective at decreasing cell viability for all exposure periods. A summary of results for 100μA ionic exposure in nitrogen is shown in *Table* 3.3.

Bacterial target	Negative polarity			Positive polarity		
	10mins	30mins	60mins	10mins	30mins	60mins
E.coli	3	9	26*	46*	82*	89*
S.aureus	2	51*	55*	2	42*	79*
Starved *P.veronii*	64*	61*	94*	37*	71*	85*
P.veronii Biofilm	7	23	40*	65*	79*	85*

Table 3.3) Summary of the mean % reduction in CFUml^{-1}number for either 100μA negative or positive exposure in nitrogen, against four different bacterial targets. * Indicates $p<0.05$ compared to control group. Highlighted boxes represent significantly greater reductions in cell viability ($p<0.05$) compared to opposite polarity exposure with the same time period.

The effect of increasing the exposure current to 200μA with a negative applied voltage is shown in *Figures* 3.31 to 3.34 (*Pages* 107 to 108).

For *E.coli* (*Figure* 3.31) exposure to 200μA negative current for ten minutes demonstrated no significant difference ($p<0.05$) between control and sample plates. Increasing the exposure time to thirty or sixty minutes did reduce the number of CFUml^{-1} by 64% and 68%, representing decreases in the mean number of CFUml^{-1} from the control value of 330 to 120 and 107 $\times$ 10^5 CFUml^{-1} respectively. Comparisons with 100μA negative exposure did show significantly greater reductions at thirty and sixty minutes.

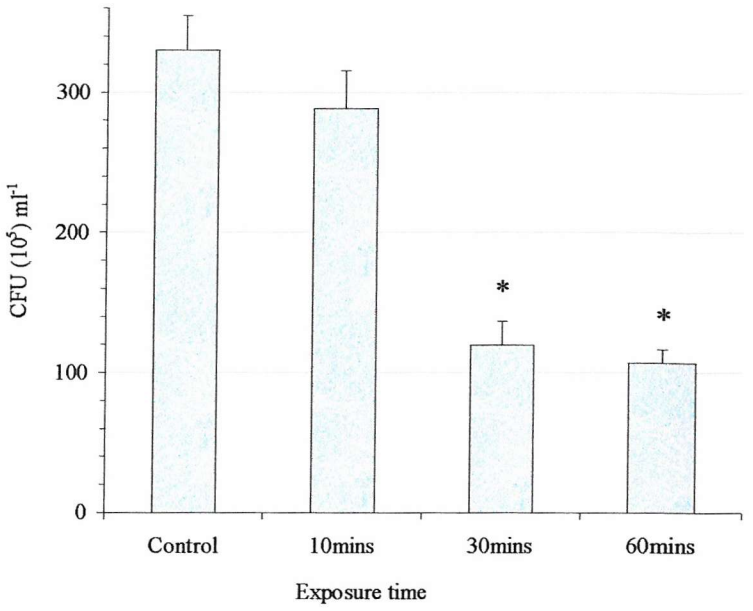

Figure 3.31) Effect of 200μA negative ionic exposure in nitrogen on *E.coli.* A set of nine pins spaced equally above an inoculated agar plate at a distance of 25mm was used. Nitrogen was flushed through the sealed chamber at a flow rate of 15L/minute for fifteen minutes prior to exposure and then reduced to 1l/min during exposure . Variable voltage was applied to the pin electrodes to produce 200μA current for a period of either 10, 30 or 60 minutes. Plates were subsequently incubated at 37°C for eighteen hours and the number of CFU counted and compared to controls. Bars represent the mean (n = 6) ± S.E.M. and * indicates $p<0.05$.

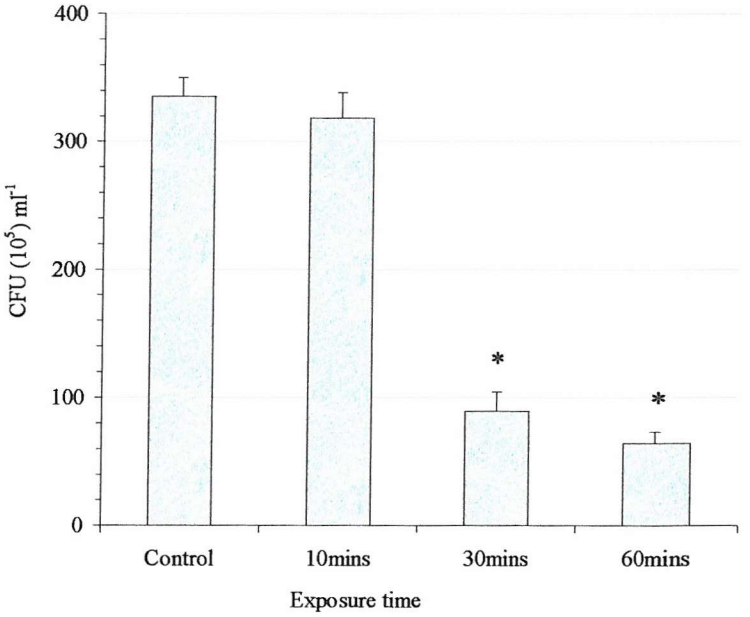

Figure 3.32) Effect of 200μA negative ionic exposure in nitrogen on *S.aureus.* A set of nine pins spaced equally above an inoculated agar plate at a distance of 25mm was used. Nitrogen was flushed through the sealed chamber at a flow rate of 15L/minute for fifteen minutes prior to exposure and then reduced to 1l/min during exposure. Variable voltage was applied to the pin electrodes to produce 200μA current for a period of either 10, 30 or 60 minutes. Plates were subsequently incubated at 30°C for nineteen hours and the number of CFU counted and compared to controls. Bars represent the mean (n = 6) ± S.E.M. and * indicates $p<0.05$.

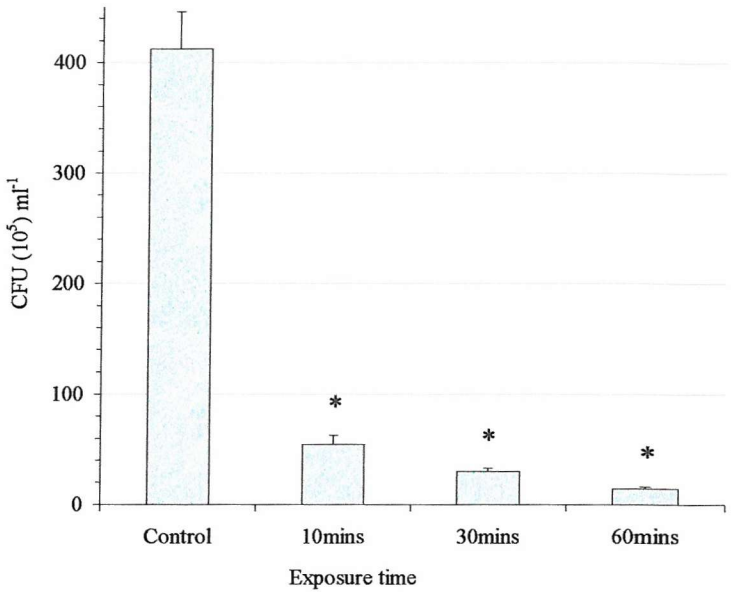

Figure 3.33) Effect of 200μA negative ionic exposure in nitrogen on starved *P.veronii*. A set of nine pins spaced equally above an 87mm diameter metal disc, at a distance of 25mm was used. Inoculated foil coupons ($2cm^2$) were positioned on the disc directly beneath a pin electrode. Nitrogen was flushed through the sealed chamber at a flow rate of 15L/minute for fifteen minutes prior to exposure and then reduced to 1l/min during exposure. Variable voltage was applied to the pin electrodes to produce 200μA current for a period of either 10, 30 or 60 minutes. Coupons were subsequently incubated in TSB for thirty minutes prior to reading in a luminometer with 50μl nonanal and compared to controls. Bars represent the mean (n = 6) ± S.E.M. and * indicates $p<0.05$.

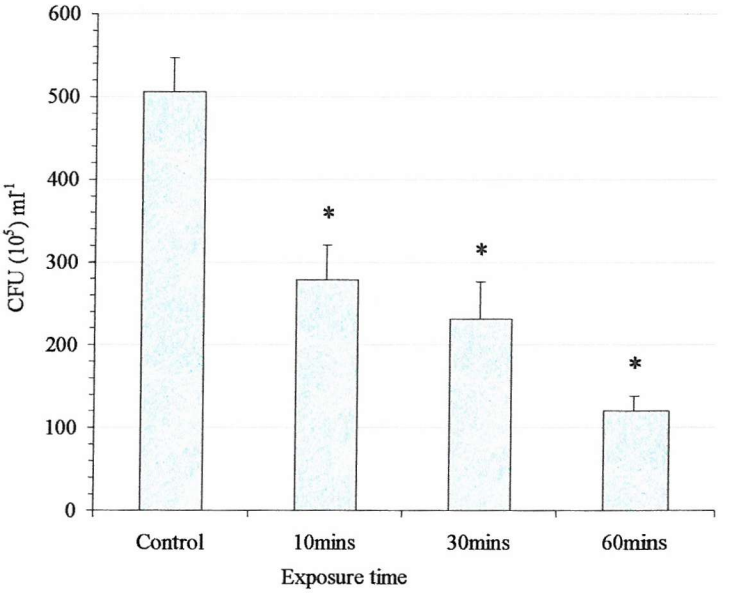

Figure 3.34) Effect of 200μA negative ionic exposure in nitrogen on *P.veronii* biofilms. A set of nine pins spaced equally above an 87mm diameter metal disc, at a distance of 25mm was used. Biofilm foil coupons ($2cm^2$) were positioned on the disc directly beneath a pin electrode. Nitrogen was flushed through the sealed chamber at a flow rate of 15L/minute for fifteen minutes prior to exposure and then reduced to 1l/min during exposure. Variable voltage was applied to the pin electrodes to produce 200μA current for a period of either 10, 30 or 60 minutes. Biofilms were subsequently incubated in TSB for thirty minutes prior to reading in a luminometer with 50μl nonanal and compared to controls. Bars represent the mean (n = 6) ± S.E.M. and * indicates $p<0.05$.

As previously seen with 100μA negative exposure, ten minutes treatment with 200μA was insufficient to affect *S.aureus* cell number (*Figure* 3.32). Thirty and sixty minute exposures did produce significantly greater reductions ($p<0.05$) when compared to sample groups for the same time periods with 100μA negative exposure. For example the mean percentage reduction in the number of $CFUml^{-1}$ after thirty minutes was 73%, compared to 51%. With sixty minutes 200μA exposure, the mean percentage reduction in the number of $CFUml^{-1}$ was 81%, representing a further decrease in cell number of 26%, compared to 100μA treatment.

With starved *P.veronii* (*Figure* 3.33) significant reductions in $CFUml^{-1}$ number were achieved for all exposure times and significant differences ($p<0.05$) were found between sample groups for ten and sixty minute exposures. Compared to the 100μA negative sample groups for ten and thirty minute time periods, reductions in cell number were significantly greater with 200μA exposure. After ten minutes of 100μA negative treatment the mean number of $CFUml^{-1}$ was 151×10^5. With 200μA negative treatment this figure was reduced to 55×10^5 $CFUml^{-1}$, representing a total mean reduction of 87% compared to the control value of 413×10^5 $CFUml^{-1}$. After thirty minutes exposure the mean number of $CFUml^{-1}$ was 30×10^5 representing a reduction of 93%, and a difference of 32% compared to the sample group for 100μA negative treatment. Sixty minutes exposure at this current level failed to elicit a significant difference ($p<0.05$) when compared to the same sample group for 100μA negative challenge.

The effect of exposure to 200μA negative corona on *P.veronii* biofilms proved effective for all time periods (*Figure* 3.34). Compared to the sample groups for 100μA negative exposure, reductions in the number of $CFUml^{-1}$ were significant for all time regimes ($p<0.05$). After ten, thirty or sixty minutes challenge with 100μA, the mean number of $CFUml^{-1}$ was 472, 392 and 306×10^5, respectively. For 200μA treatment the number of $CFUml^{-1}$ for each time period had decreased to 279, 231 and 120×10^5, respectively, and representing total mean reductions of 45%, 54% and 76%.

Comparisons between sample groups for 200μA negative exposure demonstrated no significant difference between ten and thirty minute sample groups. However, the number of $CFUml^{-1}$ for sixty minutes treatment was significantly different ($p<0.05$) when compared to thirty minutes. The effect of changing the polarity to positive with 200μA exposure current, is shown in *Figures* 3.35 to 3.38 (*Pages* 111 to 112).

Figure 3.35 shows the effect on *E.coli*. At this current level there was a significant difference ($p<0.05$) between sample groups for ten and thirty minutes, but not between sample groups for thirty and sixty minutes. Significant differences ($p<0.05$) were found in $CFUml^{-1}$ number for all time periods when compared to sample groups for 100μA positive treatment, with mean total reductions of 72%, 98% and 98% respectively. Comparisons between 200μA positive and negative exposure show significant differences ($p<0.05$) for all time periods. The mean number of $CFUml^{-1}$ for 200μA negative treatment after ten, thirty or sixty minutes was 288, 120 and 107×10^5 $CFUml^{-1}$ respectively, compared to 92, 6 and 5×10^5 $CFUml^{-1}$ for 200μA positive ionic challenge.

Even at a current level of 200μA there was no significant effect on *S.aureus* $CFUml^{-1}$ number after ten minutes positive exposure (*Figure* 3.36). Thirty and sixty minute exposures produced significant reductions in $CFUml^{-1}$ number, with mean reductions of 72% and 87%. Only the thirty minute sample group for 200μA demonstrated a significant difference when comparisons with the sample groups for 100μA were made, with a decrease from 195 to 93×10^5 $CFUml^{-1}$. Comparisons between sample groups with the same current level but with a negative applied voltage, demonstrated no significant difference for any time period.

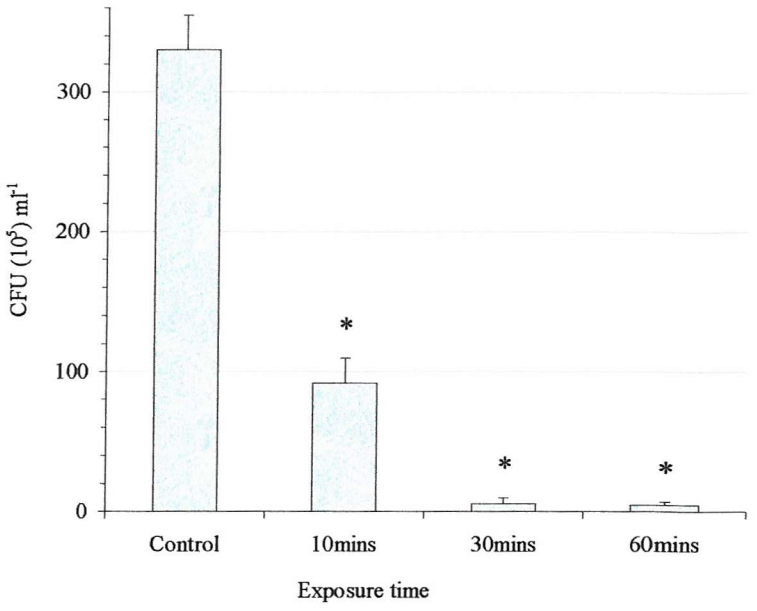

Figure 3.35) Effect of 200μA positive ionic exposure in nitrogen on *E.coli*. A set of nine pins spaced equally above an inoculated agar plate at a distance of 25mm was used. Nitrogen was flushed through the sealed chamber at a flow rate of 15L/minute for fifteen minutes prior to exposure and then reduced to 1l/min during exposure. Voltage was applied to the pin electrodes to produce 200μA current for a period of either 10, 30 or 60 minutes. Plates were subsequently incubated at 37°C for eighteen hours and the number of CFU counted and compared to controls. Bars represent the mean (n = 6) ± S.E.M. and * indicates $p<0.05$.

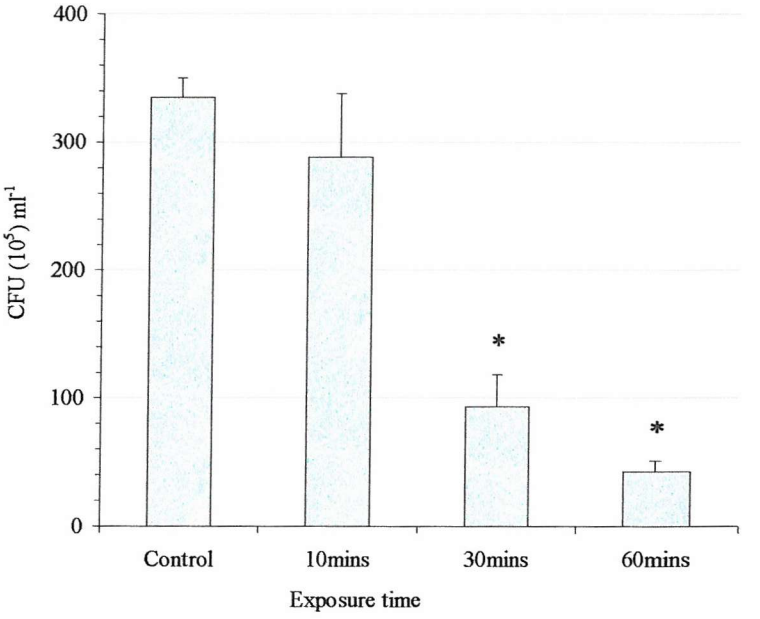

Figure 3.36) Effect of 200μA positive ionic exposure in nitrogen on *S.aureus*. A set of nine pins spaced equally above an inoculated agar plate at a distance of 25mm was used. Nitrogen was flushed through the sealed chamber at a flow rate of 15L/minute for fifteen minutes prior to exposure and then reduced to 1l/min during exposure. Voltage was applied to the pin electrodes to produce 200μA current for a period of either 10, 30 or 60 minutes. Plates were subsequently incubated at 30°C for nineteen hours and the number of CFU counted and compared to controls. Bars represent the mean (n = 6) ± S.E.M. and * indicates $p<0.05$.

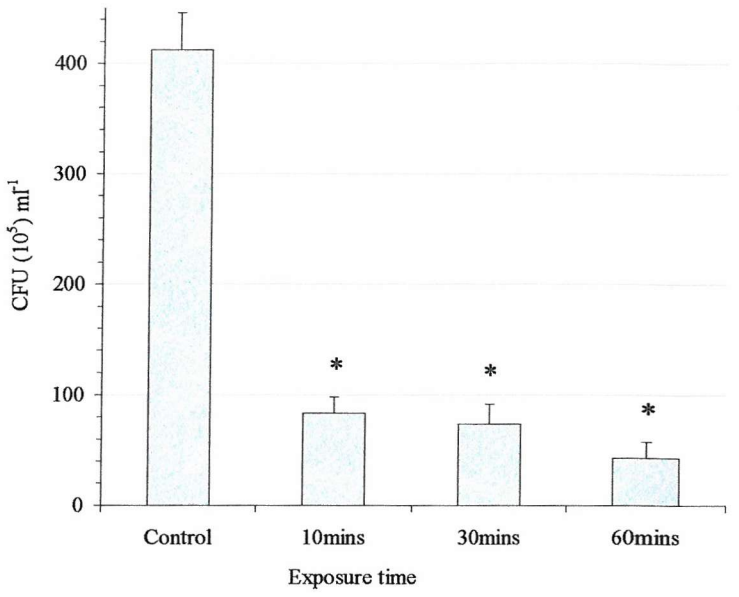

Figure 3.37) Effect of 200μA positive ionic exposure in nitrogen on starved *P.veronii*. A set of nine pins spaced equally above an 87mm diameter metal disc, at a distance of 25mm was used. Inoculated foil coupons ($2cm^2$) were positioned on the disc directly beneath a pin electrode. Nitrogen was flushed through the sealed chamber at a flow rate of 15L/minute for fifteen minutes prior to exposure and then reduced to 1l/min during exposure. Voltage was applied to the pin electrodes to produce 200μA current for a period of either 10, 30 or 60 minutes. Coupons were subsequently incubated in TSB for thirty minutes prior to reading in a luminometer with 50μl nonanal and compared to controls. Bars represent the mean (n = 6) ± S.E.M. and * indicates $p<0.05$.

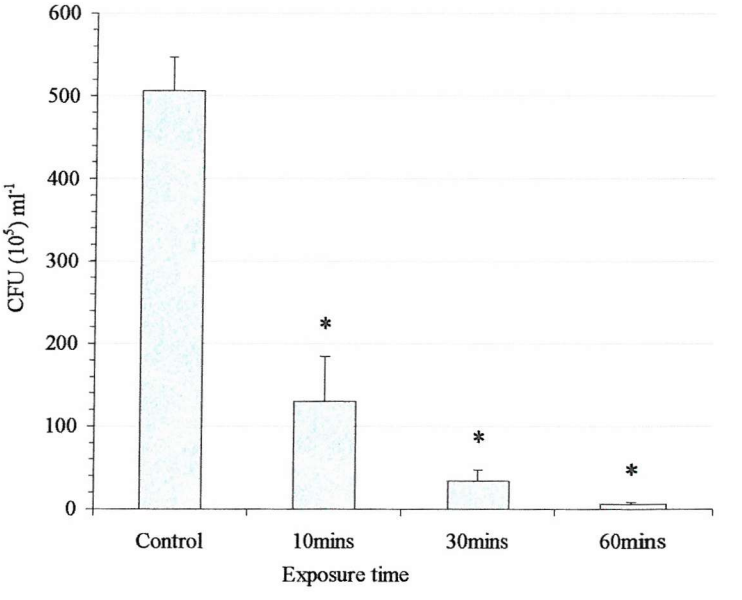

Figure 3.38) Effect of 200μA positive ionic exposure in nitrogen on *P.veronii* biofilms. A set of nine pins spaced equally above an 87mm diameter metal disc, at a distance of 25mm was used. Biofilm foil coupons ($2cm^2$) were positioned on the disc directly beneath a pin electrode. Nitrogen was flushed through the sealed chamber at a flow rate of 15L/minute for fifteen minutes prior to exposure and then reduced to 1l/min during exposure. Voltage was applied to the pin electrodes to produce 200μA current for a period of either 10, 30 or 60 minutes. Biofilms were subsequently incubated in TSB for thirty minutes prior to reading in a luminometer with 50μl nonanal and compared to controls. Bars represent the mean (n = 6) ± S.E.M. and * indicates $p<0.05$.

For starved *P.veronii* (*Figure* 3.37) increasing the exposure current to 200μA positive elicited a significant reduction after only ten minutes, with a mean reduction of 80%, in contrast to 100μA positive where the same time period produced no significant effect. Thirty and sixty minute exposures failed to significantly increase cellular death compared to 100μA positive ionic treatments. Comparisons between sample groups for ten, thirty and sixty minutes with 200μA, demonstrated no significant difference. Analysis between the time period sample groups for 200μA negative and positive treatment, demonstrated significantly greater reductions ($p<0.05$) with a negative applied voltage for thirty and sixty minute treatments. For example, with 200μA positive challenge, the mean $CFUml^{-1}$ number after thirty and sixty minutes was 74 and 43 $\times$ 10^5 respectively, compared to 30 and 14 $\times$ 10^5 $CFUml^{-1}$ with a negative applied voltage.

As shown in *Figure* 3.38, there were significant reductions ($p<0.05$) in $CFUml^{-1}$ number for all exposure periods compared to the control value of 506 $\times$ 10^5 $CFUml^{-1}$ for *P.veronii* Biofilms. Comparisons between sample groups for ten, thirty and sixty minutes demonstrated significantly greater reductions in the number of $CFUml^{-1}$ for each successive time period. After ten minutes the mean $CFUml^{-1}$ number was 131, decreasing to 34 and 6 $\times$ 10^5 for thirty and sixty minutes respectively. However, when comparisons were made with the same time period sample groups from 100μA positive exposure, there was no significant difference in the mean number of $CFUml^{-1}$. Exposure to 200μA positive current also produced significantly greater reductions in cell viability for each time period when compared to 200μA negative treatment. With a negative applied voltage the mean number of $CFUml^{-1}$ for ten, thirty and sixty minute time periods was 279, 231 and 120 $\times$ 10^5, respectively, compared to 134, 34 and 6 $\times$ 10^5 $CFUml^{-1}$ respectively, with a positive applied voltage.

A summary of results for 200μA negative or positive ionic in nitrogen exposure is shown in *Table* 3.4.

Bacterial target	Negative polarity			Positive polarity		
	10mins	30mins	60mins	10mins	30mins	60mins
E.coli	13	64*	68*	72*	98*	98*
S.aureus	5	73*	81*	14	72*	87*
Starved *P.veronii*	87*	93*	97*	80*	82*	90*
P.veronii Biofilm	45*	54*	76*	74*	93*	99*

Table 3.4) Summary of the mean % reduction in CFUml^{-1}number for either 200μA negative or positive exposure in nitrogen, against four different bacterial targets. * Indicates $p<0.05$ compared to control group. Highlighted boxes represent significantly greater reductions in cell viability ($p<0.05$) compared to 100μA exposure with the same polarity and exposure time.

Comparisons between *Table* 3.3 (*Page* 106) and *Table* 3.4 show increases in the total number of cells killed for all conditions. However, increasing the exposure current for positive applied voltage only significantly ($p<0.05$) decreased cell viability for the ten minute treatments of *E.coli* and *P.veronii*, and the thirty minute treatment of *S.aureus*. In contrast, negative exposure at 200μA significantly increased cell death for virtually all test conditions. Only the ten minute sample groups for *E.coli* and *S.aureus*, and the sixty minute *P.veronii* group failed to elicit a significant difference. With regards to total cell death, positive treatment at either 100μA or 200μA for all time periods, was significantly ($p<0.05$) more effective with a mean reduction in CFUml^{-1} number for all four bacterial targets of 72%, compared to 50% for negative. Previous tests exposing samples to a positive corona discharge in air produced significant reductions in CFUml^{-1} number, but this had been attributed to the presence of the anti-bacterial agent ozone. From these tests in nitrogen, it is clear that exposure to positive ions is detrimental to bacterial cells. Negative corona treatments in air had indicated corona components other than ozone contributing towards cell death. These tests indicate an anti-bacterial activity of negative ions.

The effect of increasing the exposure current to 350μA with a negative applied voltage is shown in *Figures* 3.39 to 3.42 (*Pages* 116 to 117).

In contrast to 200μA negative exposure, ten minutes treatment with 350μA was sufficient to significantly reduce *E.coli* $CFUml^{-1}$ number, with a mean reduction of 23% (*Figure* 3.39). Exposure times of thirty and sixty minutes produced significantly greater reductions when compared to sample groups for 200μA negative current, with total mean reductions of 91% and 93% respectively. There was no significant difference between the thirty and sixty minute sample groups at this current level. Compared to positive exposure at the lower regime of 200μA, negative exposure at 350μA is significantly less effective at decreasing cell viability. After thirty or sixty minute exposures with 350μA negative current the mean $CFUml^{-1}$ number is 31×10^5 and 23×10^5 respectively, compared to 6×10^5 and 5×10^5 $CFUml^{-1}$ respectively for 200μA positive challenge.

Figure 3.40 shows the effect on *S.aureus*. Compared to sample groups for each time period, there was no significant difference between exposures with either 200μA or 350μA negative current. For example, with 200μA challenge the mean number of $CFUml^{-1}$ for ten, thirty and sixty minute exposures was 318, 90 and 64×10^5 respectively, compared to 307, 99 and 40×10^5 for 350μA. Comparisons between 350μA negative exposure and 200μA positive exposure demonstrated no significant difference for any time period sample group.

Increasing the exposure current to 350μA proved ineffective at significantly reducing the number of starved *P.veronii* $CFUml^{-1}$, as shown in *Figure* 3.41. The mean percentage reduction in cell number for ten, thirty or sixty minutes was virtually identical to those achieved for 200μA, being 88%, 95% and 96% respectively. In contrast to 200μA negative exposure, there was no significant difference between sample groups for ten or sixty minutes with 350μA current.

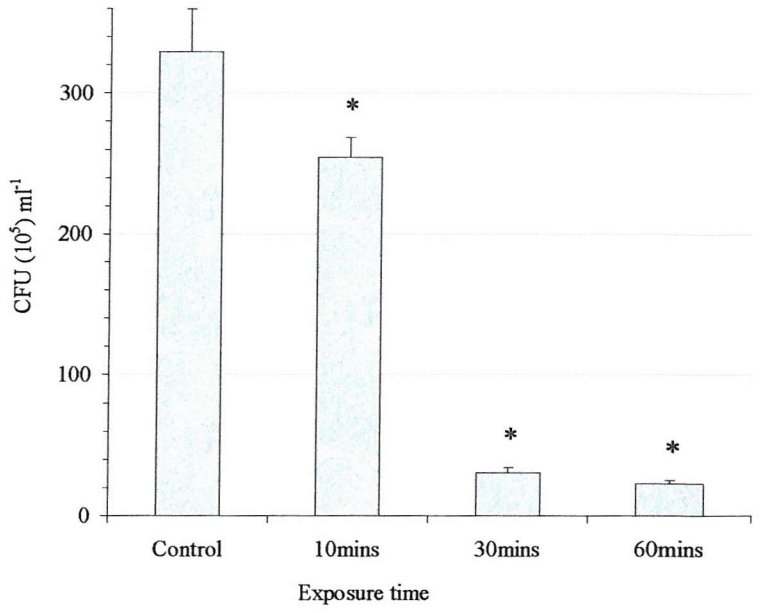

Figure 3.39) Effect of 350μA negative ionic exposure in nitrogen on *E.coli*. A set of nine pins spaced equally above an inoculated agar plate at a distance of 25mm was used. Nitrogen was flushed through the sealed chamber at a flow rate of 15L/minute for fifteen minutes prior to exposure and then reduced to 1l/min during exposure . Variable voltage was applied to the pin electrodes to produce 350μA current for a period of either 10, 30 or 60 minutes. Plates were subsequently incubated at 37°C for eighteen hours and the number of CFU counted and compared to controls. Bars represent the mean (n = 6) ± S.E.M. and * indicates $p<0.05$.

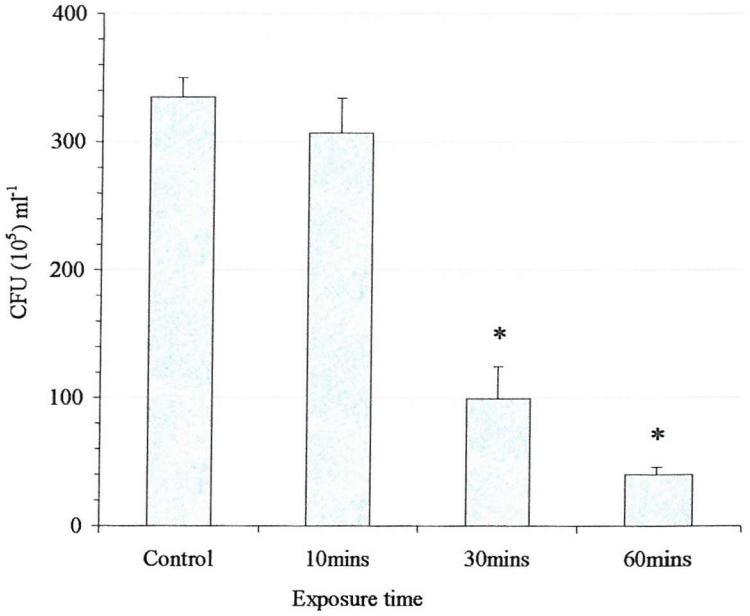

Figure 3.40) Effect of 350μA negative ionic exposure in nitrogen on *S.aureus*. A set of nine pins spaced equally above an inoculated agar plate at a distance of 25mm was used. Nitrogen was flushed through the sealed chamber at a flow rate of 15L/minute for fifteen minutes prior to exposure and then reduced to 1l/min during exposure. Variable voltage was applied to the pin electrodes to produce 350μA current for a period of either 10, 30 or 60 minutes. Plates were subsequently incubated at 30°C for nineteen hours and the number of CFU counted and compared to controls. Bars represent the mean (n = 6) ± S.E.M. and * indicates $p<0.05$.

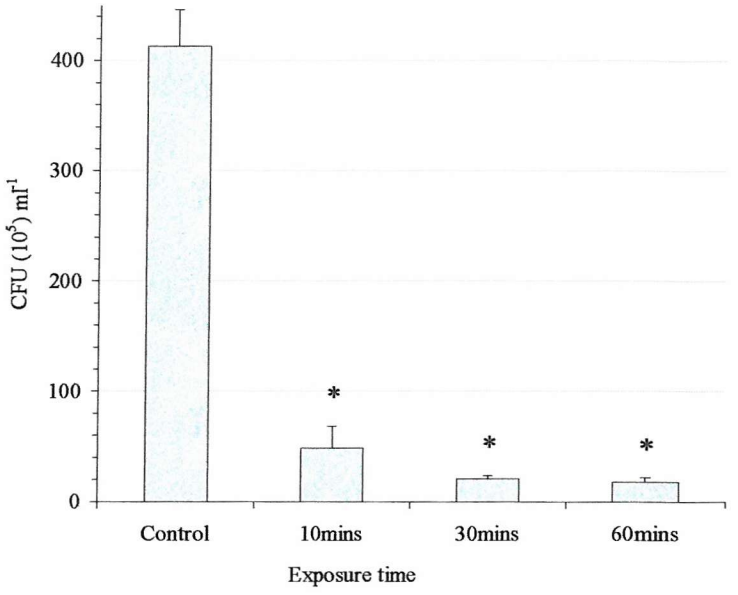

Figure 3.41) Effect of 350μA negative ionic exposure in nitrogen on starved *P.veronii*. A set of nine pins spaced equally above an 87mm diameter metal disc, at a distance of 25mm was used. Inoculated foil coupons ($2cm^2$) were positioned on the disc directly beneath a pin electrode. Nitrogen was flushed through the sealed chamber at a flow rate of 15L/minute for fifteen minutes prior to exposure and then reduced to 1l/min during exposure. Variable voltage was applied to the pin electrodes to produce 350μA current for a period of either 10, 30 or 60 minutes. Coupons were subsequently incubated in TSB for thirty minutes prior to reading in a luminometer with 50μl nonanal and compared to controls. Bars represent the mean (n = 6) ± S.E.M. and * indicates $p<0.05$.

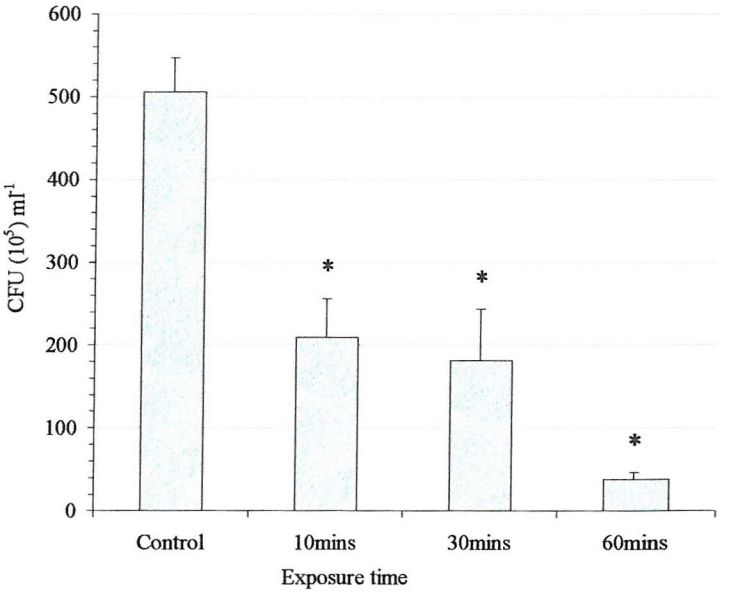

Figure 3.42) Effect of 350μA negative ionic exposure in nitrogen on *P.veronii* biofilms. A set of nine pins spaced equally above an 87mm diameter metal disc, at a distance of 25mm was used. Biofilm foil coupons ($2cm^2$) were positioned on the disc directly beneath a pin electrode. Nitrogen was flushed through the sealed chamber at a flow rate of 15L/minute for fifteen minutes prior to exposure and then reduced to 1l/min during exposure. Variable voltage was applied to the pin electrodes to produce 350μA current for a period of either 10, 30 or 60 minutes. Biofilms were subsequently incubated in TSB for thirty minutes prior to reading in a luminometer with 50μl nonanal and compared to controls. Bars represent the mean (n = 6) ± S.E.M. and * indicates $p<0.05$.

For *P.veronii* biofilms (*Figure* 3.42) the increased negative exposure current of 350μA proved effective at significantly reducing the mean number of $CFUml^{-1}$ for sixty minutes exposure only, compared to 200μA. No significant difference was found between ten and thirty minute sample groups for the 200μA and 350μA current regimes. In spite of the further reduction in cell viability for sixty minutes with 350μA negative challenge, 200μA positive exposure for the same time period was still significantly greater, with a mean number of 6×10^5 $CFUml^{-1}$ compared to 38×10^5 $CFUml^{-1}$. A summary of results for 350μA ionic exposure is shown in *Table* 3.5.

Bacterial target	Negative polarity		
	10mins	30mins	60mins
E.coli	23*	91*	93*
S.aureus	8	70*	88*
Starved P.veronii	88*	95*	96*
P.veronii Biofilm	59*	64*	92*

Table 3.5) Summary of the mean % reduction in $CFUml^{-1}$number for 350μA negative exposure in nitrogen, against four different bacterial targets. * Indicates $p<0.05$ compared to control group. Highlighted boxes represent significant greater reductions in cell viability ($p<0.05$) compared to 200μA negative exposure.

From *Table* 3.5, it can be seen that increasing the exposure current for a negative applied voltage failed to significantly increase the number of bacteria killed. Only *E.coli* elicited greater reductions in viability as a result of 350μA negative treatment. This is in contrast to the previous negative current increase from 100μA to 200μA, where significant reductions were produced for virtually all test conditions. Of the four

bacterial targets, the starved *P.veronii* cells and the *P.veronii* biofilms were the most susceptible to ionic treatment in nitrogen, either negative or positive, with mean reductions in cell number of 81% and 64% respectively (mean values of all sample data at either 100, 200 or 350μA). With regards to *E.coli* and *S.aureus* the mean reduction in $CFUml^{-1}$ number for all ionic tests conditions in nitrogen were 58% and 49% respectively. This is in contrast to results of corona exposure in air where both starved cells and biofilms proved to be significantly more resistant than *E.coli* and *S.aureus*.

3.9) Effect of exposure to either negative or positive ions within an electric field – free region in nitrogen on *E.coli, S.aureus,* starved *P.veronii or P.veronii* biofilms

Bacterial targets subjected to a corona discharge are exposed to the electric field that exists between the two electrodes. To eliminate the electric field influence, bacterial samples were exposed to negative or positive ions (mean current of 0.75μA for both polarities) within a field free zone (*Section* 2.17, *Page* 65), the effect of which is shown in *Figures* 3.43 to 3.50 (*Pages* 121 to 124).

For *E.coli* (*Figure* 3.43), only the 180-minute exposure period was sufficient to significantly affect the number of $CFUml^{-1}$ with a mean reduction of 39%. Changing the exposure polarity to positive (*Figure* 3.44) produced a significant difference in the mean number of cells after 120 minutes challenge, with a decrease from the control value of 308×10^5 to 191×10^5 $CFUml^{-1}$, representing a mean reduction of 38%. After 180 minutes positive exposure, the mean number of $CFUml^{-1}$ had been significantly reduced further to a mean value of 67×10^5 and representing a total reduction of 78%.

Field free negative exposure failed to elicit any significant effect on *S.aureus* $CFUml^{-1}$ number after 60 or 120 minutes (*Figure* 3.45). As previously seen with *E.coli*, 180 minutes treatment significantly ($p<0.05$) reduced the mean number of $CFUml^{-1}$ from the control value of 344×10^5 to 231×10^5, representing a decrease of 33%. With the application of positive field free ions (*Figure* 3.46), $CFUml^{-1}$ number was significantly

reduced ($p<0.05$) after 120 minutes, with a mean decrease of 58%. After 180 minutes positive exposure, this figure had significantly ($p<0.05$) increased to 81%.

Exposure of starved *P.veronii* to field free negative ions demonstrated significant reductions for all time regimes compared to the mean control value of 413×10^5 $CFUml^{-1}$ (*Figure* 3.47). For 60, 120 and 180 minute exposure times the mean number of $CFUml^{-1}$ was 265, 234 and 200×10^5, respectively. Comparisons between sample groups for each time period with negative field free exposure demonstrated no significant difference, with mean reductions of 36%, 43% and 52% for 60, 120 and 180 minutes respectively. Positive field free ionic exposure produced further reductions in the number of $CFUml^{-1}$ for each successive time regime, with mean reductions of 52%, 53% and 68% (*Figure* 3.48). However, only the sample group for 180 minutes demonstrated a significant difference when compared to the same sample group for negative exposure.

With negative field free treatment, only 60 minutes exposure failed to significantly reduce the number of viable *P.veronii* cells in the biofilms (*Figure* 3.49). After 60, 120 or 180 minutes, the mean number of $CFUml^{-1}$ had been reduced to 475×10^5, 24×10^5 and 16×10^5 respectively. Analysis of sample groups for each time period showed a significant difference between 60 and 120 minutes only. The sample group for 180 minutes failed to show any further significant reduction in $CFUml^{-1}$ number. Exposure to positive field free ions (*Figure* 3.50) demonstrated a significant difference in $CFUml^{-1}$ number after 60 minutes compared to negative treatment with a mean reduction of 28%. Sample groups for 120 and 180 minutes positive exposure showed no significant difference when compared to the same sample groups for negative treatment.

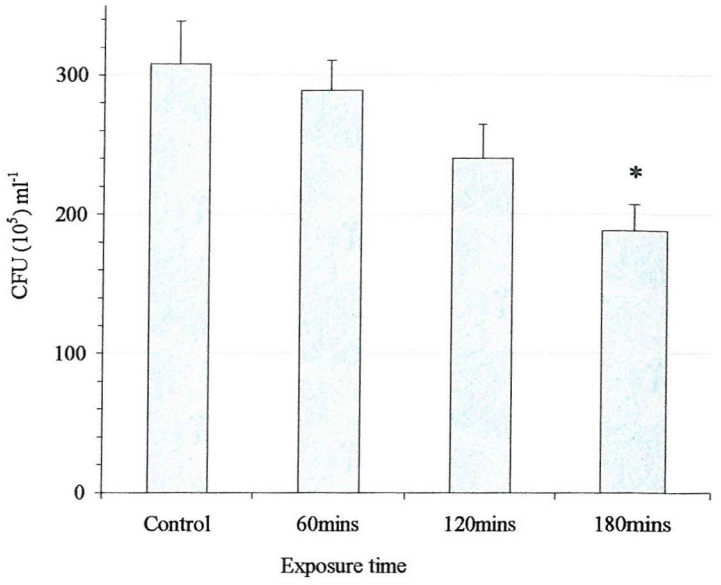

Figure 3.43) Effect of negative ionic exposure in an electric field free region on *E.coli*. A set of nine pins equally spaced above an 88mm diameter, 0.5mm^2 grid at a point to plane distance of 25mm was used. The inoculated agar plate was earthed and placed directly beneath the grid electrode at a distance of 10mm. Nitrogen was initially flushed through the sealed chamber at a flow rate of 15l/min for fifteen minutes and then reduced to 1l/min during exposure. Variable voltage was applied to the pin electrodes to generate an ion wind for either 60, 120 or 180 minutes. Plates were subsequently incubated at 37°C for eighteen hours and the number of CFU counted and compared to controls (time zero). Bars represent the mean (n = 6) ± S.E.M. and * indicates $p<0.05$.

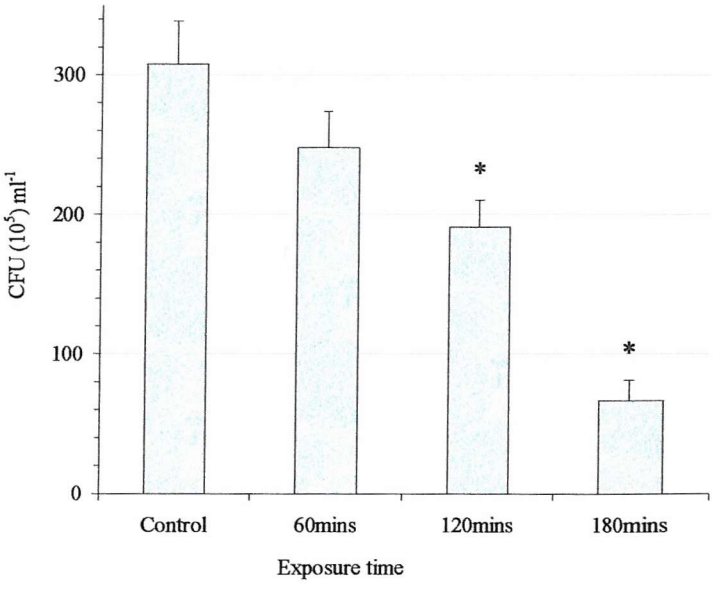

Figure 3.44) Effect of positive ionic exposure in an electric field free region on *E.coli*. A set of nine pins equally spaced above an 88mm diameter, 0.5mm^2 grid at a point to plane distance of 25mm was used. The inoculated agar plate was earthed and placed directly beneath the grid electrode at a distance of 10mm. Nitrogen was initially flushed through the sealed chamber at a flow rate of 15l/min for fifteen minutes and then reduced to 1l/min during exposure. Voltage was applied to the pin electrodes to generate an ion wind for either 60, 120 or 180 minutes. Plates were subsequently incubated at 37°C for eighteen hours and the number of CFU counted and compared to controls (time zero). Bars represent the mean (n = 6) ± S.E.M. and * indicates $p<0.05$.

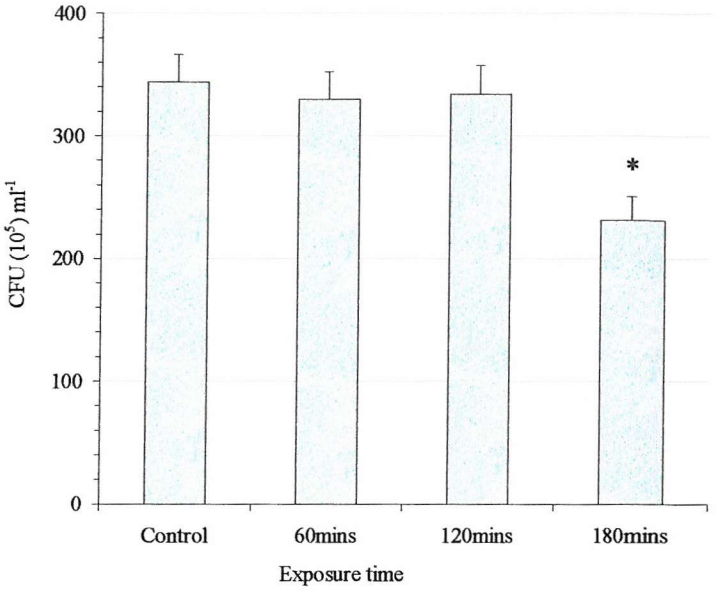

Figure 3.45) Effect of negative ionic exposure in an electric field free region on *S.aureus*. A set of nine pins equally spaced above an 88mm diameter, 0.5mm^2 grid at a point to plane distance of 25mm was used. The inoculated agar plate was earthed and placed directly beneath the grid electrode at a distance of 10mm. Nitrogen was initially flushed through the sealed chamber at a flow rate of 15l/min for fifteen minutes and then reduced to 1l/min during exposure. Variable voltage was applied to the pin electrodes to generate an ion wind for either 60, 120 or 180 minutes. Plates were subsequently incubated at 30°C for nineteen hours and the number of CFU counted and compared to controls (time zero). Bars represent the mean (n = 6) ± S.E.M. and * indicates $p<0.05$.

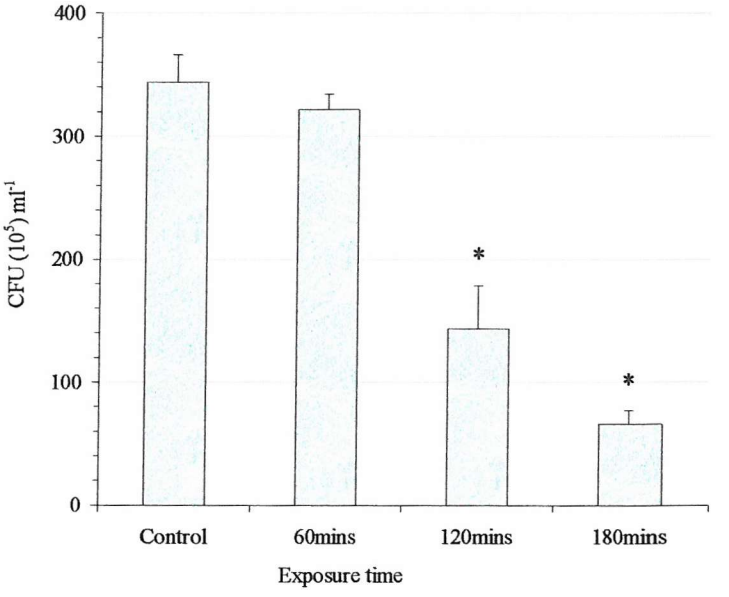

Figure 3.46) Effect of positive ionic exposure in an electric field free region on *S.aureus*. A set of nine pins equally spaced above an 88mm diameter, 0.5mm^2 grid at a point to plane distance of 25mm was used. The inoculated agar plate was earthed and placed directly beneath the grid electrode at a distance of 10mm. Nitrogen was initially flushed through the sealed chamber at a flow rate of 15l/min for fifteen minutes and then reduced to 1l/min during exposure. Voltage was applied to the pin electrodes to generate an ion wind for either 60, 120 or 180 minutes. Plates were subsequently incubated at 30°C for nineteen hours and the number of CFU counted and compared to controls (time zero). Bars represent the mean (n = 6) ± S.E.M. and * indicates $p<0.05$.

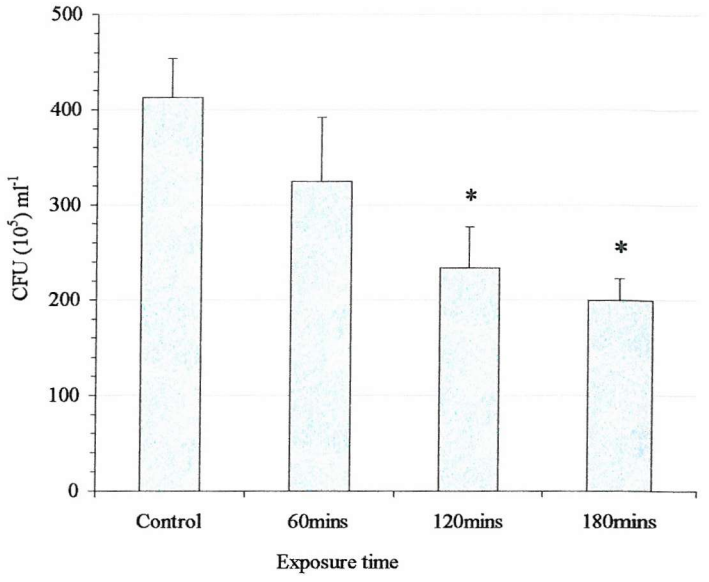

Figure 3.47) Effect of negative ionic exposure in an electric field free region on starved *P.veronii*. A set of nine pins equally spaced above an 88mm diameter, 0.5mm^2 grid at a point to plane distance of 25mm was used. The inoculated coupons were positioned on to an earthed 87mm diameter metal disc, which was positioned beneath the grid electrode at a distance of 10mm. Nitrogen was initially flushed through the sealed chamber at a flow rate of 15l/min for fifteen minutes and then reduced to 1l/min during exposure. Variable voltage was applied to the pin electrodes to generate an ion wind for either 60, 120 or 180 minutes. Coupons were subsequently incubated in TSB for thirty minutes prior to reading in a luminometer with 50µl nonanal and compared to controls. Bars represent the mean (n = 6) ± S.E.M. and * indicates $p<0.05$.

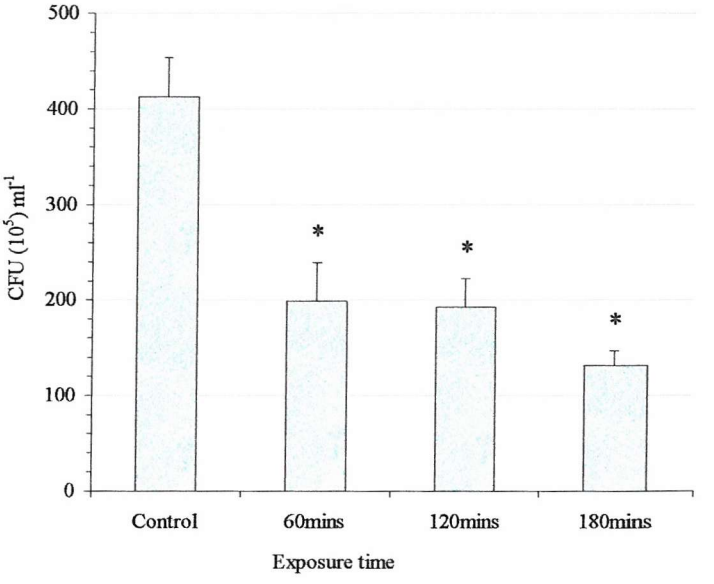

Figure 3.48) Effect of positive ionic exposure in an electric field free region on starved *P.veronii*. A set of nine pins equally spaced above an 88mm diameter, 0.5mm^2 grid at a point to plane distance of 25mm was used. The inoculated coupons were positioned on to an earthed 87mm diameter metal disc, which was positioned beneath the grid electrode at a distance of 10mm. Nitrogen was initially flushed through the sealed chamber at a flow rate of 15l/min for fifteen minutes and then reduced to 1l/min during exposure. Voltage was applied to the pin electrodes to generate an ion wind for either 60, 120 or 180 minutes. Coupons were subsequently incubated in TSB for thirty minutes prior to reading in a luminometer with 50µl nonanal and compared to controls. Bars represent the mean (n = 6) ± S.E.M. and * indicates $p<0.05$.

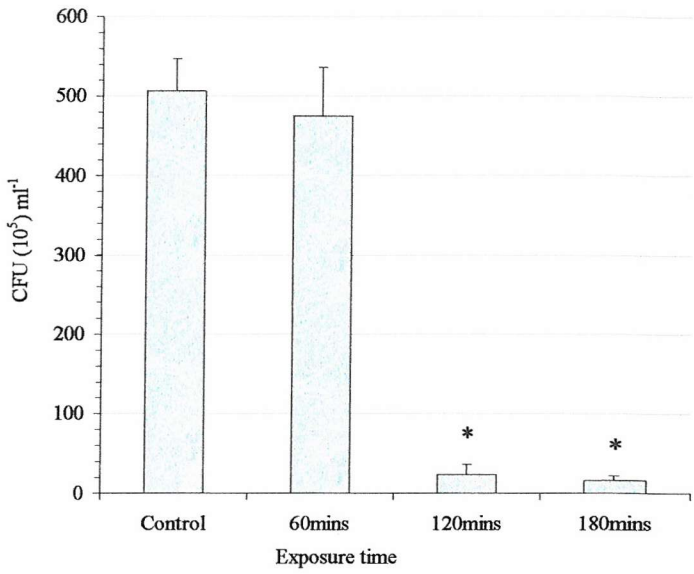

Figure 3.49) Effect of negative ionic exposure in an electric field free region on *P.veronii* biofilms. A set of nine pins equally spaced above an 88mm diameter, 0.5mm^2 grid at a point to plane distance of 25mm was used. The biofilm coupons were positioned on to an earthed 87mm diameter metal disc, which was positioned beneath the grid electrode at a distance of 10mm. Nitrogen was initially flushed through the sealed chamber at a flow rate of 15l/min for fifteen minutes and then reduced to 1l/min during exposure. Variable voltage was applied to the pin electrodes to generate an ion wind for either 60, 120 or 180 minutes. Biofilm coupons were subsequently incubated in TSB for thirty minutes prior to reading in a luminometer with 50µl nonanal and compared to controls. Bars represent the mean (n = 6) ± S.E.M. and * indicates $p<0.05$.

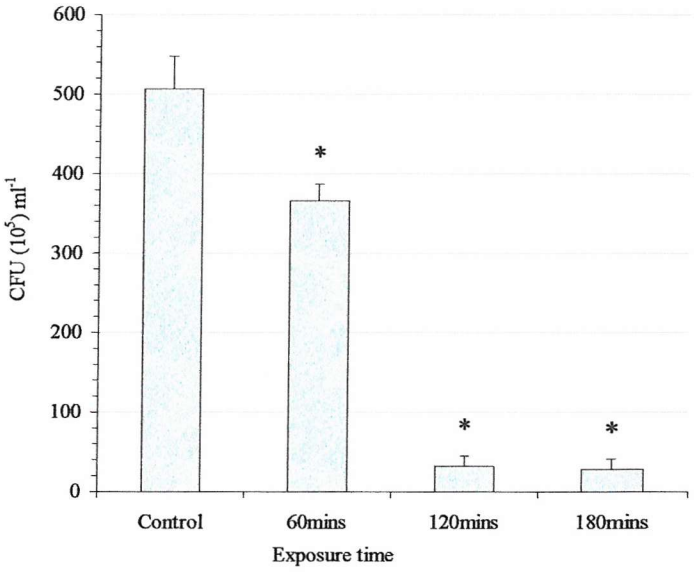

Figure 3.50) Effect of positive ionic exposure in an electric field free region on *P.veronii* biofilms. A set of nine pins equally spaced above an 88mm diameter, 0.5mm^2 grid at a point to plane distance of 25mm was used. The biofilm coupons were positioned on to an earthed 87mm diameter metal disc, which was positioned beneath the grid electrode at a distance of 10mm. Nitrogen was initially flushed through the sealed chamber at a flow rate of 15l/min for fifteen minutes and then reduced to 1l/min during exposure. Voltage was applied to the pin electrodes to generate an ion wind for either 60, 120 or 180 minutes. Biofilm coupons were subsequently incubated in TSB for thirty minutes prior to reading in a luminometer with 50µl nonanal and compared to controls. Bars represent the mean (n = 6) ± S.E.M. and * indicates $p<0.05$.

A summary of results for ionic exposure in an electric field free zone is shown in *Table* 3.6.

Bacterial target	Negative polarity			Positive polarity		
	60mins	120mins	180mins	60mins	120mins	180mins
E.coli	6	22	39*	20	38*	78*
S.aureus	4	3	33*	6	58*	81*
Starved *P.veronii*	36*	43*	52*	52*	53*	68*
P.veronii Biofilm	6	95*	97*	28*	94*	94*

Table 3.6) Summary of the mean % reduction in CFUml^{-1}number for either negative or positive ionic exposure in a field free region in nitrogen, against four different bacterial targets. * Indicates $p<0.05$ compared to control group. Highlighted boxes represent significantly greater reductions in cell viability ($p<0.05$) compared to opposite polarity exposure for the same time period.

With the influence of electric field removed, significant reductions in cell number were still achieved, although 180 minute exposure times were required for *E.coli* and *S.aureus*. Quantitatively, this was to be expected considering the exposure current was less than 1μA, compared to previous tests with exposure currents as high as 350μA. However, the magnitude of the effects seen here are surprising. For example, from *Table* 3.5, 10 minutes exposure to negative polarity at 350μA produced reductions in bacterial viability ranging from 8 to 88%. This exposure equated to a total ion flux equivalent to 200 mC. In comparison, from *Table* 3.6, 180 minutes exposure to negative polarity at 0.75μA (total charge of 8mC) produced similar reductions although the total applied charge was considerably less. At present no clear explanation can be provided and further investigation is required.

Of the two polarities, positive exposure was more effective than negative at significantly ($p<0.05$) reducing cell number for all samples, with a mean reduction of 55%, compared to 36% for negative. The most resistant organisms to either negative or positive ion treatment (field free) were *S.aureus* and *E.coli*, with mean reductions in

$CFUml^{-1}$ number of 31% and 34% respectively. Starved *P.veronii* and *P.veronii* biofilms were most susceptible with mean reductions of 51% and 69% respectively, which mimics previous results for direct ionic exposure in nitrogen (*Section* 3.8)

3.10) Scanning electron micrographs of *P.veronii* and *S.aureus*

The experiments to date have shown that exposure to either negative or positive ionic treatment in nitrogen is detrimental to both Gram-negative and Gram-positive bacterial samples. To elucidate the actual cause of this antibacterial effect, scanning electron micrographs were taken of *P.veronii* and *S.aureus* cells, which were either left untreated or exposed to 200μA negative or positive corona current. *Figures* 3.51 to 3.54 (*Page*s 127 to 128) show the effect of ionic treatment on either *P.veronii* or *S.aureus* cells. The micrographs shown represent typical results of the many pictures taken. Close inspection of the micrographs for untreated and exposed cells for both bacterial types revealed no obvious physiological differences. However, this does not mean that a physiological change has not occurred. The resolution of the micrographs was too low to reveal any physical evidence such as damage to the cell wall. In addition, it is still possible that representative cells indicating possible reasons for cellular death were simply missed by the micrographs, or masked by the physical characteristics of the electron beam with a current density in the order of 1 A cm^{-2} (Goodhew and Humphries, 1988), compared to experimental current densities of 6 μA cm^{-2}. Although it is clear that ionic exposure is fatal to both *P.veronii* and *S.aureus*, it does not necessarily mean that an external physiological alteration is responsible for cellular death. If ionic exposure induces cellular death through an internal mechanism then evidence from these pictures may not be found.

Untreated cells Treated cells

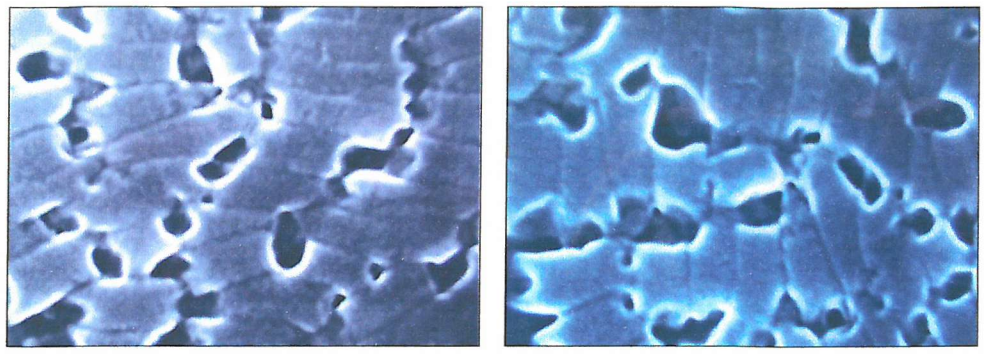

Figure 3.51) Scanning electron micrographs of *P.veronii* cells left untreated or exposed to 200μA negative ionic treatment. A set of nine pins spaced equally above an 88mm diameter metal disc, at a distance of 25mm was used. Inoculated foil coupons ($2cm^2$) were positioned on the disc directly beneath a pin electrode. Nitrogen was flushed through the sealed chamber at a flow rate of 15L/minute for fifteen minutes prior to exposure and then reduced to 1l/min during exposure. Voltage was applied to the pin electrodes to produce 200μA current for a period of 60 minutes. Post treatment, control and sample coupons were prepared and photographed. Magnification of 10^4.

Untreated cells Treated cells

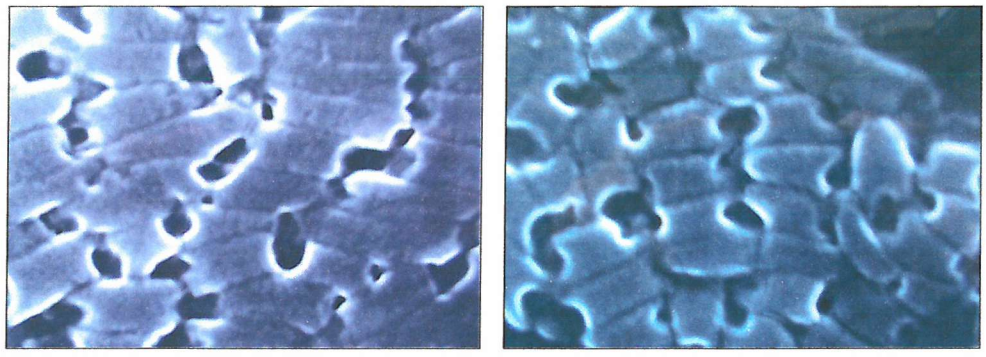

Figure 3.52) Scanning electron micrographs of *P.veronii* cells left untreated or exposed to 200μA positive ionic treatment. A set of nine pins spaced equally above an 88mm diameter metal disc, at a distance of 25mm was used. Inoculated foil coupons ($2cm^2$) were positioned on the disc directly beneath a pin electrode. Nitrogen was flushed through the sealed chamber at a flow rate of 15L/minute for fifteen minutes prior to exposure and then reduced to 1l/min during exposure. Voltage was applied to the pin electrodes to produce 200μA current for a period of 60 minutes. Post treatment, control and sample coupons were prepared and photographed. Magnification of 10^4.

Untreated cells Treated cells

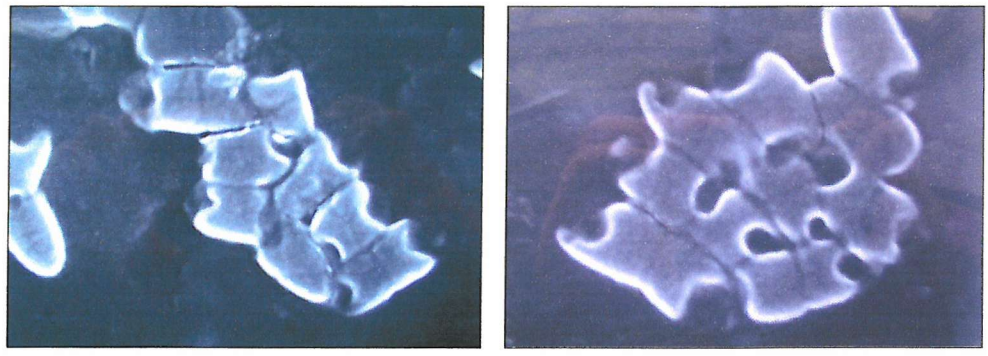

Figure 3.53) Scanning electron micrographs of *S.aureus* cells left untreated or exposed to 200μA negative ionic treatment. A set of nine pins spaced equally above an 88mm diameter metal disc, at a distance of 25mm was used. Inoculated foil coupons ($2cm^2$) were positioned on the disc directly beneath a pin electrode. Nitrogen was flushed through the sealed chamber at a flow rate of 15L/minute for fifteen minutes prior to exposure and then reduced to 1l/min during exposure. Voltage was applied to the pin electrodes to produce 200μA current for a period of 60 minutes. Post treatment, control and sample coupons were prepared and photographed. Magnification of 10^4.

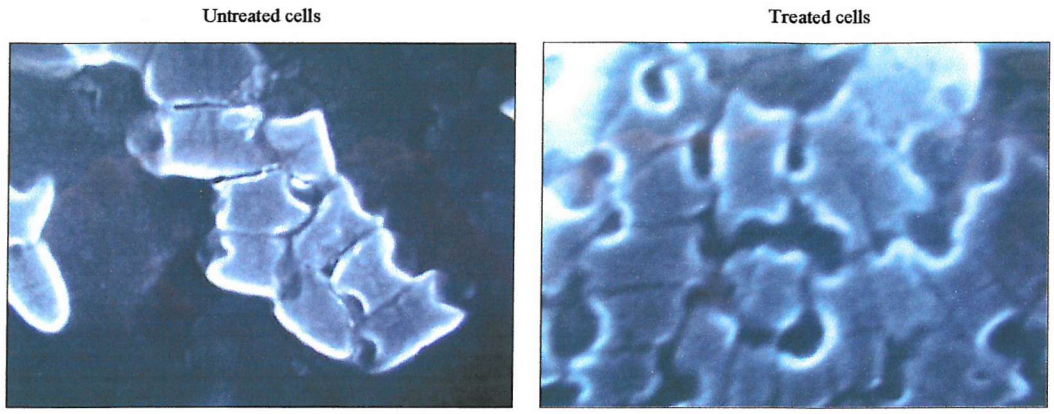

Figure 3.54) Scanning electron micrographs of *S.aureus* cells left untreated or exposed to 200μA positive ionic treatment. A set of nine pins spaced equally above an 88mm diameter metal disc, at a distance of 25mm was used. Inoculated foil coupons ($2cm^2$) were positioned on the disc directly beneath a pin electrode. Nitrogen was flushed through the sealed chamber at a flow rate of 15L/minute for fifteen minutes prior to exposure and then reduced to 1l/min during exposure. Voltage was applied to the pin electrodes to produce 200μA current for a period of 60 minutes. Post treatment, control and sample coupons were prepared and photographed. Magnification of 10^4.

3.11) Effect of negative or positive ionic exposure in nitrogen on bacterial cell wall integrity

In order to ascertain the physiological effect of ionic treatment, bacterial cells were exposed to a corona discharge in nitrogen and subsequently tested to ascertain the integrity of their cell walls using the BacLight staining technique (Section 2.19, *Page* 68). The effect of either 100μA or 200μA negative or positive exposure in nitrogen on the cell wall integrity of either *E.coli*, *S.aureus* or starved *P.veronii* can be seen in *Figures* 3.55 to 3.60 (*Pages* 130 to 132).

Exposure to 100μA negative ionic treatment for *E.coli* (*Figure* 3.55) produced a significant reduction ($p<0.05$) in the ratio of Syto–9 to Propidium iodide (S9: P.I) of 46% after sixty minutes. Positive treatment at the same current level induced significant reductions for both thirty and sixty minute treatments of 54% and 71%

respectively. Increasing the current to 200μA (*Figure* 3.56) produced significantly greater reductions in the S9: P.I exposure for both polarities. With negative applied voltage the mean S9: P.I was 0.957 and 0.473 after thirty and sixty minutes respectively, compared to 1.3 and 0.80 for 100μA. With positive polarity at this current level only the sample group for sixty minutes was significantly different compared to 100μA, with a mean reduction of 86%.

For *S.aureus* (*Figure* 3.57) 100μA negative exposure produced no significant reduction after thirty minutes. However, increasing the exposure time to sixty minutes significantly reduced the S9: P.I by 26%. In contrast, positive challenge at 100μA significantly reduced the S9: P.I by 50% and 52% after thirty and sixty minutes. Applying 200μA (*Figure* 3.58) negative exposure, significantly increased the mean reduction in the S9: P.I to 86% after sixty minutes compared to 100μA. Positive exposure at 200μA produced reductions of 72% and 79% for thirty and sixty minute treatments respectively, that were significantly different ($p<0.05$) compared to sample groups for 100μA.

With starved *P.veronii* (*Figure* 3.59) 100μA negative treatment induced significant reductions of 43% and 77% after thirty and sixty minutes respectively. With 100μA positive exposure there were 63% and 90% reductions for the same time periods. Exposure to 200μA with negative applied voltage significantly increased the reductions after thirty and sixty minutes to 77% and 92% respectively. Representing a decrease from the mean control S9: P.I value of 1.8 to 0.41 and 0.13 respectively, compared to 1.03 and 0.42 for 100μA. Positive polarity at 200μA significantly decreased the S9: P.I further for thirty minutes to a mean of 0.17, but not for sixty minutes.

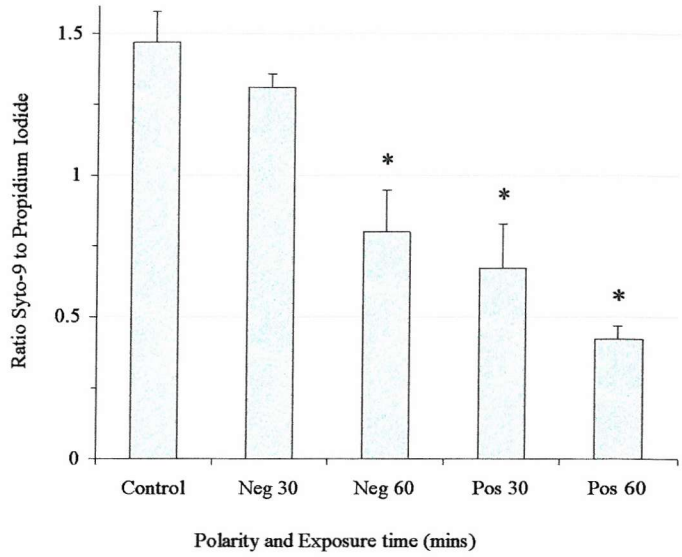

Figure 3.55) Effect of 100µA negative or positive ionic exposure in nitrogen on *E.coli* cell wall integrity. A set of nine pins spaced equally above an 87mm diameter metal disc, at a distance of 25mm was used. Inoculated foil coupons ($2cm^2$) were positioned on the disc directly beneath a pin electrode. Nitrogen was flushed through the sealed chamber at a flow rate of 15L/minute for fifteen minutes prior to exposure and then reduced to 1l/min during exposure. Voltage was applied to the pin electrodes to produce 100µA current for a period of either 30 or 60 minutes. Residue spots were subsequently rehydrated in distilled water for sixty minutes, then 80µl was transferred into wells of a white, 96 well plate. 80 µl of BacLight dye was added to each well. The plate was then placed in the dark for 15 minutes. Following incubation with the dye, the plate was read using a luminescence spectrometer. Bars represent the mean (n = 6) ± S.E.M. and * indicates $p<0.05$.

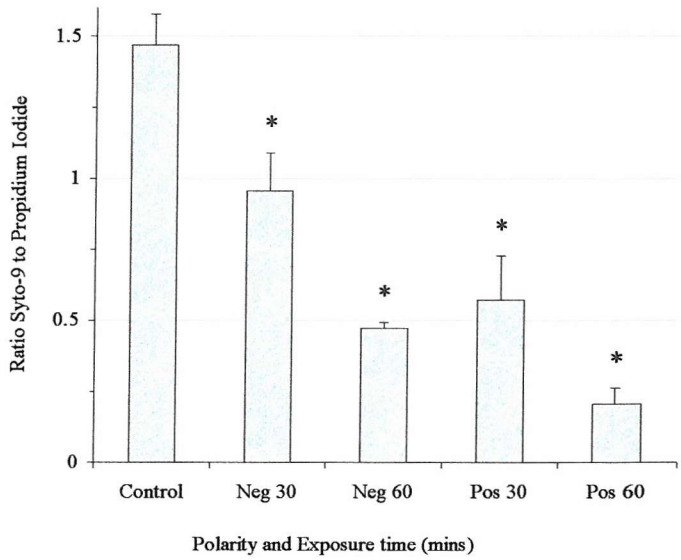

Figure 3.56) Effect of 200µA negative or positive ionic exposure in nitrogen on *E.coli* cell wall integrity. A set of nine pins spaced equally above an 87mm diameter metal disc, at a distance of 25mm was used. Inoculated foil coupons ($2cm^2$) were positioned on the disc directly beneath a pin electrode. Nitrogen was flushed through the sealed chamber at a flow rate of 15L/minute for fifteen minutes prior to exposure and then reduced to 1l/min during exposure. Voltage was applied to the pin electrodes to produce 200µA current for a period of either 30 or 60 minutes. Residue spots were subsequently rehydrated in distilled water for sixty minutes, then 80µl was transferred into wells of a white, 96 well plate. 80 µl of BacLight dye was added to each well. The plate was then placed in the dark for 15 minutes. Following incubation with the dye, the plate was read using a luminescence spectrometer. Bars represent the mean (n = 6) ± S.E.M. and * indicates $p<0.05$.

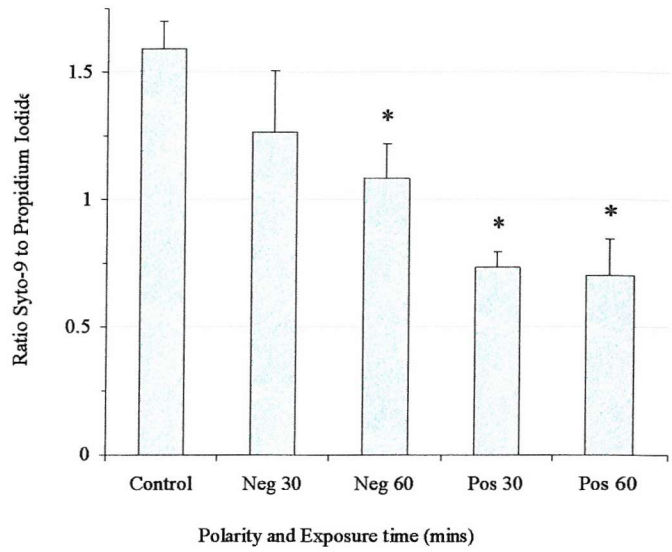

Figure 3.57) Effect of 100µA negative or positive ionic exposure in nitrogen on *S.aureus* cell wall integrity. A set of nine pins spaced equally above an 87mm diameter metal disc, at a distance of 25mm was used. Inoculated foil coupons ($2cm^2$) were positioned on the disc directly beneath a pin electrode. Nitrogen was flushed through the sealed chamber at a flow rate of 15L/minute for fifteen minutes prior to exposure and then reduced to 1l/min during exposure. Voltage was applied to the pin electrodes to produce 100µA current for a period of either 30 or 60 minutes. Residue spots were subsequently rehydrated in distilled water for sixty minutes, then 80µl was transferred into wells of a white, 96 well plate. 80 µl of BacLight dye was added to each well. The plate was then placed in the dark for 15 minutes. Following incubation with the dye, the plate was read using a luminescence spectrometer. Bars represent the mean (n = 6) ± S.E.M. and * indicates $p<0.05$.

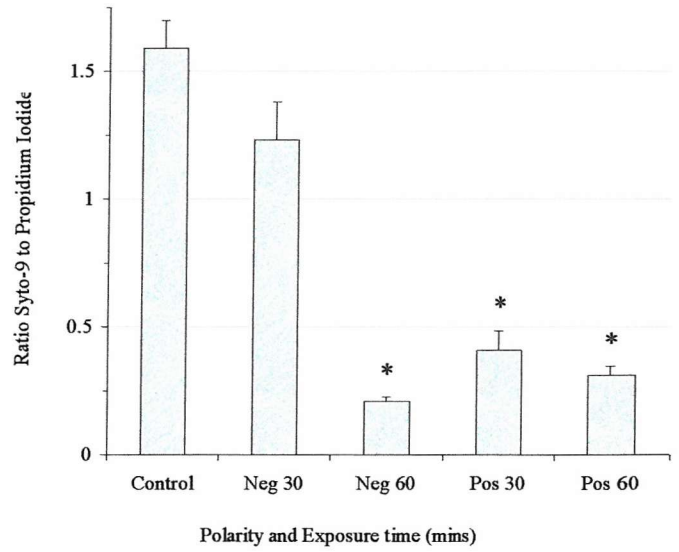

Figure 3.58) Effect of 200µA negative or positive ionic exposure in nitrogen on *S.aureus* cell wall integrity. A set of nine pins spaced equally above an 87mm diameter metal disc, at a distance of 25mm was used. Inoculated foil coupons ($2cm^2$) were positioned on the disc directly beneath a pin electrode. Nitrogen was flushed through the sealed chamber at a flow rate of 15L/minute for fifteen minutes prior to exposure and then reduced to 1l/min during exposure. Voltage was applied to the pin electrodes to produce 200µA current for a period of either 30 or 60 minutes. Residue spots were subsequently rehydrated in distilled water for sixty minutes, then 80µl was transferred into wells of a white, 96 well plate. 80 µl of BacLight dye was added to each well. The plate was then placed in the dark for 15 minutes. Following incubation with the dye, the plate was read using a luminescence spectrometer. Bars represent the mean (n = 6) ± S.E.M. and * indicates $p<0.05$.

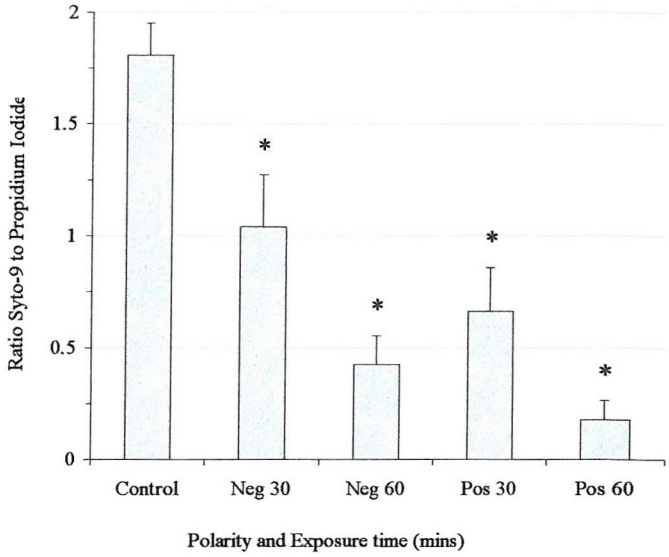

Figure 3.59) Effect of 100μA negative or positive ionic exposure in nitrogen on starved *P.veronii* cell wall integrity. A set of nine pins spaced equally above an 87mm diameter metal disc, at a distance of 25mm was used. Inoculated foil coupons ($2cm^2$) were positioned on the disc directly beneath a pin electrode. Nitrogen was flushed through the sealed chamber at a flow rate of 15L/minute for fifteen minutes prior to exposure and then reduced to 1l/min during exposure. Voltage was applied to the pin electrodes to produce 100μA current for a period of either 30 or 60 minutes. Residue spots were subsequently rehydrated in distilled water for sixty minutes, then 80μl was transferred into wells of a white, 96 well plate. 80 μl of BacLight dye was added to each well. The plate was then placed in the dark for 15 minutes. Following incubation with the dye, the plate was read using a luminescence spectrometer. Bars represent the mean (n = 6) ± S.E.M. and * indicates $p<0.05$.

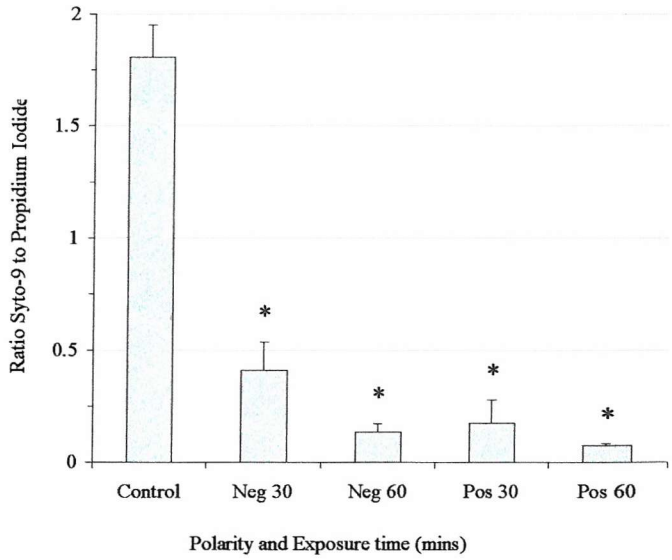

Figure 3.60) Effect of 200μA negative or positive ionic exposure in nitrogen on starved *P.veronii* cell wall integrity. A set of nine pins spaced equally above an 87mm diameter metal disc, at a distance of 25mm was used. Inoculated foil coupons ($2cm^2$) were positioned on the disc directly beneath a pin electrode. Nitrogen was flushed through the sealed chamber at a flow rate of 15L/minute for fifteen minutes prior to exposure and then reduced to 1l/min during exposure. Voltage was applied to the pin electrodes to produce 200μA current for a period of either 30 or 60 minutes. Residue spots were subsequently rehydrated in distilled water for sixty minutes, then 80μl was transferred into wells of a white, 96 well plate. 80 μl of BacLight dye was added to each well. The plate was then placed in the dark for 15 minutes. Following incubation with the dye, the plate was read using a luminescence spectrometer. Bars represent the mean (n = 6) ± S.E.M. and * indicates $p<0.05$.

A summary of results for ionic exposure and cell wall disruption is shown in *Table* 3.7.

Bacterial target	Negative polarity				Positive polarity			
	100μA		200μA		100μA		200μA	
	30mins	60mins	30mins	60mins	30mins	60mins	30mins	60mins
E.coli	11	46*	35*	68*	54*	71*	61*	86*
S.aureus	14	26*	16	86*	50*	52*	72*	79*
Starved P.veronii	43*	77*	77*	90*	63*	90*	90*	96*

Table 3.7) Summary of the mean % reduction in S9: P.I for either negative or positive ionic exposure in nitrogen, against three different bacterial targets. * Indicates $p<0.05$ compared to control group. Highlighted boxes represent significantly greater reductions in S9: P.I compared to 100μA treatment with the same polarity.

From these results it is apparent that cell wall damage is occurring as a direct response to ionic challenge. In addition, a pattern previously seen with ionic exposure in nitrogen exists i.e. for all bacterial types, either increasing the exposure current and time resulted in greater cell wall disruption. However, only certain test regimes produced significant increases as shown by *Table* 3.7. Nevertheless, previous results have shown that viability decreases with increasing current and exposure time, and these data indicate that cell wall damage is the possible cause. Exposure to positive ionic treatment in nitrogen produced significantly greater cell wall disruption, with a mean reduction in the S9: P.I of 72%, compared to 49% with negative treatment. Starved *P.veronii* was the most susceptible, with a mean reduction for either negative or positive exposure of 78%, compared to 54% and 49% for *E.coli* and *S.aureus* respectively.

3.12) Effect of negative or positive ionic exposure on nutrient agar

In order to eliminate any direct effect of a corona discharge on either the TSB or CGB agar medium, plates were exposed to either a negative or positive corona discharge for a period of sixty minutes, prior to inoculation with bacteria. The effect of prior exposure to either 200μA negative or positive corona current in air or nitrogen on the ability of TSB or CGB agar to support bacterial growth, is shown in *Figures* 3.61 and 3.62 (*Page* 135). As can be seen from both figures, there was no significant effect ($p>0.05$) on either nutrient medium type with pre-treated plates supporting bacterial colony formation to the same level as control plates.

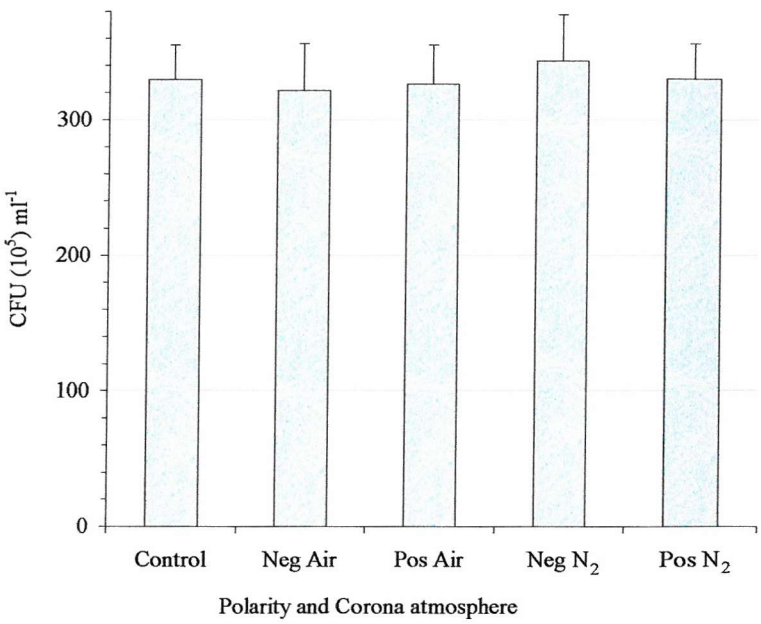

Figure 3.61) Effect of corona discharge in air or nitrogen on TSB agar. A set of nine pins spaced equally above an uninoculated TSB agar plate, at a distance of 25mm was used. Voltage was applied to the pin electrodes to produce 200μA negative corona current for a period of 120minutes. For exposure in nitrogen a sealed chamber was used and nitrogen was flushed through it at a flow rate of 15L/minute for fifteen minutes prior to exposure and then reduced to 1l/min during exposure. Following treatment the plates were inoculated with *E.coli* and incubated at 37°C for eighteen hours and the number of CFU counted and compared to controls. Bars represent the mean (n = 6) ± S.E.M.

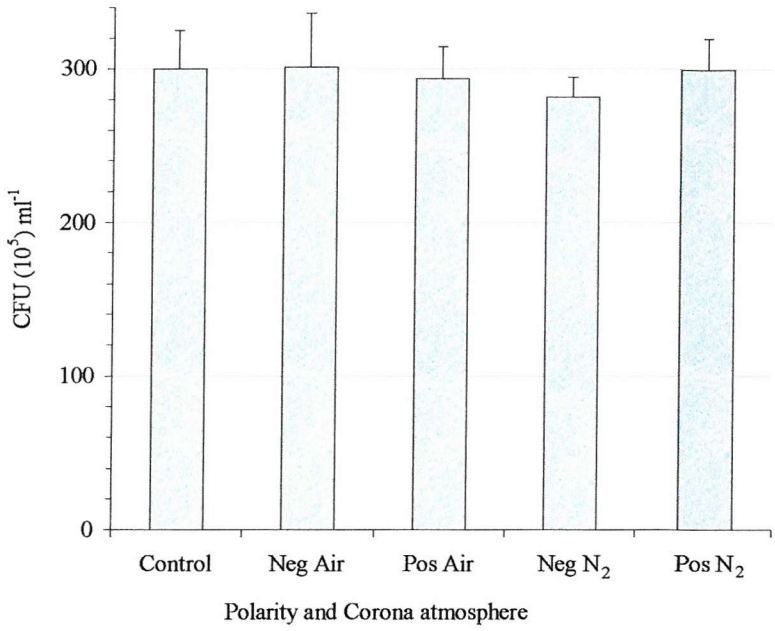

Figure 3.62) Effect of corona discharge in air or nitrogen on CGB agar. A set of nine pins spaced equally above an uninoculated CGB agar plate, at a distance of 25mm was used. Voltage was applied to the pin electrodes to produce 200μA negative or positive corona current for a period of 120minutes. For exposure in nitrogen a sealed chamber was used and nitrogen was flushed through it at a flow rate of 15L/minute for fifteen minutes prior to exposure and then reduced to 1l/min during exposure. Following treatment the plates were inoculated with *S.aureus* and incubated at 30°C for nineteen hours and the number of CFU counted and compared to controls. Bars represent the mean (n = 6) ± S.E.M.

3.13) Negative or positive ionic exposure and aluminium foil

The effect of pre-exposing aluminium foil coupons to either a corona discharge in air or nitrogen can be seen in *Figure* 3.63 (*Page* 136). The number of viable $CFUml^{-1}$ recorded from ionic pre-treated coupons showed no significant difference ($p<0.05$) compared to untreated foil coupons.

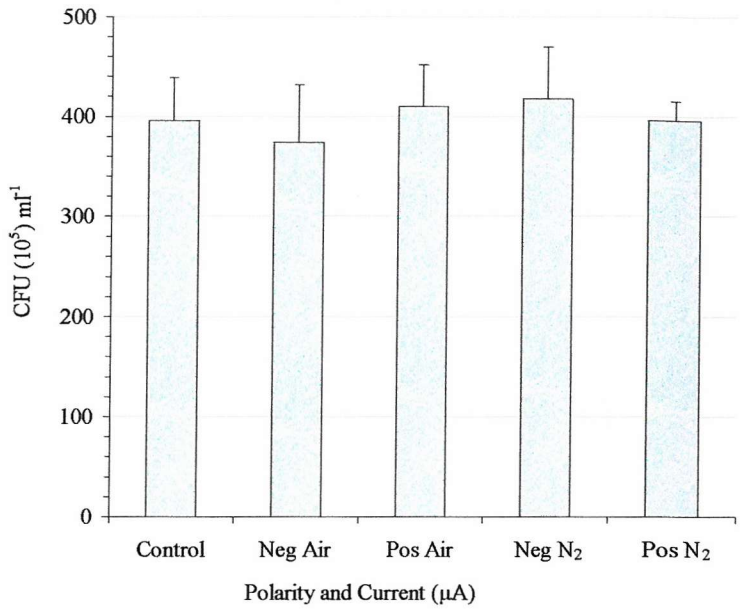

Figure 3.63) Effect of corona discharge in air or nitrogen on aluminium foil. A set of nine pins spaced equally above an 87mm diameter metal disc, at a distance of 25mm was used. Foil coupons ($2cm^2$) were positioned on the disc directly beneath a pin electrode. Voltage was applied to the pin electrodes to produce either 200μA positive or negative corona current for a period of 120minutes. For exposure in nitrogen a sealed chamber was used and nitrogen was flushed through it at a flow rate of 15L/minute for fifteen minutes prior to exposure and then reduced to 1l/min during exposure. Following treatment the coupons were inoculated with *P.veronii* and once dry, incubated with TSB for thirty minutes, followed by luminometer reading with 50μl nonanal. Bars represent the mean ($n = 6$) ± S.E.M.

3.14) Effect of current on bacterial viability

To ascertain the effect of an electrical current generated without a corona discharge on bacterial samples, inoculated samples were subjected to a 500μA current using a low voltage supply (*Section* 2.22, *Page* 70) for 180 minutes as shown in *Figures* 3.64 and 3.65 (*Page* 137). As shown by both figures, 180 minutes treatment with 500μA current failed to generate any significant difference ($p<0.05$) between control and sample groups for all bacterial types.

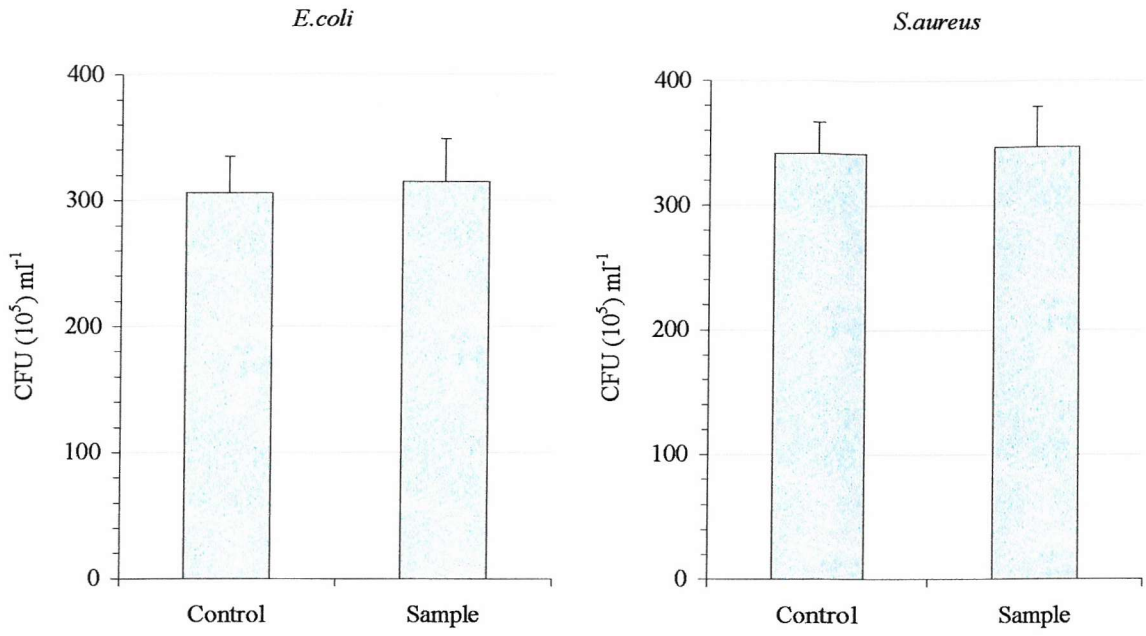

Figure 3.64) Effect of exposure to 500µA electrical current on *E.coli or S.aureus*. Electrodes from a low voltage power supply were placed at either end of inoculated dishes. Voltage was applied to the electrodes to generate 500µA current for a period of 180 minutes. Post treatment *E.coli* and *S.aureus* plates were incubated at 37°C for eighteen hours or 37°C for nineteen hours respectively and the number of CFU counted and compared to controls. Bars represent the mean (n = 6) ± S.E.M.

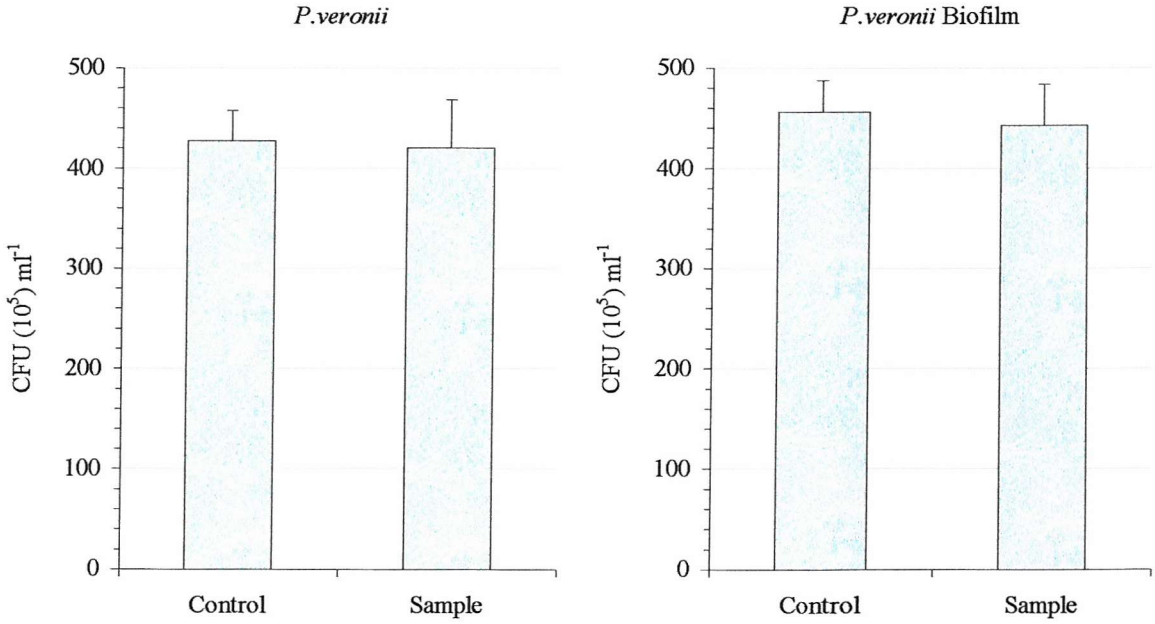

Figure 3.65) Effect of exposure to 500µA electrical current on starved *P.veronii* cells or *P.veronii* biofilms. Electrodes from a low voltage power supply were placed at either end of an aluminium plate with inoculated coupons placed on it. Voltage was applied to the electrodes to generate 500µA current for a period of 180 minutes. Coupons were subsequently incubated in TSB for thirty minutes prior to reading in a luminometer with 50µl nonanal and compared to controls. Bars represent the mean (n = 6) ± S.E.M.

3.15) Effect of RH on ionic treatment of *E.coli* and *S.aureus* cells

The use of nutrient agar plates as the plane electrode in a corona discharge set up leads to water evaporation from the plate surface as a consequence of ventilation by the ion wind. Consequently the RH levels of the experimental apparatus increased with time. In order to determine if the RH contributed towards the antibacterial effect of ionic exposure on either *E.coli* or *S.aureus* cells, bacterial samples inoculated onto foil coupons were exposed to 200μA negative or positive treatment in nitrogen with mean RH levels ranging from 8% to 70% (*Figures* 3.66 to 3.69, *Page*s 139 to 140).

From *Figures* 3.66 and 3.67 it can be seen that exposure to 200μA negative corona current for sixty minutes was effective at reducing the number of *E.coli* $CFUml^{-1}$. However, This effect is independent of RH level as there was no significant difference between sample groups for 8%, 20%, 40% and 70% RH for both polarities. Although there was a greater reduction in $CFUml^{-1}$ number with a positive applied voltage, the difference between sample groups for negative and positive tests was not significant.

As shown in *Figures* 3.68 and 3.69, the RH level had no effect on the amount of *S.aureus* disinfection achieved from negative or positive exposure in nitrogen. No significant difference ($p<0.05$) was found between the RH sample groups. Analysis between negative and positive sample groups did show a significantly greater reduction in cell number for positive exposure with a mean decrease of 61%, compared to 35% for negative.

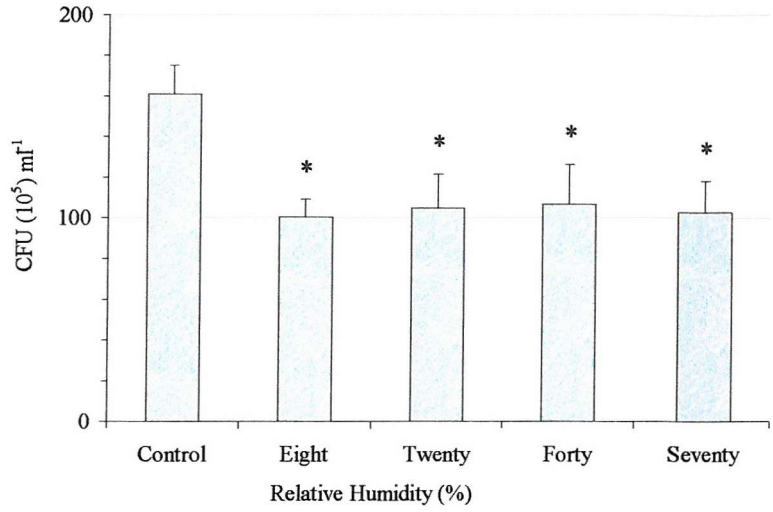

Figure 3.66) Effect of relative humidity on 200μA negative ionic exposure in nitrogen on *E.coli*. A set of nine pins spaced equally above an 87mm diameter metal disc, at a distance of 25mm was used. Inoculated foil coupons ($2cm^2$) were positioned on the disc directly beneath a pin electrode. Nitrogen was flushed through the sealed chamber at a flow rate of 15L/minute for sixteen minutes prior to exposure and then reduced to 1l/min during exposure. The nitrogen gas was passed through distilled water and then different quantities of silica gel to provide relative humidity levels of either 8, 20, 40 or 70%.Voltage was applied to the pin electrodes to produce 200μA current for a period of sixty minutes. Residue spots were subsequently rehydrated in TSB for sixty minutes, then 100μl was removed and serially diluted to 10^{-4}. TSB agar plates were then inoculated and incubated at 37°C for eighteen hours and the number of CFU counted and compared to controls. Bars represent the mean (n = 6) ± S.E.M. and * indicates $p<0.05$.

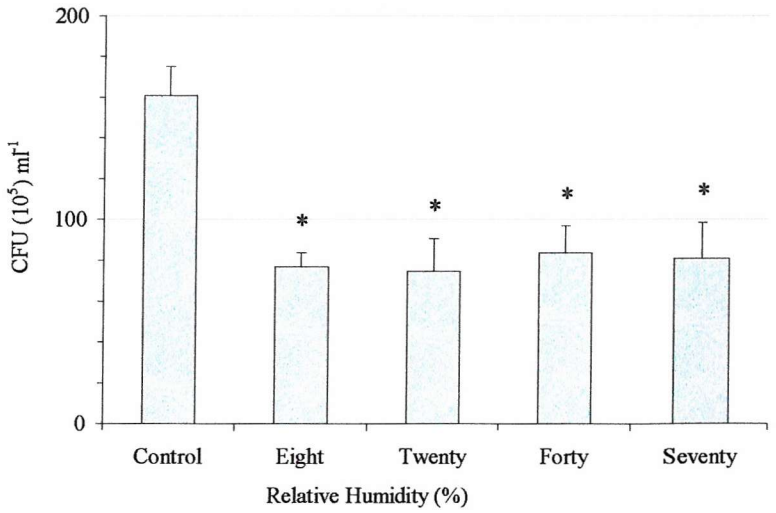

Figure 3.67) Effect of relative humidity on 200μA positive ionic exposure in nitrogen on *E.coli*. A set of nine pins spaced equally above an 87mm diameter metal disc, at a distance of 25mm was used. Inoculated foil coupons ($2cm^2$) were positioned on the disc directly beneath a pin electrode. Nitrogen was flushed through the sealed chamber at a flow rate of 15L/minute for sixteen minutes prior to exposure and then reduced to 1l/min during exposure. The nitrogen gas was passed through distilled water and then different quantities of silica gel to provide relative humidity levels of either 8, 20, 40 or 70%.Voltage was applied to the pin electrodes to produce 200μA current for a period of sixty minutes. Residue spots were subsequently rehydrated in TSB for sixty minutes, then 100μl was removed and serially diluted to 10^{-4}. TSB agar plates were then inoculated and incubated at 37°C for eighteen hours and the number of CFU counted and compared to controls. Bars represent the mean (n = 6) ± S.E.M. and * indicates $p<0.05$.

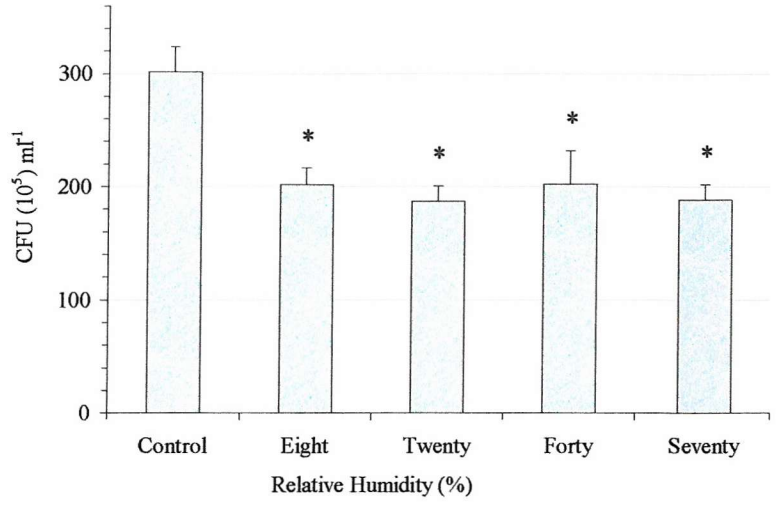

Figure 3.68) Effect of relative humidity on 200μA negative ionic exposure in nitrogen on *S.aureus*. A set of nine pins spaced equally above an 87mm diameter metal disc, at a distance of 25mm was used. Inoculated foil coupons ($2cm^2$) were positioned on the disc directly beneath a pin electrode. Nitrogen was flushed through the sealed chamber at a flow rate of 15L/minute for sixteen minutes prior to exposure and then reduced to 1l/min during exposure. The nitrogen gas was passed through distilled water and then different quantities of silica gel to provide relative humidity levels of either 8, 20, 40 or 70%.Voltage was applied to the pin electrodes to produce 200μA current for a period of sixty minutes. Residue spots were subsequently rehydrated in TSB for sixty minutes, then 100μl was removed and serially diluted to 10^{-4}. CGB agar plates were then inoculated and incubated at 30°C for nineteen hours and the number of CFU counted and compared to controls. Bars represent the mean (n = 6) ± S.E.M. and * indicates $p<0.05$.

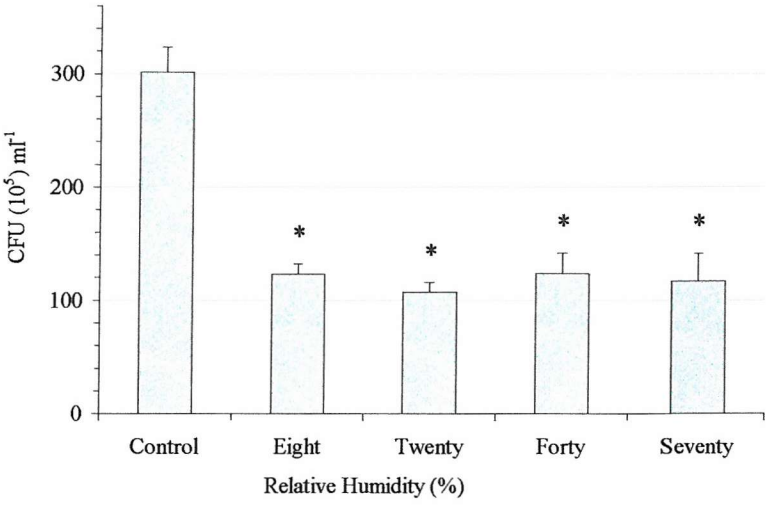

Figure 3.69) Effect of relative humidity on 200μA positive ionic exposure in nitrogen on *S.aureus*. A set of nine pins spaced equally above an 87mm diameter metal disc, at a distance of 25mm was used. Inoculated foil coupons ($2cm^2$) were positioned on the disc directly beneath a pin electrode. Nitrogen was flushed through the sealed chamber at a flow rate of 15L/minute for sixteen minutes prior to exposure and then reduced to 1l/min during exposure. The nitrogen gas was passed through distilled water and then different quantities of silica gel to provide relative humidity levels of either 8, 20, 40 or 70%.Voltage was applied to the pin electrodes to produce 200μA current for a period of sixty minutes. Residue spots were subsequently rehydrated in TSB for sixty minutes, then 100μl was removed and serially diluted to 10^{-4}. CGB agar plates were then inoculated and incubated at 30°C for eighteen hours and the number of CFU counted and compared to controls. Bars represent the mean (n = 6) ± S.E.M. and * indicates $p<0.05$.

3.16) Effect of exposure to evaporation on *E.coli*, starved *P.veronii*, *S.aureus* or *P.veronii* biofilms

Exposure to a corona ion wind was causing evaporative loss in the mass of the agar plates. The effect of corona polarity and current level on the loss in plate mass is shown in *Figure* 3.70 (*Page* 143). Loss in mass from plates exposed to positive corona was significantly greater ($p<0.05$) than plates exposed to negative, with a mean loss in mass of 1.53g for 200μA current, compared to 1.15g for 350μA negative current. This difference was considered to be due to the greater ion wind velocity that was generated by a positive corona in nitrogen (1.7 m s^{-1} for a positive corona compared to 1.1 m s^{-1} for negative).

To establish if this evaporative loss in mass had an effect on the reduction in the number of $CFUml^{-1}$, inoculated plates or coupons were exposed to a nitrogen gas flow of $1.7ms^{-1}$ for a period of sixty minutes. As shown in *Figures* 3.71 (*Page* 143) and 3.72 (*Page* 144), there was no significant difference ($p<0.05$) in $CFUml^{-1}$ number between sample and control groups for all bacterial types.

3.17) Effect of exposure to a nitrogen only atmosphere on *E.coli*, *S.aureus*, starved *P.veronii or P.veronii* biofilms

E.coli, *S.aureus* and *P.veronii* are not obligate aerobes i.e. organisms that can only use oxygen for respiration. Nevertheless, the possibility remained that exposure to a nitrogen only atmosphere was contributing to the reduction in $CFUml^{-1}$.

Figure 3.73 (*Page* 144) shows the effect on $CFUml^{-1}$ number when plates inoculated with either *E.coli* or *S.aureus* were exposed to nitrogen only i.e. without corona. After 180 minutes there was no significant difference ($p<0.05$) between control and sample plates for both organisms. A pattern that was repeated with starved *P.veronii* cells and *P.veronii* biofilms as shown in *Figure* 3.74 (*Page* 145), where no significant difference ($p<0.05$) was found between sample and control groups.

3.18) Effect of temperature on negative or positive ionic treatment in nitrogen

Figures 3.75 to 3.78 (*Pages* 145 to 147) shows the effect of exposing bacterial samples to either 100μA negative or positive ions in nitrogen, at two different temperature regimes chosen to represent winter and summer ambient laboratory conditions.

For both polarity regimes, experiments conducted at either 18°C or 24°C produced no significant difference ($p<0.05$) between sample groups for all bacterial types. Differences were found between control and sample groups, but not significantly different to the previous data for 100μA negative or positive exposure in nitrogen (Section 3.8)

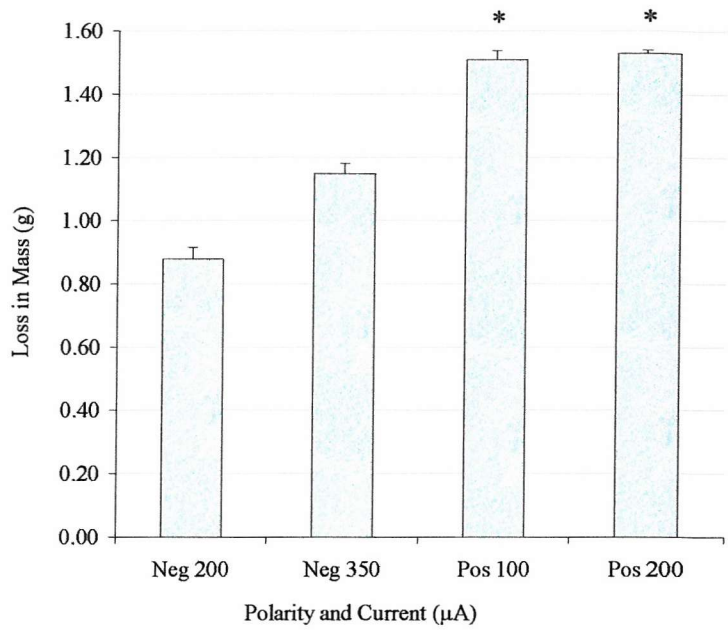

Figure 3.70) Effect of corona polarity and current on agar plate mass. A set of nine pins spaced equally above an agar plate at a distance of 25mm was used. Nitrogen was flushed through the sealed chamber at a flow rate of 15L/minute for fifteen minutes prior to exposure and then reduced to 1l/min during exposure. Voltage was applied to the pin electrodes to produce either 200μA or 350μA of negative current or 100μA or 200μA of positive current for a period of 60 minutes. Plate mass was recorded before and after exposure and the difference in mass calculated. Bars represent the mean (n = 6) ± S.E.M. and * indicates $p < 0.05$ between polarity groups.

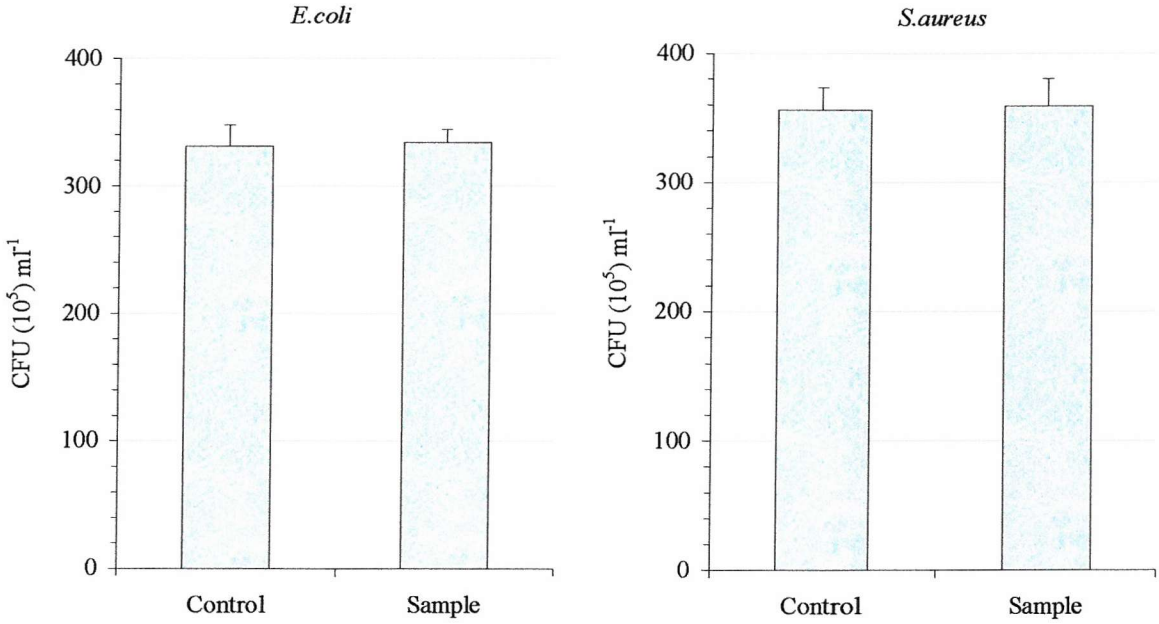

Figure 3.71) Effect of evaporation on *E.coli* and *S.aureus*. Inoculated agar plates were placed at a distance of 80mm beneath an electric fan situated within a 10 litre sealed container. Nitrogen was flushed through the chamber at a flow rate of 15l/min for fifteen minutes and then 1l/min during exposure. The fan was then switched on to generate a nitrogen airflow of $1.7ms^{-1}$ for a period of 180 minutes. Plates were subsequently incubated at 37°C for eighteen hours or 30°C for nineteen hours and the number of CFU counted and compared to controls. Bars represent the mean (n = 6) ± S.E.M.

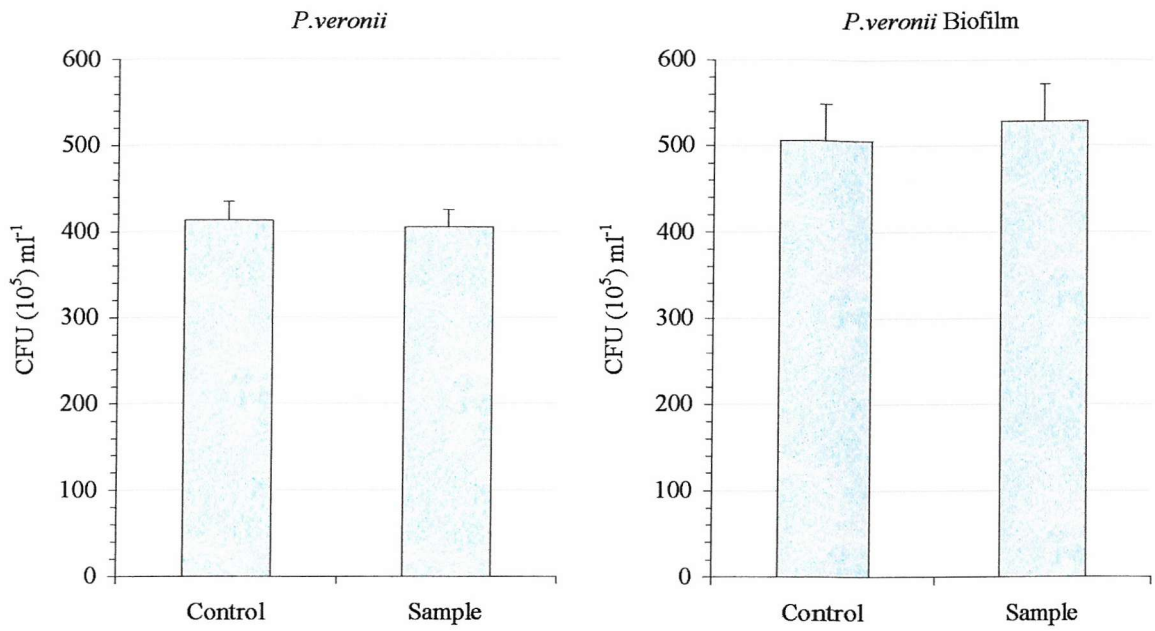

Figure 3.72) Effect of evaporation on starved *P.veronii* cells and *P.veronii* biofilms. Inoculated coupons were placed at a distance of 80mm beneath an electric fan situated within a 10 litre sealed container. Nitrogen was flushed through the chamber at a flow rate of 15l/min for fifteen minutes and then 1l/min. The fan was then switched on to generate a nitrogen airflow of $1.7ms^{-1}$ for a period of 180 minutes. Coupons were subsequently incubated in TSB for thirty minutes prior to reading in a luminometer with 50µl nonanal and compared to controls. Bars represent the mean (n = 6) ± S.E.M.

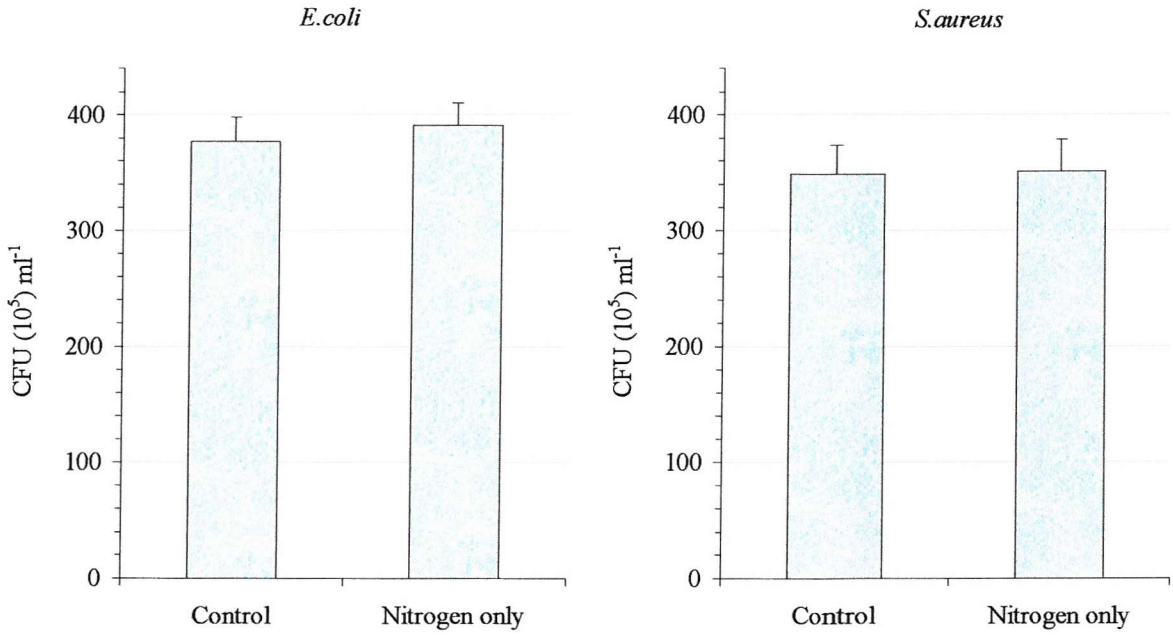

Figure 3.73) Effect of exposure to a nitrogen only atmosphere on *E.coli or S.aureus*. Inoculated agar plates were placed in a sealed container (volume 10 litres). Nitrogen was flushed through the chamber at a flow rate of 15l/min for fifteen minutes and then 1l/min for 180 minutes. *E.coli* and *S.aureus* plates were subsequently incubated at 37°C for eighteen hours or 37°C for nineteen hours respectively and the number of CFU counted and compared to controls. Bars represent the mean (n = 6) ± S.E.M.

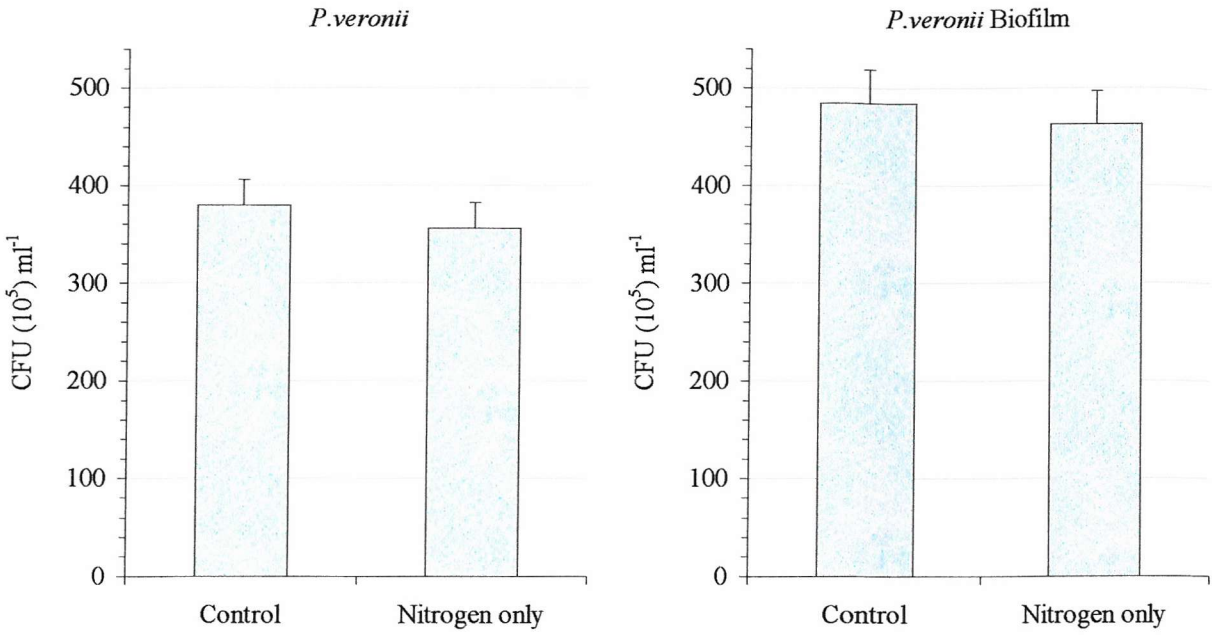

Figure 3.74) Effect of exposure to a nitrogen only atmosphere on starved *P.veronii* cells or *P.veronii* biofilms. Inoculated foil coupons ($2cm^2$) were positioned in a sealed container (volume 10 litres). Nitrogen was flushed through the chamber at a flow rate of 15l/min for fifteen minutes and then 1l/min for 180 minutes. Coupons were subsequently incubated in TSB for thirty minutes prior to reading in a luminometer with 50µl nonanal and compared to controls. Bars represent the mean (n = 6) ± S.E.M.

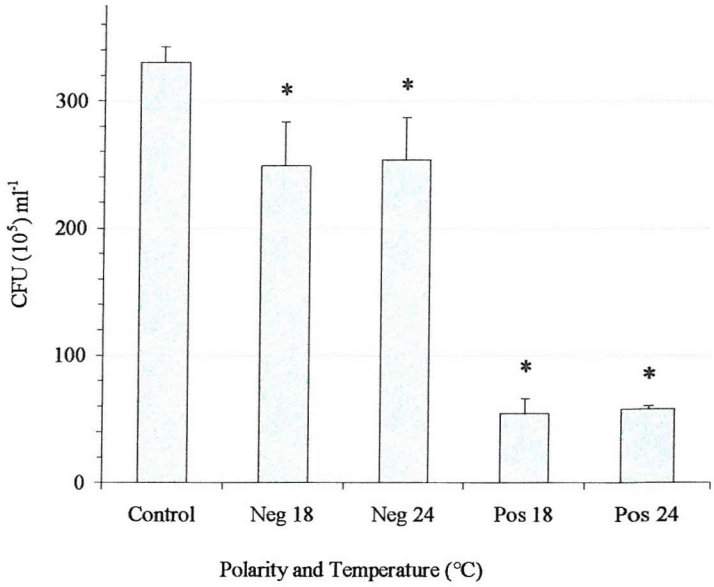

Figure 3.75) Effect of temperature on 100µA negative or positive ionic exposure in nitrogen on *E.coli*. A set of nine pins spaced equally above an agar plate at a distance of 25mm was used. Nitrogen was flushed through the sealed chamber at a flow rate of 15L/minute for fifteen minutes prior to exposure and then reduced to 1l/min during exposure. A heating element within the chamber was activated to produce an internal temperature of either 18°C or 24°C. Voltage was applied to the pin electrodes to produce 100µA constant current for a period of sixty minutes. Plates were subsequently incubated at 37°C for eighteen hours and the number of CFU counted and compared to controls. Bars represent the mean (n = 6) ± S.E.M. and * indicates $p<0.05$.

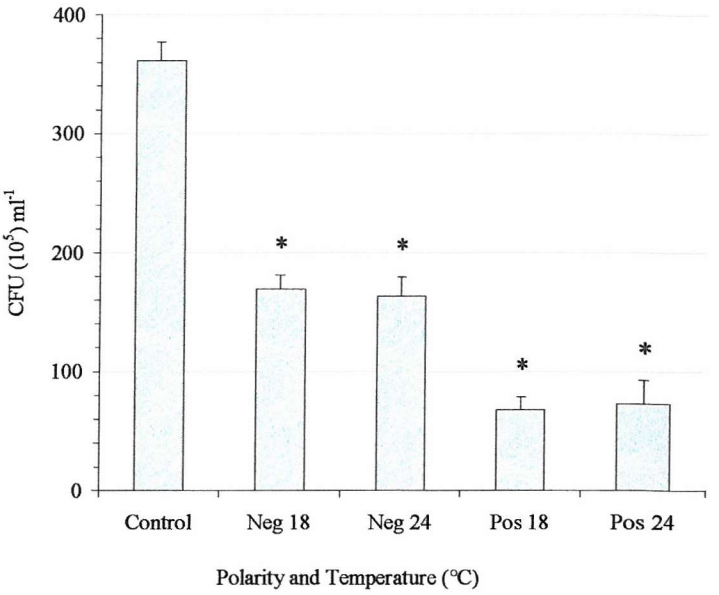

Figure 3.76) Effect of temperature on 100µA negative or positive ionic exposure in nitrogen on *S.aureus*. A set of nine pins spaced equally above an agar plate at a distance of 25mm was used. Nitrogen was flushed through the sealed chamber at a flow rate of 15L/minute for fifteen minutes prior to exposure and then reduced to 1l/min during exposure. A heating element within the chamber was activated to produce an internal temperature of either 18°C or 24°C. Voltage was applied to the pin electrodes to produce 100µA constant current for a period of sixty minutes. Plates were subsequently incubated at 30°C for nineteen hours and the number of CFU counted and compared to controls. Bars represent the mean (n = 6) ± S.E.M. and * indicates $p<0.05$.

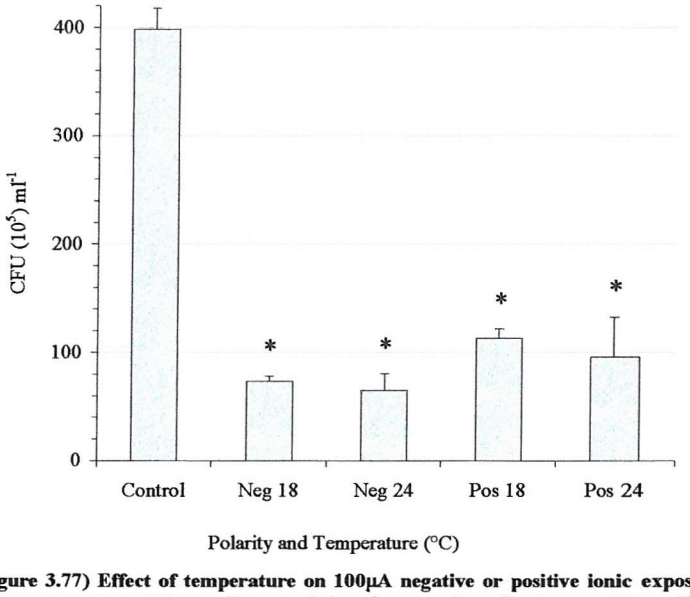

Figure 3.77) Effect of temperature on 100µA negative or positive ionic exposure in nitrogen on starved *P.veronii*. A set of nine pins spaced equally above an 87mm diameter metal disc, at a distance of 25mm was used. Inoculated foil coupons ($2cm^2$) were positioned on the disc directly beneath a pin electrode. Nitrogen was flushed through the sealed chamber at a flow rate of 15L/minute for fifteen minutes prior to exposure and then reduced to 1l/min during exposure. A heating element within the chamber was activated to produce an internal temperature of either 18°C or 24°C. Voltage was applied to the pin electrodes to produce 100µA constant current for a period of sixty minutes. Coupons were subsequently incubated in TSB for thirty minutes prior to reading in a luminometer with 50µl nonanal and compared to controls. Bars represent the mean (n = 6) ± S.E.M. and * indicates $p<0.05$.

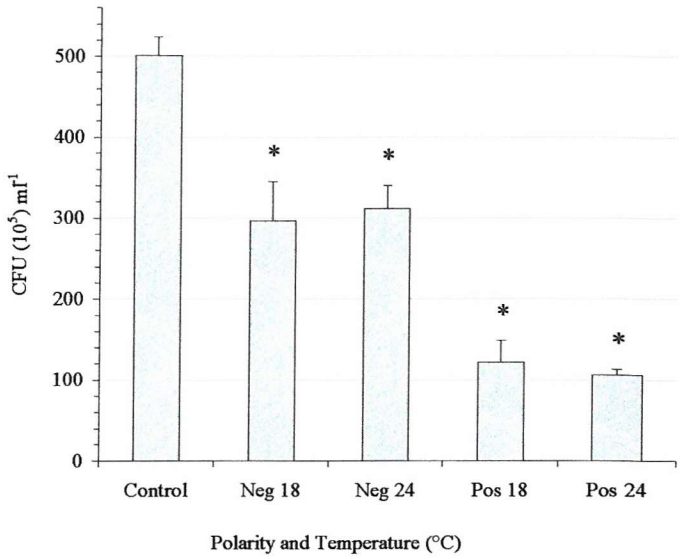

Figure 3.78) Effect of temperature on 100µA negative or positive ionic exposure in nitrogen on *P.veronii* biofilm. A set of nine pins spaced equally above an 87mm diameter metal disc, at a distance of 25mm was used. Biofilm foil coupons ($2cm^2$) were positioned on the disc directly beneath a pin electrode. Nitrogen was flushed through the sealed chamber at a flow rate of 15L/minute for fifteen minutes prior to exposure and then reduced to 1l/min during exposure. A heating element within the chamber was activated to produce an internal temperature of either 18°C or 24°C. Voltage was applied to the pin electrodes to produce 100µA constant current for a period of sixty minutes. Biofilms were subsequently incubated in TSB for thirty minutes prior to reading in a luminometer with 50µl nonanal and compared to controls. Bars represent the mean (n = 6) ± S.E.M. and * indicates $p<0.05$.

Chapter Four

Discussion

4.1) Discussion

Resistance to all contemporary antibiotics and a range of disinfectants is becoming widespread for many bacterial species. Continued overuse of antibiotics in humans, animals and the plant industry, has been the major factor in the development of multi-drug resistant strains, including vancomycin resistant *Enterococcus* species and methicillin resistant *Staphylococcus aureus*. With this in mind, the development of new chemical and physical methods for bacterial decontamination is paramount. Contemporary sterilisation methods include dry heat, moist heat (boiling and autoclaving), filtration, and ultra violet radiation. For each particular situation the applied method of sterilisation depends principally on the materials involved, safety factors, disposal requirements and expense. The objective of this study was to determine if either negative or positive unipolar ions could counteract the growth of bacterial populations, with the potential to be applied as a broad-spectrum and inexpensive method of reducing log numbers of microbial cells.

To ascertain the effect of unipolar ion treatment, bacterial samples were selected for the study to represent both Gram-negative and Gram-positive species, and naturally occurring resistant phenotypes that exist in everyday environmental conditions. Using a purpose built point to plane corona discharge, either *Escherichia coli*, *Staphylococcus aureus*, starved *Pseudomonas veronii* cells or *Pseudomonas veronii* biofilms were subjected to either negative or positive ionic exposure in air or nitrogen. The results from this study have demonstrated an antibacterial effect of both negative and positive unipolar ions with significant reductions (up to two log) in bacterial numbers.

Initial experiments utilising exposure to a corona discharge in air failed to demonstrate a specific role for unipolar ions with regards to bacterial death. This was despite significant differences between control and sample groups, for both corona polarities. Any effect of a negative or positive corona discharge on the nutrient agar media or aluminium foil itself was tested with no significant difference between controls and

samples. In addition, the effect of any evaporative contribution towards the reduction in $CFUml^{-1}$ number, was also investigated and results demonstrated no significant effect on bacterial viability.

The corona discharge in air provides one of the most intense oxidising environments available to science, with products including electrons, unipolar ions, ozone and hydrogen peroxide (Hoenig *et al*, 1980). Thus, under such conditions a reduction in the viable cell count was to be expected, particularly with the presence of ozone and hydrogen peroxide. Inactivation of both Gram-negative and Gram-positive bacteria by ozone and hydrogen peroxide is a complex process. This is due to the numerous cellular targets including proteins, unsaturated lipids, peptidoglycan and cell membrane respiratory enzymes. However, cell death is primarily attributed to oxidation of the sulfhydryl groups and the double bonds of unsaturated lipids in the cell wall, leading to structural failure and cell lysis (Khadre *et al*, 2001).

From the antibacterial agents produced by a corona discharge in air, Sigmond *et al* (1999) concluded that ozone was the principal agent responsible for bacterial death. Ozone concentrations were recorded for tests in air at 1.0ppm for a negative corona and 1.4ppm for a positive corona. Subsequent tests utilising ozone exposure at the same concentrations but without corona, indicated that additional components of the corona discharge were responsible for bacterial death. This was due to the significantly greater numbers of cells killed for all bacterial targets by the discharge in air with a negative applied voltage. The application of a positive corona in air only demonstrated a significantly greater reduction for the biofilm sample group, indicating ozone to be the single corona product responsible for killing *E.coli*, *S.aureus* and *P.veronii*. However, the increased bacterial kill rate seen with a discharge in air compared to ozone treatments could have simply been due to the production of other detrimental oxide species. Therefore, the results from negative or positive corona tests in air were insufficient to support a theory of bacterial death by a process of ionic interactions. If a harmful ionic process were occurring, it was simply hidden by the other documented

biocidal agents. Thus, to conclusively designate a role for unipolar ions using an electrical discharge in air, additional tests would be required, documenting, recording and exposing bacterial samples to each individual antibacterial corona product.

The implementation of a pure nitrogen atmosphere for subsequent experiments removed the possibility of ozone and additional oxide species intervention. The application of an electrical corona discharge in nitrogen has clearly demonstrated a role for ionic treatment with significant reductions in $CFUml^{-1}$ number for all the microbial targets. This effect is also independent of the nitrogen atmosphere, relative humidity, temperature, electric field, electrical current and evaporation from the ion wind. From the results it is apparent that a relationship exists between the applied corona current, exposure time and bacterial viability, as either increasing the current or time of exposure, significantly decreased the number of viable bacterial cells for both positive and negative ions. Based on these observations there appears to be a critical ion density for microbial death, with a higher threshold for negative exposure than positive, and varying levels for each bacterial type and species. Once this threshold is breached, bacterial cell death occurs rapidly until a subsequent limit is met, when further disinfection of the inoculated material is considerably reduced.

For example, with an exposure current of 100μA significant reductions were seen in the number of $CFUml^{-1}$ for all bacterial targets after sixty minutes treatment, and for both polarities. However, doubling the exposure current to 200μA only proved effective for negative polarity tests, with significant increases in cellular death for all target organisms except the starved *P.veronii* cells. For positive ionic exposures at 200μA there was no further significant increase in cell death after sixty minutes treatment, for any of the four bacterial samples. In effect the upper limit for positive exposures was attained with an applied corona current of only 100μA. Once again with a negative applied voltage, increasing the exposure current to 350μA only significantly decreased viability for *E.coli*, with the other bacteria types remaining unaffected. Thus the upper threshold for negative ionic exposure was achieved with 200μA exposure.

Therefore the threshold limit for positive ions to initiate cellular death appears to be significantly lower than negative, with 100μA exposures producing significantly greater kill rates for all sample organisms except starved *P.veronii*. Further disinfection of samples beyond the upper limit may be possible through extended exposure periods (>2hours), although this is yet to be established.

The tests where samples were exposed to ions under field-free conditions also support the argument for the lower positive ionic threshold. These experiments not only demonstrated the influence of the electric field (ranging from $80kVm^{-1}$ to $400kVm^{-1}$) on bacterial viability to be insignificant, but also allowed samples to be exposed to previously unattainable current regimes. With either a negative or positive discharge in nitrogen, applying currents of <10μA was extremely difficult as corona onset would only begin with currents greater than this value for either polarity. With an exposure current of <1μA, longer treatment periods of up to 180 minutes were required to produce similar kill rates, which were previously achieved with either 30 or 60 minute direct exposures with 100μA. However, even with a 100 fold reduction in exposure current, positive ionic treatment was sufficient to significantly reduce $CFUml^{-1}$ number after only sixty minutes for both the starved *P.veronii* cells and the biofilm sample groups. In contrast, negative exposures with <1μA required a minimum of 120minutes to produce a significant reduction in microbial viability for all the sample types, further supporting the theory that higher inception values were required to induce bacterial death with negative ions.

Of the two polarities, positive ions in nitrogen were significantly more effective than negative at reducing microbial load, with a mean kill rate from all test conditions of 72% compared to 50%. This could possibly be due to the net negative surface charge that exists on the cell walls of both Gram-negative and Gram-positive bacteria (James, 1991). For Gram-negative bacteria this is due to the presence of lipopolysaccharide (LPS) in their secondary outer membrane, with its numerous phosphate groups. LPS is composed of a polysaccharide chain covalently attached by way of an oligosaccharide

core to a glycolipid moiety. For *Escherichia coli* it has been estimated that for every 6 μm^2 of cell surface area there is approximately 3.5 million LPS molecules, constituting a significant permeability barrier. For Gram-positive bacteria, the negative cell wall charge results from teichoic acids that are covalently linked to muramic acid residues in the peptidoglycan. They exist as polymers up to forty units long consisting of glycerol, phosphates and ribitol. The phosphate groups in these polymers are fully ionised above pH 2.5, so a typical teichoic acid of forty repeating units would contain forty negatively charged phosphates per molecule (Jucker *et al*, 1996).

With an electrostatic attraction between the charged groups in the cell wall and the positive ions from the discharge, the accumulation of positive charge at the cell wall surface would be rapid, in contrast to negative ions that would have to counteract the repulsive force of the net surface charge. The resulting electrostatic interaction between the positive ions and the numerous negatively charged groups in the LPS and teichoic acid molecules, could interfere with the selective permeability properties of the cell wall, possibly initiating a cascade of events that ultimately proves fatal to the organism.

For either negative or positive exposure at each time period and current regime, *S.aureus* had the lowest mean reduction in cell number at 47%, which suggests that Gram-negative cells, as represented by *E.coli* and *P.veronii* may be more susceptible to ionic treatment. The primary difference between Gram-negative and Gram-positive bacteria, except the outer membrane, is peptidoglycan. Gram-negative cells have significantly lower amounts of this stress bearing component in their cell walls, representing 10-20% (2nm width) of their total cell mass, compared to ~50% (ranging from15-80nm in width) for Gram-positive bacteria. Although an additional outer membrane is present, this primarily acts as a permeability barrier and does not provide mechanical support to the cell wall. The significantly lower quantities of peptidoglycan could be insufficient to provide the additional strength and rigidity required to

withstand disruption through ion accumulation, and subsequent electrical breakdown of the cell wall.

In addition, the increased resistance to contemporary microbial treatments provided through starvation or biofilm habitation, appears to be ineffective for the Gram-negative cell *P.veronii*, with both sample groups exhibiting significantly greater mean reductions in cell viability than *S.aureus*. The starved bacterial cell implements a substantial programme of gene expression and morphological alteration to withstand the environmental stress of reduced nutrient availability. With regards to ionic exposure the implemented changes to either cell wall structure or internal metabolism appear to be ineffective at defending the cell. Ionic treatment of *P.veronii* biofilms was also highly effective at decreasing viability, indicating a potential weakness in the usually protective extracellular matrix. However, in a fashion similar to the bacterial cell wall, the matrix does contain numerous charged groups that would provide interaction points for ionic challenge. Thus, it is feasible that ionic exposure could alter the properties of the matrix to such an extent that subsequent penetration of the biofilm becomes possible, with individual cells subject to exposure.

For ionic tests using agar plates, the majority of surviving bacteria were located on the outer edge of the petri dish where the ion density would be lower, particularly compared to regions of the plate directly beneath the point electrodes. However, some colonies were formed beneath the point electrodes, indicating that additional factors other than ion concentration were responsible for killing *E.coli* or *S.aureus* cells. For these tests it was unclear whether the bacteria were actually rendered non-viable or whether they were simply unable to form colonies after exposure, particularly as bacteria exposed to physical and chemical stresses can enter a viable but unculturable state. However, viability determination from *P.veronii* was achieved through bioluminescent readings, which were shown to directly correlate to actual numbers of living cells. Sixty minutes exposure to either negative or positive ions in nitrogen

significantly reduced *P.veronii* cell numbers by 97% and 90% respectively, which reduces the possible existence of viable but unculturable cells.

The precise mechanism responsible for the death of bacterial cells, as a result of unipolar ionic exposure, is yet to be fully established. Unfortunately the resolution of the scanning electron micrographs taken of *S.aureus* and *P.veronii* after ionic treatment in nitrogen, were insufficient to clearly demonstrate any physiological damage to the microbes. This would have at least corroborated disruption to the cell wall. However, in spite of this, a theoretical model is beginning to form. Laroussi *et al* (2000) published some work on the effects of a glow discharge at atmospheric pressure on *Escherichia coli* (pbr 322) and *Pseudomonas aeruginosa* (frd 1). The glow discharge is fundamentally different to a corona discharge in that two planar electrodes are utilised, one of which is insulated by a dielectric material. The application of voltage between the electrodes results in the formation of non-thermal plasma containing charged particles, free radicals and radiation, both infrared and ultraviolet. Bacterial cells were prepared and inoculated onto nitrocellulose filter membranes (4×10^6 CFU per filter) and subsequently placed into the plasma. Significant kill rates were achieved for both organisms with complete sterilisation of the membrane after only 3.5 minutes in the case of *E.coli*. To complement the plasma experiments, a series of scanning electron photomicrographs were taken of *E.coli* before and after 30 seconds glow discharge treatment. According to Laroussi, the treated cells appeared to be in the process of leaking internal matter, and from this he concluded that the outer membrane of the cells was punctured and subsequently vulnerable to the reactive environment of the discharge.

In response to this publication, Mendis *et al* (2001) proposed a theory on the mechanism for the demise of Gram-negative bacteria in a glow discharge that was additionally applicable to a corona discharge. They proposed that the disruption of the cell structure was a physical process, specifically the electrostatic disruption of the cell wall, induced when sufficient electric charge has accumulated at the outer membrane

to exceed its material tensile strength (*Figure* 4.1, *Page* 157). In theory, the accumulation of charge at the outer membrane initiates contraction, as oppositely charged groups on both sides attract each other. The membrane thickness decreases rapidly as the electrical contraction increases, with the elastic restoring force of the membrane unable to cope. Eventually a local breakdown of the membrane occurs resulting in cell lysis.

Mendis proposed a model where the *Escherichia coli* bacterium was idealised as a sphere of radius 1μm, with a hemispherical irregularity of radius 0.02μm to account for the surface roughness, and an outer membrane thickness of 0.008μm. The tensile strength of the outer membrane was assumed to be between 1 and 5 $kgcm^{-2}$, based on a gram-negative bacterium's ability to withstand osmotic pressure of up to five atmospheres. If the upper tensile strength value of 5 $kgcm^{-2}$ was taken, then the potential difference across the membrane required to cause disruption was calculated to be $\geq$ 6V, reducing to 3V if the lower value of 1 $kgcm^{-2}$ was substituted. Mendis concluded that although the model was simple, electrostatic disruption was possible, particularly if the surface of the bacterium contained irregularities with regions of higher local curvature. In fact, the cell surfaces of gram-negative cells are typically rough and convoluted as shown by electron micrographs. Therefore, such a model would support the existence of a critical ion density i.e. a specific number of ions required to generate the cell wall potential necessary for structural failure. Additional support has come from mathematical analysis provided by Vaughn (2003), confirming the theoretical mechanical failure of a 10 nm cell wall due to applied electrostatic forces.

However, the proposed Mendis model noted that the physical mechanism for the structural disruption of bacteria is only effective for Gram-negative ones like *E.coli* and *P.veronii*, which possess thin outer membranes and small quantities of peptidoglycan.

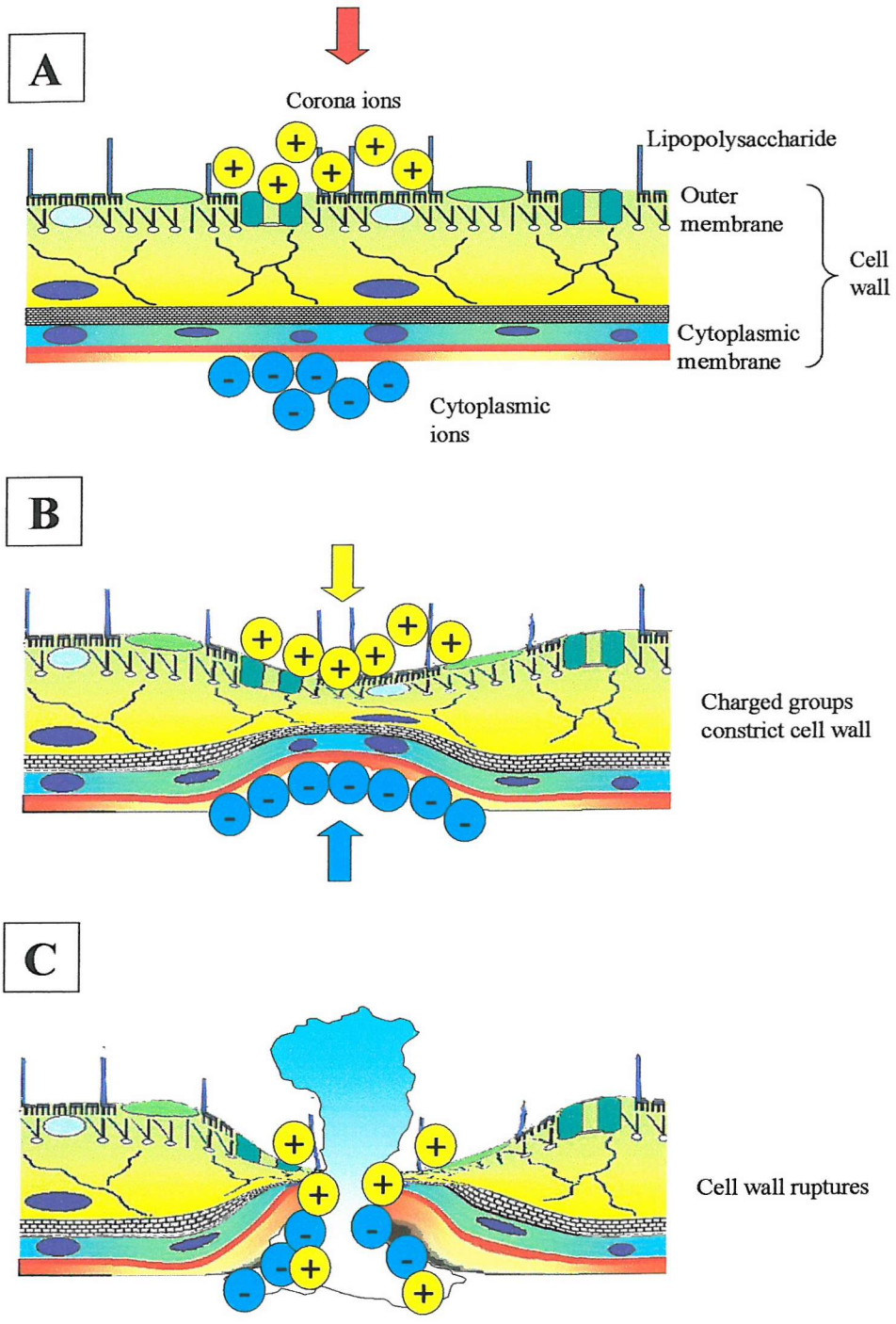

Figure 4.1) Diagram of the theoretical disruption of the Gram-negative cell wall by charge accumulation. **A)** Accumulation of charge at the outer membrane attracts oppositely charged groups to the cytoplasmic membrane. **B)** Electrostatic attraction applies a constriction force to the cell wall. **C)** The tensile strength is exceeded and electrical breakdown of the cell wall occurs with leakage of cytoplasm and subsequent death by cell lysis.

Mendis suggested that Gram-positive bacteria such as *S.aureus* with their thicker peptidoglycan layer and greater levels of rigidity would be highly resistant to this form of attack. In which case, an alternative explanation of ionic induced cell death is required. Whatever the alternative process, data provided by the BacLight tests reveals a relationship between ionic exposure and cell membrane disruption, which is applicable for both Gram-negative and Gram-positive cells. Therefore, ionic disruption of the cell wall does occur for Gram-positive bacteria, but not in theory by the mechanisms proposed by Mendis. However some form of ionic-based damage is apparent, with an increase in the exposure current from 100μA to 200μA, generating significantly greater numbers of bacteria with broken membranes. If ionic constriction is not the process responsible, then possibly some form of interference with the selective permeability properties of the cell wall may be apparent.

4.2) Conclusions and further work

The application of corona discharges for the production of bactericidal products is well known, although bactericidal activity has been primarily attributed to the production of ozone. Using the experimental set up described here, significant reductions ($p<0.05$) in the microbial load of inoculated surfaces, has been achieved using a corona discharge in nitrogen gas and without ozone contamination. It has been shown that both Gram-negative and Gram-positive bacteria are susceptible to either negative or positive ionic challenge, with viability decreasing with increasing exposure time and current level. A minimum ion threshold limit appears to exist that once exceeded, induces bacterial death, with a lower value for positive ions than negative.

An upper limit is also apparent where further increases to the exposure current, produces no further significant reduction in microbial viability. Detrimental ionic effects have additionally been established against resistant phenotypes of starved *P.veronii* cells and *P.veronii* biofilms, which represent actual environmental conditions, as opposed to bacterial cells inoculated onto nutrient agar plates. Of the two charges, positive ions were the most effective at reducing the number of viable

bacteria, with reductions of two log achieved for both *E.coli* and *P.veronii* biofilm samples, after sixty minutes with 200μA.

Gram-negative bacteria have been shown to be more susceptible to ionic challenge than Gram-positive, with *S.aureus* achieving higher viability results after treatment, compared to both *E.coli* and *P.veronii*. It has been postulated that microbial death by ionic exposure is due to electrostatic constriction of the cell wall, leading to eventual breakdown of the integral membranes. In support of this hypothesis is the data provided by the BacLight tests, which have conclusively shown cell wall disruption to *E.coli*, *P.veronii* and *S.aureus*. However, the mechanism for disruption to the Gram-positive cell wall remains undetermined, as the higher peptidoglycan content provides sufficient strength and rigidity to contradict the hypothesised Mendis disruption model.

Now that the corona disinfection technique is well established, the possibility for extending this line of research is highly feasible, as some key points remain unanswered. A theoretical model is in place to explain the death of Gram-negative bacteria. However, this is just a model. Further studies are required to reveal the actual mechanism responsible for bacterial death. Why do some bacteria survive ionic challenge? Is there some form of a shielding effect occurring from surrounding bacteria? Is complete sterilisation of inoculated surfaces possible? With the actual mechanism determined, the parameters of ionic challenge could be modified to further increase the numbers of non-viable bacteria.

Further work should include the taking of higher resolution micrographs of bacteria after ionic treatment, to confirm the findings of the BacLight tests. Pictures conclusively showing damage to the cell wall would further enforce the theory of electrostatic breakdown and possibly reveal clues to the mechanism for Gram-positive bacteria. Tests conducted so far have confirmed ionic disinfection with up to two log reductions in microbial numbers. However, further experiments could develop and modify the present apparatus to increase efficiency of the discharge. This could

potentially reveal the criteria for complete sterilisation of all samples, particularly as there appears to be a threshold where subsequent reductions in viability are affected.

Experiments to date have utilised a corona discharge with an inter-electrode distance of 25mm, confined to a 10litre chamber flushed with nitrogen gas. Experimentally sound, but not really conducive for other applications. However, modification of the enhanced corona discharge described in *Chapter One* (Garate *et al*, 1998) to completely prevent ozone formation, could allow large-scale tests to be conducted. Test conditions reflecting domestic room environments could be created to establish the degree of disinfection possible, through long-distance ionic exposure. With this arrangement, additional substrates could be inoculated such as glass, plastic and kitchen work surfaces, to establish is disinfection is possible when directed against these domestic surfaces.

Potential applications of this technology could possibly include both industrial and domestic devices particularly where the use of disinfectants is inappropriate. In fact, any situation that requires a level of disinfection could use the technology, including medical situations, food processing and air conditioning systems.

Publications arising from this work:

Noyce, J.O., and Hughes, J.F., (2002), Bactericidal Effects Of Negative and Positive Ions Generated in Nitrogen on Escherichia Coli, *Journal of Electrostatics*, **54**, 179-187

Noyce, J.O., and Hughes, J.F., (2003), Bactericidal Effects Of Negative and Positive Ions Generated in Nitrogen on Starved *Pseudomonas veronii*, *Journal of Electrostatics*, **57**, 49-58

Appendix

Appendix A: Statistical analysis

Levels of measurement

Nominal – At this level numbers are used to classify things, e.g. the digits seen on the back of football player's shirts.
Ordinal – Involves an ordering or ranking of the variable under consideration e.g. race positions such as 1st, 2nd and 3rd.
Interval scale – Numbers are ordered, but also the intervals between each step, at all points along the scale are of equal size. Interval scales have no absolute zero point e.g. the centigrade temperature scale where temperatures lower than zero are indicated by a negative sign.
Ratio scale – ranked numbers with equal intervals between the numbers throughout the scale in addition to having an absolute zero e.g. length, weight, speed and temperature on the Kelvin scale.

Parametric and Non-parametric tests

Statistical tests are either parametric or non-parametric. The conditions for using a parametric test are more stringent than for non-parametric tests. Data for use in parametric tests should be on an interval or ratio scale of measurement and the data must be normally distributed. Parametric tests compare means and variances of sample data. Non – parametric may be used with actual observations or those converted to ranks. They can be used with observations on nominal, ordinal or interval scales. Non-parametric tests compare medians and do not require data to be normally distributed. They are suitable for data that are counts.

Normal distribution, standard deviation and standard error

A normal distribution is when data are dispersed fairly symmetrically either side of the mean with very few extremely high or low values. The standard deviation is a measure of the spread of the data around the mean. It is calculated by

$$S = \sqrt{\frac{\Sigma(x-\bar{x})^2}{n-1}}$$

Where s is the standard deviation from the mean, x is the value of an observation, $\bar{x}$ is the sample mean and n is the number of observations. The standard error of a sample mean (SEM) is a representation of the spread of data around the sample mean. It is calculated by,

$$SEM = \frac{s}{\sqrt{n}}$$

Where s is the standard deviation and n is the number of observations. The standard error of a sample mean is an indication of the quality of an estimate of the sample mean, equating to a 68% confidence that the mean lies within one standard error of the mean.

The Mann-Whitney *U*-test

The Mann-Whitney *U*-test is a non-parametric test for the comparing the medians of two unmatched samples. It may be used with as little as four observations in each sample and the sample sizes may be unequal. It is suitable for the comparison of data that are counts or percentages. All of the observations of the two samples to be compared are listed in ascending order. The samples are distinguished by underlining

the values of the second data set. These observations are then assigned ranks. The ranks of each sample are then summed.

R_1 = sum of ranks of sample 1
R_2 = sum of ranks of sample 2

The test statistics U_1 and U_2 are then calculated.

$$U_1 = n_1 n_2 + \frac{n_2(n_2 + 1)}{2} - R_2$$

$$U_2 = n_1 n_2 + \frac{n_1(n_1 + 1)}{2} - R_1$$

The smaller of the two U values is then selected and compared to the critical value in the tabulated values for the appropriate values of n_1 and n_2. if the smallest value of U is less than the critical value, there is a statistically significant difference between the medians. A Mann Whitney U-test can also be performed using specialist software such as SPSS.

The Spearman Rank Correlation

The spearman rank correlation involves the calculation of a coefficient r_s. The two-paired sets of observations consisting of interval data, are listed in a table and ranked. The difference (d) between the ranks of sample 1 and sample 2 is calculated for each pair of samples. The value of d^2 is then calculated for each pair of samples and summed to obtain Σd^2. The calculation of r_s is then conducted as follows,

$$r_s = 1 - \left[\frac{6\Sigma d^2}{n3 - n}\right]$$

Where n is the number of units in a sample and d is the difference between ranks. The r_s value can then be compared to an appropriate table of values for the specified n values (Fowler and Cohen, 1990). If the calculated value exceeds the critical value at the appropriate n value at p=0.05, the correlation is significant. A spearman rank correlation can also be performed using specialist software such as SPSS.

Appendix B: Developmental stages in the design and construction of the multi point corona discharge apparatus.

Stage one design:

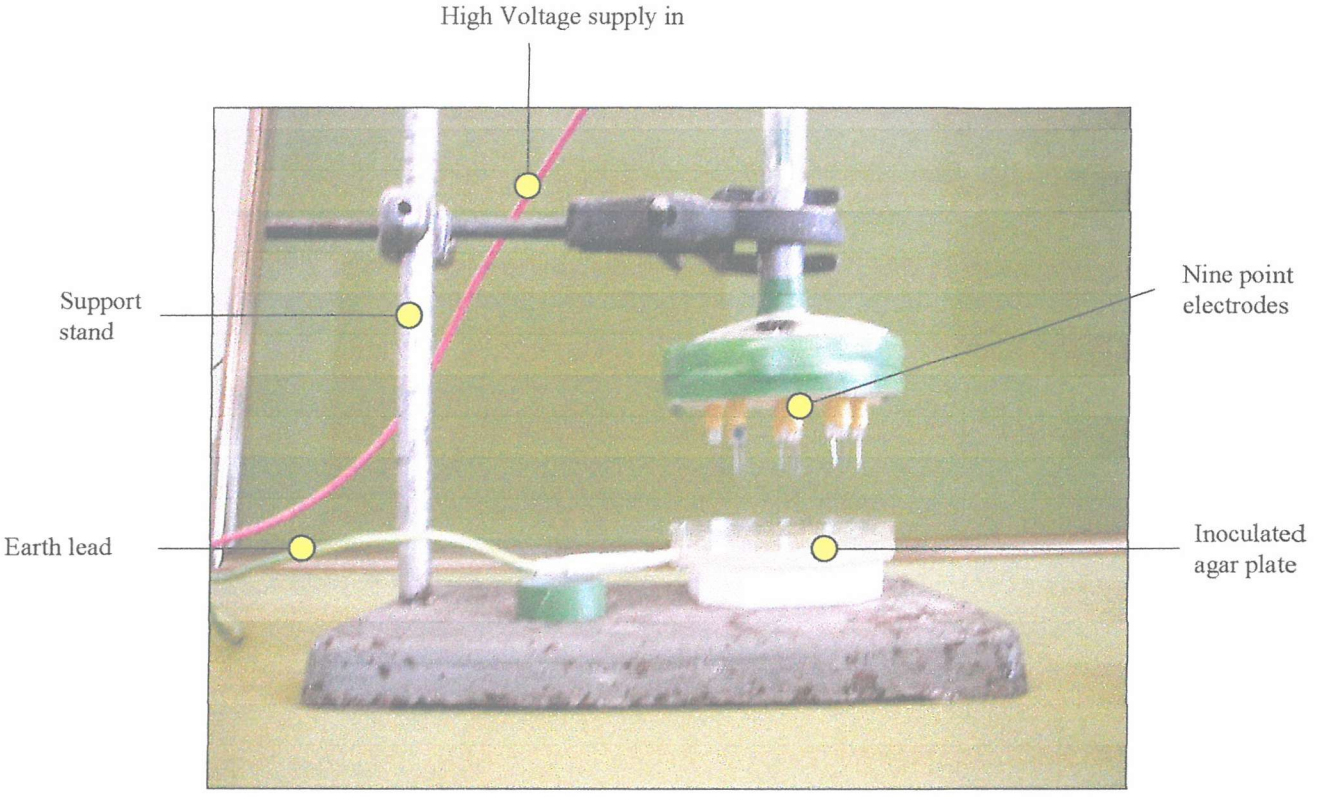

Stage two design:

- Upper elevation

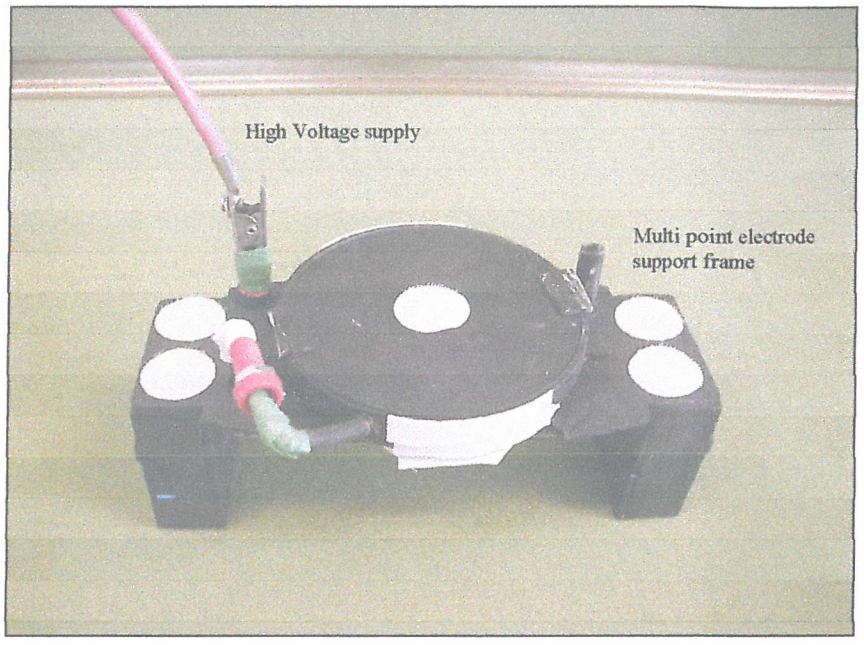

- Side elevation

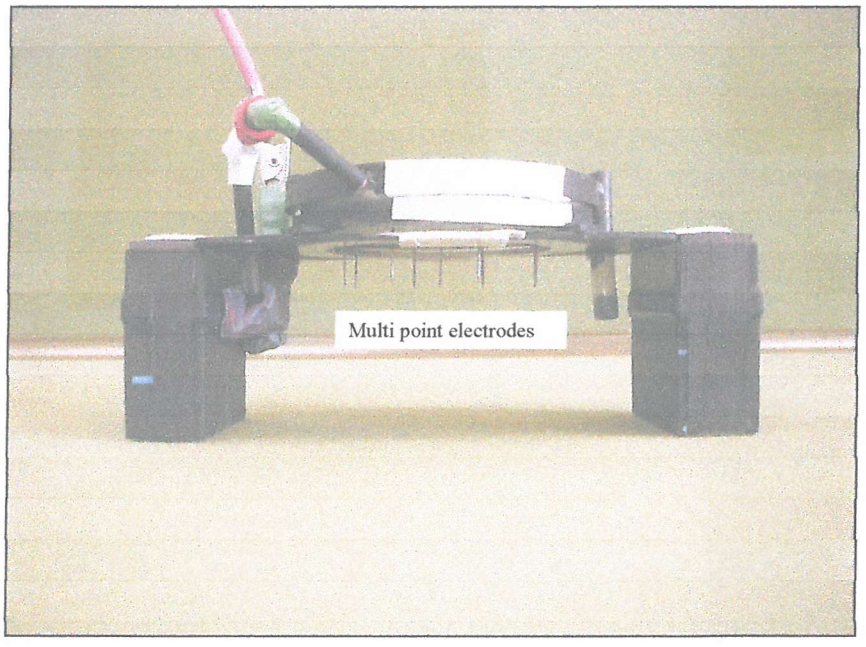

- Corona electrode support frame and bacterial plate housing as separate units

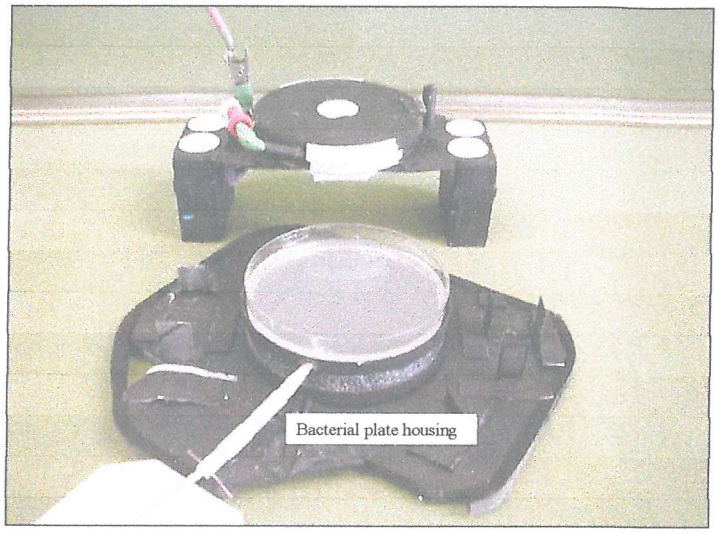

- Corona electrode support frame and bacterial plate housing as experimental set up

Stage three design:

- Side elevation

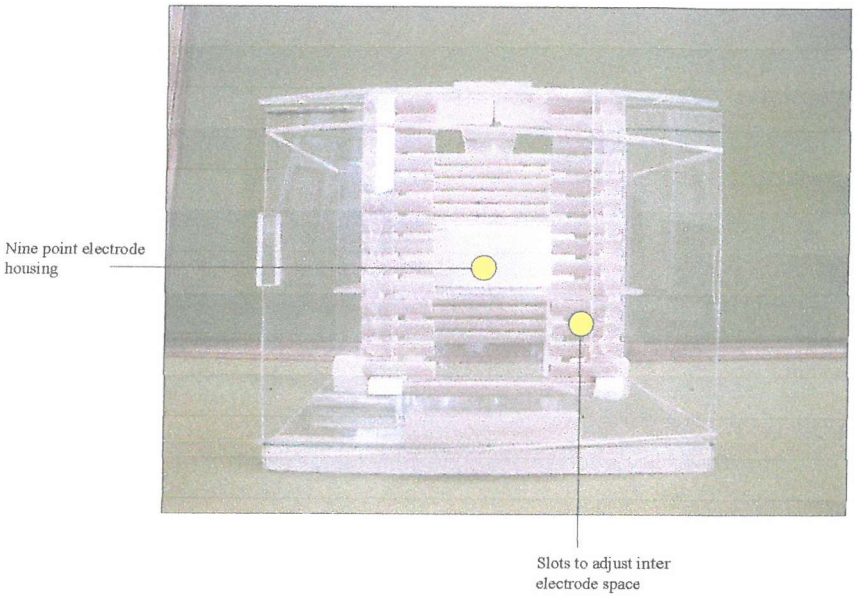

Front elevation

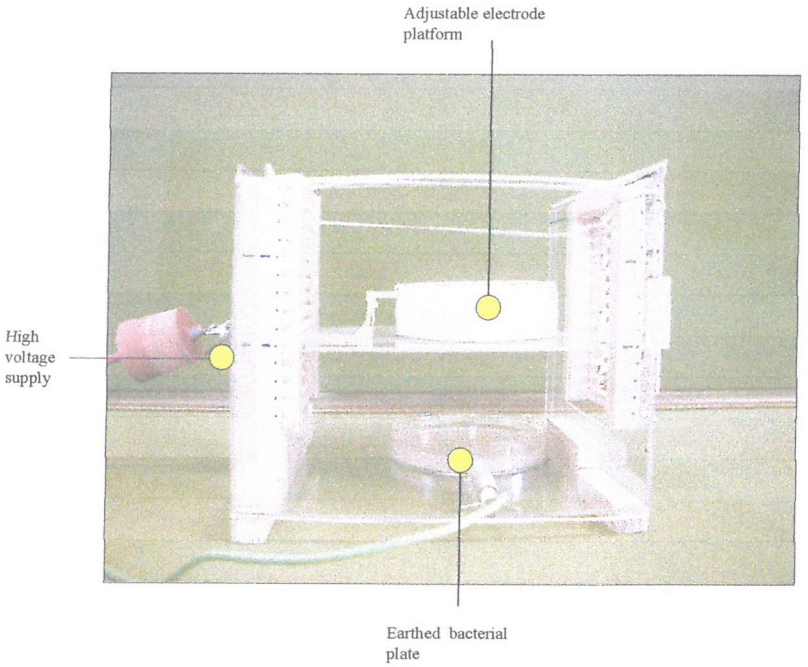

- Upper elevation

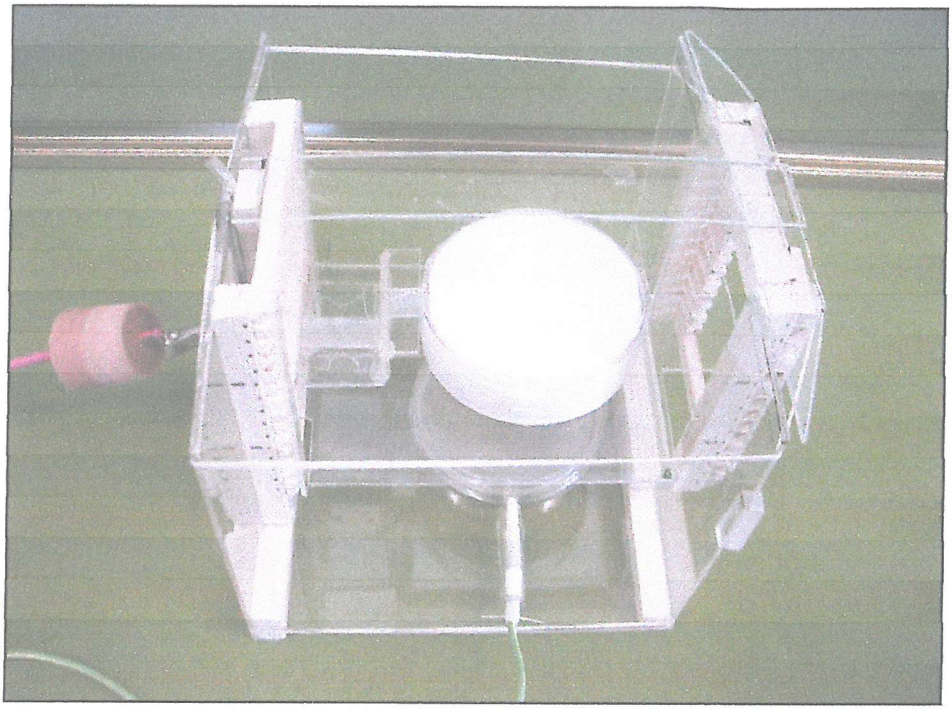

- Corona apparatus housing

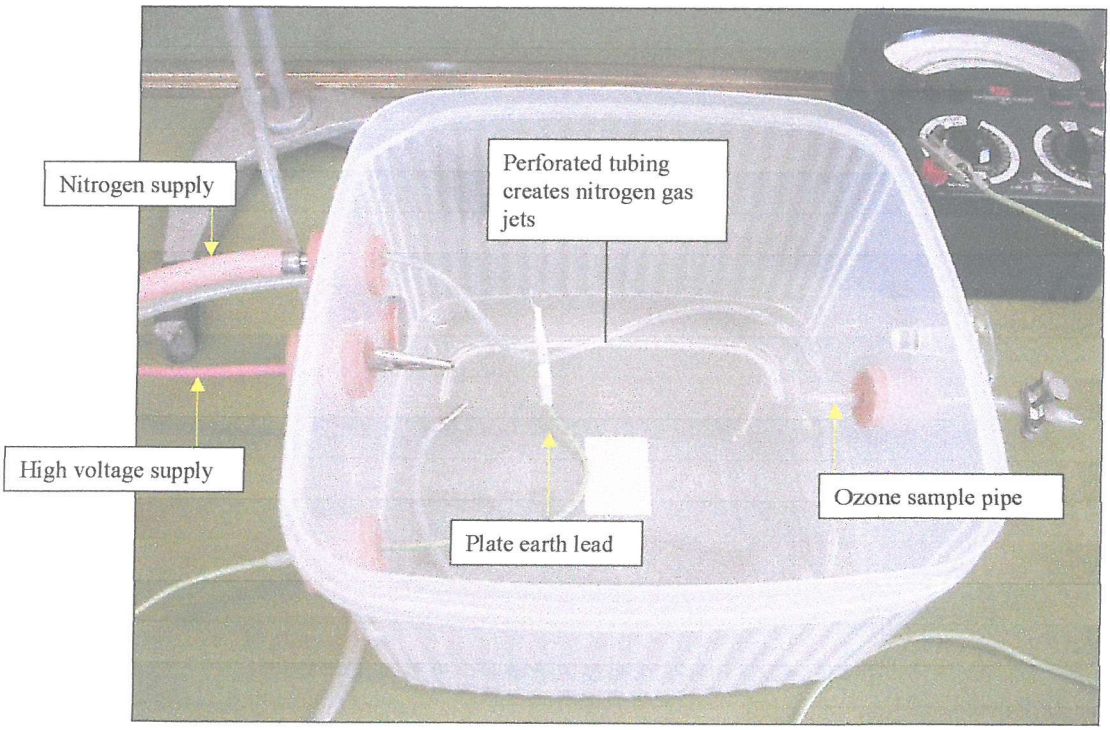

- Corona apparatus in housing

- Experimental set up

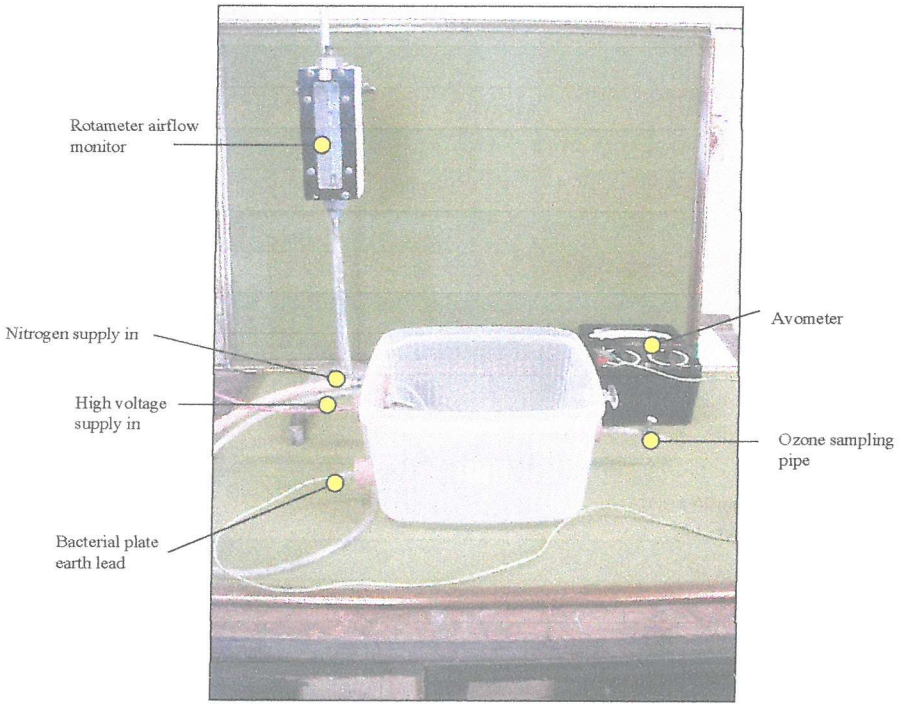

- The chamber is sealed ready for nitrogen flushing

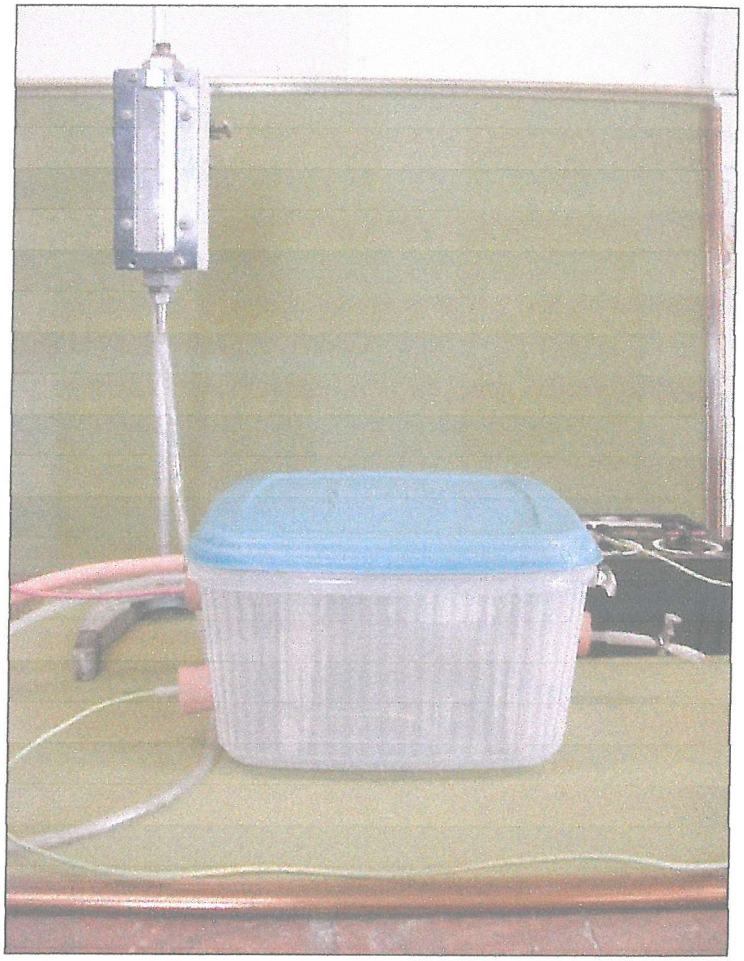

References

Allison D.G., and Sutherland I.W., (1984), A Staining Technique for Attached Bacteria and its Correlation to Extracellular Carbohydrate Production, *Journal of Microbiological Methods*, **2**, pt2, 93-99

Blin-Stoyle, R.J., (1997), Eureka: Physics of Particles, Matter and the Universe, Institute of Physics, Bristol.

Brown, M.R.W., and Gilbert, P., (1993), Sensitivity of Biofilms to Antimicrobial Agents, *Journal of Applied Bacteriology Symposium*, **74**, 87S-97S

Busscher, H.J., and Weerkamp, A.H., (1987), Specific and Non-Specific Interactions in Bacterial Adhesion to Solid Substrata, *F.E.Ms Microbiology Reviews*, **46**, pt2, 165-173

Busscher, H.J., Stokroos, I., and Schakenraad, J.M., (1991), 2-Dimensional, Spatial Arrangement of Fibronectin Adsorbed to Biomaterials with Different Wettabilities, *Cells and Materials*, **1**, pt1, 49-57

Costerton, J.W., Lewandowski, Z., Caldwell, D.E., Korber D.R., and Lappinscott, H.M., (1995), Microbial Biofilms, *Annual Review of Microbiology*, **49**, 711-745

Costerton, J.W., Stewart, P.S., and Greenberg, E.P., (1999), Bacterial Biofilms: A Common Cause of Persistent Infections, *Science*, **284**, 1318-1322

Cross, J.A., (1987), Electrostatics: Principles, Problems and Applications, Adam Hilger, Bristol, England.

Dasgupta, M.K., Read, R.R., Eberwein, P., Grant, S.K., Lam, K., Nickel, J.C., and Costerton JW, (1989), Peritonitis In Peritoneal-Dialysis - Bacterial-Colonization By Biofilm Spread Along The Catheter Surface, *Kidney International*, **35**, pt2, 614-621

Davies, J.E, (1996), Bacteria on the Rampage, *Nature*, **383**, 219-220

Davies, J.E., (1997), Origins, Acquisition and Dissemination of Antibiotic Resistance Determinants, *Antibiotic Resistance: Origins, Evolution, Selection and Spread, Ciba Foundation Symposia*, **207**, 15-27

Fiorenza, G., and Ward, C.H., (1997), Microbial Adaptation to Hydrogen Peroxide and Biodegradation of Aromatic Hydrocarbons, *Journal of Industrial Microbiology and Biotechnology*, **18**, 140-141

Fowler, J. and Cohen, L. (1990), Practical Statistics for Field Biology, John Wiley and Sons Ltd, Chichester, England.

Frère, J.M., (1995), Beta-Lactamases and Bacterial Resistance to Antibiotics, *Molecular Microbiology*, **16**, 385-395

Garate, E., Evans, K., Gornostaeva, O., Alexeff, I., Kang, W., Rader, M., and Woods, T., (1998), Atmospheric plasma induced sterilisation and chemical neutralisation, *Proc. IEEE International Conference on Plasma Science*, Raleigh, NC.

Giard, J.C., Hartke, A., Flahaut, S., Benachour, A., Boutibonnes, P., and Auffray, Y., (1996), Starvation-Induced Multi-Resistance in *Enterococcus faecalis* JH2-2, *Current Microbiology*, **32**, pt5, 264-271

Gilbert, P., and McBain, A.J., (2001), Biocide Usage in the Domestic Setting and Concern About Antibacterial and Antibiotic Resistance, *Journal of Infection*, **43**, pt1, 85-91

Goldman, M., Goldman, A., and Sigmond, R.S., (1985), The Corona Discharge, It's Properties and Specific Uses, *Pure and Applied Chemistry*, **57**, 1353-1362

Goodman, P.J., and Humphries, (1988), F.J., Electron Microscopy and Analysis 2nd Edt, Taylor and Francis, London

Gordon. G., and Bubnis. B., (2000), Environmentally Friendly Methods of Water Disinfection: The Chemistry of Alternative Disinfectants, *Progress in Nuclear Energy*, **37**, (1-4), 37-40

Greene, A.K., Few, B.K., and Serafini, J.C., (1993), A Comparison of Ozonation and Chloronation for the Disinfection of Stainless Steel Surfaces, *Journal of Dairy Science*, **76**, 3617-3620

Habash, M., and Reid, G., (1999), Microbial Biofilms: Their Development and Significance for Medical Device-Related Infections, *Journal of Clinical Pharmacology*, **39**, pt9, 887-898

Handal, T., and Olsen, I., (2000), Antimicrobial Resistance with Focus on Oral Beta-Lactamases, *European Journal of Oral Sciences*, **108**,163-174

Hartke, A., Giard, J.C., Laplace, J.M., and Auffray, Y., (1998), Survival of *Enterococcus faecalis* in an Oligotrophic Microcosm: Changes in Morphology, Development of General Stress Resistance, and Analysis of Protein Synthesis, *Applied and Environmental Microbiology*, **64**, pt11, 4238-4245

Heir, E., Sundheim, G., and Holck, A.L., (1995), Resistance to Quaternary Ammonium-Compounds in *Staphylococcus sp.* Isolated from the Food-Industry and Nucleotide Sequence of the Resistance Plasmid pst827, *Journal of Applied Bacteriology*, **79**, pt2, 149-156

Hoenig, S.A., Sill, G.T., Kelley, L.M., and Garvey, K.J., (1980), Destruction of Bacteria and Toxic Organic Chemicals by a Corona Discharge, *Journal of the Air Pollution Control Association*, **30**, 227-228

Ishida, H., Ishida, Y., Kurosaka, Y., Otani, T., Sato, K., and Kobayashi, H., (1998), In Vitro And in Vivo Activities of Levofloxacin Against Biofilm Producing *Pseudomonas Aeruginosa*, *Antimicrobial Agents and Chemotherapy*, **42**, pt7, 1641-1645

James, A.M., (1991), In: "Microbial Cell Surface Analysis: Structural and Physiochemical Methods", Mozes, N., VCH, New York

Jenkins, D.E., Schultz, J.E., and Matin, A., (1988), Starvation Induced Cross Protection Against Heat Or H_2O_2 Challenge In *Escherichia Coli*, *Journal of Bacteriology*, **170**, 3910-3914

Jenkins, D.E., Chaisson, S.A., and Matin, A., (1990), Starvation-induced Cross Protection Against Osmotic Challenge in *Escherichia-coli*, *Journal of Bacteriology*, **172**, pt5, 2779-2781

Jucker, B.A., Harms, H., and Zehnder, J.B., (1996), Adhesion of the Positively Charged Bacterium *Stenotrophomonas (Xanthomonas) malphilia* 70401 to Glass and Teflon, *Journal of Bacteriology*, **178**, 5472-5479

Kerr, C., Jones, C., Hillier, V., Robson, G., Osborn, K., and Handley, P., (2000), Statistical Evaluation of a Newly Modified Robbins Device Using a Bioluminescent *Pseudomonad* to Quantify Adhesion to Plastic, *Biofouling*, **14**, 267-277

Khadre, M.A., Yousef, A.E., and Kim, J.G., (2001), Microbiological Aspects of Ozone Applications in Food: A Review, *Journal of Food Science*, **66**, 1242-1251

Kim, J.G., (1998), Ozone As an Antimicrobial Agent in Minimally Processed Foods, PhD Thesis, The Ohio State University, Columbus, U.S.A.

Kim, J.G, Yousef, A.E, and Dave, S., (1999), Application of Ozone for Enhancing the Microbiological Safety and Quality of Foods: A review, *Journal of Food Protection*, **62**, (9), 1071-1087

Kjelleberg, S., Hermansson, M., and Marden, P., (1987), The Transient Phase Between Growth and Non-Growth of Heterotrophic Bacteria, with Emphasis on the Marine-Environment, *Annual Review of Microbiology*, **41**, 25-49

Kolter, R., Siegele, D.A., and Tormo, A., (1993), The Stationary-Phase of the Bacterial Life Cycle, *Annual Review of Microbiology*, **47**, 855-874

Kowalski, W.J., Bahnfleth, W.P., Whittam, T.S., (1998), Bactericidal effects of high airborne ozone concentrations on *Escherichia coli* and *Staphylococcus aureus*, *Ozone Science and Engineering*, **20**, 205-221

Kumar, C.G., and Anand, S.K., (1998), Significance of Microbial Biofilms in Food Industry: a Review, *International Journal of Food Microbiology*, **42**, pt1-2, 9-27

Lambe, D.W., Ferguson, K.P., Mayberrycarson, K.J., Tobermeyer, B., and Costerton, J.W., (1991), Foreign-Body-Associated Experimental Osteomyelitis Induced with Bacteroides-Fragilis and *Staphylococcus-Epidermidis* In Rabbits, *Clinical Orthopaedics and Related Research*, **266**, 285-294

Lange, R., and Henggearonis, R., (1991), Identification of a Central Regulator of Stationary-Phase Gene-Expression in *Escherichia-coli*, *Molecular Microbiology*, **5**, pt1, 49-59

Laroussi, M., Alexeff, I., and Kang.W.L., (2000), Biological Decontamination by Nonthermal Plasmas, *IEEE Transactions on Plasma Science*, **28**, 184 - 188

Lederberg, J., (2000), Encyclopaedia of Microbiology, Academic Press, San Diego, U.S.A.

Leelaporn, A., Paulsen, I.T., and Skurray, R.A., (1994), Multidrug Resistance to Antiseptics and Disinfectants in Coagulase-Negative *Staphylococci*, *Journal of Medical Microbiology*, **40**, 214-220

Levy, S.B., (1998), The Challenge of Antibiotic Resistance, *Scientific American*, **278**, 46-53

Levy, S.B., (2000), Antibiotic and Antiseptic Resistance: Impact on Public Health, *Paediatric Infectious Disease Journal*, **19**, pt10, S120-S122

Mann, J., (1996), Bacteria and Antibacterial Agents, Spectrum, Oxford, England

Matin, A., Auger, E.A., Blum, P.H., and Schultz J.E., (1989), Genetic-Basis of Starvation Survival in Non-Differentiating Bacteria, *Annual Review of Microbiology*, **43**, 293-316

Marrie, T.J., Nelligan, J., and Costerton J.W., (1982), A Scanning And Transmission Electron-Microscopic Study of an Infected Endocardial Pacemaker Lead, *Circulation*, **66**, pt6, 1339-1341

McBain, A.J., and Gilbert, P., (2001), Biocide tolerance and the harbingers of doom, *International Biodeterioration & Biodegradation*, **47**, pt2, 55-61

McDonald, G. and Russell, A.D., (1999), Antiseptics and Disinfectants: Activity, Action and Resistance, *Clinical Microbiology Review*, **12**, 147-179

McMurry, L.M., Oethinger, M., and Levy, S.B., (1998), Triclosan Targets Lipid Synthesis, *Nature*, **394**, 531-532

Mendis, D.A., Rosenberg, M., and Azam, F., (2000), A Note on the Possible Disruption of Bacteria, *IEEE Transactions on Plasma Science*, **28**, 1304 - 1881306

Miller, P.S., Kipp, S.A., and McGill, C., (1999), A Psoralen-Conjugated Triplex-Forming Oligodeoxyribonucleotide Containing Alternating Methylphosphonate-Phosphodiester Linkages: Synthesis and Interactions with DNA, *Bioconjugate Chemistry*, **10**, pt4, 572-577

Moore, G., Griffith, C., and Peters, A., (2000), Bactericidal Properties of Ozone and its Potential as a Terminal Disinfectant, *Journal of Food Protection*, **63**, 1100-1106

Morita, R.Y., (1982), Starvation-Survival of Heterotrophs in the Marine-Environment, *Advances in Microbial Ecology*, **6**, 171-198

Mozes, N., (1991), Microbial Cell Surface Analysis: Structural and Physiochemical Methods, VCH, New York, U.S.A.

Mukherjee, T.K., Raghavan, A., and Chatterji, D., (1998), Shortage of Nutrients in Bacteria: The Stringent Response, *Current Science*, **75**, pt7, 684-689

Neis, D.H., and Silver, S., (1995), Ion Efflux Systems Involved in Bacterial Metal Resistance, *Journal of Industrial Microbiology*, **14**, 186-199

Nikaido, H., (1994), Prevention of Drug Access to Bacterial Targets - Permeability Barriers and Active Efflux, *Science*, **264**, 382-388

Nystrom, T., and Kjelleberg, S., (1989), Role of Protein-Synthesis in the Cell Division and Starvation Induced Resistance to Autolysis of a Marine *Vibrio* During the Initial Phase of Starvation, *Journal of General Microbiology*, **135**, 1599-1606

Okabe, H., (1978), Photochemistry of small molecules, John Wiley and Sons, New York, U.S.A.

Palmer, R.J., and White, D.C., (1997), Developmental Biology of Biofilms: Implications for Treatment and Control, *Trends in Microbiology*, **5**, pt11, 435-440

Philips, J., and Murray, P., (1995), The Biology of Disease, Blackwell Science, London, England

Pichereau, V., Hartke, A., and Auffray, Y., (2000), Starvation and Osmotic Stress Induced Multi-Resistances Influence of Extracellular Compounds, *International Journal of Food Microbiology*, **55**, pt 1-3, 19-25

Rang, H.P., Dale, M.M., and Ritter, J.M., (1998), Pharmacology, Churchill Livingstone, London, England

Reid, G., Teizer, C., and Bailey, R.R., (1995), Bacterial Biofilms on Devices used in Nephrology, *Nephrology*, **1**, 269-275

Roccanova, L. and Rappa, P., (2000), Antibiotic Rotation, *Science*, **287**, 803

Russell, A.D., and Russell, N.J., (1995), Biocides: Activity, action and resistance, *Symposium of the society for general microbiology*, **53**, 327-365

Russell, A.D., (1997), Plasmids and bacterial resistance to biocides, *Journal of Applied Microbiology*, **82**, 155-165

Russell, A.D., (1998), Mechanisms of Bacterial Resistance to Antibiotics and Biocides, *Progress in Medicinal Chemistry*, **35**, 133-197

Russell, A.D., (1998), Bacterial Resistance to Disinfectants: Present Knowledge and Future Problems, *Journal of Hospital Infection*, **43** (Supplement), S57 – S68

Russell, A.D., (2000), Do Biocides select for antibiotic resistance?, *Journal of Pharmacy and Pharmacology*, **52**, 227-233

Russell, A.D., and McDonnell, G., (2000), Concentration: A Major Factor in Studying Biocidal Action, *Journal of hospital infection*, **44**, pt1, 1-3

Setti, E.L., and Micetich, R.G., (1998), New Trends in Antimicrobial Development, *Current Medicinal Chemistry*, **5**, 101-113

Siegele, D.A., and Kolter R., (1992), Life after log, *Journal of bacteriology*, **174**, pt 2, 345-348

Sigmond, R.S., (1989), Mass Transfer in Corona Discharges, *Rev. Int. Hautes Temper. Refract.*, **25**, 201-206

Sigmond, R.S., Kurdelova, B., and Kurdel, M., (1999), Action of Corona discharges on Bacteria and Spores, *Czechoslovak Journal of Physics*, **49**, 405-420

Sihorkar, V., and Vyas, S.P., (2001), Biofilm Consortia on Biomedical and Biological Surfaces: Delivery and Targeting Strategies, *Pharmaceutical Research*, **18**, pt 9, 1247-1254

Slavkin, H.C., (1997), Emerging and Re-emerging Infectious Diseases: a Biological Evolutionary Drama, *JADA*, **128**, 10855-113

Sondossi, M., Rossmoore, H.W., and Wireman, J.W., (1985), Observations of Resistance and Cross-Resistance to Formaldehyde and a Formaldehyde Condensate Biocide in *Pseudomonas-aeruginosa*, *International Biodeterioration*, **21**, pt2, 105-106

Stewart, P.S., (1998), A Review Of Experimental Measurements of Effective Diffusive Permeabilities and Effective Diffusion Coefficients in Biofilms, *Biotechnology and Bioengineering*, **59**, pt3, 261-272

Stoodley, P., Boyle, J.D., DeBeer, D., and Lappin-Scott, H.M., (1999), Evolving Perspectives of Biofilm Structure, *Biofouling*, **14**, pt1, 75-84

Suci, P.A., Siedlecki, K.J., Palmer, R.J., White, D.C., and Geesey, G.G., (1997), Combined Light Microscopy and Attenuated Total Reflection Fourier Transform Infrared Spectroscopy for Integration of Biofilm Structure, Distribution, and Chemistry at Solid-Liquid Interfaces, *Applied and Environmental Microbiology*, **63**, pt11, 4600-4603

Suller, M.T.E., and Russell, A.D., (2000), Triclosan and antibiotic resistance in *Staphylococcus aureus*, *Journal of Antimicrobial Chemotherapy*, **46**, pt1, 11-18

Tan, Y.T., Tillett, D.J, and McKay, I.A., (2000), Molecular Strategies for Overcoming Antibiotic Resistance in Bacteria, *Molecular Medicine Today*, **6**, 309-314

Taylor, D.M., and Secker, P.E., (1994), Industrial Electrostatics, John Wiley and Sons, New York, U.S.A.

Vanloosdrecht, M.C.M., Lyklema, J., Norde, W., and Zehnder, A., (1989), Bacterial Adhesion - a Physicochemical Approach, *Microbial Ecology*, **17**, pt1, 1-15

Vaughn, A.S., (2003), Private communication

Veenstra, G.J.C., Cremers, F.F.M., VanDijk, H., and Fleer, A., (1996), Ultrastructural Organization and Regulation of a Biomaterial Adhesion of *Staphylococcus Epidermidis*, *Journal of Bacteriology*, **178**, pt2, 537-541

Volk, W.A., (1996), Essentials of Medical Microbiology - 5th Ed, Lippincott-Raven, Philadelphia, U.S.A.

Ward, K.H., Olson, M.E., Lam, K., and Costerton, J.W., (1992), Mechanism of Persistent Infection Associated with Peritoneal Implants, *Journal of Medical Microbiology*, **36**, pt6, 406-413

Wessells, N.K., and Hopson, J.L., (1988), Biology, Random House, New York, U.S.A.

White, D., (1995), The Physiology and Biochemistry of Prokaryotes, Oxford University Press, New York, U.S.A.

White, D.G., and McDermott, P.F., (2001), Biocides: Drug Resistance and Microbial Evolution, *Current opinion in microbiology*, **4**, pt3, 313-317
